SINGLE USER DIVERSITY RECEIVERS FOR FREQUENCY SELECTIVE WCDMA CHANNELS

A Thesis Submitted to The University

of Kent

For the Degree of DOCTOR OF PHILOSOPY

In ELECTRONIC ENGINEERING

By
CHARAN LITCHFIELD
MAY 2006

If the doors of perception were cleansed,

everything would appear as it is,

infinite.

-William Blake

ABSTRACT

Wideband code division multiple access (WCDMA) forward links are susceptible to performance degradation incurred by multiple access interference (MAI) when the radio channel is frequency selective. This places a tight limit on the channel capacity of the cellular downlink since computationally efficient receiver technologies such as the 2D Rake receiver do not yield significant attenuation of the interference floor for high data rates. The application of optimum spatial processing employing two or more antenna elements is a topic of some interest since an optimum beamformer is one where the desired signal is decoupled into a matched filter while interfering signals are spatially nulled or filtered. However, for realistic radio environments and low number of sensors, array overloading prevents optimum information retrieval (and the required target bit error floor to be met) from a doubly selective spatial radio channel.

The work undertaken in the first part of this thesis investigates adaptive two element array receiver structures to enhance the downlink performance. In addition to per-path adaptive beamforming, oversampling can form several technologies utilizing this basic structure. In particular, an oversampled receiver with additional finger assignment (not necessarily matched to the channel delay spectra) forms the basis of a channel equalizer. This thesis extends upon this criterion by developing adaptive dual antenna interference suppressing receivers that jointly optimize the spatial and temporal multipath channel signatures at chip or symbol level. In particular, a chip-level optimization (forming a 2D chip equalizer) can decorrelate the multipath channel spectra allowing interference suppression with a chip-matched filter. This receiver is a generalized broadband antenna beamformer, where the resultant improvement in performance over the 2D Rake receiver is significant with only moderately increased complexity.

Optimum spatio-temporal diversity receivers require that the multipath delay spectra are known and the channel phase/attenuation parameters perfectly reproducible with negligible error. However, matched filtering applying estimation of the channel parameters is unlikely to be error free, nor devoid of the effects of quantization. The second part of this thesis investigates the effect of quantization and logarithmic arithmetic on the 2D Rake receiver and 2D Chip equalizer. Logarithmic arithmetic was found to augment many useful properties such as reducing receiver filter inner products into trivial additions by transforming a linear algorithm into the logarithmic domain using the logarithmic number system. This method was found to offer superior error performance even when utilizing very simple codecs. This makes it a promising technique for integrating an adaptive WCDMA receiver onto low power multiplierless programmable hardware devices.

ACKNOWLEDGEMENTS

First and foremost, I would like to thank Prof. R.J. Langley for being a compassionate, supportive and flexible supervisor throughout the duration of the PhD project.

I would also like to extend immense gratitude to Dr. P. Lee for making an invaluable contribution to this project by providing expertise on digital signal processing - in particular the numeric coding aspect from both a practical and theoretical level.

I wish to extend my warm regards and appreciation to Harada Industries Europe for funding the project and offering technical advice on many aspects of the Ph.D.

To the following people of the communications group, namely Dr, J.C. Batchelor, Prof. M. Sobhy, Dr. N. Gomes, and Mr. A. Jabstrebski, I extend warm gratitude for supplying advise and assistance on the more difficult aspects of the project - particularly during the introductory phase of my PhD.

I also wish to acknowledge the contributions by Dr. Eryl Bassett and Dr. Alfred Kume from the Department of Statistics for their assistance in the development of many mathematical derivations yielded by this thesis.

Next, I wish to thank my parents, Roy and Adrienne Litchfield, and my brothers, Dustin and Aryn, for their encouragement and support. The largest appreciation however, must be bequeathed to my wife Julie. Her continual words of encouragement, love, and support wiped away all reservations I may have held during the write-up phase of the project.

Finally, I wish to thank my friend, Gurinder Singh Dayal.

LIST OF PUBLICATIONS

1. Litchfield. C, Langley. R, and Lee. P. (2005). "The use of Hybrid Logarithmic Arithmetic for Root Raised Cosine Matched Filters in WCDMA Downlink Receivers". *Proceedings of the IEEE International Conference on Wireless Communications and Networks.*

2. Litchfield. C, Langley. R, and Lee. P. (2005). "Least Squares Adaptive Algorithms Suitable for Multiplierless LMMSE Detection in 3rd Generation Mobile Systems". *Proceedings of the IEEE International Conference on Personal, Indoor and Mobile Radio Communications.*

3. Litchfield. C, Langley. R, and Lee. P. "Low-Precision Logarithmic Coding for Application in low power WCDMA Receivers". *Submitted for publication in the Electronics Letters Journal.*

4. Litchfield. C, Langley. R, and Lee. P. "Error Bounds for LMMSE WCDMA Receivers Employing Finite-Precision Logarithmic Coding". *Submitted for publication in IEEE Transactions on Vehicular Technology.*

5. Litchfield. C, Langley. R, and Lee. P. "On Linear Equalization Employing Logarithmic Coding". *Submitted for publication in IEEE Transactions on Signal Processing.*

CONTENTS

LIST OF FIGURES

LIST OF TABLES

ABBREVIATIONS

3GPP	Third Generation Partnership Project
AGC	Automatic Gain Control
AOA	Angle of Arrival
ARAKE	All Rake
ASIC	Application Specific Integrated Circuit
AWGN	Additive White Gaussian Noise
BER	Bit Error Rate
BPSK	Binary Phase Shift Keying
CDMA	Code Division Multiple Access
CMF	Chip Matched Filter
CNR	Chip to Noise Ratio
CPICH	Common Pilot Channel
D/A	Digital to Analog
DFE	Decision Feedback Equalizer
DOA	Direction of Arrival
DDPCH	Dedicated Data Physical Channel
DS-CDMA	Direct Sequence-Code Division Multiple Access
DSP	Digital Signal Processing
FIR	Finite Impulse Response
EGC	Equal Gain Combining
EDGE	Enhanced Data Rates for Global Evolution
ESPRIT	Estimation of Signal Parameters via Rotation Invariance Techniques
FDMA	Frequency Division Multiple Access
FLP	Floating Point
FM	Frequency Modulation
FPGA	Field Programmable Gate Array
FSE	Fractionally Space Equalizer
GPS	Global Positioning System
GPRS	General Packet Radio System
GRAKE	Generalized RAKE
GSM	Global System for Mobile Communication
H-LNS	Hybrid-Logarithmic Number System
IC	Interference Cancelling
ICI	Interchip Interference
ITU	International Telecommunication Union
ISI	Inter-Symbol-Interference
LMMSE	Linear Minimum Mean Square Error
LNS	Logarithmic Number System
LOG	Logarithm
LSB	Least Significant Bit
LUT	Look Up Table
MAC	Multiply Accumulate
MAI	Multiple Access Interference
MAP	Maximum A Posteriori
MDL	Minimum Description Length
MF	Matched Filter
MIMO	Multiple Input Multiple Output
ML	Maximum Likelihood
MLSD	Maximum Likelihood Sequence Detector
MMSE	Minimum Mean Square Error

MSB	Most Significant Bit
MSINR	Maximum Signal to Interference Ratio
MOE	Minimum Output Energy
MRC	Maximum Ratio Combining
MSB	Most Significant Bit
MSE	Mean Square Error
MUSIC	Multiple Signal Classification
MV	Minimum Variance
MVU	Minimum Variance Unbiased
NFR	Near Far Ratio
LMS	Least Mean Squares
NLMS	Normalized Least Mean Squares
NP	Neyman-Pearson
OFDM	Orthogonal Frequency Division Multiplexing
PCH	Physical Channel
PIC	Parallel Interference Cancellation
PN	Pseudo Noise
PSD	Power Spectral Density
QOS	Quality of Service
QPSK	Quadrature Phase Shift Keying
RLS	Recursive Least Squares
RMS	Root Mean Square
ROM	Read Only Memory
RRC	Root Raise Cosine
RV	Random Variable
SD	Soft Decision
SER	Signed Exponent Regressor
SIC	Successive (or Serial) Interference Cancellation
SIR	Signal to Interference Ratio
SINR	Signal to Interference plus Noise Ratio
SIMO	Single Input Multiple Output
SISO	Single Input Single Output
SLNS	Signed Logarithmic Number System
SNR	Signal to Noise Ratio
SR	Signed Regressor
STTD	Space Time Transmit Diversity
TDMA	Time Division Multiple Access
TOA	Time of Arrival
UMTS	Universal Mobile Terrestrial System
UTRA-FDD	Universal Terrestrial Radio Access-Frequency Division Duplex
V	Versus
UTRAN	Universal Terrestrial Multiple Access Network
WCDMA	Wireless Code Division Multiple Access
WMF	Whitening Matched Filter
WSSUS	Wide-Sense Stationary Uncorrelated Scattering

CHAPTER 1
INTRODUCTION

PREFACE

To enable high capacity and combat multipath fading for medium-broad bandwidth applications, 3rd Generation mobile networks have integrated diversity applications for both uplink and downlink. Uplink basestation receivers generally incorporate spatial and multiuser interference cancellation techniques to circumvent the asynchronous nature of multiple access interference, while the forward link is generally only supported with a rake receiver. The multiple access downlink channel carries synchronous multirate transmissions spread with variable spreading factor orthogonal codes (with all users sharing the same radio channel) where the optimum detector in frequency-non-selective multipath channels is a code-matched filter. However, dispersive channels can induce multiple access and inter-channel interference that is particularly prevalent in frequency selective fading generating non-orthogonality between the multiple scattered signals. Overcoming the interference generated in WCDMA fading channels (at a cost of greatly accentuated complexity) include traditional multiuser detection algorithms such as the Maximum Likelihood detector or Decorrelator [Verdu1998] provided knowledge of all active signatures are given to the receiver by the network. Blind single or multi-user detection techniques [Wang2004] have strong applicability for downlink scenarios when only the desired channel code is known, but offer little accentuation in performance for long-code CDMA (where the code varies from symbol to symbol). The problems incurred by optimizing the downlink detection problem based on constraints regarding knowledge of the active signatures and/or cyclic second order statistics has led to industrial and academic research on chip-level estimation employing beamforming [Litva1996] or channel equalization to restore the orthogonality of the multiple access channel [Hooli1999A]. This thesis focuses on receiver techniques employing both antenna array and equalization technologies to reduce the interference floor incurred by doubly selective fading channels. Of particular importance in the context of single user detection is the receiver complexity, where the other main thesis objective is to present solutions overcoming the strict requirement of multiplication in traditional fixed or floating-point arithmetic and associated effects on receiver performance. The motivation behind this thesis is given in section 1.2, and the thesis outline discussed in section 1.3.

1.1 Overview of CDMA Receiver Technologies

Research involving detection problems for CDMA employing single or multiple sub-carriers has been extremely active in the past two decades, particularly when noting the rise of very commercial wireless mobile networks utilizing this technology (IS-95, and more recently the UMTS). However, most industrial and academic research has concentrated on the mobile uplink where a plethora of optimization techniques have been proposed to enable more optimum multi-user demodulation in the presence of severe near-far interference (which can also be combated with dynamic power control) and/or high system capacity. Such schemes are extremely diverse, ranging from computationally expensive likelihood optimization problems to the more simplistic generic multi-user equalization employing fairly basic statistical techniques- such as those involving minimization of a Bayesian cost function or a zero-forcing criterion (see [Verdu1998] for a general introduction to multiuser demodulation covering the widely acknowledged Decorrelator and vector based LMMSE detector). As antenna arrays (used as spatial filters) have become more practical for handsets and basestations, many proposals have followed by academic or industrial researchers in their utilization as part of the detection problem- mainly exploiting the beamforming properties of a linear array of elements to separate out multiple user transmissions from a multipath field and hence suppress interference. Improved diversity application is also another widely acknowledge use of antenna arrays- including application for the shadowing phenomena where macrodiversity is a common method for ensuring at least one good quality channel per user. The global research and development of novel and improved uplink detection (and power control) schemes is not surprising since the fundamental limits of system performance and capacity are ultimately determined by the mobile reverse link- mainly due to the nature of multiple access and the information limits imposed by a variable and harsh fading channel when users are connected to the terrestrial network via a fixed basestation. This being said, it is not inconsequential considering the mobile downlink, where some research has occurred mainly in presenting simplistic diversity algorithms (generally based on the rake receiver) and/or channel equalizers to improve performance. Of course the mobile downlink is generally not as harsh as the uplink- mainly due to the near-far problem (in downlink we treat this as a far-near problem) being significantly less than an uplink scenario (the uplink has to deal with both asynchronous transmissions as well as temporal dispersion of channel fading). However, this does not mean that the near-far problem or number of simultaneously active users is insignificant since the performance of the downlink with doubly selective channels ultimately

depends on these parameters (even when channel coding or transmit diversity is employed by the network).

The drive and ambition of advanced detection in 3rd Generation mobile and beyond is chiefly related to the fact that mobile operators offer high quality of service and guaranteed connection to their networks. In order to maximize the network throughput and the potential for offering wideband and real-time multimedia services to many users simultaneously, it is essential that connection quality be maintained even when a micro/macro-cell is at near full capacity. To ensure connection quality to a wide variety of users, the current network standards incorporate power control, antenna arrays (for the uplink reception and downlink beamforming/diversity) and rake receivers for mobile devices [Prasad2000]. Efficient channel coding schemes are also invoked for both link directions in the form of turbo and convolutional coding. Although realistically, even with perfect power control, traditional correlation type receivers (i.e. despreading devices employing a chip-matched filter or integrate-dump style detector) with single or multi-branch diversity in frequency selective multipath environments are only sub-optimal where the efficiency (and thus asymptotic efficiency) is degraded and dependent on the number and power of the adjacent users, as well as the accuracy of channel acquisition affecting synchronization and code tracking [Verdu1998]. This fact alone has motivated the research and development of more advanced detection, power control and channel coding for multipath environments. An antenna array receiver would in some sense yield significant diversity gain (especially when utilizing STTD codes) for frequency non-selective channels since code-orthogonality amongst adjacent channels would be observed and the diversity receiver required just to track, cophase and combine uncorrelated (spatially) fading signals. Adaptive array receivers have been shown to suppress adjacent-cell and adjacent-channel interference [Litva1996] in cellular CDMA, but the significant performance gain offered by this technique is generally only realizable in the mobile uplink due to optimization constraints and the available dimensions regarding sufficient antenna spacing. The use of linear receivers (for single or multiple sensor communications) applying some form of statistical optimization to increase the probability of successful acquisition are well-known alternatives to the conventional matched filtering, where over the course of the last two decades, innumerable receivers have been published and documented that propose greater performance advantages. While many optimum/sub-optimum receiver architectures and algorithms exist, most are totally unsuitable for implementation in the forward-link of the WCDMA-FDD interface due to the "number of user" dependent complexity, knowledge of adjacent user signatures or powers (where other users get demodulated by the algorithm), the cyclostationarity requirement for symbol level detection,

and the non-trivial operation of performing matrix inverses [Verdu1998]. The downlink interference problem can be combated using chip-level estimation or equalization [Werner1999] rather than explicit symbol level optimization[1]. Equalization is an age-old technique for dealing with channels incurring ISI in point-to-point communications where applications in telephony go as far back as 1928 [Zobel1928]. In a similar manner, the synchronous multiple access channels can be treated as a single user channel with multi-level/phase chip constellation, hence multipath channel decorrelation/inverse filtering via an equalizer can restore the original transmitted information (where interference can be removed with a simple matched filter). The difficulty of equalizer application in WCDMA channels relates to the chip or symbol level optimizations in the downlink where knowledge of the multiuser signatures is limited (and techniques to estimate the active user signatures are too exhaustive complexity-wise for practical application [Li1996]). Advances in blind channel identification and equalization in the latter part of the 1990's [Honig1995, Heikkila1999] at least present an alternative to the more formalized decision-directed or pilot symbol training usually associated with traditional equalizer optimization algorithms [Leus2003]. Symbol level equalizers [Moonen2000, Bottomly2000, Krauss2002] studied in the literature overcome the requirement of explicit first-order MAI knowledge (since it can be reasoned that a chip matched filter should significantly reduce the interference floor) at a cost that training will be either slow or impossible in very fast fading channels.

1.2 PROBLEM DEFINITION

In the synchronous downlink employing orthogonal multiple access, MAI occurs when multipath dispersion causes replicas of the transmitted basestation signal to arrive at the receiver terminal with a time and frequency shift. The cross-correlation between the spreading + scrambling sequences of any two paths with a timing offset is a non-zero quantity – thus generating self interference and MAI at the output of each rake finger matched filter. In flat or narrow band fading channels (caused by low data rate or delay spread), the MAI can be considered virtually negligible where the error floor of the receiver usually will allow a fairly low target BER performance. In frequency selective vehicular channels, the interference effect

[1] To prevent confusion of "symbol level optimization", it is referred here that a symbol level optimization approach minimizes/maximizes a cost function formed from the output of an unknown detector. In other words, the input to the detector is the multi channel received sequence, and the detector output is a single or multi-dimensional (for multiuser or sequential detection) symbol estimate. The other form of a symbol level detector would be one based on applying despreading prior to optimization.

for the Rake receiver may cause severe BER degradation unless the system loading is very low. Traditional multiuser demodulation techniques (such as the MLSE or LMMSE receivers) appearing in the literature for interference suppression or cancellation are not generally practical in the WCDMA downlink for a variety of reason including: Lack of cyclostationarity in the transmitted signals for applying symbol level detection, lack of knowledge of the "active" adjacent channel signatures, and the complexity of the receivers in question (usually linearly complex with number of users or exponentially complex in the case of the MLSE with the Viterbi algorithm).

Optimum or near-optimum chip level estimation of the access channel (utilizing the optimum maximum likelihood sequence estimator or the near-optimum decision feedback equalizer) is very difficult to apply in the WCDMA downlink since all users require demodulation and the constellation of the total basestation signal (commuting over all physical channels) somewhat resembles a very high order quadrature amplitude modulation constellation with non-symmetric spacing (that also changes due to power control and discontinuous multiuser transmissions). The "classical" decision feedback or Viterbi approaches to chip level estimation is therefore largely impractical for most channel loading situations. The LMMSE serial equalizer, on the other hand, is a practically achievable chip estimator where limitations only incur for very sparse fading channels (where inverse filtering transforms may be ill-conditioned or singular). This device only requires knowledge of the channel, the second order moments of the additive noise and the basestation signal covariance. The LMMSE chip estimator also transfers easily into an adaptive filter, where training can be applied with a composite of the Common Pilot Channel and other physical channels. A decentralized receiver would have to be adapted blindly[2] or with partial information resulting in slower convergence and performance degradation.

Antenna arrays have long been considered as a viable approach for removing interference contributions arising from multipath scattering and dispersion – particularly when the radio channel scatters the energy over an incident angle distribution. Adaptive arrays unfortunately suffer from overloading effects when the number of interferers exceeds the number of array elements, as would be likely for handsets employing a low number of sensors. This approach can be partially overcome considering rake-assisted beamforming [Affes1999] when the channel is temporally and spatially dispersive. However, the link between the broadband beamformer and a channel equalizer can render another approach – that being joint

[2] The classic blind equalizer applying the constant modulus algorithm is not applicable for chip-level channel equalization due to the constellation of the access channel. Other blind approaches such as Griffith's algorithm and adaptive MOE receiver will be discussed in the proceeding chapter.

beamforming and equalization (or rather the broadband antenna array) to overcome the limited array dimensionality. In this thesis, the suppression of MAI is studied employing dual antenna equalizer structures. The thesis scope is predominately concerned with adaptive serial equalization rather than nonlinear or frequency domain equalization due to technical difficulties applying these techniques in the WCDMA downlink (the frequency domain approach is more commonly associated with the OFDM standards being proposed for 3.5G and 4G networks).

The issue of finite quantization and arithmetic round-off effects in matched filtering for mobile communication are not a very well explored topic in the literature. In particular, the computational cost of applying a large number of multiplications and the associated round-off error for low precision receivers is an area requiring some research scope – particularly if matched filters become ill conditioned due to finite quantization. This thesis studies the effect of linear and logarithmic domain arithmetic on the proposed dual antenna receivers. Logarithmic domain implementations are proposed in this thesis due to lower complexity and better robustness to the effects of arithmetic round-off error.

1.3 Outline of the Thesis

In this thesis, receivers negating interference by utilizing broadband adaptive antennas is studied. The application of logarithmic domain algorithms and computations are proposed to reduce numerical errors and complexity by circumventing the requirement of hardware multipliers. The rest of the thesis is organized as follows:

In Chapter 2, a generic model of the WCDMA downlink is given for the case of SISO or SIMO fading channels. The WCDMA downlink model is the generalized UMTS-FDD model without transmitter diversity. This second section of this chapter reviews the current state of the art receiver techniques for single or multi-carrier CDMA derived from the literature. The final section of this chapter reviews the problem definition by giving a brief overview of the rake receiver and dual antenna diversity receivers with result verification for the WCDMA downlink.

Chapter 3 presents an algorithmic approach to delay acquisition and the channel estimation algorithms required for building multi-sensor diversity receivers and one-shot chip estimators. The specific delay acquisition algorithms consider the minimum variance, multiple signal

classification, minimum mean square error, and matched filter approaches. The delay diversity acquisition schemes are compared and contrasted in terms of performance, complexity and practicality for WCDMA downlink detection. The contributions of this chapter are the application of well-known antenna direction of arrival estimation and beamforming techniques applied specifically for the downlink delay acquisition procedure.

Chapter 4 investigates the performance of various adaptive antenna receivers exploiting temporal diversity. The first part of the chapter considers the rake-beamformer where adaptive combining is instigated on a "per-finger" basis and the outputs combined according to the maximum ratio-combining rule (applying the inverse channel noise + interference variance). The second part of this chapter investigates the application of two types of equalization technique to the adaptive beamformer – namely the symbol equalizer (or GRAKE) optimized with MMSE or Whitening hypothesis, and the MMSE chip equalizer. The similarity between the different receivers is mathematically modelled and verified with simulation against the computationally simpler rake-beamformer. The contributions of this chapter involve the implementation of an improved diversity combiner for the adaptive beamformer, and the study of broadband antenna arrays for the WCDMA downlink.

Chapter 5 studies the effect of finite precision arithmetic on the performance of the diversity receivers investigated in Chapter 4 for the WCDMA downlink. A logarithmic domain computer arithmetic algorithm first studied in the 1960's (and still an ongoing topic of research in industry for efficient and highly accurate computer arithmetic units) is the main topic of investigation in Chapter 5 to allow not only improvement in performance for low-precision receivers, but also entirely multiplierless receiver algorithms. The contributions of the chapter (accounting for all published and submitted papers arising from the thesis) are the multiplierless rake receiver and equalizer employing two antennas. The logarithmic part of this work presents the main aspect of originality in this chapter.

Chapter 6 presents the conclusion to this thesis and reviews current open issues in wireless mobile computing and optimization. Further improvements to the work undertaken in this thesis and aspects for further research are also mentioned.

CHAPTER 2
PRELIMINARIES

PREFACE

This chapter presents the mathematical preliminaries for the WCDMA Forward link and yields a review of discrete channel modelling. This chapter also gives an overview of the state of the art research incurred in single and multiuser detection prior to the conception of this thesis. The aspects covered in this chapter have important repercussions in the development of data detection algorithms for single user terminals, where in particular, the linear mathematical models presented in Section 2.1 have applications for discrete signal processing rendering relatively simple optimizations that are prevalent in definitions for optimum and sub-optimum matched filters. Section 2.2 yields a literature survey on past and present developments in the field of detection of single carrier DS-CDMA channels. The particular focus of this section is on single user and multiuser detection applying statistical optimization. The section 2.3 shifts the focus of single user detection to the case of antenna arrays. Only low cost solutions are presented. A brief overview of the rake receiver is given in section 2.4, with relevant discussions given in section 2.5.

2.1 SYSTEM MODEL

This section concentrates purely on the mathematical preliminaries for the WCDMA downlink transmissions.

2.1.1 MODEL OF THE WCDMA DOWNLINK

The model for the synchronous WCDMA-FDD downlink will consider the reception of signals with K multiplexed users and L propagation paths. In this case, information bearing multiple users (multiplexed and coded with unique channel signatures) will contribute L QPSK modulated RF signals to the received field at a mobile terminal antenna. For brevity, the mathematical analysis considers just the baseband spectrum. The baseband signal consists of a continuous stream of chips at a fixed baud rate, where the spreading sequences can be generically defined for the kth user as

$$s_k(t) = \sum_{i=0}^{G^{(k)}-1} s_k(i) \cdot \varphi(t - iT_c) \tag{2.1}$$

with $s_k(i) \in \{1+j,\ 1-j,\ -1-j,\ -1+j\}$ the ith complex spreading chip of user k and $\varphi(t)$ the chip waveform of chip interval, T_c and chip index iT_c. The variable $G^{(k)}$ is the spreading factor (commonly known as the processing gain) for user k. The component chip waveforms[1], $\varphi(t)$ are unit energy and non zero for $0 \le t < T_c$. Each multiuser modulating waveform built with chips exhibits Root Raised Cosine (RRC) response (2.2) having excess bandwidth of $\alpha = 0.22$ and frequency transfer function

$$\vartheta(f) = \begin{cases} 1 & 0 \le |f| \le \dfrac{1-\alpha}{2 \cdot T} \\ \cos\left[\dfrac{\pi \cdot T}{2 \cdot \alpha} \cdot \left(|f| - \dfrac{1-\alpha}{2 \cdot T}\right)\right] & \dfrac{1-\alpha}{2 \cdot T} \le |f| \le \dfrac{1+\alpha}{2 \cdot T} \\ 0 & |f| > \dfrac{1+\alpha}{2 \cdot T} \end{cases} \tag{2.2}$$

with $T = T_c$. Application of the inverse Fourier transform yields the Root-Raised Cosine impulse response,

[1] Systems like UMTS have tight bounds on the ACLR, hence agreement to the spectral emissions mask is mandatory where non-linear power amplifiers and pulse shaping filters are two such cases where transmitting equipment must have conformance.

$$\varphi(t) = \frac{\sin\left(\pi \cdot \frac{t}{T}\right) \cdot \cos\left(\pi \cdot \alpha \cdot \frac{t}{T}\right)}{\pi \cdot \left(\frac{t}{T}\right) \cdot \left[1 - 4 \cdot \alpha^2 \cdot \left(\frac{t^2}{T^2}\right)\right]} \tag{2.3}$$

where at the receiver, the discrete sampled version yields the coefficients of a digital FIR filter realization [3GPP2001]. The autocorrelation function of the RRC pulse (at the matched filter of the receiver) yields a traditional Raised Cosine (RC) response, which is then down sampled for further signal processing such as despreading and/or equalization. The coding used in modern communications (i.e. like the UMTS) consists usually of short (dependant on the spreading factor), cyclic spreading sequences that are typically overlaid with scrambling sequences (which generally have greater duty cycle than the chip-modulated symbol duration). The channelization codes (or short spreading sequences) are variable spreading factor and taken from orthogonal Walsh-Hadamard code set [3GPP2002] where $\boldsymbol{C}_{(m)}^{(k)} \in \begin{bmatrix} +1 \\ -1 \end{bmatrix}$ is the spreading modulation code (m is the chip index), and $\boldsymbol{C}^{(k)}$ a vector with a predefined sequence (selected by the network during dial up) of unity autocorrelation and rank $G^{(k)}$. The complex chip rate[2] sequence of user k is denoted as:

$$\boldsymbol{X}_k^{(n)} = \sqrt{\varepsilon_{(n)}^{(k)}} \cdot b_{(n)}^{(k)} \cdot \boldsymbol{C}^{(k)} \tag{2.4}$$

where $b_{(\mathrm{n})}^{(k)} \in \begin{bmatrix} I_k(n) \\ j * Q_k(n) \end{bmatrix}$ is the temporal antipodal data symbol (simulating the k$^{\text{th}}$ user I and Q channel) and $\sqrt{\varepsilon_{(\mathrm{n})}^{(k)}}$ the square root of the signalling energy[3] for the user k. n is the symbol sampling index with $n = i T_s^{(k)} \; \forall \, i, \; i = 1 : N_b^{(k)}$ where $T_s^{(k)}$ is the data symbol period for user k, and $N_b^{(k)}$ is the total number of information symbols transmitted in the traffic channel. The normalized codes exhibit orthogonal properties, where if synchronous transmission is observed, then $G^{-1} \sum_{g=1}^{G-1} X_{l,g}^{(n)} X_{k,g}^{(n)} = 0$. The scrambling overlay code, $S(t)$ is multiplied complex-wise

[2] Defined in this thesis as 3.84Mcps and is limited to the alphabet $\Xi = \{1 + j, 1 - j, -1 - j, -1 + j\}$.

[3] The spatial coding (such as STTD coding), number of transmitting antennas and power control varies this parameter which ultimately exhibits dependency on the mobile-base station distance and the fading channel to determine the transmitted power per user.

(where all users share the same scrambling code) with the spreaded data sequence of each user. Considering (2.1) and altering the definition for the scrambling overlay model, let $\boldsymbol{X}_k^{(n)}\boldsymbol{S}^{(n)}$ be the spreaded-scrambled data block for user k, i.e $\boldsymbol{X}_k^{(n)}\boldsymbol{S}^{(n)} = \sqrt{\varepsilon_{(n)}^{(k)}} \cdot b_{(n)}^{(k)} \cdot \boldsymbol{C}^{(k)}\boldsymbol{S}^{(n)}$ where $\boldsymbol{S}^{(n)}$ are the sampled complex scrambling signatures defined as $\boldsymbol{S}^{(n)} = [S(nT_s), S(nT_s + T_c), ..., S(nT_s + (G^{(k)} - 1) \cdot T_c)]^T \in \Xi^G$. Hence (2.1) can be rewritten as

$$s_{k,n}(t) = \sum_{i=0}^{G^{(k)}-1} [(\boldsymbol{C}^{(k)}\boldsymbol{S}^{(n)}) \cdot \partial(n-i)] \cdot \varphi(t - iT_c) \tag{2.5}$$

where Ξ is the set of complex modulation symbols (for QPSK this is a 4 element set) and $\partial(n)$ the Kronecker delta. The complex envelope $r(t)$ of the received signal can be expressed as (see Fig 2.1 for the model):

$$r(t) = \sum_{k=1}^{K} \sum_{n=0}^{N_b^{(k)}-1} \left[\sqrt{\varepsilon_{(n)}^{(k)}} \cdot b_{(n)}^{(k)} \cdot s_{k,n}(t - nT_s^{(k)})\right] * h(t) + \eta(t) \tag{2.6}$$

where $h(t)$ represents the filter impulse response modelling the time invariant fading channel and the "*" operator representing convolution. $\eta(t)$ is a complex zero mean additive bandlimited white noise (modeling the thermal noise and narrow band interference from other systems) with double sided PSD, σ_n^2. $h(t)$ can be simplified to denote a multiplicative process where:

$$h(t) = \sum_{d=1}^{L} \alpha_d^{(n)} \cdot \partial(t - \tau_d) \tag{2.7}$$

with the assumption that all users share the same radio channel where $\alpha_d^{(n)}$ represents the complex channel coefficient at the sample index, n. τ_d is the d^{th} propagation delay represented as an integer scalar (which was normalized to the oversampled chip period giving rise to a dimensionless integer useful for expressing delays in samples). Substitution of (2.7) into (2.6) yields the received signal as:

$$r(t) = \sum_{k=1}^{K} \sum_{d=1}^{L} \sum_{n=0}^{N_b^{(k)}-1} \sqrt{\varepsilon_{(n)}^{(k)}} \cdot b_{(n)}^{(k)} \cdot \alpha_d^{(n)} \cdot s_{k,n}(t - nT_s^{(k)} - \tau_d) + \eta(t). \tag{2.8}$$

It would be useful to expatiate upon (2.8) to yield an equivalent discrete time model such that a signal processor or statistical optimization can be applied. The received signal is time-discretized by sampling (after anti-aliasing filtering) $r(t)$ at a rate $s^{-1}T_c$, where s is the oversampling factor

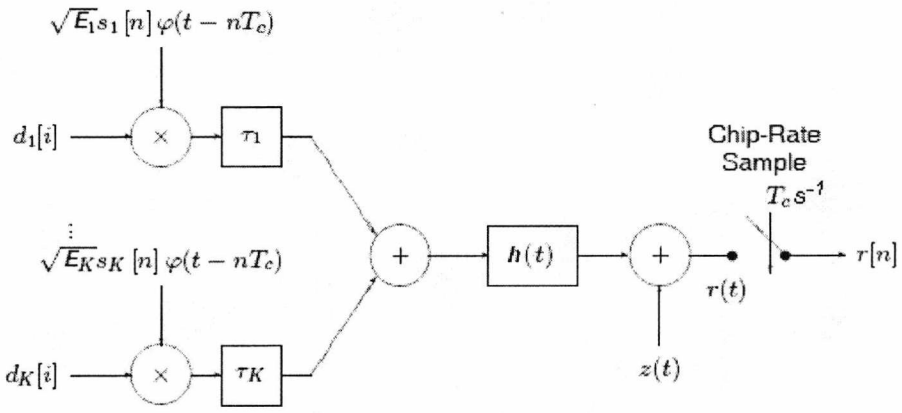

Fig 2.1. A general block diagram of the WCDMA transmitter

(normally greater than 7 to prevent spectral regrowth from the received RRC matched filter). If s is not equal to the number of receiver matched filter taps (encompassing over the chip period), then the sample index must be sufficiently spaced so as not to cause ISI. In the case of $s=8$, then $n= s^{-1}T_c$ for the time sample domain representation where $r[n] = r(is^{-1}T_c)$ for all integer values of i, and $r(is^{-1}T_c)=0$ elsewhere. The digital FIR version of the RRC filter was built with 129 taps at the receiver front end, and is preceded by a filter applying linear regression. The model can also be written in matrix format, where assuming that the linear generic system model $\boldsymbol{\chi} = \boldsymbol{H\theta} + \boldsymbol{\eta}$ is desired, a vectoral alteration to (2.8) yields the same sampled received signal. This alteration yields the matrix $\boldsymbol{H} = \boldsymbol{Q}$, where $\boldsymbol{Q}$ is the delay shifted Pulse shaping matrix defined in part by the RRC filter. The vector parameter $\boldsymbol{\theta}$ in this case is defined as $\boldsymbol{\theta} = \boldsymbol{FS}_1\boldsymbol{\xi}_1\boldsymbol{b}_1$ where the synchronous multiplexed adjacent channel signals are treated as noise with the discernable quality of being orthogonal to the desired user provided the channel is delay equalized. The discrete-time signal can be presented by the matrix equation

$$\boldsymbol{r} = \boldsymbol{QF}\left[\boldsymbol{S}_1\boldsymbol{\xi}_1\boldsymbol{b}_1 + \sum_{i=2}^{K}\boldsymbol{S}_i\boldsymbol{\xi}_i\boldsymbol{b}_i + \boldsymbol{P}_s\boldsymbol{\xi}_s\boldsymbol{p}\right] + \boldsymbol{\eta} \in \mathrm{C}^{\mathrm{N_s GN_b}} \tag{2.9}$$

where **r** is the received sample vector. $\boldsymbol{Q}$ is the delay path chip pulse convolution matrix where

$$\boldsymbol{Q} = \left[\boldsymbol{Q}^{(0)}, \boldsymbol{Q}^{(1)}, \ldots, \boldsymbol{Q}^{(GN_b)}\right] \in \mathrm{R}^{\mathrm{N_s GN_b} \times \mathrm{GLN_b}} \tag{2.10}$$

and

$$\boldsymbol{Q}^{(m)} = \left[\boldsymbol{q}^{(\tau_0)}, \boldsymbol{q}^{(\tau_1)}, \ldots, \boldsymbol{q}^{(\tau_L)}\right] \in \mathrm{R}^{\mathrm{N_s GN_b} \times \mathrm{L}} \tag{2.11}$$

with

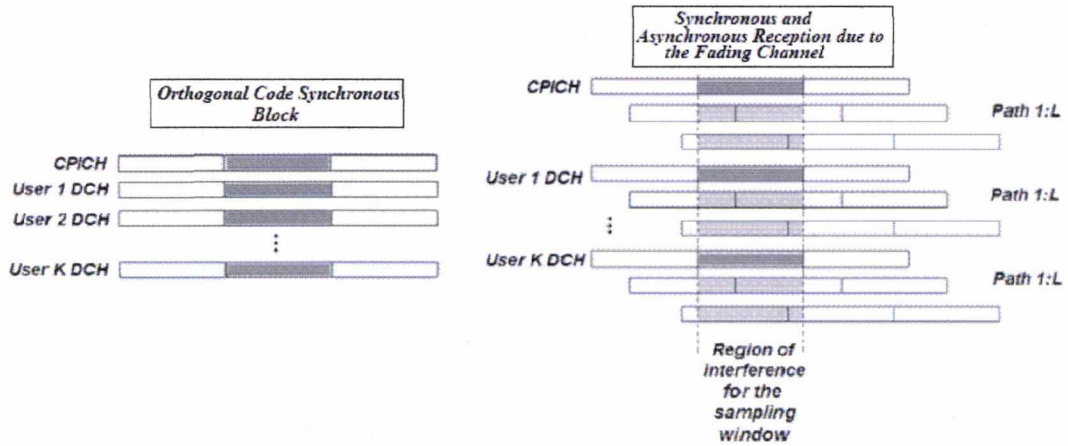

Fig 2.2. A pictorial representation of the effects of the fading channel dispersion, where code-orthogonal channels are delay spread rendering a region of interference within a sampling window used for symbol demodulation. The light grey shading is the region in this window where adjacent channel and multiple access interference can be problematic in detection.

$$q^{(\tau_d)} = \left[\boldsymbol{0}^{\mathrm{T}}_{mN_s + \tau_d}, \boldsymbol{P}^{\mathrm{T}}, \boldsymbol{0}^{\mathrm{T}}_{N_s(\mathrm{GN_b} - \mathrm{m}) + \Delta} \right]^{\mathrm{T}} \in \mathrm{R}^{\mathrm{N_s GN_b}} \tag{2.12}$$

the sample delay vector where $\mathbf{P} \in \mathrm{R}^{\mathrm{N_s}}$ are the filter coefficients, N_s the number of equally spaced discrete RRC samples, and $\Delta = \tau_{max} - \tau_d$ the path distance from the maximum. $\boldsymbol{F}$ is the matrix of channel coefficients with

$$\boldsymbol{F} = \mathrm{diag}\left[\boldsymbol{F}^{(0)}, \boldsymbol{F}^{(1)}, \ldots, \boldsymbol{F}^{(GN_b)} \right] \in \mathrm{C}^{\mathrm{GLN_b} \times \mathrm{GN_b}} \tag{2.13}$$

and the vector

$$\boldsymbol{F}^{(\mathrm{m})} = \left[\boldsymbol{\alpha}_0^{(m)}, \boldsymbol{\alpha}_1^{(m)}, \ldots, \boldsymbol{\alpha}_L^{(m)} \right]^{\mathrm{T}} \in \mathrm{C}^{\mathrm{L}} \tag{2.14}$$

containing channel coefficient samples at the m^{th} chip interval for paths $1{:}L$. $\boldsymbol{S}_i$ is the code signature matrix for the i^{th} user (the suffix 1 indicates the desired user of interest) with

$$\boldsymbol{S}_{\mathrm{i}} = \left[\boldsymbol{S}_i^{(0)}, \boldsymbol{S}_i^{(1)}, \ldots, \boldsymbol{S}_i^{(N_b - 1)} \right] \in \Xi^{\mathrm{GN_b} \times \mathrm{N_b}}. \tag{2.15}$$

$$\boldsymbol{S}_{\mathrm{i}}^{(\mathrm{n})} = \left[\boldsymbol{0}^{\mathrm{T}}_{G(n-1)}, \boldsymbol{s}^{\mathrm{T}}_{i,n}, \boldsymbol{0}^{\mathrm{T}}_{G(N_b - n)} \right]^{\mathrm{T}} \in \Xi^{\mathrm{GN_b}} \tag{2.16}$$

where the $\boldsymbol{s}_{i,n} \in \Xi^{\mathrm{G}}$ row vector represents the sampled signature sequence at discrete chip intervals for the i^{th} user with Ξ the chip alphabet.

$$\boldsymbol{\xi}_i = \mathrm{diag}\left[\sqrt{\varepsilon_i^{(0)}}, \sqrt{\varepsilon_i^{(1)}} \ldots, \sqrt{\varepsilon_i^{(N_b - 1)}} \right] \in \mathrm{R}^{\mathrm{N_b} \times \mathrm{N_b}} \tag{2.17}$$

is the block diagonal matrix of received bit amplitudes for the user i. $\boldsymbol{b}_i$ is the data vector for the

i^{th} user represented with quadrature modulation symbol, which is processed in fixed blocks given by

$$\boldsymbol{b}_{\mathrm{i}} = \left[\boldsymbol{b}_{\mathrm{i},(0)}^{\mathrm{T}}, \boldsymbol{b}_{i,(1)}^{\mathrm{T}}, \ldots \boldsymbol{b}_{i,(N_b-1)}^{\mathrm{T}}\right]^{\mathrm{T}} \in \Xi^{\mathrm{N_b}}. \tag{2.18}$$

The vector $\boldsymbol{P}_s \boldsymbol{\xi}_s \boldsymbol{p} \in \mathrm{C}^{\mathrm{N_s GN_b}}$ represents the modulated Pilot signal where $\boldsymbol{P}_s$ is the matrix of scrambling signatures, $\boldsymbol{\xi}_s$ the matrix of received Pilot signaling energies, and $\boldsymbol{p}$ the vector of pilot symbols with predefined sequence (that is known to the receiver to invoke channel + delay acquisition).

Note that this model is actually an altered definition normally reserved for equalizer derivation (where modelling variable spreading factors for the other users is not necessary to form the estimator- since the only interesting information for demodulation is contained in the radio and single user channel), with the equalizers studied in [Krauss2000] and [Heikkila2001] using the $\boldsymbol{\chi} = \boldsymbol{H\theta} + \boldsymbol{\eta}$ notation by denoting $\boldsymbol{H}$ as the channel convolution matrix and $\boldsymbol{\theta}$ the synchronous multiplex of the desired single (or multi) user channel and adjacent channels. The model, in this case, assumes rectangular pulses. The difficulty of this model for signal estimation involves the application of $\boldsymbol{H}$, where in this case the channel fading and delay parameters have to be known or estimated beforehand (where channel estimation is normally fairly noisy in fast fading channels).

The model does not account for other adjacent channels apart from the Pilot channel and the multiplexed multiuser channels. In other words, Multicode transmissions, Space Time Transmit Diversity (STTD) (employing two or more transmit antennas) and Macrodiversity are not considered for this thesis. Issues such as interleaving, channel coding- including convolutional [Viterbi1967, Viterbi1971] and turbo coding [Berrou1993], impair the simplicity of simulation where estimating the probability of error metrics for different SNR bounds is difficult to perform for low additive noise channels (due to low BER of coding techniques unless channel interference is very high). In real communication systems, rate matching [Prasad2000] is an important technique for ensuring the product between the generated baud rates and spreading chips renders the required chip rate. For different QOS and bandwidth in a variety of data/voice applications will yield the requirement of inserting tail bits or puncturing of the parity bits to ensure correct operation. This is a complexity and system related issue, where it is not particularly insightful to the performance of receivers particularly when simulations would ideally contain as few a number of variables as possible. It is improbable that a real communications system would contain uncoded transmissions- particularly 3rd and 4th generation

wireless mobile systems where QOS requirements are stringent. A reasonable assumption is that improvement to the uncoded error rate should correspondingly also yield improvements in the coded error rate (particularly when removing the asymptotic bound of interference) hence inclusion of a turbo decoder or hybrid turbo decoding with interference cancellation/equalization [Koetter2004, Yeap2002] is not considered.

2.1.2 MODELLING MULTIPATH FADING CHANNELS

Most cellular wireless systems, like the UMTS WCDMA downlink, operate in urban environments where direct line-of-sight between transmitter and receiver is rarely observed. It is discernible [Lee1985] that in such environments consisting of man made and natural obstacles, multiple signal scattering and reflection cause a random distribution of signals arriving via different paths (at different times, frequencies and phases) thus creating a fading profile [Proakis1998].

2.1.2.1 MULTIPATH GENERATION WITH RANDOM SCATTERING ASSUMPTION

This section briefly introduces the statistical models for generating a Rayleigh distributed fading channel. Models that are commonly applied to multipath for cellular communications with no line of sight and small coverage areas involve Jakes, Clark's or Aulin's approach [Jakes1993, Clarke1968, Aulin1979]. All approaches are rather similar in principle. This thesis considers the ideas from Clark's model mainly due to its simplicity of implementation. The models are generic and do not apply to specific fading channels where empirical approaches based on measured statistics would be more useful in such a scenario. The assumptions for the generation of the multipath signals are given herewith:

i) Each multipath component is generated by an individual scattering source. Each path incident to the scattering source has a uniformly and independently distributed phase and attenuation factor, G.

ii) Each scatter source generates multiple spectral copies of the received incident signal with different phase and amplitude variations. Each scattered ray is modeled as a wave bundle with minimal delay times between each wave component (when combined, the wave bundle will have spectrally a flat fading multipath response). Time delays (contributing to a different time of arrival at the mobile antenna and

hence delay spread) of each retransmitted signals from the scatterers are assumed random.

iii) The multipath phases are uniformly distributed and the envelope induced by multipath treated as being Rayleigh distributed.

iv) The angular spread is uniform and random.

v) The scatterers are electrically far from the sensor, thus over a relatively short duration of motion the angular spread is stationary.

The Multiple scattering model (Fig 2.3) based on the assumptions can be shown to produce the necessary statistics for creation of a frequency selective Rayleigh fading channel. In wireless transmission scenarios where the receiver undergoes motion relative to the transmitter with no line of sight component, Rayleigh fading is often a fairly good approximation of the real channel conditions. A Rayleigh fading channel for pedestrian speed refers to a multiplicative distortion, $h(t)$ of the original transmitted signal (with $h(t)$ being a constant in this situation). This channel waveform, $h(t) = \sum_{i=0}^{N} A_i \cdot e^{-j2\pi cos(\theta_i)}$ is modelled as wide-sense stationary complex Gaussian process with zero mean (where A is a complex source magnitude and θ the angle of incidence), which, according to [Blaunstein2002] makes marginal distributions on the phase and attenuation/gain factor as being Uniform and Rayleigh (see Appendix A for proof).

The problem of generating one, or in channels with frequency selectivity, more than one random complex Gaussian process with the required Doppler PSD has been modeled as a combination of an approach first mentioned by Bello [Bello1963], and expatiated upon by Jakes [Jakes1993] via introducing a multiplicative time varying waveform (sum of complex sinusoids) approximating the frequency domain convolution with a filter defined by (2.25) as suggested in [Blaunstein2002].

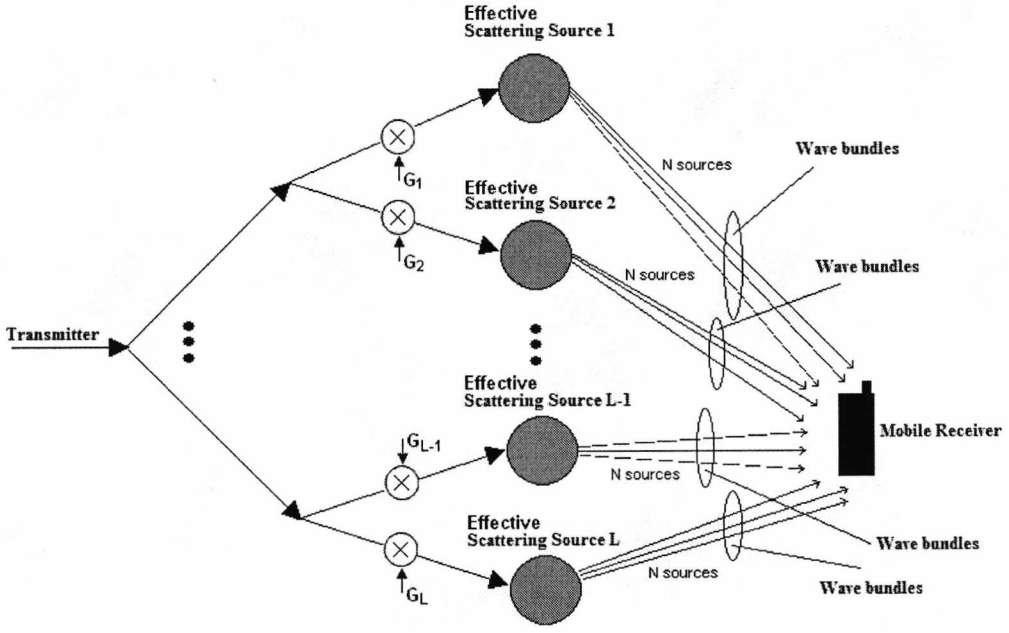

Fig. 2.3. The Physical Scattering model used to define the fading channel

The autocorrelation properties of the random process $h(t)$ in a non-stationary flat fading environment (with moving vehicle or moving scatterers) is governed by the Doppler frequency f_d and is given by

$$\begin{aligned} R(\tau) &= E\left\{h(t)\cdot h^*(t-\tau)\right\} \\ &= E\left\{|h(t)|^2\right\}\cdot \Im_0(2\pi f_d \tau) \end{aligned} \tag{2.19}$$

which gives rise to the well-known, non-rational power spectral density (PSD) of the channel process

$$P_{hh}(f) = \begin{cases} \dfrac{1}{\pi f_d}\dfrac{1}{\sqrt{1-\left(\dfrac{f}{f_d}\right)^2}}, & |f| \le f_d \\ 0, & otherwise \end{cases} \tag{2.20}$$

where $\Im_0(\bullet)$ is a zero order Bessel function of the first kind and $f_d = \dfrac{v}{v_{light}} f_c$ the maximum Doppler frequency with f_c the carrier frequency, v the speed of the vehicle and v_{light} the velocity of light. The model generating $h(t)$ for a moving vehicle can be defined by [Steele1992]

$$h(t) = U(t)\sum_{i=0}^{N} A_i \cdot exp\left\{-j2\pi\left(\frac{vf_c}{v_{light}}\right)cos(\theta_i)t\right\} \tag{2.21}$$

Note that the thesis assumes here forth that the channel is slowly fading (as would be expected in a pedestrian channel) when $f_d T_s << 1$ and fast fading when $f_d T_s >> 1$ where the coherence time $T_{ch} \propto (f_d)^{-1}$. General real depictions would fall somewhere in-between the two extreme cases- i.e. a pedestrian channel with voice/low data rate application up to a fairly fast vehicular channel (where the channel fading will be fast for voice applications and fairly slow for data applications).

2.1.2.2 Time Invariant FIR Filter Implementation for Modelling Frequency Selective Rayleigh Fading

The approach by Bello [Bello1963] renders a rather simplistic, but nevertheless effective model for a channel exhibiting frequency selectivity in some situations. The time-invariant channel coefficients in the channel coefficient matrix are assumed to be independent complex Gaussian random processes with zero means and variances normalized so that the channel coefficients are also assumed to be stationary over the observation window. This together with the independence assumption is equivalent to the wide-sense stationary uncorrelated scattering (WSSUS) model, where if multiple delays are introduced, the model can be simplified to a linear FIR equivalent filter to represent convolution with channels having a delay spread (Fig. 2.4). A discrete time mathematical expression of the SIMO channel is given herewith

$$h_M(t) = \sum_{i=1}^{X} \sum_{u=0}^{N} G_i \cdot \left[A_{i,u} \cdot exp\left\{ -j\left(\frac{2\pi}{\lambda_0}\right) D_M sin(\theta_{i,u}) \right\} \right] \cdot exp\left\{ -j2\pi \left(\frac{vf_c}{v_{light}}\right) cos[(\theta_{i,u})t] \right\} \cdot \partial(t-\tau_i) \quad (2.22)$$

yields the coefficients of the equivalent channel filter (X =number of delay sources, N =number of scatterers, λ_0 the carrier wevelength, and D_M the metric distance of the Mth antenna from the zeroth antenna reference element where M is any integer ≥ 0). Denote the time-variant impulse response by $h(\tau, t)$ yielding the response of the channel (at time t) to an impulse at time $t-\tau$. If $x(t)$ represents the transmitted signal through mobile radio channel, the received signal, $y(t)$, can be expressed

$$y(t) = \int_{-\infty}^{\infty} \boldsymbol{h}(\tau, t)\, \boldsymbol{x}(t-\tau)\, d\tau \quad (2.23)$$

If the time-variation of the channel is slow, it is often treated as quasi-stationary, i.e. a linear system whose parameters vary with time but are constant for a finite period. If the maximum Dopper shift ν_{max} is much less than the maximum delay in the channel, τ_{max}, then the channel is separable, so that the delay parameter τ and the time t can be treated separately. This is of

course an extremely useful property that can be exploited by classical delay and channel estimators [Steele1992]. If the signals on different paths are uncorrelated with complex Gaussian amplitudes including the channel phase (that are time variant), i.e. the Gaussian wide-sense stationary uncorrelated scattering model, the impulse response can be represented by the sum of impulses delayed with respect to τ_i, (the path delay). The channel can be sampled at the chip rate (or fractions of it), yielding the tapped delay-line-model where delayed signals on the different paths are lumped into delays of multiples of the fractional chip period. The channel covariance matrix $\Sigma_F = E\{FF^H\}$ for the downlink is given as

$$\Sigma_F = diag\left[A^{(0)}, A^{(1)}, \ldots, A^{(GN_b)}\right] \in \mathrm{R}^{\mathrm{GLN_b} \times \mathrm{GLN_b}} \tag{2.24}$$

with $A^{(m)} = diag[\sigma_0^2, \sigma_1^2, \ldots, \sigma_L^2] \in \mathrm{R}^{\mathrm{L} \times \mathrm{L}}$.

The assumption of independent channel coefficients is idealistic for link performance in some environments with multiple input, multiple output (MIMO) sensors [Varanisi1993, Klein1993, Vaughan2003] although it is reasonable for the scope of this thesis involved with the development and evaluation of adaptive receivers. The RMS delay spread and average power of the multiple scatter paths in the model reflect the properties of the propagation channel, hence several channel models have been proposed for different environments. The channel profiles used in the thesis are based on International Telecommunication Union (ITU) models [ITU1997] that are commonly accepted and used for reference purposes – see Appendix B for more information.

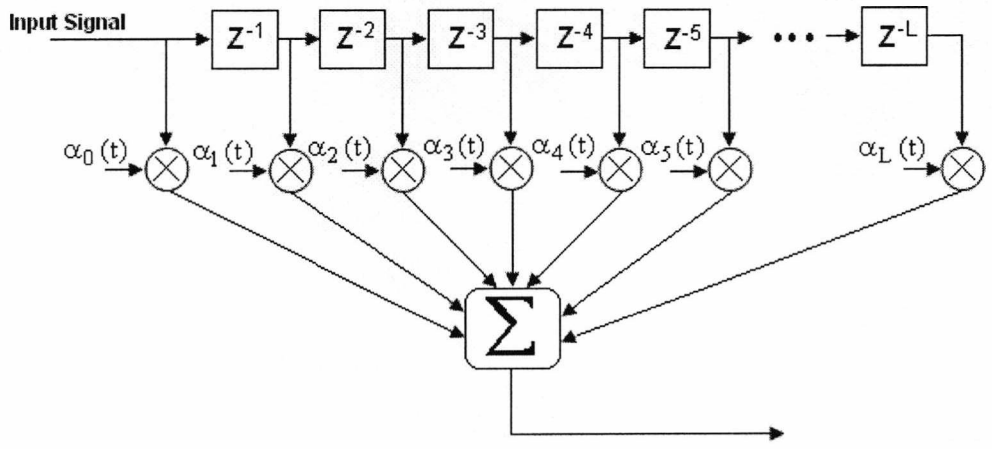

Fig. 2.4 A Generic FIR Filter Implementation of the fading channel.

2.2 Receiver Techniques for Direct Sequence CDMA: An Overview

Spread Spectrum [Viterbi1979] has been realized as a communication and multiple access technique for digital radio since the 1970's. Spread spectrum differs from traditional binary signalling techniques employed in early wireless transmission and fixed terrestrial networks in that information-bearing digital signals are coded (and spread) with random signature sequences. It has long been recognized that spread spectrum enables markedly superior reception for a modulated digital signal in noise over conventional amplitude and phase shift keyed modulation formats without coding [Pickholtz1982]. Indeed, for digital signals coded and spread with pseudo-noise (PN) random sequences over a large bandwidth, it is possible to obtain coherent reception with low probability of error even if the received power is below the noise floor [Sholtz1977]. Furthermore, as a multiple access technique, multiple users employing orthogonal code sequences can be demodulated in the presence of noise with simple correlation receivers yielding no cross talk provided the propagation medium maintains perfect orthogonality between users. In dispersive channels or asynchronous transmission, cross talk (often termed in the literature as multiple access interference) is a degrading effect caused by non-orthogonality between multiple user codes. Hence, the correlation receiver decorrelates not only the desired user waveform but also a random noise signal with moments relative to the statistical distribution of powers for the multi-user signals [Flikkema1997].

The early 1990's marked a new epoch in the evolution from the inaugural first generation analogue mobile telecommunication system to the second-generation digital revolution. These systems had the original aim of providing only voice traffic and simple text based services. However the immense, perhaps surprising success of GSM directed a demand and evolution to provide more advanced multimedia based applications; hence leading to proposals for the General Packet Radio System (GPRS) incorporating Enhanced Data Rates for Global Evolution (EDGE) and eventually the third generation concept [Samukic1998]. While the European second-generation digital mobile systems used the then more traditional time and frequency division multiple access (TDMA and FDMA), the United States system (IS-95) incorporated code division multiple access (CDMA) using the spread spectrum philosophy [Pickholtz1991]. Code division multiple access is a multiplexing technique where users simultaneously accessing the network (either synchronously or asynchronously) are modulated with different preassigned signature sequences whilst sharing the same time and frequency space [Kohno1995]. This technique has been noted as being more robust than TDMA and FDMA

when negating multipath channel frequency selectivity and environments with impulse noise, hence yielding significant capacity gains [Gilhousen1991, Jung1993]. The CDMA philosophy as the primary multiple access technique for third generation mobile systems and beyond is generically based on the spread-spectrum proposals reported in [Fukasawa1996, Milstein2000]. CDMA is certainly not limited to single carrier systems, where proposals for 3rd generation systems and beyond will no doubt consider multi-carrier CDMA, OFDM and hybrid-technologies of it to deliver high data rates and broadband services to every user in highly loaded, smaller micro/pico cells [Adachi1998]. The work conducted in this thesis concentrates on the 3rd Generation wireless interface, where it would be useful to expatiate the CDMA concept and current system bottlenecks. The aims for 3rd generation (and beyond) mobile telecommunications systems are to integrate a wide range of services to augment wireless voice telephony [Hara1997], such as the provision of multimedia based applications and broadband wireless Internet, including real time video conferencing, entertainment etc [Konhauser1998]. For the network to support a wide range of services with variable data rates (from low 12.2Kbps voice to 384Kbps connections on a single 3.84Mcps channel) presents a plethora of technical issues at the system wireless interface that require consideration from the mobile system operators for the proposition of offering high system capacity with guaranteed quality of service. This is a somewhat demanding requirement to fulfil when some consideration is given to an unreliable and difficult to estimate radio channel which often yields a severe impediment to high quality, high bandwidth radio communication [Prasad2000]. The nature and type of multipath fading propagation channel presented to wireless operators is unfeasible to define in a deterministic sense (and often even in a statistical sense accurately), although its effects on the radio signal are quite profound [Pursley1977, Turin1984, Polydoros1994]. The main issue for the quality of the RF signal is the multipath fading which induces a random fading envelope to the signal, frequency and time dispersion creating inter-channel interference, and in synchronous CDMA communication, causing multiple access interference (MAI). Indeed, it is a challenging science to fully develop and implement procedures to overcome the effect of multipath fading since coherent and synchronized diversity receivers are difficult to optimize [Bello1963, Verdu1986]. Procedures such as optimum diversity receivers [Lupas1989, Honig1995, Madhow1998], beamforming [Godara1997], pre-channel-distortion [Derryberry2002, Simeone2004] (for smaller Micro and Pico-cells), macro-diversity [Kim2002] and adaptive power control [Hanly1999] are currently proposed for use in 3rd generation mobile systems to overcome the problems incurred by transmission through a radio channel. These methods are presently under heavy research and development.

The Mobile system operators collaborating under the third generation partnership project (3GPP) defined a set of standards to which the 3rd generation system must adhere to [Richardson2000]. The system is aptly named the Universal Mobile Telecommunications System (UMTS) and the radio access network defined as the Universal Terrestrial Radio Access Network (UTRAN) [Bauer2003]. The bulk of standards defined for the UTRAN involve not only the wireless terrestrial interface, but also the concepts and mechanisms for the interface of radio over fiber backbone networks to macro-micro cellular radio planning which will not be discussed in this thesis. The wireless terrestrial interface defined for the UMTS is deemed as Wideband Code Division Multiple Access (WCDMA) [Dahlman1998A, Dahlman1998B]. This has the capability of supporting services with different data rates and provides good protection from inter-channel and inter-cell interference when overlaid with long or short scrambling codes. The integration of Macro-diversity within the WCDMA interface allows connectivity with one or more transmitters/receivers in a cellular structure composing of a Macro-cell and several underlying smaller Micro-cells in a coverage area. This allows for temporal, spatial and spatial-temporal type receivers [Winters1984, Lamarca1997, Welburn2004] that can either optimize or select channels that are of higher quality in a multipath spread (this technique is one such method to combat shadowing). This is one of the key newer developments of the WCDMA interface where uplink channels can be combined using rake and/or antenna arrays with radio-over fiber networks, and downlink channels combined using a rake receiver [Mudulodu2004].

Since the mid-part of the twentieth century, wireless mobile radio communications in fading channels have been studied intensively. The bulk of research over the past 40 years have considered optimum single-user receivers [Poor1998], Optimum [Verdu1986, Schneider1979] and Sub-optimum multiuser receivers [Madhow1998], diversity techniques for transmission and reception [Lehnert1987, Lenardi2001], advanced signal detection and estimation schemes [Varanasi1991, Wang1999], interference rejection [Vanghi1996], adaptive signal processing methodology [Rapajic1994], Modulation [Steele1992], coding techniques [Hanzo2002], and numerous other technical aspects that are well documented in existing literature (see [Kay1993A] for a detailed overview of general statistical estimation covering the various information theory and physical layer features). CDMA has emerged as a leading technology in the field of wireless mobile communication where information bottlenecks involving detection and high quality of service for interference limited channels have at least been largely overcome with the design of more intelligent receivers. Notable contributions in this field are given by Verdu [Verdu1998], Schneider [Schneider1979] and Zhenhua et al [Zhenhua1990] whom

developed interference resistant detectors capable of delivering system capacities and error performances approaching the theoretical upper bounds of additive noise only channels.

The traditional detector for synchronous CDMA channels consists of a bank of chip-matched filters (for non-coherent multiuser detection) or despreading devices (consisting of an integrate-dump detector) for coherent detection[4] [Simon1994]. The classic diversity receiver for demodulation in WCDMA is the single user matched filter (commonly known as the rake receiver) originally proposed by Green for FM based systems in 1958 with his classic paper [Green1958]. This receiver was shown to split the various components of a multipath delay spread provided that the multiple propagation paths did not arrive and combine at an antenna with delays so closely spaced such that the receiver equipment had insufficient resolution to detect the paths using correlation techniques (for wideband systems, this case would make the channel frequency-non-selective). Each multipath component that could be resolved was assigned a 'finger' (in future literature with equally spaced multipath delays, the finger management system would be considered in a DSP sense as a tap-delay-line). Each 'finger' would contain detection filters (typically with low pass response) and a weighting coefficient assigned for maximum-ratio diversity combining (or Equal Gain combining which appears to be the most common implementation). The rake receiver was realized as an equalizer or optimum matched filter for Spread Spectrum systems provided that only a single user was occupying the system bandwidth [Turin1980]. Further research in the 1980's [Kohno1983] concluded that the rake receiver in direct-sequence-spread-spectrum-multiple-access channels was not optimum for single and multi-user detection due to inherent problem of inter-symbol-interference (ISI) for short spreading codes (or inter-path interference for long spreading codes), and multiple-access interference (MAI). Longer spreading codes reduce ISI in multipath channels at a cost to the system bandwidth requirements, but do not counteract MAI entirely in the asymptotic limits.

Both ISI and MAI (for synchronous multiplexing and transmission) occur due to frequency selective wireless channels, with the severity of these degrading effects depending on the Near-Far Ratio (NFR), the number of users synchronously (or asynchronously) accessing the channel, the level of fading, the Doppler and Delay Spread [Glisic1997]. The effects and type of errors introduced by multipath propagation on spread-spectrum code and carrier tracking, rake receivers, and wireless engineering in general are well documented in [Chan1994, Glance1993, Stein1987]. A simple optimization scheme for the rake receiver in multiple-access networks was denoted the General Rake Receiver (Grake) and developed by Bottomly in 1993 [Bottomly1993]. This expatiates upon Green's initial Rake concept by introducing a fractionally

[4] Single User Detection requires only one despreading device per diversity channel.

spaced tap delay line with diversity combining coefficients matched to the multipath channel. It was found in this case, that provided the channel spread was small, the number of taps required do not have to be overly large. Bottomley concluded that the rake receiver was sub-optimal in a CDMA downlink due to intercell interference being present on the desired user channel. Hence using the assumption that the intracell interference is colored Gaussian noise, the GRAKE was derived to maximize the SINR. The rake-finger weights were found to be precisely the solution to the MMSE equalizer. Indeed, this receiver is in actual fact an equalizer [Frank2002]. It is well known that filtering applying inverse transformation generally yields an infinite impulse response, where truncation of the number of filter taps usually creates residue ISI [Proakis2001]. However, despite this fact, the performance of the Grake and Equalizers are usually very good for synchronous point-multi-point communications utilizing DS-CDMA with orthogonal coding [Lenardi2000].

Alternative and more advanced detection schemes are designed to combat some of the properties of the aforementioned terminology of the wireless access channel (to bring the channel back to it's ideal state, that being an Additive Gaussian Noise Channel). Many detection algorithms can actually be shown to loosely relate to the conventional rake receiver (i.e. the receiver architecture can be based on the rake principle but have additional linear FIR filters or filter transformations to improve the detection). In many instances, the authors have noted the similarity and expatiated upon the basic rake detector [Latva-Aho2000, Lenardi2000, Hooli2001]. Two types of receivers are often mentioned in the literature: Centralized and Decentralized receivers. Centralized receivers would be more commonly expected on the reverse link and as such, knowledge of the multiuser signatures would be mandatory for demodulation (forming so called multiuser receivers). Decentralized is an applied term usually noted for single user detection- and as such, is indicated for a receiver in the forward link. Algorithms that drive single and multi-user detection are unsurprisingly different- since many techniques such as Decorrelation [Lupas1990] and interference cancellation [Patel1994] have limited practicality in single user detection. Furthermore, the IS-95 and UMTS forward link generally utilize long scrambling sequences that yield many blind/semi-blind and decision directed single user detection algorithms [Honig1995, Latva-Aho2000] practically useless in such a scenario.

Relevant topics in the area of detection for CDMA communications are briefly reviewed hereforth. Comprehensive surveys are given in [Duel-Hallen1995, Moshavi1996, Verdu1998, Wang2004] for multiuser CDMA receivers. Single user detection in multiple access channels have received comparatively little interest for numerous reasons that mainly relate to the fact that

synchronous uplink transmission is impractical (due to roaming and multipath making synchronous multiplexing and timing exceedingly difficult to achieve with linear prediction and/or GPS) and that every user occupying the Basestation coverage sector transmits information via separate multipath channels. This incurs a cost of making uplink reception a major factor in ensuring that the network capacity requirements are maintained. Of course, this does not mean that downlink reception and QOS requirements are treated as being trivial, where work carried out in [Ghauri1998] and [Hooli1999A] show that computationally inexpensive methods can be invoked in generating fairly robust receivers with/without channel coding (and power control) that greatly increase the performance of the downlink. Statistical optimization techniques that may be applied for digital communications (uplink or downlink depending on assumptions and system parameters) are described in great detail in [Kay1993A]. The more commonly encountered algorithms, that being Maximum Likelihood (ML), Linear Minimum Mean Square Error (LMMSE) and Minimum Variance Unbiased (MVU) have appeared in the literature for interference negation [Verdu1986, Honig1994, Tsatsanis1998] and diversity reception [Balaban1992]. MAI is often observed as being coloured or white Gaussian noise, where, on the provision that a sufficient observation interval is applied, the statistics can be determined and optimization applied which yields significant performance enhancement [Verdu1998]. Detectors for CDMA can be further classified as being either direct or indirect interference cancelling (IC) applying linear transformation, the Viterbi algorithm (or other dynamic programming algorithms for optimum receivers), and/or linear FIR structures. In addition, detection can be considered in two cases: Optimum and Sub-optimum. It is often quoted that Maximum Likelihood (ML) detection is optimum provided that the likelihood estimator exists. Generally speaking, sub-optimum detection is of most interest due to the computational complexity of Maximum A Posteriori (MAP) or ML estimation- particularly for real-time communication [Mitra1995A, Verdu1998]. Research to simplify ML estimation[5] is a hot topic- since ML complexity [Verdu1989, Forney1972, Forney1973, Schlegel1997] is a bottleneck for statistical signal processing (particularly for signal processing applications dealing with channels requiring infinite memory).

The optimal receiver for single-user communications in multipath channels causing inter-symbol interference (ISI), is the maximum likelihood sequence detector (MLSD) [Forney1972, Proakis1973] requiring that the channel is known. The general approach to MLSD for synchronous and asynchronous channels usually considers maximizing the log-likelihood

[5] Which is generally conducted with dynamic programming algorithms (such as the Viterbi algorithm with the corresponding trellis to compute the minimum distance metrics).

function based on a reception model (as in Chapter 2) where the channel is estimated, and the matched filter outputs decoupled into a detector that obtains the received noiseless signal and correlates the received signal with this estimate [Van Trees1971, Proakis2001]. Due to the more realistic asynchronous transmission in CDMA channels, tree search techniques or dynamic programming is considered since an exhaustive search through all possible symbol sequences (over the entire transmission time interval) is not practical. Verdu derived the optimal MLSD receiver for multi user CDMA communications [Verdu1986] where, due to a high complexity that grows exponentially with the number of users, several suboptimal receivers have been proposed [Lupas1989, Zhenhua1990, Honig1994]. The simplest suboptimal single-user receiver for CDMA systems is the aforementioned RAKE receiver, which consists of a bank of correlators to receive several multipath components [Green1958]. Coherent or non-coherent RAKE receiver structures can be used depending on the bit error rate requirements and signalling formats. As the radio frequency for wireless mobile increased beyond 2GHz for third generation systems, recent interest has sparked the possibility of applying spatio-temporal diversity for the forward link, and has led to some interesting developments and concepts noted in [Naguid1994, Dahlhaus1997]. These algorithms are often quoted in the literature as being two-dimensional rake receivers (also commonly known as interference suppressing adaptive antenna arrays). The practicality of advanced array detection and/or MIMO processing is limited on dimensionally small handsets, where closely spaced antennas compromise diversity gain [Vaughan2003]. Furthermore, large linear arrays are not realistic hence the receiver will generally be limited to two or three spatial diversity channels at most.

Other sub-optimum techniques for multiple-access fading channels include linear multi user suppression receivers [Zhenhua1990, Honig1994]. The simplest linear multi user receiver is the zero-forcing equalizer applying a simple linear transformation after chip-matched filtering-commonly denoted as being the Decorrelator [Verdu1988, Lupas1989]. This receiver has a complexity that grows linearly with the number of users to be demodulated, hence rendering a valid trade-off in performance compared with the MLSD receiver. These have been studied for AWGN and multipath fading channels in [Zhenhua1990, Varanasi1993, Klein1993, Zvonar1994, Zvonar1995, Madhow1998]. Finite length windowed Decorrelation (with feasible application for MMSE detection) was studied in [Verdu1986, Lupas1990, Duel-Hallen1993, Wijayasuriya1996, Tsatsanis1996, Bravo1997, Junnti1997]. An alternative to the Decorrelator yielding superior performance with minimal complexity gain is the Linear Minimum Mean Squared Error (LMMSE) Equalizer [Honig1994]. The LMMSE receiver is often termed the Best Linear Unbiased Estimator for multi user, multipath channels in the presence of Gaussian

noise since the LMMSE estimator minimizes the noise variance and hence the signal-to-interference-plus-noise ratio (SINR) [Whalen1971]. LMMSE receivers have been proposed for AWGN channels and multipath fading SIMO, MISO and MIMO channels in [Lupas1990, Rapajic1995, Jung1995, Bernstein1996, Klein1996, Poor1997, Latva-Aho1998, Latva-Aho2000]. The LMMSE receiver is interesting due to the existence of simplified adaptive versions being applicable as a blind or decision directed single-user receiver (requiring training symbols). Adaptive LMMSE receivers for AWGN channels have been studied in [Roy1994, Miller1995, Mitra1995B, Miller1996, Opperman1997, Latva-Aho1997, Barbosa1998]. A constrained form of the LMMSE estimator was presented in [Kim2000, Hong2004] and improves the multiuser efficiency over the classical LMMSE receiver (the authors denote this particular receiver as the CMMSE Rake receiver). The mean squared error and constrained minimum output energy (MOE) criteria have been studied extensively for multi user CDMA detection [Honig1995], where one-shot and blind adaptation utilizing the MOE constraint have been considered for AWGN and Fading channels in [Tsatsanis1997, Shodorf1997, Wang1998, Iltis1998, Fan2000]. The MOE criterion was originally developed in the 1960's by Capon [Capon1969] as a beamforming technique for arrays- where the beamformer weights are separated into fixed and adaptive parts. Part of this exciting development also yielded the Minimum Variance algorithm for Blind beamforming, which has been applied for centralized DS-CDMA receivers in [Tsatsanis1998, Xu2001] utilizing both one-shot parametric optimization and recursive adaptation for sequential detection.

Another concept generating great interest is the idea of matched filtering for forward and reverse links to suppress interference created by a multiple propagation channel. One such matched filter is the GRAKE receiver exploiting the colouration of interference- and as such could be treated as an interference-whitening detector. Related to the interference-whitening criterion is the general equalizer (often called the zero forcing equalizer). Equalization is a pervasive technique for building channel-matched filters, which can be broken down into two subsets- Linear Equalization [Barhumi2003] and Decision Feedback Equalization [Al-Dahir1995]. Equalization has the useful property of restoring multi-user orthogonality, where interference cancellation can be achieved with a traditional CDMA correlation type receiver. Klein [Klein1993, Klein1996] studied Linear detectors in depth and derived sub-optimal symbol-rate equalization techniques for CDMA systems. Of particular note, she concluded that the Decision Feedback Equalizer, Zero Forcing Equalizer and MMSE equalizer could all be considered extensions to the Whitening Matched Filter hypothesis and hence are related to each other via linear transformation. Her solutions required computationally intensive algorithms

where the receiver is centralized (in that knowledge of the all Multi-user spreading codes and the Channel is available). The significance of her work was extended to the Single-User case in [Klein1997], which developed blind algorithms (requiring no training symbols) for suppressing Multiple-Access Interference and Inter-Symbol Interference with equalization methodology. Ghauri [Ghauri1998, Slock2000] modelled the downlink where the signal was spread by relatively short orthogonal signatures and scrambled with long overlaying sequences. The orthogonality of the synchronous multiple access channel was destroyed by a frequency selective multipath channel. His contribution involved the design of zero forcing and MMSE equalizers that were multi-channel (due to oversampling) and retained the goal of restoring orthogonality of users via removing the MAI by despreading (or chip-matched filtering). Werner, [Werner1999, Werner2000] implemented chip spaced equalizers rather than fractionally spaced, where these equalizers were adaptive rather than deterministic based on matrix optimization. Frank, [Frank1998] published a paper on equalization for a generic CDMA forward link and suggested descrambling and despreading the equalized output prior to generating an error signal. This equalizer was implemented using tentative bit decisions, hence was updated at symbol rate rather than chip-rate. Madhow [Frank2002] derived a scrambling code dependent equalizer and obtained an equivalent MMSE detector. It was found that the resultant equalizer performance was identical for random and orthogonal sequences overlayed with scrambling codes. This equalizer was found to suppress non-zero mean coloured noise and the receiver significantly outperformed the rake detector. The GRAKE algorithm was also shown to yield the solution to the MMSE equalizer. Krauss and Zoltowski et al [Zoltowski1999, Chowdhury2000, Krauss2000A, Krauss2002, Chowdhury2002] similarly researched multi-channel equalizers for long code CDMA systems and compared Zero forcing to MMSE and Rake solutions. Their main assumptions were that the channel was known, as was the interference signatures of other users. Chip-level, Symbol-level, and subspace-constrained symbol-level MMSE equalizers were derived in [Krauss2000B, Zoltowski2000]. The chip-level MMSE equalizer minimizes the quadratic form of the cost function between the desired (the tentative bit decision multiplied by the signature sequence) and equalized signal, while the symbol-level MMSE equalizer minimizes the MSE between the bit estimate and tentative bit decision. Kari Hooli [Hooli1999A, Hooli2002] made essentially the same assumptions, where the LMMSE chip equalizer formulated in his research contributions used the common pilot channel to restore orthogonality amongst users for interference cancellation. Hooli also stated that the problem of LMMSE interference cancelling type receivers [Hooli1999B] was that the long-overlay sequences used in most 3GPP standards required either long training windows (and hence high

complexity), or cyclostationary in the scrambling code. It was concluded that the LMMSE adaptive interference-cancelling receivers required shorter scrambling code. His work is essentially a logical extension on prior work from Latva Aho and Juntti in Pre and Post Combining LMMSE receivers [Latva-Aho2000]. A blind equalizer, [Li1999], was applied for short and long codes when the chip-rate signal was equalized prior to linear projection (where the scrambling code used at the transmitter rotated the code-space from symbol to symbol, where the codes remained orthogonal due to the unitary operation of the scrambling signatures). The blind equalizer essentially projects the received signal energy into the orthogonal code space in the direction of the desired user's code such that chip matched filtering can remove MAI. Slock and Ghauri show that the blind equalizer maximizes SINR in the case of random scrambling codes [Slock2000]. A similar baud-rate, pilot-trained Recursive Least Squares (RLS) equalizer developed by Frank and Visotsky [Frank2002] showed that fractionally spaced equalization had superior performance to chip-spaced equalization [Petre2000]. A semi-blind approach is taken in [Petre2001], where a filter is generated such that when the equalized signal is projected onto the subspace orthogonal to the multi-user codes, the projection is close to the pilot signal in a least squares sense. Block processing and adaptive algorithms are derived that rely on a model with at least two received channels. Further contributions considering the WCDMA/DS-CDMA downlink and channel decorrelation for Pilot trained chip rate, Blind, Blind MOE, and subspace constrained adaptive equalizers are given here-with [Hooli2001, Hooli2002, Komulainen2000, Heikkila1999, Komulainen2001, Heikkila2001, Mailaender2002, Mudulodu2000, Darwood2001, Ghosh2001].

Decision feedback equalizer (DFE) methods for single and multi user detection have been proposed since the late 1970's [Belfiore1979, Duel-Hallen1995, Varanasi1999], where in the case of detection in time dispersive CDMA channels, the algorithms generally equalize and decode the received signal to provide multiuser bit estimates that are respread and input into a delayed chip-level DFE for re-processing [Choi2004]. A DFE that exploits the finite alphabet of the desired user's transmitted symbols is proposed in [Yang2002] for the DS-CDMA downlink, where a single feed-forward filter is used in conjunction with several feedback filters. In the case of BPSK, only two possible values of the current antipodal symbol exist (and are either $+1$ or -1). There are two feedback paths. For one of these paths, the input is the code chips of the current symbol. For the other path, the input is the sign-inverted code chips of the current symbol. The outputs of these two paths are despread separately. A minimum distance decoder is then used that decides in favor of $+1$ if the despread signal corresponding to the first path is closer to $+1$ than the output of the despread second path is to -1. This method is quite complex

since the number of feedback paths is MN, with M is the number of symbols in the alphabet and N the number of desired bit-streams. However the DFE was found to offer superior performance over the conventional MMSE receiver.

Finally, it will be of interest to briefly mention Interference Cancelling (IC) receivers. The methodology of IC receivers is to estimate the multiple-access and multipath induced interference and then subtracts the interference estimate from the received signal. There are several principles of estimating the interference leading to different IC techniques. The interference can be cancelled simultaneously from all users leading to parallel interference cancellation (PIC) [Divsalar1998, Buehrer1996], or on a user-by-user basis leading to successive (or serial) interference cancellation (SIC) [Kohno1983, Patel1994]. The interference cancellation utilizing tentative data decisions is called hard decision (HD) interference cancellation and requires explicit channel estimation. The soft decision (SD) interference cancellation utilizes only the composite signal of the data and the channel coefficient hence no explicit channel estimation is needed. Usually the interference is estimated iteratively in several receiver stages (utilizing linear/non-linear decision functions) leading to multistage receiver algorithms [Varanasi1990, Fawer1995]. These receivers are generally not suitable for single user detection- mainly due to the modulating waveforms for adjacent users being considered an unknown quality that must be estimated.

2.3 Spatial Diversity Reception in the WCDMA Downlink Applying Two Sensors

The relatively large bandwidth offered by 3G wireless networks employing the WCDMA interface has lead to several proposals invoking both transmitter and receiver diversity application to combat the impeding qualities of multipath fading. The UMTS in Europe and Japan has moved toward the Multiple-Input Multiple Output (MIMO) ideals by providing diversity for the downlink utilizing multiple transmitter antennas (and spatial coding schemes such as STTD). However, combating a flat fading channel with spatial coding and multiple transmitter-receiver antennas generates a somewhat milder constraint on performance than that of a frequency selective fading channel, where the relatively short spreading codes yield traditional matched filters incapable of fully interference resistant detection. This effect is less prevalent for narrow-band systems where diversity employing multiple transmitter-receiver

antennas is near optimum in terms of performance. In frequency selective environments conventional CDMA matched filters do not alleviate the effects of fading and inter-code, inter-symbol interference entirely and hence an alternative detection/estimation hypothesis must ensue to improve the quality of the channels. One approach for improving the performance of downlink receivers involves an estimation hypothesis using two or more antennas to implement diversity and/or suppress interference. This section presents the results of diversity and adaptive combining for a dual antenna handset receiver. Adaptive combining techniques are shown in [Dolmans1999, Kim2000] and this section to improve the performance of the downlink compared with the more traditional techniques normally employed for combating frequency-flat fading (that being selective, equal gain, and maximum ratio combining). Furthermore, adaptive combining solutions can be formulated without necessitating exact knowledge of the fading environment (other than the desired path phase if the array is used to suppress interference due to echo paths). This is particularly important since the Direction of Arrival (DOA) can be exceedingly difficult to estimate for low-order diversity arrays, where the bulk of optimization techniques for antenna arrays require that the receiver incur such knowledge accurately.

2.3.1 Numerical Examples for Diversity Combining

Diversity and adaptive antennas [Winters1998] are highly useful for spatial processing application and have far reaching consequences in interference negation and multipath fading suppression. A popular conception of the diversity antenna takes the form of an antenna array. An antenna array consists of a set of antenna elements that are spatially distributed at known locations referenced to a common fixed node [Vaughan2003, Van Veen1988, Godara1997B, Razavilar1999] and can be implemented with various geometries (such as Linear, Circular and Planar). In systems that transmit with vertical or horizontal polarization, polarization diversity [Dietrich2001] can be instigated to exploit the random fading channel with horizontal and vertically aligned elements. In a linear array, the centers of the elements of the array are aligned along a straight line, where in this thesis it is assumed the elements of a linear array are equally spaced by a distance d, i.e. a Uniform Linear Array. The incident signals are assumed plane waves (i.e. the scatterers are assumed to be infinitely distant from the array) that arrive at the array from a direction θ off the array broadside.

A generic diversity receiver for information coded multiple access systems is displayed in Fig. 2.5. This diagram illustrates the main receiver processing blocks- which consider timing requiring delay acquisition and tracking, cophasing requiring separate channel estimation filters,

matched-filtering (matched to the single-user codes and pulse shape), and the diversity combiner employing channel weighting prior to summation.

The Equal Gain and Maximum Ratio diversity-combining schemes [Brennan1959, Litva1996] (also see Appendix E, section E.1 for a brief discussion on these techniques) can be tested in the WCDMA downlink employing QPSK modulation and Transmitter/Receiver front-end RRC filters with impulse response truncated to nine chip intervals (the impulse response is symmetrical, hence four symbol intervals each side of the axis of symmetry). The structure of the receiver in this case is given generically with Fig. 2.5 where the waveform demodulator is a chip-matched filter, and the timing acquisition and channel estimation performed with traditional techniques[6] [Steele1992]. The following simulation parameters are applied: The transmitter employed a carrier of 2.15GHz, and the multipath channel was the Vehicular A Rayleigh fading model. The vehicle speed was 36Km/Hr translating to maximum Doppler shift of 139.5Hz. The dual antenna receiver employed separate mixers and RF amplifiers on each diversity branch, where the conventional CDMA correlation detector [Steele1992] was used for detection pre-array combining. The single user channel was based on the UMTS radio frame with processing gain of 15dB. The scrambling overlay code was a long duty cycle (repeating every 38400 chips) gold code that is multiplied complex-wise with the quaternary spreaded information. The in-phase channel contained the user-specific information, and the quadrature channel used for transmitting the Common Control Channels. The spreading codes for all multiple access channels were obtained from the Hadamard matrix (all users were assumed to have equal processing gain for this example), hence are orthogonal.

[6] Timing Acquisition can be employed using code-matched filters and delay locked loops for coherent receivers. The acquisition process is determined by selecting a delay scalar that maximizes the receiver output power. Channel estimation is implemented using the CPICH, which is descrambled and smoothed with a moving average filter.

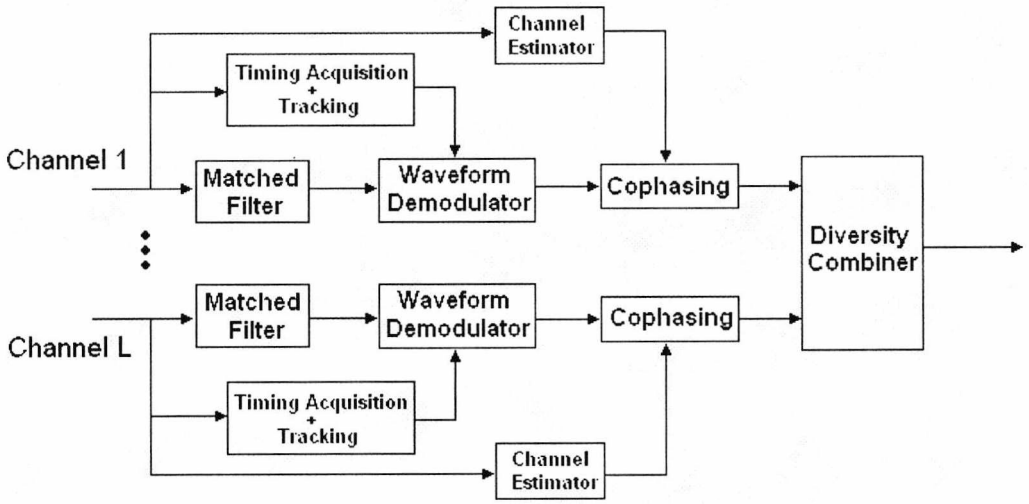

Fig 2.5. A general block diagram of a diversity combiner

The multiplexing for all users at the transmitter end were synchronous and all users shared the same scrambling overlay code. The number of active users was made variable for the simulations, where signaling powers were uniformly distributed but made no greater than 5dB above the desired channel. The CPICH power was 10dB greater than that of the multiplexed data channels.

The Fig. 2.6 shows an array combining solution for a nearly frequency-flat channel (Pedestrian A with pedestrian velocity of 4Km/Hr) utilizing a two-element array considering EGC and MRC. The number of users accessing this channel was made equal to zero- i.e. only the desired physical channels were transmitted along with the CPICH. It can be seen that both techniques improve the probability of error performance over the singular antenna case employing just a correlation receiver to demodulate the single user channel. For convenience, the theoretical single path fading bound [Proakis2001, page 837] is included for the single antenna case and it can be seen the measured result matches well. The MRC technique slightly outperforms the EGC technique for this channel, where the MRC was dynamically adjusted per data symbol considering just the envelope power of three Pilot symbols. The Single User Bound included for visual comparison is the hypothetical AWGN channel bound, which cannot be exceeded by any estimator.

The Fig. 2.7 yields the results from an investigation into the effect of antenna separation on the output SINR and the probability of error. The simulation results were obtained by using semi-analytical techniques where the SINR was calculated from averaging the detector output SNR utilizing a known\pre-calculated noise floor for 1000 channel realizations (Pedestrian A with pedestrian velocity of 4Km/Hr) and a 10000 random (Bernoulli) bit pattern for which a

noise free decision variable was calculated. The bit error probabilities were obtained by averaging over the instantaneous decision probabilities calculated from the SINR realizations. No multiple access interference was included in simulation where the SINR is used instead of the SNR due to the self-interference incurred by the propagation channel (which is in fact negligibly low for the Pedestrian A channel). It is well known that closely spaced antennas yield less diversity gain over antennas that are mutually uncoupled and separated by an order greater or equal to half a wavelength. However, despite the SINR (Fig. 3.7A) and probability of symbol acquisition (Fig. 3.7B) being significantly lower for antenna separations < 0.5λ, the results still show that some improvement is offered by employing two antennas instead of one. The foremost issue requiring consideration in beamforming networks is that related to the spatial selectivity of the channel that yield deliberations relating to the antenna array physical properties (i.e. the distance of antenna separation and thus array factor). One such property of antenna separation in fading channels was observed by Clarke [Clarke1968] that renders the envelope correlation between adjacent antenna elements for various displacements in any plane of polarization. One discernable quality was that for decrimental antenna separation less than half a wavelength, the envelope correlation increases (that in turn compromises diversity gain). Due to system complexity and power consumption (via separate RF amplifiers, mixers etc per antenna feed), adaptive and diversity antennas have normally being considered mainly as mobile uplink devices (or mobile downlink transmitter devices for diversity algorithms such as those using spatial coding such as STTD [Alamouti1998]). Part of this consideration accounts mainly for the generally upheld belief that antenna's yield only effective performance for signal processing applications if the physical dimensions of the array incur individual elements to be spaced by at least half a wavelength. While there is some validity in this assumption, Clarke's approach is actually a somewhat idealistic model (i.e. assuming the antennas were isotropic), where the envelope correlation is modeled by

$$\rho_e = \Im_0^2\left(\frac{2\pi d}{\lambda}\right) \tag{2.25}$$

with ρ_e the envelope correlation between the antennas, $\Im_0$ a Bessel function of the first kind with zero order, d the antenna spacing, and λ the RF signal wavelength. Field measurements conducted by other researchers reported that even when $d = 0.15\lambda$ the correlation was low enough to provide diversity gain [Dietrich2001]. Generally measurements concur that $0.14 \leq \rho_e \leq 0.74$ for various environments based on antenna separations $0.1\lambda \leq d \leq 0.5\lambda$ [Colburn1998]. It is noteworthy to mention that the derivation of the spatial envelope correlation coefficient was

based on the primary assumption that the antennas were isotropic elements. Obviously for directional antennas, this correlation function would not take the exact form of (3.1) and will relate to other parameters (such as the mean effective antenna gain dependence on the spatial distribution of scatterers). The results thus far have only included a single user channel for a relatively mild fading channel. Obviously in practical systems, it is highly likely that the radio channel will be shared with other users and hence the rest of this section (and the thesis) will assume a multiple access scenario (and problem). For a frequency selective channel (as with the Vehicular A channel), it is a fairly standard assumption (see [Klein1993] and the references within) that the performance of detectors optimized for synchronous AWGN channels are very sensitive to the effects of near-far (or far-near in the downlink case) and system loading.

The Fig 2.8 shows the results for the WCDMA downlink for a single user when the access channel is subject to varying numbers of users. For the Vehicular A fading channel, the first result considered shows the effect of system loading on the diversity receiver output SINR (Fig 2.8A). It can be seen that increasing the number of users (given the simulation parameters) drastically degrades this metric by as much as 22dB for K = 30. It can also be noted that the effect of self-interference is evident by degrading the channel quality by about 7dB in the asymptotic bound (as the input SNR becomes large). The bit error probability (Fig. 2.8B) similarly shows that for larger numbers of users, the achievable diversity gain (over the ideal fading channel) degrades by approximately 10dB for 16 users. It is clear that the receiver performance exhibits asymptotic nature where increasing the input SNR yields little effect on the detector error performance.

The final simulation result considers the effect of the spreading factor on the diversity receiver performance for various numbers of users (Fig. 2.9). This result was obtained from the Monte Carlo method described in [Balaban1992] (also see Appendix C) where the accuracy of estimation was set to 95% to speed up the simulation time. It can be seen that for low spreading factor (i.e. high data rate channels) the channel loading significantly degrades the probability of error. However for low data rate channels (G = 128), the effect of loading and self-interference yields somewhat less degradation on the receiver performance. Hence it can be concluded that the search for more optimum detection methods is not motivated by the requirement to drastically improve the quality of voice traffic or high processing gain channels. The next section investigates the application of adaptive antenna arrays as a means for reducing the interference thus improving the quality of the single user channel.

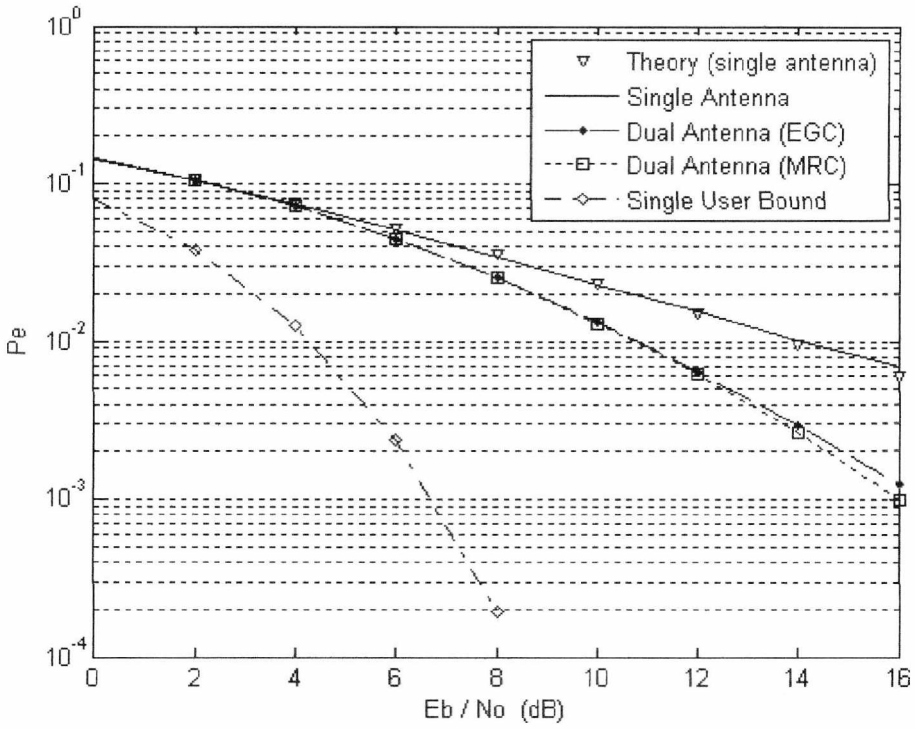

Fig 2.6 Performance of the diversity combining solutions (K=0) compared with the single antenna for a Pedestrian A Channel.

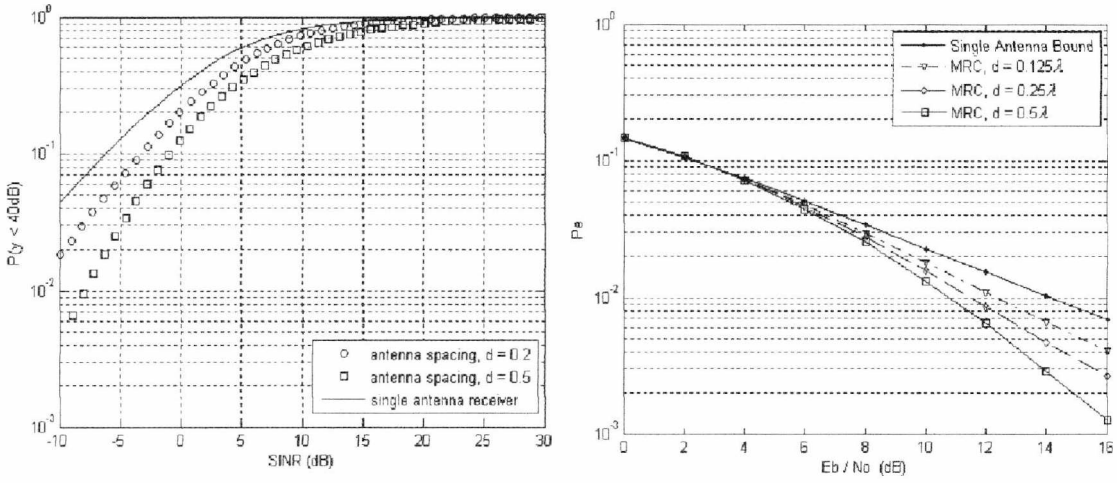

(A) **(B)**

Fig 2.7 (A) Cumulative probability function for the receiver output SINR for different antenna distances.

Fig 2.7 (B) Probability of error Vs the input symbol-noise ratio for different antenna distance for a Pedestrian A Channel.

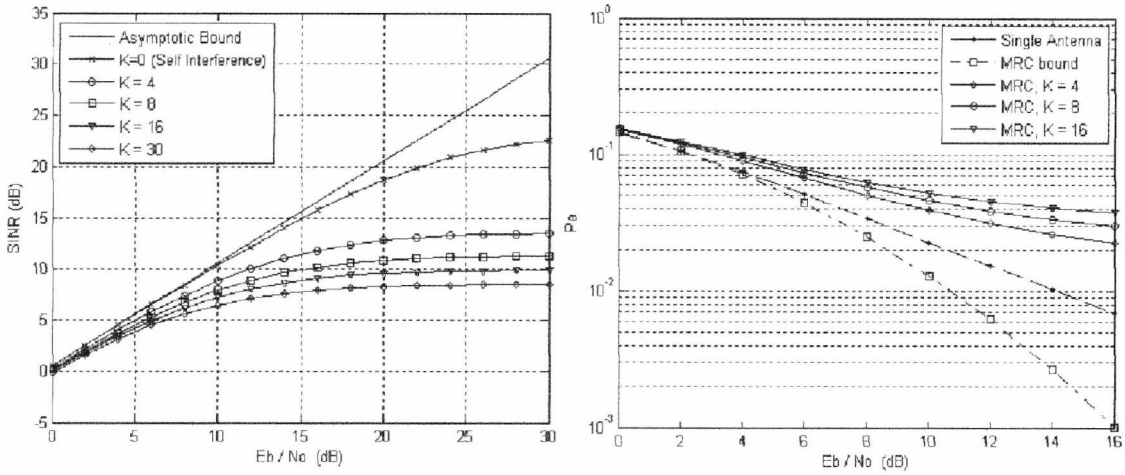

(A) **(B)**

Fig 2.8 (A) Output SINR Vs the input symbol-noise ratio for different numbers of adjacent channels (K).

Fig 2.8 (B) Probability of error Vs the input symbol-noise ratio for different numbers of adjacent channels (K).

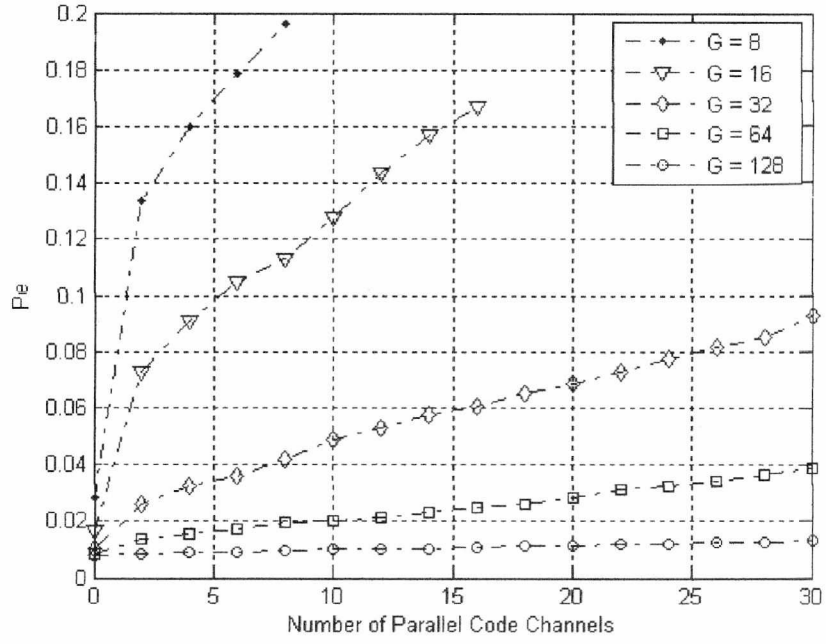

Fig 2.9. Bit Error Probability of the diversity Receiver Vs Number of Users for Spreading Factors G = 8, G = 16, G = 32, G = 64, G = 128. The SNR = 10dB.

2.3.2 NUMERICAL EXAMPLES OF ANTENNA BEAMFORMING

Generally, an adaptive antenna array continuously adjusts its complex gain coefficients via a recursive scheme. Optimization techniques are frequently referred to in the literature for estimating the optimum adaptive combining coefficients (to maximize the output SINR) and include the MMSE or minimum variance criterion [Litva1996]. In additive noise only channels, the adaptive antenna receiver becomes identical (in terms of the diversity gain metrics) to the classical diversity antenna employing MRC. When the system parameters include high loading, the receiver performance is interference limited, where the adaptive antenna yields generally superior performance compared with the classical diversity antenna utilizing MRC – even for cases when the number of interference sources (number of multipaths and separate path intercell interference) exceeds the number of antennas [Dolmans1999, Kim2000, Krauss2000]. This thesis assumes the antennas are spaced by less than or equal to half a wavelength to prevent spatial aliasing from being a significant problem. This is quite different from the diversity trend where antennas should ideally be placed several wavelengths apart.

The analysis for all beamformers investigated in this section ignores the multipath induced phase on the desired specular carrier (and hence on the information after down-conversion) when considering suppression of the echo paths in a multipath channel. For a practical implementation, this phase needs to be eliminated from the information and is conducted post-beamforming using a channel estimator for a fixed reference channel (such as the CPICH in UMTS). Since the idea of beamforming in the downlink is to eliminate unwanted temporally dispersive multipath channels from the desired TOA channel (coherently fixed and tracked by the spread-spectrum acquisition stage), if known reference symbols are provided by the system, then the reference signal should be formed by modulating the symbols with the desired channel attenuation + phase variables. In the case of hybrid beamformers exploiting the frequency selectivity of the channel, then multiple phase coefficients are required to form an "*N-Dimensional*" training signal – one per antenna per path. Two cases for a two-element antenna beamformer can be considered namely where the DOA is known and unknown (leading to adaptive antenna algorithms). If all DOA's are known and the antenna array factor is large enough to prevent overloading, an optimum solution to the beamformer would be to adjust its coefficients to the zero forcing solution (see [Litva96] and Appendix E, Section E.2) leading to perfect interference cancellation provided the angular spread is wide and random. In cases where the interference components arrive too closely spaced (in an angular sense) to the desired

components, the antenna array may not be able to attain zero forcing response (unless the antenna elements are extremely directional).

It is worth noting that the following assumption was endorsed in this thesis- being that the bandwidth of the intruding signal is much smaller than the reciprocal of the propagation time across the array. This supposition, commonly known as the narrowband assumption [188], for the signal represents the propagation delay within the elements of the array by a linear phase shift. Although exacting for sinusoidal signals, the approximation for a situation where the bandwidth of the signal is very small compared to the inverse of the propagation time across the array is usually fairly good for even WCDMA networks with high data/chip rates.

In cases where the receiver does not have prior knowledge of the array response to the multipath and interference signal DOA parameters, an alternative hypothesis must ensue where the receiver must estimate the optimum combining weights based on the measured data. Such algorithms can be formulated to exploit certain well-known parameters of the signaling medium- i.e. a training waveform is provided by the system or the access channel employing phase modulation on the desired signal (or any constant envelope modulation like FSK) that can be optimized (requiring no training signals) via exploitation of the constant modulus of the signal envelope [Treichler1983, Gooch1986]. A simple method for calculating the antenna combiner weights can be formed by minimizing the mean square error between combined "L" space signals and a training signal that is known by the receiver [Litva1996]. Such a combiner, minimizing the quadratic form $\frac{\partial}{\partial \boldsymbol{w}} = E\left\{\left(d(t) - \boldsymbol{w}^H \boldsymbol{x}(t)\right)^H \left(d(t) - \boldsymbol{w}^H \boldsymbol{x}(t)\right)\right\}$ yields the continuous unbiased estimate $y(t) = \boldsymbol{w}^H \boldsymbol{x}(t)$, with

$$\boldsymbol{w} = \Sigma_{xx}^{-1} \boldsymbol{\Lambda}_{dx} \tag{2.26}$$

the beamformer coefficients where $\Sigma_{xx} = E\left\{\boldsymbol{x}(t) \cdot \boldsymbol{x}^H(t)\right\}$, $\boldsymbol{\Lambda}_{dx} = E\left\{d(t) \cdot \boldsymbol{x}(t)\right\}$, $d(t)$ = the reference waveform exhibiting correlation with the desired DOA signal(s), and the vector $\boldsymbol{x}(t) = \left[x_1(t) \quad x_2(t)\right]^T$ denoting the input diversity signals (sum of interference and desired signaling waveforms). This reference signal can be obtained either using the Pilot channel in WCDMA or regenerating the data and/or the multiplexed interference + Pilot channels (provided all interference arrives via the same paths as the desired data channels). Let Σ_{xx} be decomposed where $\Sigma_{xx} = \Sigma_s + \Sigma_u$ with $\Sigma_s = E\left\{\|d(t)\|^2\right\} \boldsymbol{A}(\theta_d) \boldsymbol{A}^H(\theta_d)$ the covariance of the desired multivariate array signal and $\Sigma_u = \Sigma_I + \sigma_n^2 \boldsymbol{I}$ the interference + noise covariance (using

the assumption the noise variables on each antenna element are IID and hence uncorrelated). $\boldsymbol{A}(\theta_d)$ is the array propagation vector for the desired signal (that being the multipath specular component synchronized to the receiver code acquisition). With good approximation, $\boldsymbol{\Lambda}_{dx} = E\left\{\|d(t)\|^2\right\}\boldsymbol{A}(\theta_d)$ if the interference is assumed IID and uncorrelated with the desired signal[7]. Applying Woodbury's identity to Σ_{xx}^{-1} [Litva1996], the weight vector for the antenna combiner can be alternatively given by

$$\boldsymbol{w} = \frac{E\left\{\|d(t)\|^2\right\}\Sigma_u^{-1}\boldsymbol{A}(\theta_d)}{1 + E\left\{\|d(t)\|^2\right\}\boldsymbol{A}^H(\theta_d)\Sigma_u^{-1}\boldsymbol{A}(\theta_d)} \tag{2.27}$$

which, upon close inspection, contains an interference whitening transformation and henceforth does not eliminate the spatial signatures entirely from the undesirable components. Direct coefficient calculation (2.31) requires the covariance (Σ_{xx}) matrix and cross correlation ($\boldsymbol{\Lambda}_{dx}$) vector to be estimated applying windowing and averaging [Godara1997B]. Due to the requirement for adaptivity in non-stationary multipath environments, Σ_{xx} must be estimated and updated from time to time as environmental factors alter. Hence we can either treat this problem with sampled matrix inversion [Haykin1996] by fixing the observation window and updating recursively (introducing a forgetting factor in the process as in the Kalman [Kalman1960] algorithm) or by using the generally more popular steepest descent techniques such as the Normalized Least Mean Squares algorithm. Applying the method of least squares, the antenna coefficients utilizing a known reference signal (such as the CPICH in WCDMA) can be updated with $\boldsymbol{w}^{(n)} = \boldsymbol{w}^{(n-1)} + \mu\left(\boldsymbol{\Lambda}_{dx} - \hat{\Sigma}_{xx}\,\boldsymbol{w}^{(n-1)}\right)$ with $\hat{\Sigma}_{xx}$ the instantaneous covariance estimate (at sample time n). The NLMS algorithm is given by the following equation,

$$\boldsymbol{w}_k^{(n)} = \boldsymbol{w}_k^{(n-1)} + \left(\frac{\mu}{\rho + \left\|\boldsymbol{\chi}_{(n)}^H\boldsymbol{\chi}_{(n)}\right\|}\right)\cdot\left[d_{(n)} - \hat{d}_{(n)}\right]^*\cdot\boldsymbol{\chi}_{(n-1)} \tag{2.28}$$

where $\hat{d}^{(n)} = \boldsymbol{w}_{(n-1)}^H\boldsymbol{\chi}_{(n)}$ is the array output estimate, and μ, ρ are small fractional constants. The NLMS algorithm has a "per-step" complexity that is much lower than the direct solution and can track non-stationary channels where the tap weights of spatial processor are updated on

[7] The basic assumption is that all individual multipath components are identically distributed (with different mean) but uncorrelated. This is true if the second TOA lags by more than one chip and of course is incident to the array with different AOA.

a sample-by-sample basis [Widrow1976A], [Widrow1976B, Slock1993]. The NLMS algorithm is known to have a far larger misadjustment and slower convergence than the direct block estimator offered by (2.31) where the input sample streams are arranged in fixed, finite blocks. However, the disadvantage of the direct solution is higher computational complexity. A tradeoff is thus offered with the RLS (Recursive Least Squares) algorithm that offers reasonable convergence in most practical situations [Haykin1996] – see Appendix D for the derivation of the algorithm.

A major issue to be addressed is whether the beamformer coefficient adjustment occurs at the front end (dealing with a chip rate signal) or after chip matched filtering (where the baud rates are much lower). A front – end diversity combiner would require the receiver to be centralized in providing a suitable training waveform where, if the Pilot channel were to be used, the random chip sequences incurred by the adjacent data channels would be treated as noise. This will incur a cost where convergence is likely to be slow in such a situation (due to the relatively low SINR) unless the pilot is far more dominant over other channels to increase the relative pilot SINR when utilizing adaptive techniques (realistically, the pilot channel accounts for only a portion of the base-station transmitted power). However, in only partially interference suppressing receivers, it would be expected and logical to assume that increasing the Pilot channel SINR without bound is not only impractical (due to limitations on the transmit power and non-linearities of the power amplifier) but would also offer a severe degradation to the desired physical channels. If we assume the fading is constant over the data symbol duration, it is not necessary to update the antenna weights at full chip baud rate. Symbol level combining would be more practical both computationally and allow improvement in the channel quality when a moving average filter is used to decrease the adjacent channel interference. In this set up (Fig. 2.10), the despread CPICH would be used to excite the modes of adaptation for the NLMS or RLS algorithm.

Numerical examples are presented for MMSE and the Blind Maximum SINR algorithm (see [Kwon1999, Choi2000] and the Appendix E, section E.3) implemented for a dual antenna array using the same downlink simulation parameters (and set-up) in section 2.3.1. Logically speaking, "beamforming only" application (i.e. antenna array followed by a spread spectrum code matched filter/integrate dump filter) for the WCDMA downlink is actually not an entirely optimum solution for circumvention of the interference mechanism generated from fading channels. The reasons for this will be visualized from the results presented for relatively harsh (Vehicular A) fading channels, where for channels with number of paths >> number of sensors, the receiver still has an irreducible interference floor and thus is asymptotically bounded for K=

8 and K = 16 users (Fig. 2.11A, 2.11B, 2.11C, and 2.11D). The Vehicular channel for this simulation was set to 36Km/hr. The results show that the exact solutions to the MMSE and MSINR array outperform the MRC solution presented in the section 3.1. It is also clear that the MMSE solution yields superior error performance, however this is not surprising since the MSINR algorithm was implemented with the approximations regarding the interference and desired signal autocovariance's suggested in [Choi2002] and Appendix E.3. Realistically, the exact MSINR solution [Rapajic1995] would offer identical SINR (and hence BER) performance; hence this solution is not shown. The adaptive MMSE (applying 2.32 and the RLS algorithm) and MSINR (see [Choi2002], and Appendix E.3) arrays were also presented in the results. The adaptive step size was a small fractal constant = 2^{-8} to ensure convergence. A larger step size may improve the convergence, but this usually comes at a cost of higher misadjustment [Jung1995] and possible instability.

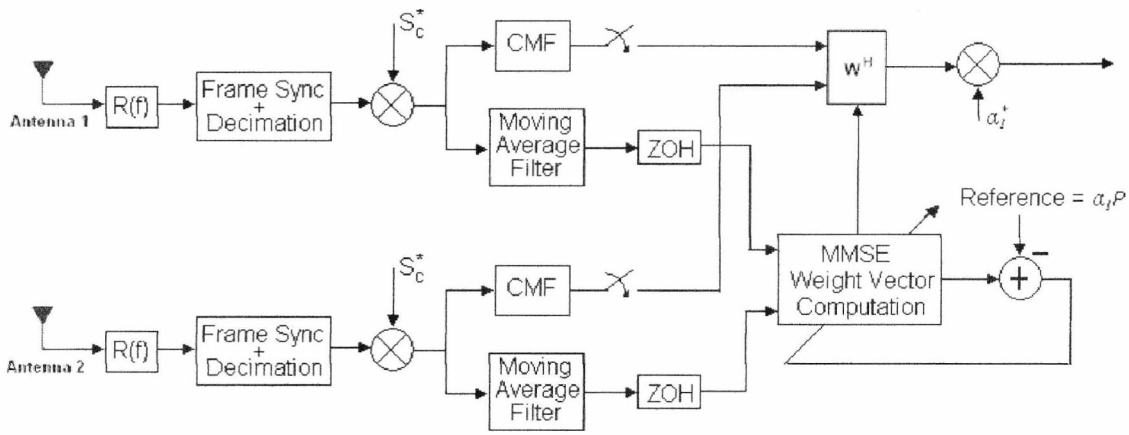

Fig. 2.10 A Dual Antenna beamformer employing symbol level adaptive combining. R(f) is the front end RRC Matched filter. S_c denotes the descrambling code.

Of the adaptive schemes, the MMSE solution employing the RLS algorithm offered best performance. With exception of the blind adaptive MSINR algorithm, both RLS and NLMS schemes improved the receiver performance over the MRC diversity combiner. The blind adaptive MSINR algorithm actually performed worse than the MRC receiver for K = 16 users (although did offer some diversity improvement over the single antenna case). This type of problem with blind detection is commonly observed with the MOE and Griffiths algorithm [Honig1995, Hooli2002, Griffiths1969] where the convergence is usually slower (and with greater MSE) than the corresponding Least Squares algorithms utilizing an exact training signal. It can be concluded that the mechanism generating interference arising from not only the angular spread of the incident waves, but also that the echo paths (and all waves incident to the array associated with the sounding echo) of variable DOA's are not going to be cancelled entirely from what is a small array (Fig. 2.12). The Fig. 2.12 shows the beamformer response for the zero forcing, MSINR, and MMSE algorithms, where it can be seen that the MSINR and MMSE array approximate the optimum response well for a single interferer. The problem is of course multiple interferers created by the access and fading channel. As discussed in Chapter 1, the interference from other users (including Pilot channel, and self-data channel interference- IPI) is generated only in dispersive channels[8] creating non-orthogonality between the spreading codes in the column space of Spreading matrix. The Fig. 2.13 shows the results of the adaptive NLMS receiver for different vehicular speeds. The observation here is that for vehicular speeds > 60Km/hr, the performance of the estimator degrades significantly due to slow tracking of the algorithm (and error in the generated reference signal where the channel is no longer flat over relatively long processing windows).

[8] In flat fading channels this interference is negligible unless the Doppler spread is very high causing channel-induced interference due to a non-stationary, non-linear channel coefficient during the despreading interval. We ignore the modulation based interference caused by non-uniform fading profiles within a symbol interval by assuming the channel is reasonably flat over short durations.

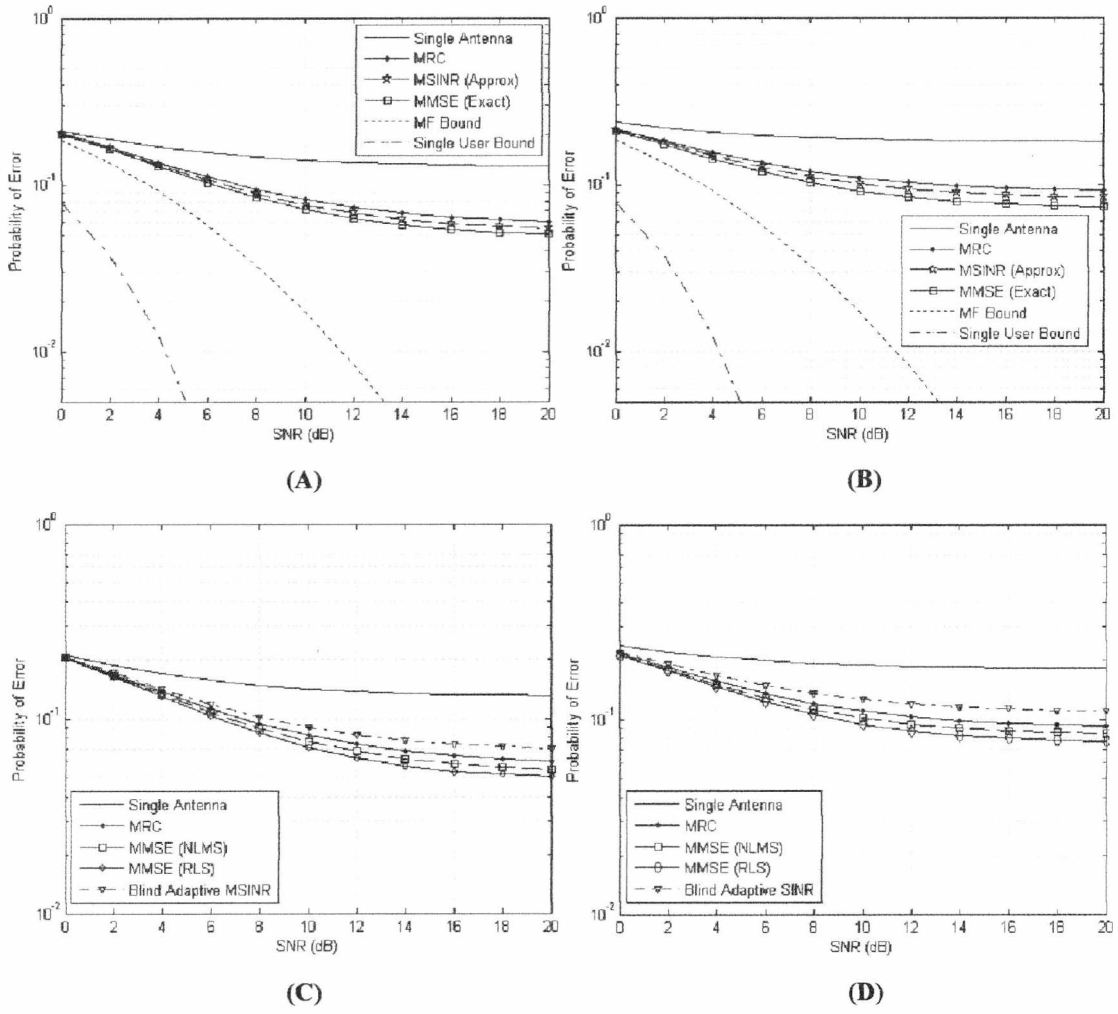

Fig 2.11A Probability of error Vs the input symbol-noise ratio with K = 8 for the MMSE and approximate MSINR dual antenna combining algorithm.

Fig 2.11B Probability of error Vs the input symbol-noise ratio with K = 16 for the MMSE and approximate MSINR dual antenna combining algorithm.

Fig 2.11C Probability of error Vs the input symbol-noise ratio with K = 8 for the adaptive dual antenna NLMS, RLS and MSINR algorithm.

Fig 2.11D Probability of error Vs the input symbol-noise ratio with K = 8 for the adaptive dual antenna NLMS, RLS and MSINR algorithm.

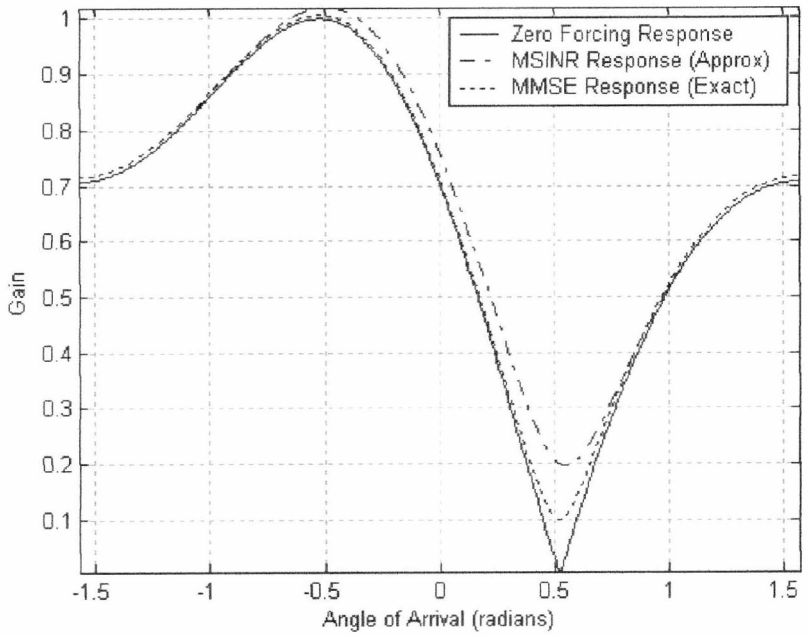

Fig 2.12 The antenna gain Vs. direction of arrival for diversity coefficients obtained based on zero-forcing, MMSE, and approximate MSINR for the desired and interference signal

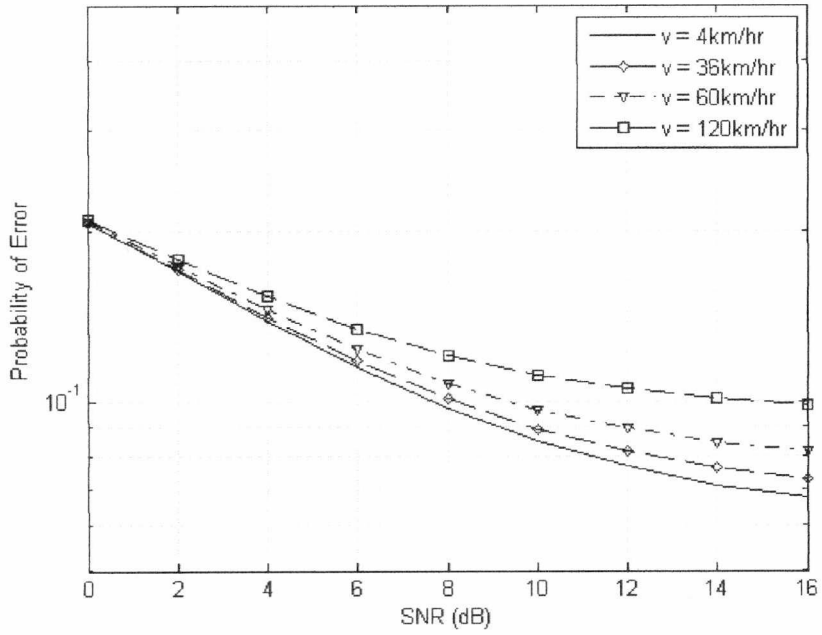

Fig 2.13 The Probability of Error Vs SNR for the NLMS dual antenna receiver with different Vehicular speeds.

2.4 Temporal Diversity Application Employing the Rake Receiver for Channels with Frequency-Selectivity

The fact that the propagation channel incurs a convolutive process on the desired signalling source makes optimal diversity reception [Brennan1959] very difficult to achieve in practice. A technically sound solution not applying traditional diversity algorithms would be the inverse filter that requires the fading channel is known. However, inverse filtering is constrained to only certain types of channels since the impulse response applying the Deconvolution theorem is infinite and not always stable. Furthermore, equalization does not generally yield large diversity gains (in a puritan sense) for additive noise channels and may actually worsen the detection problem if the channel is noise rather than interference limited. Equalization based on measured channel statistics are also very intolerant to delay and channel estimation errors when the weight vector is calculated via matrix transformation/optimisation. On the other hand, standard techniques like the Rake receiver (overcoming the requirement of applying exact inverse transforms) yield cross talk between the diversity channels- the negation of which may require an advanced statistical signal processing methodology [Kay1993A]. A generic diversity receiver based on splitting the multipath components into "L" channels is shown in Fig. 2.14. This forms the basis of the rake receiver requiring timing acquisition and tracking of all the multipath components (or, rather the resolvable paths), and channel estimation filters for providing sufficient diversity combining coefficients. Channel coding is not considered and hence receiver decisions are based on the sign detector.

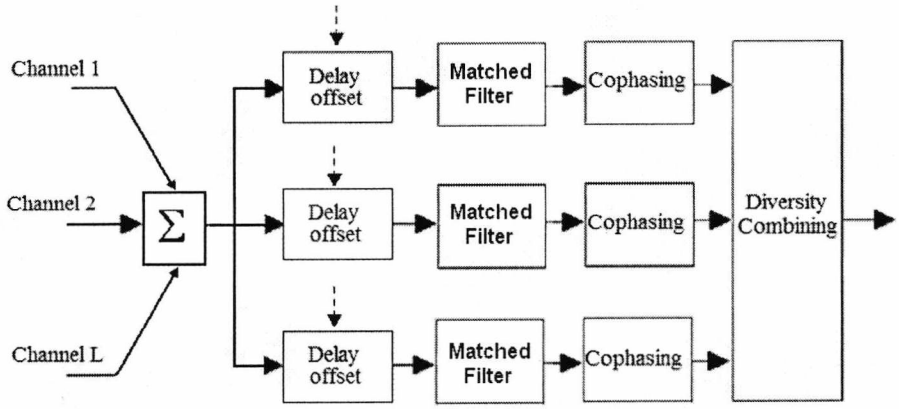

Fig 2.14 A generic Temporal Diversity Receiver

This section explores the Rake receiver performance for the Vehicular A channel with varying loading conditions (where each user power is uniformly distributed). The semi-analytical approach based on the Gaussian approximation (see [Latva-Aho1998] and Appendix C, Section C.3) was used to estimate the probability of error. This was conducted for blocks of 1200 symbols[9] with the result averaged over 1000 independent channel and data sequence realizations. The channel for all simulations was set for vehicular speed of 36Km/hr. For simplicity of simulation, the chip waveforms were rectangular pulses and perfect delay and channel acquisition at the receiver are assumed. The vehicular channel delays were set to be proportional to the chip period. The first result (Fig. 2.15) obtained shows the Rake receiver BER Vs SNR performance under various loading conditions (K = 4, 8, and 16). It can be seen that the Rake receiver yields very similar performance to the spatial two-antenna maximum ratio combiner (performance of the rake is slightly better). The results here reflect the self-interference for K = 0. It is also noted that the probability of error for any fixed channel SNR is highly dependent on the number of users accessing the network. The Fig. 2.16 shows that some performance gain is realized when the Rake fingers are weighted proportionately to the inverse channel interference variance (see [Kuo2001] and the Appendix F) and can be interpreted as a capacity gain for the network when a better MRC criterion is used over the traditional Rake combiner. The performance of the rake receiver was also expatiated further in Fig. 2.17 when the number of adjacent synchronous channels was the variable argument against probability of error (for fixed ideal channel SNR = 20dB). The result shows that the performance of rake reception is superior against fading and system loading over the dual antenna combiner (employing the MRC scheme). This factor led to the proposal of 2D-Rake receivers in [Kohno1998] where both spatial and temporal diversity is utilized to combat frequency selective fading. However, it is necessary from a diversity perspective to equalize a frequency selective channel, since unless the system loading is either low (or the desired channel having significant processing gain), the performance targets of third and forth generation mobile systems are unlikely to be met due to the interference generated in CDMA based systems. The performance of 2D-Rake receivers, Rake assisted beamformers, and broadband antenna arrays are scrutinized more elegantly in Chapter 4.

[9] Translating to a 1 TTI radio frame for the UMTS with G = 32. The quadrature component contains the common control channel, while the in-phase component is information bearing- i.e. the dedicated physical data channel for the user under investigation.

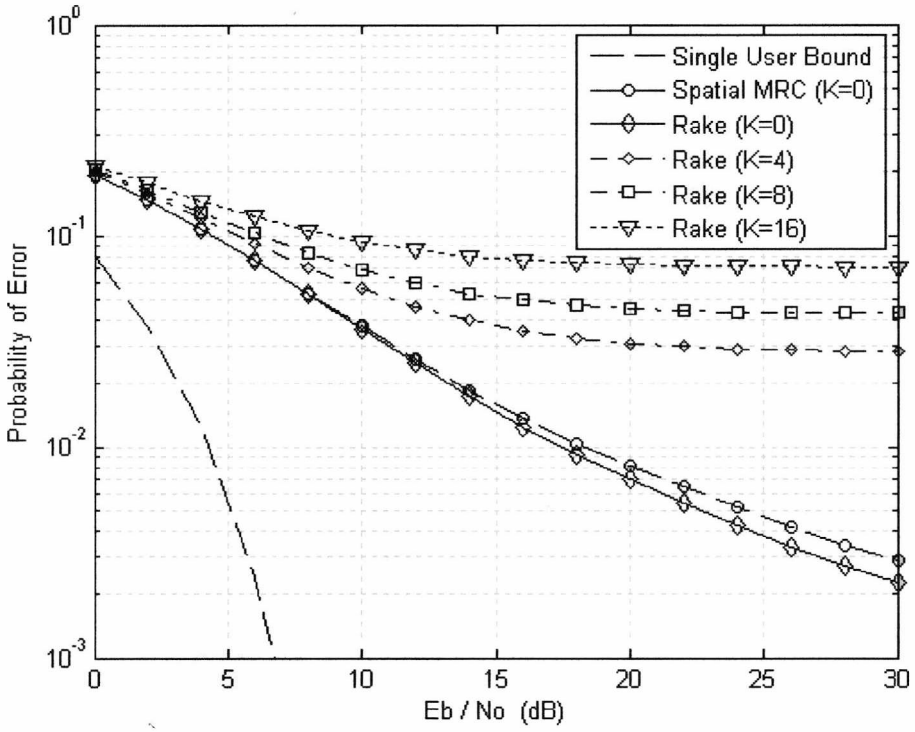

Fig. 2.15 Rake Receiver BER Vs SNR performance for K = 0, 4, 8, and 16 users with uniformly distributed powers.

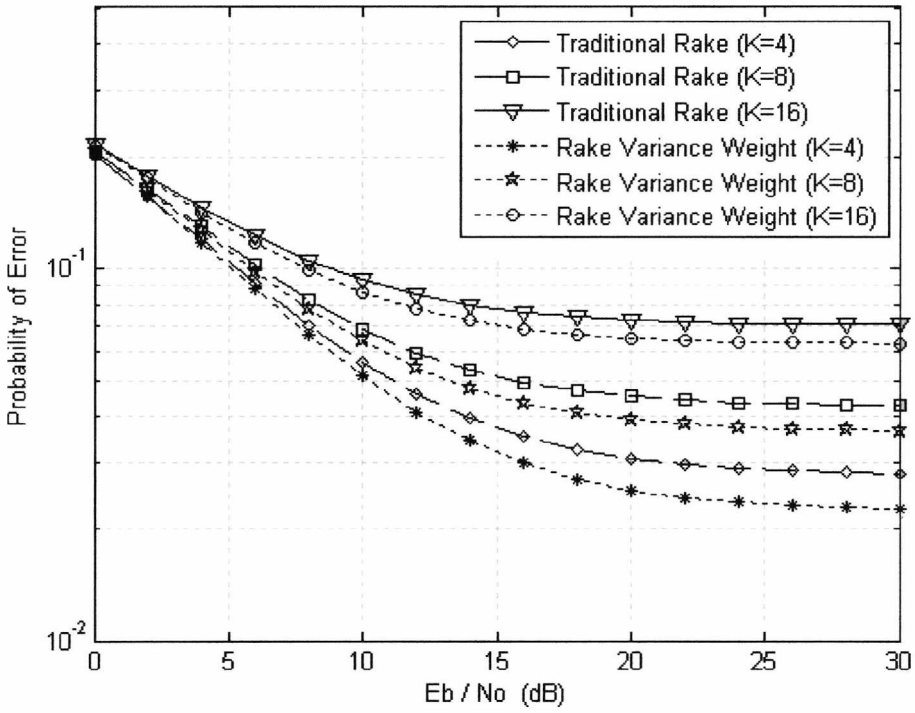

Fig. 2.16 Rake Receiver BER Vs SNR performance for K = 4, 8, and 16 users with the conventional and inverse finger variance diversity combining solutions.

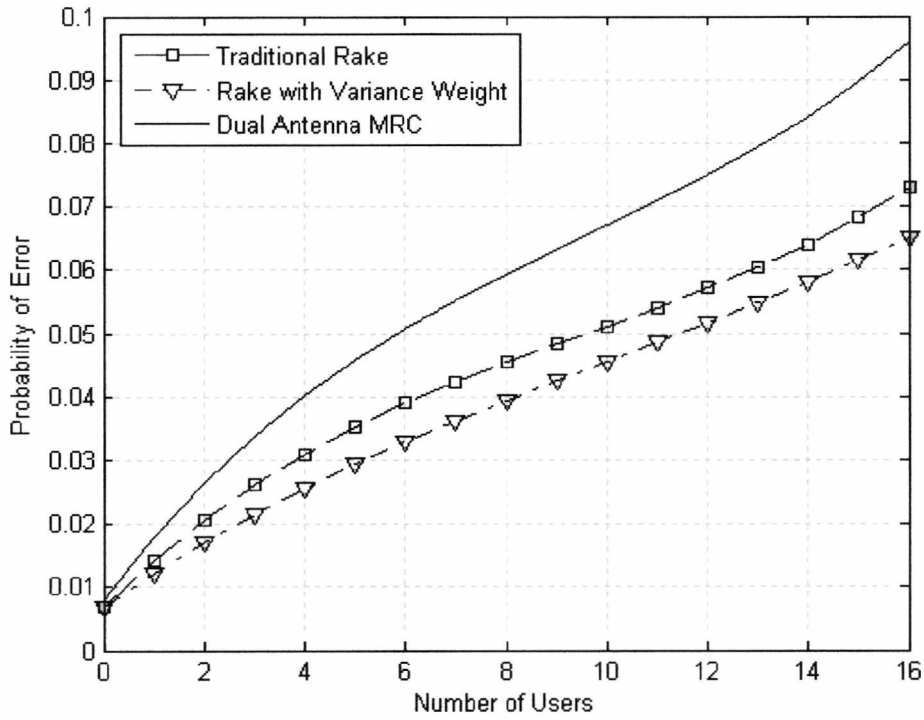

Fig. 2.17 Rake Receiver BER Vs Number of users for SNR = 20dB with the conventional and inverse finger variance diversity combining solutions.

2.5 Discussion

Blind MSINR and MMSE receivers have been shown to improve the receiver performance for the WCDMA downlink. However, since the MSINR receiver is computationally more demanding and performs worse than the MMSE receiver, its implementation in the WCDMA downlink is irrelevant if the network provides a Pilot channel (taking form as an adjacent code channel or a multiplexed preamble/midamble known by the receiver). If no Pilot channel is available (or is far too noisy to use with any degree of accuracy), then the MSINR criterion would be the most logical solution. The MMSE receiver in fact does not even require a Pilot channel- since decision directed beamforming has been conducted for many years in array processing problems if a reference is not available (decision directed training involves making soft or hard decisions on the data waveform and using this as the reference signal). Of course, the problem with decision directed beamforming is if the demodulated channel has low SINR (where $P_e \rightarrow 0.5$) meaning the training waveform is uncorrelated with the real information

bearing waveform (essentially making training useless). An issue of some importance is that the statistical solution for the MMSE algorithm does not consider the multiplex of adjacent users in the data stream (i.e. the receiver is assumed blind to the active multiple access codes) and uses only the descrambled pilot channel for referencing purposes. This solution is not overly erratic provided the pilot channel appears spectrally as the "dominant" channel (as one would expect in a power controlled scenario), however, if a Pilot channel was not available or the adjacent data channels yielded comparable or greater power, then this method is imperfect. In summary, both beamforming cases yielded superior results in both vehicular channels (with K = 8 and K = 16 interferers), however it can be clearly seen that the performance is asymptotically bounded, where increasing the channel SNR does not decrease the probability of error without bound. Hence it can be concluded that both beamformers are in fact interference limited offering marginal performance gains over the MRC technique. Of course increasing the degrees of freedom via utilizing a greater number of equally spaced sensors will eventually remove this interference constraint- however, this approach is impractical on dimensionally small handsets with battery power limitations (since a digital beamformer would require separate RF demodulation units that include a low noise amplifier on each diversity branch). A summary of the three key antenna optimization criterions is given in Table 2.1.

A more logical approach in CDMA systems would be to employ and consider all the aspects of diversity in frequency selective multipath channels- this being the spatial-frequency channel selectivity. The standard forms of frequency selective channel resistant detection normally begins (applying some fairly standard assumptions) with the rake receiver, which has evolved into more complicated algorithms exploiting the coding orthogonality between all multiuser channels and/or the multipath channel itself if the parameters of fading are known (forming the inverse filter commonly denoted as being the zero forcing equalizer). It would be extremely useful for the purpose of discussion to reflect on the rake receiver in the WCDMA downlink and extend its diversity range by considering the spatial selectivity of the multipath channel- forming the classic 2D Rake receiver. Despite the limitations of Rake reception in highly loaded cells with/without power control, the actual generic solution is extremely powerful in assisting more effective detection algorithms in providing sufficient statistics in hypothesis testing.

The 2D Rake receiver (investigated more thoroughly in Chapter 4) can be further developed into a Rake beamformer, where each path (on each antenna element) is combined adaptively and then cophased and fed into a maximum ratio combiner [Kim2001]. This receiver can be considered a per-path beamformer, although array overloading due to widely dispersive

multipath channels would still present an issue to interference negation for a low number of antenna sensors. Chapter 4 extends the rake hypothesis to investigate more optimum beamformers that decorrelate the channel based on the measured spatial signals. Such receivers, denoted as being broadband beamformers [Madisetti1997], exploit chip or symbol level equalizers optimized according to the spatial and temporal signatures of the channel. The best linear unbiased 2D Rake receiver would be the broadband beamformer (with the rake receiver being generalized as an equalizer by exploiting additional fingers/taps not necessarily aligned to the multipath delay spectra).

Table 2.1 Statistically optimum beamforming techniques

	MMSE	**Max SINR**	**MV**
Criterion	*Minimize the difference between the output of the array and the desired response.*	*Maximize the ratio between desired signal energy component and the interference + noise energy components at the array output*	*Minimize the variance at the output of the array subject to a linear constraint forcing the beam pattern to be a constant in a particular direction.*
Cost Function	$J(\mathbf{w})= \mathrm{E}[\,\lvert \mathbf{w}^H \mathbf{r}(t)-d(t)\rvert^2\,]$ *r(t) is the array input and d(t) is the desired response.*	$J(\mathbf{w})= \dfrac{\mathbf{w}^H \Sigma_s \mathbf{w}}{\mathbf{w}^H \Sigma_u \mathbf{w}}$	$\min_{\mathbf{w}} \{\mathbf{w}^H \Sigma_u \mathbf{w}\}$ *subject to the constraint* $\mathbf{w}^H A(\theta_d) = 1$ *This is the Minimum Variance Distortionless Response (MVRD) beamformer.*
Solution	$\mathbf{w} = \Sigma_{xx}^{-1} \Lambda_{dx}$	$\Sigma_s \cdot \mathbf{w} = \lambda_{max} \Sigma_u \cdot \mathbf{w}$	$\mathbf{w} = \dfrac{\Sigma_u^{-1} A(\theta_d)}{A^H(\theta_d)\Sigma_u^{-1} A(\theta_d)}$
Advantages	*Knowledge of the interference statistics or desired signal DOA are not required. Solution is fairly simple.*	*Maximization of SINR. Solution is identical to the MMSE criterion requiring no information-based training signal.*	*No Training signal required and solution is similarly identical to the MMSE solution in terms of the output SINR. Solution not overly complex.*
Disadvantages	*Requires generation of a reference signal. Difficulty in CDMA environment is interference from other channels causing slow convergence for adaptive schemes utilizing training signals composed of only the desired or pilot channel when coexisting with simultaneously active physical channels.*	*Must know second order statistics of noise, interference and the DOA of desired signal. Computationally cumbersome particularly for large array factors.*	*Must know second order statistics of noise, interference and the DOA of desired signal.*

CHAPTER 3
ALGORITHMS FOR DELAY DIVERSITY APPLICATION IN SINGLE USER MOBILE TERMINALS

PREFACE

This chapter deals primarily with the rake algorithm and the channel/delay acquisition stages required for generating receivers that exploit the temporal nature of diversity. The estimation of the propagation delay and phase variables yield particular scope focussed for rake receivers, linear single/multi user estimation and equalization techniques designed specifically for diversity in frequency selective fading channels. This chapter yields an algorithmic perspective of channel acquisition mainly for the rake receiver since this technique is the receiver of choice in current mobile technology for the downlink. The rake receiver is inherently sub-optimum in frequency selective channels due to temporal dispersion creating an irreducible noise floor when waveform demodulation is applied with the traditional matched filter [Prasad2000]. However, to maximize the performance of the rake receiver, accurate timing acquisition and channel estimation are mandatory. The implementation aspects for channel estimation are quite diverse, depending largely on the structure of the linear detection algorithm. From a more generic sense, the channel and coded information symbols are jointly estimated if the properties of the delay channel are known or estimated beforehand. This is the case certainly for linear multiuser receivers such as the Decorrelator and LMMSE detector. However, some single user techniques such as adaptive equalization [Qureshi1985] do not always necessitate knowledge of the channel at- where the only requirement is that the most significant delay path (yielding the highest average power) is tracked and synchronized by the detector (for timing purposes and code acquisition). Channel and delay estimation are among the most important criterion for diversity combining receivers, where algorithmic complexity varies greatly depending on the level of optimization applied and the assumptions made in doing so. This thesis does not concentrate on a maximum likelihood channel estimator due to high complexity [Bensley1996, Strom1998], however several sub-optimum techniques exist that includes Minimum Variance estimation [Tsatsanis1998], Vector Subspace estimation [Schmidt1986, Bensley1996], and Correlation

[Simon1994] type receivers utilizing smoothing filters. Delay and channel estimation employing matched filters or linear unbiased estimators are generally quite robust to interference and additive noise provided the transmission power of the Pilot channel is greater than the mean power of the interference sources (which include the "own" user data channel). However, considering the limitations of power control for the Common Pilot Channel (CPICH), the additive noise and interference in highly loaded networks will create errors in relatively fast fading channels – particularly so by degrading the accuracy of channel estimation. For delay estimation, the probability of successful path acquisition is an important metric, where this probability is interference and noise limited- being close to 1 for low noise channels, and exhibiting asymptotic limiting behaviour for very highly loaded channels. It is assumed in this thesis that a pilot channel of higher energy is transmitted to every user sharing the access channel to enable estimation of the convolutive processes incurred in radio transmission. This Chapter is summarized as follows: The Section 3.1 describes several delay acquisition algorithms predominantly for short code WCDMA. Section 3.2 overviews the channel estimation process employing fixed or dynamically adjusted filters. The numeric results are presented in section 3.3, with appropriate conclusions generated in section 3.4.

3.1 DELAY ACQUISITION

3.1.1 MATCHED FILTERS FOR DELAY ESTIMATION

The general approach to delay and channel estimation utilizes one shot correlation composed of multiple delay shifted replicas of the original coding waveform (utilizing a tap delay line with fractionally spaced sample offsets), where the peaks of correlation are compared to a threshold and the channel timing/delay (in samples) offsets obtained from the hard decisions. Such an algorithm, defined by (3.1) operates on the received pilot symbols of maximum block length $M = 3N_s GN_{symb} \cdot \left(\frac{max(T_{delay})}{T_c} \right)$ and applying a tracking loop based on the early-late principle with dual channel latency of half a chip [Simon1994]. N_{symb} = number of symbols encompassed by the estimator, which is defined as $N=3$ unless stated otherwise. Large swings in the delay spread of the channel can cause timing synchronization to be lost, hence the receiver can be modified to periodically recalculate the delay estimates if need be (where detection

employing sliding window based Decorrelation requires the diversity order to be sequential). The conventional matched filter estimates the delay paths by sweeping through the pilot code vector realizations with different timing offset and obtaining the offset that maximizes the output power. Formally this can be written as

$$\hat{\tau}_l = \underset{\tau_l}{argmax}\ P_{MF}\left(\bar{s}(\tilde{\tau}_l)\right) \tag{3.1}$$

where $P_{MF}\left(\bar{s}(\tau_l)\right) = \dfrac{\left|\bar{s}^H(\tau_l)\cdot \boldsymbol{r}\right|^2}{\left\|\bar{s}^H(\tau_l)\cdot\bar{s}(\tau_l)\right\|}$ is the figure of merit with $\bar{s}(\tilde{\tau}_l) = \left[\boldsymbol{0}^T_{NsG+\tau_l},\ \boldsymbol{s}_k,\ \boldsymbol{0}^T_{(NsG-\tau_l)}\right]^{\mathrm{T}}$ the sampled Raised Cosine pulse shaped signature sequence (N symbolises the data overlapping due to multipath and is usually $N=2$) as a function of delay offset τ_l. Note P_{MF} is more convenient to write as being without normalization since the scalar dot product between the code vectors is always equivalent regardless of the delay shift. In this case, $P_{MF}\left(\bar{s}(\tau_l)\right) = \bar{s}^H(\tau_l)\,\Sigma_{\mathrm{r}}\,\bar{s}(\tau_l)$ with $\Sigma_{\mathrm{r}} = E\left(\boldsymbol{r}\cdot\boldsymbol{r}^{\mathrm{H}}\right)$ the received signal covariance matrix[1]. Also it is noteworthy that the received covariance matrix is completely unknown to the receiver, hence it must be estimated from the samples where $\Sigma_{\mathrm{r}} \approx \dfrac{1}{M}\sum_{i=0}^{M-1}\boldsymbol{r}_i\cdot\boldsymbol{r}_i^H$ with M the maximum iteration and $\boldsymbol{r}_i$ the received vector spanning the length of the matched filter.

3.1.2 WHITENING APPROACH TO DELAY ACQUISITION

The sliding correlator matched filter performance can be significantly improved if the received vector is whitened with the matrix $\boldsymbol{L}^{-1} = \Sigma_Z^{-1/2}$ obtained with the Cholesky decomposition [Alexander1998] where Σ_Z is the received interference + noise covariance matrix [Xiao2003]. In this case the delay estimate is given by the

[1] Note the superscript symbol H represents the Hermitian transpose. E represents the stastistical expectation.

$$\hat{\tau}_l = \underset{\tau_l}{argmax}\, P_{WMF}\left(\bar{s}(\tilde{\tau}_l)\right) \tag{3.2}$$

where $P_{WMF}\left(\bar{s}(\tau_l)\right) = \dfrac{\left|\left\{\boldsymbol{L}^{-1}\bar{s}(\tau_l)\right\}^H \boldsymbol{L}^{-1}\boldsymbol{r}\right|}{\left\|\boldsymbol{L}^{-1}\bar{s}(\tau_l)\right\|^2} = \dfrac{\bar{s}^H(\tau_l)\Sigma_Z^{-1}\boldsymbol{r}}{\bar{s}^H(\tau_l)\Sigma_Z^{-1}\bar{s}(\tau_l)}$ is the figure of merit with interference and noise whitening. The operation of the whitening transform is to whiten the interference and it is rather simple to show mathematically.

Let $\boldsymbol{r}$ be modelled at the receiver side to a definition of single user + adjacent users, thus if $\boldsymbol{r} = \boldsymbol{S}_c\boldsymbol{P} + \boldsymbol{Z}$ with $\boldsymbol{Z}$ the interference, data and noise signal (with $\boldsymbol{P}$ the channel modulated pilot signal vector with complex non-zero mean Gaussian amplitude distribution and $\boldsymbol{S}_c$ the scrambling code matrix), then the output of the whitening filter can be modelled as $\boldsymbol{Y} = \boldsymbol{L}^{-1}\boldsymbol{S}_c\boldsymbol{P} + \boldsymbol{L}^{-1}\boldsymbol{Z}$. The expectation of the interference autocorrelation matrix is $E\{(\boldsymbol{L}^{-1}\boldsymbol{Z})^H(\boldsymbol{L}^{-1}\boldsymbol{Z})\} = \Sigma_Z^{-1}\Sigma_Z = \boldsymbol{I} \sim N(0,1)$, i.e. a Gaussian distributed vector with unity variance.

3.1.3 MMSE Approach to Delay Estimation

An alternative optimization to the conventional delay estimator considers a Bayesian approach, where one class of estimator can be formed from the minimization of a cost function, that being the mean square error (MSE) between the input and a training waveform that shares some correlation with the desired signalling parameter. The general form for this unbiased estimator in short or cyclic code applications can be formed from the partial derivative $\dfrac{\partial}{\partial\boldsymbol{\alpha}} = E\left\{\left(P - \boldsymbol{\alpha}^H\boldsymbol{r}\right)^H\left(P - \boldsymbol{\alpha}^H\boldsymbol{r}\right)\right\}$ where equating to zero (note the non-bold P means a single sample and not a vector) yields the Wiener estimator [Xiao2003, El-Tarhuni1998] and the parameter vector is

$$\boldsymbol{\alpha} = \Sigma_r^{-1}\boldsymbol{\Lambda} \quad \in \quad C^M \tag{3.3}$$

with $\boldsymbol{\Lambda} = E\left\{P^*\boldsymbol{r}\right\}$ and M the number of taps defined earlier. The delay estimator in this case correlates the delayed signature sequence $\bar{s}(\tau)$ with the filter vector; hence the figure of merit

$P_{MMSE}(\bar{s}(\tau_l)) = \frac{\left|\bar{s}^H(\tau_l)\cdot\alpha\right|^2}{\left\|\bar{s}^H(\tau_l)\cdot\bar{s}(\tau_l)\right\|} = \frac{\bar{s}^H(\tau_l)\sum_\alpha \bar{s}(\tau_l)}{\left\|\bar{s}^H(\tau_l)\cdot\bar{s}(\tau_l)\right\|}$ is used to enforce receiver decisions on the delay estimates where the test statistic in this case is given by

$$\hat{\tau}_l = \underset{\tau_l}{argmax}\, P_{MMSE}(\bar{s}(\tilde{\tau}_l)). \tag{3.4}$$

The practicality of the delay estimator for long-code CDMA is questionable due to large observation windows required to observe cyclostationary in the interference signals (and large scale matrix inversion). In this case, the matched filter must be extended to impractical lengths. Another approach can utilize brute force calculation over an extended but not impractical matched filter, where in this case the parameter vector $\alpha = \sum_r^{-1}\bar{s}(\tau_l) \in C^M$ will be the approximate MMSE optimization with the covariance matrix estimated only during a long observation window comprised of finite, smaller length time spans assigned for a limited capture of constant phase modulated pilot symbols (where it will only yield an approximate expectation). This technique would only realistically be applicable for a one shot approach to delay acquisition and does not incur any significant and implemental delay-tracking algorithm, i.e. the delay tracking could only be implemented on a limited number of symbols per radio frame which would yield some useful statistical information provided delays are stationary during the extended observation window (where the cross correlation and covariance matrix would have to be updated based on this finite observation).

3.1.4 Minimum Variance Delay Estimation

Minimum Variance [Tsatsanis1998] and Sub-Space delay estimators are extensions to the matched filter hypothesis and yield near-far resistance. The Minimum Variance (MV) delay estimator is just an extension to the subspace techniques suggested in [Bensley1996, Strom1996] by utilizing the entire signal space, where the algorithm of applying constrained optimization is well known in blind beamforming techniques [Hamid1996, Lorenz2005]. The usual approach to solving constrained optimization problems (and obtaining the detector based on the MV or MSE criterion at the point where the gradient function is at local minima) involves the use of Lagrange multipliers, which convert a constrained predicament to one that is unconstrained. Consider the unknown parameter vector $\boldsymbol{w}$ acting on the received signal vector $\boldsymbol{r}$ where the

output variance $\sigma_r^2 = E\left\{\left|\boldsymbol{w}^H \boldsymbol{r}\right|^2\right\} = \boldsymbol{w}^H \Sigma_r \boldsymbol{w}$. The optimization problem is therefore to minimize σ_r^2, i.e. $\min_{\boldsymbol{w}} \left\{\boldsymbol{w}^H \Sigma_r \boldsymbol{w}\right\}$ subject to the constraint $\boldsymbol{w}^H \bar{s}(\tilde{\tau}_l) = 1$. The Lagrangian function is

$$L(\boldsymbol{w}, \lambda) = \boldsymbol{w}^H \Sigma_r \boldsymbol{w} + \lambda\left(\boldsymbol{w}^H \bar{s}(\tilde{\tau}_l) - 1\right) \tag{3.5}$$

with λ the Lagrange multiplier. To remove the constraint, the gradient of the Lagrangian function is set to zero, i.e. $\frac{\partial L(\boldsymbol{w}, \lambda)}{\partial \boldsymbol{w}} = 0$ giving rise to the weight vector $\boldsymbol{w} = -\frac{\lambda}{2} \Sigma_r^{-1} \bar{s}(\tilde{\tau}_l)$. Since $\boldsymbol{w}^H \bar{s}(\tilde{\tau}_l) = 1$ then λ can be found from $-\frac{\lambda}{2} \bar{s}^H(\tau_l) \Sigma_r^{-1} \bar{s}(\tilde{\tau}_l) = 1$ where $\lambda = -2\left\{\bar{s}^H(\tau_l) \Sigma_r^{-1} \bar{s}(\tilde{\tau}_l)\right\}^{-1}$. Hence the unknown parameter vector is given as

$$\boldsymbol{w} = \frac{\Sigma_r^{-1} \bar{s}(\tilde{\tau}_l)}{\bar{s}^H(\tau_l) \Sigma_r^{-1} \bar{s}(\tilde{\tau}_l)} \tag{3.6}$$

where the denominator to this expression is a scalar quantity. The figure of merit is $P_{MV}\left(\bar{s}(\tilde{\tau}_l)\right) = \boldsymbol{w}^H \Sigma_r \boldsymbol{w}$ which yields[2] $P_{MV}\left(\bar{s}(\tilde{\tau}_l)\right) = \frac{1}{\bar{s}^H(\tau_l) \Sigma_r^{-1} \bar{s}(\tilde{\tau}_l)}$.

The received pilot channel can be sampled at any discrete offset τ, and thus the delay estimator finds the delayed spreading sequence $\bar{s}(\tau)$ that maximizes $P_{MV}\left(\bar{s}(\tau)\right)$, i.e.

$$\hat{\tau}_l = \underset{\tau_l}{argmax}\, P_{MV}\left(\bar{s}(\tilde{\tau}_l)\right). \tag{3.7}$$

The Minimum Variance Estimator does not have to take a block matrix form. It was shown in [Xu2001, Godara1997B] that sequential recursive approaches could be undertaken to estimate the MV filter, including utilizing a blind least squares tracking algorithm forming the so-called blind Minimum Output Energy (MOE) filter [Madhow1998B]. This technique has great validity and implemental aspect for the blind minimum variance receivers proposed in [Xu2001, Godara1997B] for demodulation of single or multiple user channels if the coding is cyclic and deterministic. Such receivers are generically similar to the rake.

---

[2] $P_{MV}\left(\bar{s}(\tilde{\tau}_l)\right) = \frac{\bar{s}^H(\tau_l) \Sigma_r^{-1} \Sigma_r \Sigma_r^{-1} \bar{s}(\tilde{\tau}_l)}{\bar{s}^H(\tau_l) \Sigma_r^{-1} \bar{s}(\tilde{\tau}_l)} \cdot \frac{1}{\bar{s}^H(\tau_l) \Sigma_r^{-1} \bar{s}(\tilde{\tau}_l)}$

3.1.5 SUBSPACE DELAY ESTIMATION

Subspace estimators for timing acquisition have been proposed for single and multiple-user scenarios in frequency flat and frequency selective channels [Bensley1996, Strom1996, Xiao2003]. Subspace techniques are well known in antenna array applications for optimizing a beam based on the direction of arrival (DOA), where a subspace classifier utilizes the geometric properties of an assumed data model to apply a near-optimum parameter estimate close in quality to the Cramer-Rao lower bound [Stoica1989]. There exist many algorithms exploiting the geometric properties and decomposition of the signal covariance matrix for subspace estimation- where the more famous techniques in the literature are namely the Multiple Signal Classification (MUSIC) [Schmidt1986] and the Estimation of Signal Parameters via Rotation Invariance Technique (ESPRIT) [Roy1989]. The ESPIRIT estimation technique is more robust and less computationally expensive than the MUSIC technique, although it requires a displacement structure within the covariance matrix and the algorithm performs poorly with correlated sources. Hence it will not be considered in this thesis. MUSIC applies parameter estimation (in this case the delays) by splitting/decomposing the received vector space into a signal space (containing the subspace spanned by all the multi-user signals) and an orthogonal noise subspace. The general approach considers Eigen-decomposition of the covariance matrix [Johnson1982] where the signal and noise contributions are taken from the vector space in descending orders- where a sample trial of the largest eigenvalues correspond to the sources, and the remaining assigned to be noise. With the modelling assumption $\boldsymbol{r} = \boldsymbol{S}\boldsymbol{d} + \boldsymbol{n}$ (with $\boldsymbol{d}=\xi\boldsymbol{b}$) where the M fractionally spaced samples (for the nth Pilot symbol) of $\boldsymbol{r}$ are stored in an M element vector, the covariance matrix $\sum_{\mathrm{r}} = E\left(\boldsymbol{r}\cdot\boldsymbol{r}^{\mathrm{H}}\right)$ can be decomposed into $\sum_{\mathrm{r}} = \boldsymbol{S}\,E\left(\boldsymbol{d}\cdot\boldsymbol{d}^{\mathrm{H}}\right)\boldsymbol{S}^{H} + \sum_{\mathrm{n}}$. Assuming further that the matrices $\boldsymbol{S}$ and $E\left(\boldsymbol{d}\cdot\boldsymbol{d}^{\mathrm{H}}\right)$ are full rank[3], the signal subspace is deemed the column space of $\sum_{\mathrm{r}}$ i.e. the $range[\boldsymbol{S}\,E\left(\boldsymbol{d}\cdot\boldsymbol{d}^{\mathrm{H}}\right)\boldsymbol{S}^{H} + \sum_{\mathrm{n}}]$ with the noise subspace assumed as the orthogonal complement to the signal subspace. Since $\sum_{\mathrm{r}}$ is Hermitian and positive definite, there is an Eigenvalue decomposition where assuming the covariance $\sum_{\mathrm{r}}$ in the metric of $\sum_{\mathrm{n}}$ is known [Smith1994]

[3] The matrix $\boldsymbol{S}_c$ is of full rank when all its columns are independent for all delay realizations. This is probable in DS-CDMA employing random orthogonal coding for different user signatures.

$$\Sigma_r = \begin{bmatrix} \boldsymbol{E}_c & \boldsymbol{E}_z \end{bmatrix} \begin{bmatrix} \boldsymbol{\Lambda}_c & \boldsymbol{0} \\ \boldsymbol{0} & \boldsymbol{\Lambda}_z \end{bmatrix} \begin{bmatrix} \boldsymbol{E}_c & \boldsymbol{E}_z \end{bmatrix}^H \in C^{M \times M}. \tag{3.8}$$

$\boldsymbol{E}_c \in C^{M \times N}$ is the matrix of eigenvectors (deemed the signal subspace) corresponding to the $N=L(K+1)$ largest eigenvalues (with $N < M$), where $\boldsymbol{\Lambda}_c = diag[\lambda_1, \lambda_2, \cdots, \lambda_N] \in R^{N \times N}$ with λ_i being the non zero eigenvalues ($\forall\ i, i \leq N$)of the vector space Σ_r. $\boldsymbol{E}_z \in C^{M \times (M-N)}$ are the eigenvectors corresponding to the $(M-N)$ smallest non-zero eigenvalues $\boldsymbol{\Lambda}_z \in R^{M \times (M-N)}$ of Σ_r and is thus the noise subspace. The fundamental observation [187] is that the columns of $\boldsymbol{S}_c$ are orthogonal to the noise subspace, i.e. $E\left\| \boldsymbol{E}_z^H \bar{\boldsymbol{s}}(\tau_l) \right\|^2 = 0$. In practice the covariance matrix in the metric of Σ_n must be estimated with $\hat{\Sigma}_r \approx \frac{1}{M} \sum_{i=0}^{M-1} \boldsymbol{r}_i \cdot \boldsymbol{r}_i^H \approx \hat{\boldsymbol{E}}_c \hat{\boldsymbol{\Lambda}}_c \hat{\boldsymbol{E}}_c^H + \hat{\boldsymbol{E}}_z \hat{\boldsymbol{\Lambda}}_z \hat{\boldsymbol{E}}_z^H$ where the columns of $\hat{\boldsymbol{E}}_z$ are estimated to be the M -N smallest eigenvalues of $\hat{\Sigma}_r$ after decomposition. However, based on this estimation, the columns of $\boldsymbol{S}$ will only be approximately orthogonal to the columns of $\hat{\boldsymbol{E}}_z$ hence this technique will only be suboptimum. Based on the property $E\left\| \boldsymbol{E}_z^H \bar{\boldsymbol{s}}(\tau_l) \right\|^2 = 0$, it is possible to build a subspace delay estimator for finding the delay code $\bar{\boldsymbol{s}}(\tau_l)$ that minimizes this expression (with $\bar{\boldsymbol{s}}(\tau_l)$ acting as a steering vector where if the directions are orthogonal to the noise in an eigenvector sense, the delay variable τ_l is likely to have occurred). Formally, this can be denoted with a figure of merit $P_{MUSIC}\left(\bar{\boldsymbol{s}}(\tau_l)\right) = \frac{\left\| \boldsymbol{E}_z^H \bar{\boldsymbol{s}}(\tau_l) \right\|^2}{\left\| \bar{\boldsymbol{s}}^H(\tau_l) \cdot \bar{\boldsymbol{s}}(\tau_l) \right\|} = \frac{\bar{\boldsymbol{s}}^H(\tau_l) \boldsymbol{E}_z \boldsymbol{E}_z^H \bar{\boldsymbol{s}}(\tau_l)}{\left\| \bar{\boldsymbol{s}}^H(\tau_l) \cdot \bar{\boldsymbol{s}}(\tau_l) \right\|}$ and the delay estimator becomes

$$\hat{\tau}_l = \underset{\tau_l}{arg\ min}\ P_{MUSIC}\left(\bar{\boldsymbol{s}}(\tilde{\tau}_l)\right). \tag{3.9}$$

Note this algorithm is one where the power must be minimized rather than maximized to obtain the delay estimate. Also in real single user detection, the dimensionality of the signal space must be estimated or assumed a priori for best performance. A general approach utilizing the

Minimum Description Length (MDL) criterion [Wax1985] can be applied to estimate the number of sources prior to the subspace technique described in this section.

3.1.6 Acquisition Time for Delay Path Estimation

Acquisition of the variable delays is based on the selection of the maximum (or in the case of the MUSIC algorithm, the minimum) matched filter output per code shift that cause the optimum/near-optimum quality factor. In this case, the work presented in 1984 on Spread-Spectrum code acquisition [Weber1984A, Weber1984B] will give a useful insight into the timing acquisition for any delay approach rendering a correlative/FIR convolution process. The so-called "Unified Theory of Timing Acquisition" is henceforth used for analysis of each technique. The process state diagram presented in these papers is a simple finite state machine allowing the acquisition state function $P_A(Z) = \dfrac{P_T Z^M}{1-(1-P_T)Z^{M+T_F}}$ to be formulated and the mean acquisition time determined where $T_{ACQ}(Z) = \left(\dfrac{\partial}{\partial Z} P_A(Z)\big|_{Z=1} \right)$ and hence

$$T_{ACQ} = [M + T_F(1-P_T)]P_T^{-1}T_C. \tag{3.10}$$

P_T is the probability of successful delay acquisition within the observation interval, T_F is a chip index metric obtained from the false alarm acquisition probability and denotes the number of chip delays incurred by false acquisition (i.e. it is a penalty factor highlighting the length of time until a new trial can ensue to find the correct delay). T_C is the chip interval in seconds, and z is the sample delay parameter in the z-domain.

3.2 Channel Estimation

The simplest channel estimator utilizing the CPICH [Fantacci2005] is formed by splitting the channel into a set of L delay path elements (after delay estimation), where each delay channel is descrambled and the pilot symbol modulation removed by multiplication with its conjugate. The initial channel estimates will be extremely noisy due to the additive noise and interference; hence it is proposed to employ smoothing filters (with moving average) to yield an approximate expectation calculation at the sample decision instant. This technique has very variable noise

and interference robustness depending on the rate of fading- i.e. in slow fading channels, long filtering windows will yield accurate channel estimates, but in fast fading channels, the length of the averaging filter has to be short and hence channel estimates will be noisy. Generally, moving average filter lengths of 32 chips should yield acceptable performance for most cases provided interference is not too limiting. The channel estimates at the output of a moving average filter are defined as

$$\hat{c}(\tau) = \sum_{i=0}^{M} \frac{P^*}{M+1} \tilde{c}(n-i) \tag{3.11}$$

with $\tilde{c}(n) = S_c^*(n) \otimes r(n)$ the noisy initial pilot symbol estimate and n the symbol index. P^* is the conjugate of the pilot symbol and S_c a row vector of scrambling signatures for the received symbol block processed within the averaging filter. The Fig 3.1 shows a generic block diagram of the channel estimator as used in a conventional matched filter data estimator. Several sub-optimum approaches can be undertaken to improve the quality of the estimate for short code CDMA. Long-code CDMA channel estimation is extremely difficult to optimize without having to resort to algorithmic approaches requiring unreasonable assumptions and complexity. This is due to the fact that useful statistical information regarding interference cannot be obtained since the coding only exhibits cyclostationary on a frame by frame basis, hence the multipath parameters that require estimation need an implausible assumption incurring that the channel is completely stationary over the length of time for gathering sufficient statistics (needing a high number of 10ms radio frames).

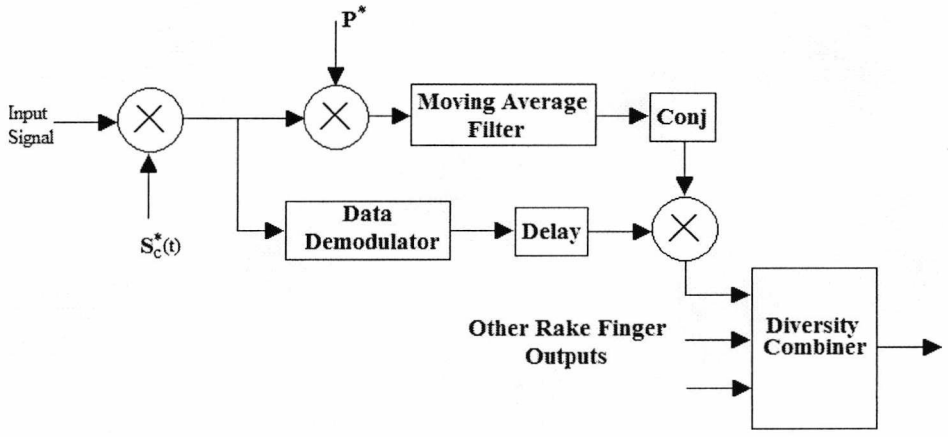

Fig. 3.1 A diagrammatic interpretation of the channel estimator as used in a Rake receiver.

An alternative approach to channel estimation can be applied for short-code CDMA systems using FIR Linear prediction, where the adjacent channel interference can be mitigated to improve the quality of estimate. The linear predictor minimizes the partial derivative of the quadratic cost function $\frac{\partial}{\partial w} = E\left\{\left(\hat{c}(\tau) - w^H r\right)^H \left(\hat{c}(\tau) - w^H r\right)\right\}$ leading to the unbiased estimate $\hat{c}(\tau) = w^H r(\tau)$ with

$$w = \sum_r^{-1} \Lambda \tag{3.11}$$

and $\Lambda = E\{\hat{c}(\tau) \cdot r\}$. The weight vector, w does not have to be calculated utilizing sampled matrix inversion. Stochastic gradient estimation applying arithmetically simpler recursive filters built with algorithms such as the Least Mean Squares or Recursive Least Squares [Kay1996] can be used to form the estimator. Such algorithms require training, where the channel estimator will initially use the soft outputs from the moving average filter estimator presented at the beginning of this section. The adaptive filter weights are initially set to the Moving Average filter definition prior to training. The Fig 3.2 yields a general block diagram of the channel estimator employing adaptive learning based initially on the error between the output of the filter and the soft outputs of the low pass filter (defined as the moving average filter). When the filter starts to converge, the training waveform is then the one symbol delayed previous output.

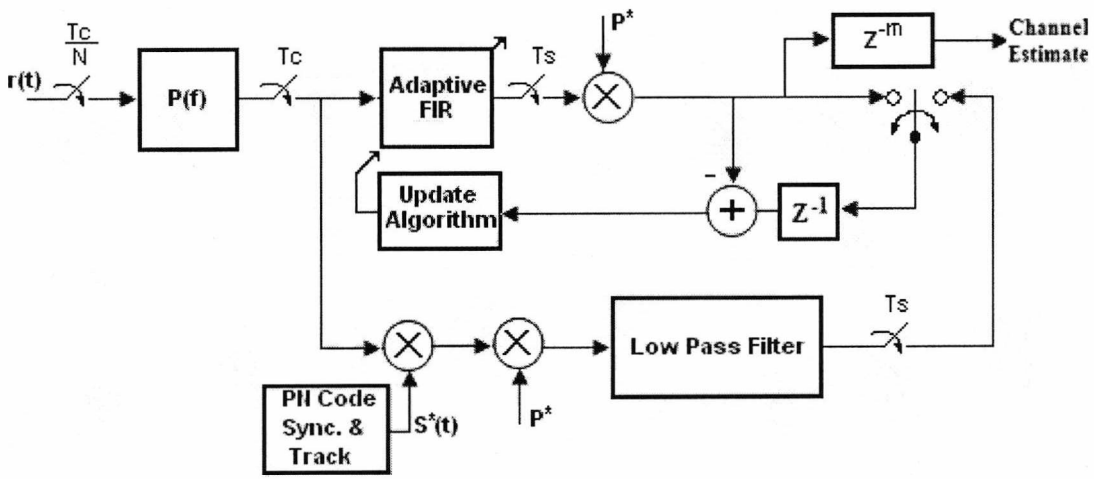

Fig. 3.2 A diagrammatic interpretation of the adaptive linear predictor channel estimator.

Channel estimation in advanced signal processing techniques for detection is usually obtained during data demodulation utilizing the structure and properties of the detector in use. However, assuming a generic model not applying interference cancelling or equalization techniques, an unconstrained likelihood approach can be undertaken to remove the content of the delay channel for inter-code interference suppression on the pilot channel itself (at a cost of increasing the noise floor including the adjacent channel interference). Detectors employing the unconstrained likelihood minimization are often called Decorrelators [Verdu1998], where the matrix transformation utilizes the structure of the scrambling code matrix (with delays) to project the interference code channels into the space spanned by the noise thus allowing interference suppression. In such a case, the unmodulated Pilot vector must be treated as information in the multiplexed data stream along with adjacent code channels, hence the algorithm necessitates knowledge of all active codes and requires that all available channels are jointly estimated. This level of optimization is not usually achievable in single user demodulation unless overhead is yielded in the radio frame to make such information available.

3.3 NUMERICAL EXAMPLES

The first set of results that can be obtained for delay acquisition will examine the effect of cell loading and near-far ratio on the probability of successful acquisition. Using the results obtained, it is then possible to use a semi-analytical approach to attain the mean acquisition times per algorithm in use, and hence validate each technique for trade-offs in complexity, acquisition time, and overall performance. The next set of results will examine the accuracy of the channel estimation schemes presented in terms of the MSE between expected and calculated estimates for different pilot channel signal to noise + interference (SINR) ratios. This will allow a direct comparison of the schemes when used in a conventional rake receiver- allowing a further consideration on the effect on the QOS offered by the device in channel uncoded multiuser WCDMA downlink. The following simulation parameters were observed: The carrier frequency was 2.1GHz and the channel was considered the ITU Vehicular channel A with normalized Doppler shift of 5.135×10^{-3} (translating to a Vehicular speed of 36Km/Hr). The data rate on the adjacent channels (including the multiple access channels) was set to 16Kbps for the single user, with a random spread of data rates for the multiple access channels with one channel set to a high power 384Kbps rate. The statistical observation interval for the covariance matrix

optimizations was set to 100 Pilot symbols. The probability of successful acquisition and false alarm probability was observed for two cases where: (A) The multiple access interference had random near-far ratio (with maximum NFR = 3dB for one channel comparison to the single user channel) when the observed parameter was made a function of the number of users, (B) The number of users occupying the downlink capacity was set to two, with the NFR varied by simulation. The probability of acquisition was measured using Monte Carlo simulation, where this metric was considered yielding a successful trial if the significant delay paths were captured within 0.0625 of a chip interval from the ideal time delay. Note that some biasing was made to the real delays due to the sampling resolution of Matlab, hence in such a case the delays of the Vehicular A channel were modified and quantized to be within a maximum 0.125 chip error from the real delays. The mean acquisition times were analyzed using (2.50), where the chip period was set to 0.26μs, the observation intervals were set to 100 Pilot symbols (for the MV, Whitening and MMSE algorithms to gather sufficient statistics), the false alarm time was set to 10ms (corresponding to 150 Pilot symbols), and the mean SNR for the single user channel set to 15dB. The number of users was a variable. The channel estimation schemes and simulations considered the same parameters used for the delay acquisition probability (A), where the length of the moving average filter was variable for the first estimation scheme (the SNR metric for this simulation is in fact the SINR). The second set of channel estimation results used the same simulation parameters, except now the desired channel SNR was used as the argument against the mean square error for the conventional and MMSE channel estimator. The rake receiver simulation considered a multiple user scenario (10 users were considered to be simultaneously operating in the access channel) where observations were generated for its diversity performance with a variety of channel estimation schemes.

The first observation (Fig 3.3) considered the probability of delay acquisition of the MV, MUSIC, Whitening, conventional MF, and MMSE algorithm for a variable number of users. It can be seen in this case that all techniques offer similar and good performance for low loading, where divergence of the schemes occur when the number of users > 11. In highly loaded cells, the MV technique offers the best performance while the MUSIC estimator performs very poorly. The MMSE, Whitening and conventional MF operate poorly when the number of users > 21, but offer reasonable performance below this margin. The case (Fig 3.4) for a 2-channel transmission (excluding the Pilot) investigating the false alarm probability shows that the MV and Subspace largely mitigate the Near-Far effect, whilst the conventional scheme performs poorly when the NFR > 10dB. The Whitening and MMSE estimators offer intermediary performance, and exhibit some near-far resistance. The second observation (Fig 3.5) considered the effect of the

MV, MUSIC and MF delay acquisition on the probability of error performance of the Rake receiver. It is seen here (where the simulation result was obtained by averaging the error performance over 1000 bit sequence and channel realizations) that the performance of all schemes operate quite close to the theoretical lower bound until K > 10. For K > 10, the probability of acquisition decreases (and probability of false alarm increases) hence yielding significantly higher probability of error particularly for the MUSIC algorithm. Note that the length of the matched filters was 32 chips (one symbol interval). The third observation (Fig 3.6) considered the acquisition time for all the algorithms discussed thus far for delay estimation. The overriding observation is that the MV algorithm performs with the least acquisitions time, whilst the other techniques yield amicable performance in comparison until the number of users increase beyond about ten, after which the MUSIC algorithm yields unacceptable performance. The conventional, Whitening and MMSE schemes (along with the MUSIC scheme) become rather limited (i.e. long acquisition times) for high cell loading. The forth observation (Fig 3.7) considered just the moving average channel estimator with thee SNR boundaries namely at 0dB, 10dB, and 20dB. The length of the moving average filter was observed for this Vehicular channel, where it is clear a minima was observed for the moving average filter taps close to 16. It was stated in section 2.3.5 that filter lengths of 32 were acceptable, where the simulation concurs with this observation. This filter length of 32 is not arbitrary; where Pedestrian channels that are relatively slowly faded can incur a cost of longer filtering windows for improved accuracy. Realistic implementation of channel estimation will be largely oblivious to the channel environment (which could indeed include any sort of terrain, possible line of sight, pedestrian or vehicular channels and non-deterministic delay spread) hence a mid-level trade off between accuracy and complexity is proposed between the vehicular channel and pedestrian channel optimum operating point. The fifth observation (Fig 3.8) concurred that the short-code channel estimation schemes employing the more advanced adaptive linear predictor improved the quality of the channel estimate over the moving average filter implementation. It can be seen the MMSE estimator offers worse performance than even the conventional scheme when the channel quality is low (for high channel quality it yields the best performance out of all the channel schemes). Although for SINR > 5dB, the performance advantage at little cost to complexity is obvious.

However, this estimator is not suitable for long-code CDMA, whereas the conventional scheme is largely code-independent in terms of performance[4]. The sixth observation (Fig 3.9) considers the effect of the different channel estimation schemes on the performance of the rake receiver. In this case it is clear that the MMSE scheme offers the best diversity performance in terms of the probability of error metric. However, the performance difference between is rather minimal hence unless exceedingly accurate channel estimates are required, the conventional moving average approach should yield acceptable performance for a variety of sub-optimum detectors including the Rake receiver.

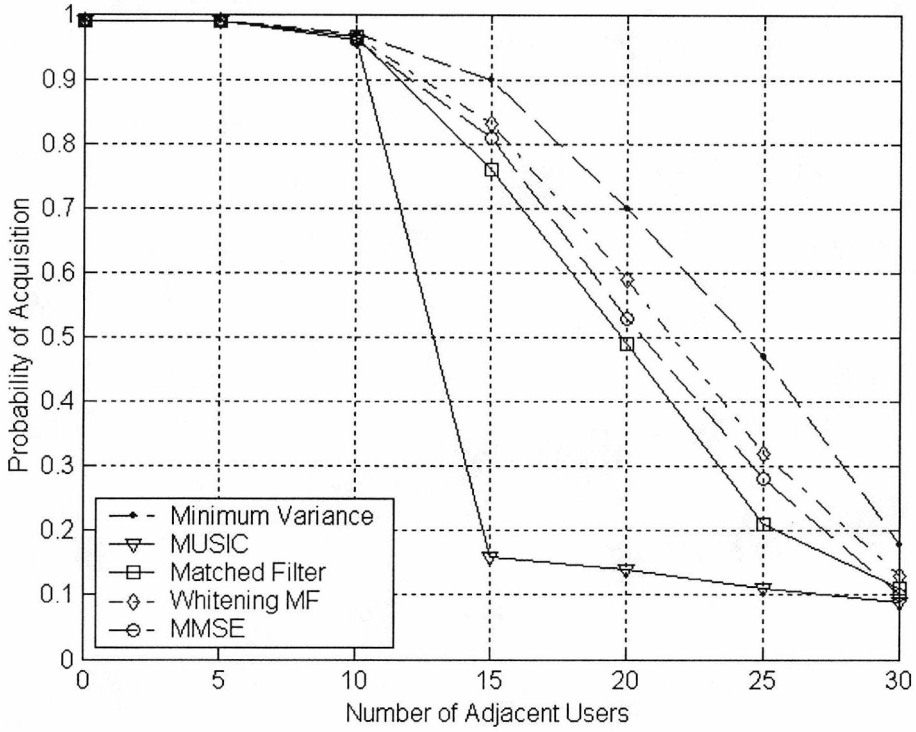

Fig. 3.3 The Probability of acquisition as a function of the number of the users for the Minimum Variance, MUSIC, MMSE, Interference Whitening, and Matched filter correlator.

[4] By code independent, we still assume that the scrambling code is cyclic but spans an interval longer than a single symbol period thus negating the severe impediment when short Hadamard codes are unmodulated and transmitted through a dispersive channel causing ISI. The receiver under conditions where the delay spread is similar to the chip interval, the delay acquisition would only see one path thus resulting in a loss of diversity.

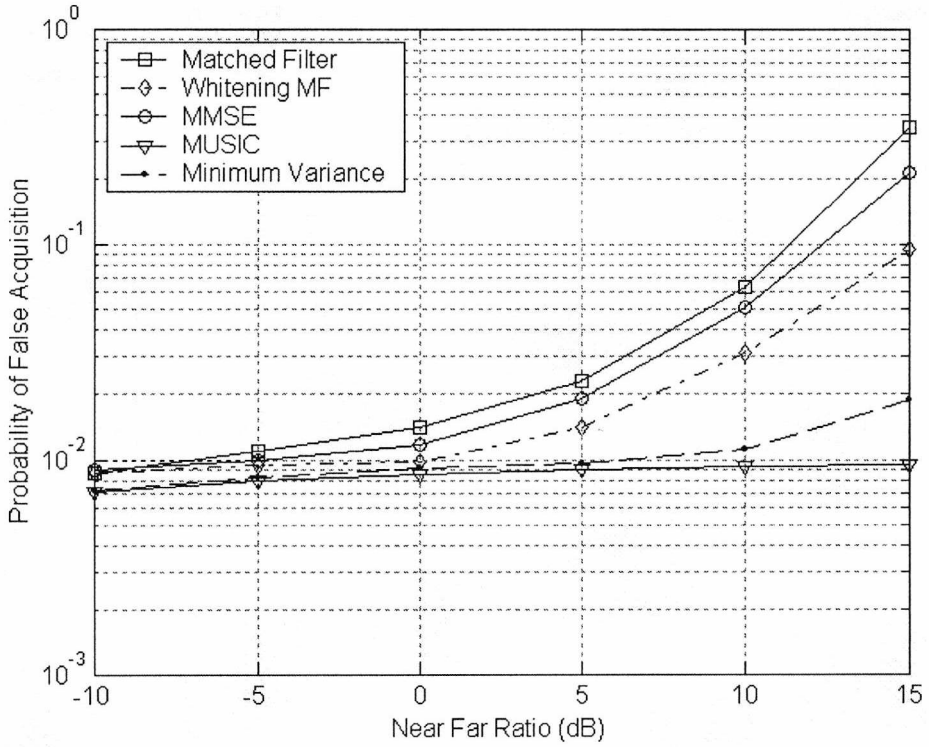

Fig. 3.4 The Probability of false acquisition as a function of the number of the near far ratio between two users for the Minimum Variance, MUSIC, MMSE, Interference Whitening, and Matched filter correlator.

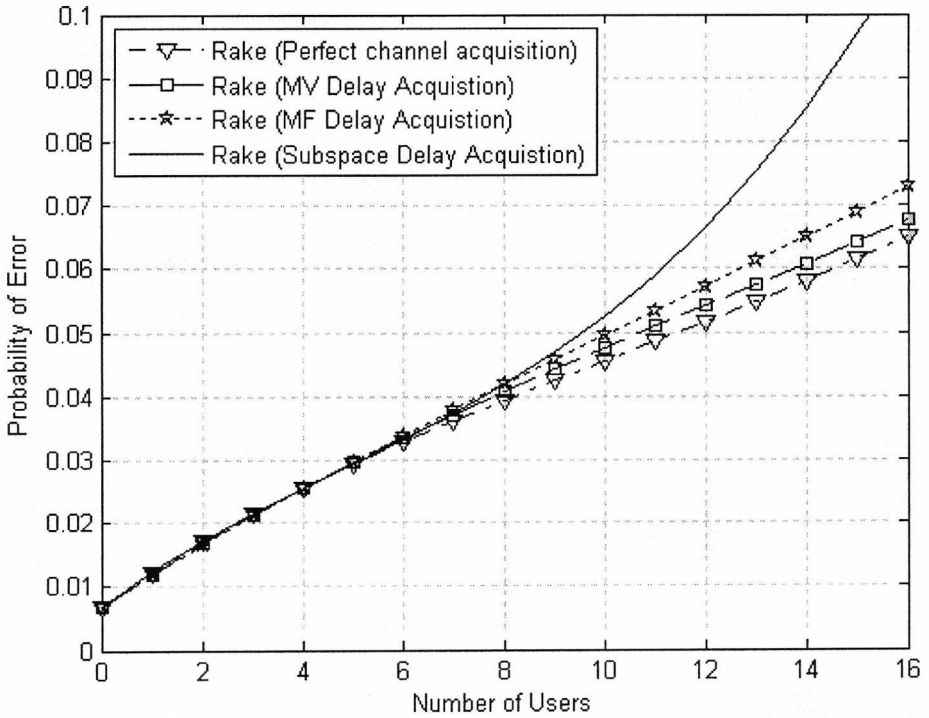

Fig. 3.5 The Rake receiver probability of error Vs number of users for the MUSIC, MV and MF delay estimators.

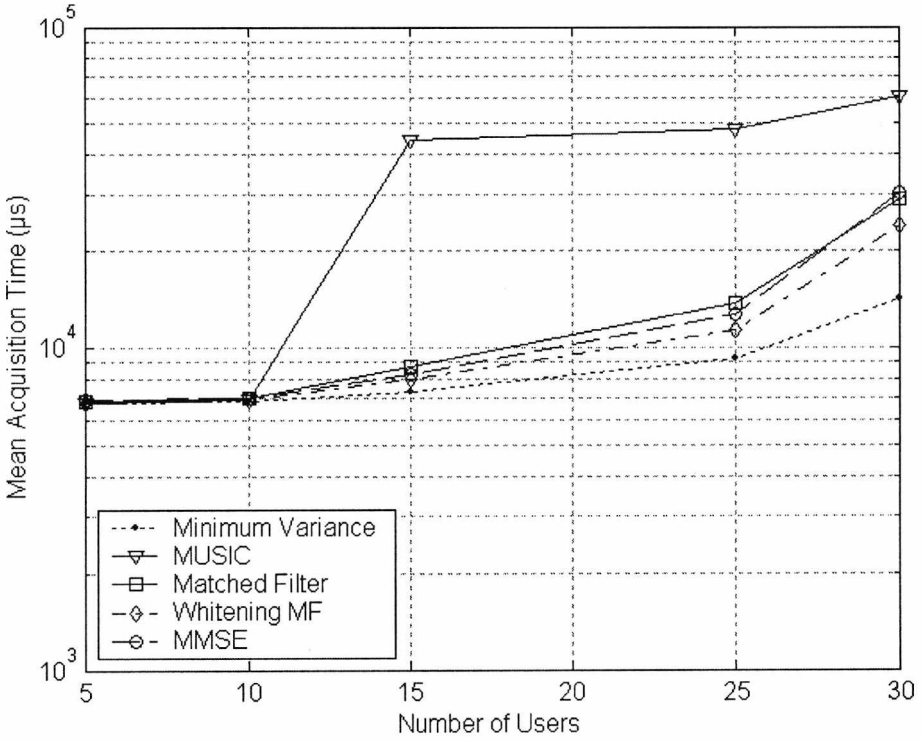

Fig. 3.6 The mean acquisition time as a function of the number of the users for the Minimum Variance, MUSIC, MMSE, Interference Whitening, and Matched filter correlator.

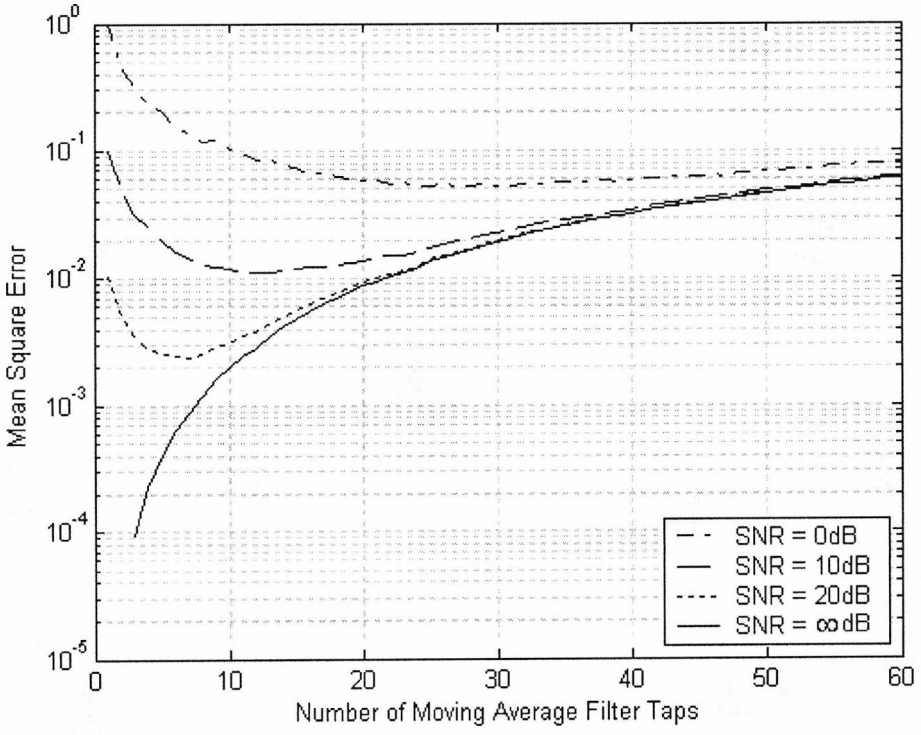

Fig. 3.7 The mean square error as a function of the number of moving average filter taps for the conventional channel estimator for three cases where the SINR = 0dB, 10dB and 20dB.

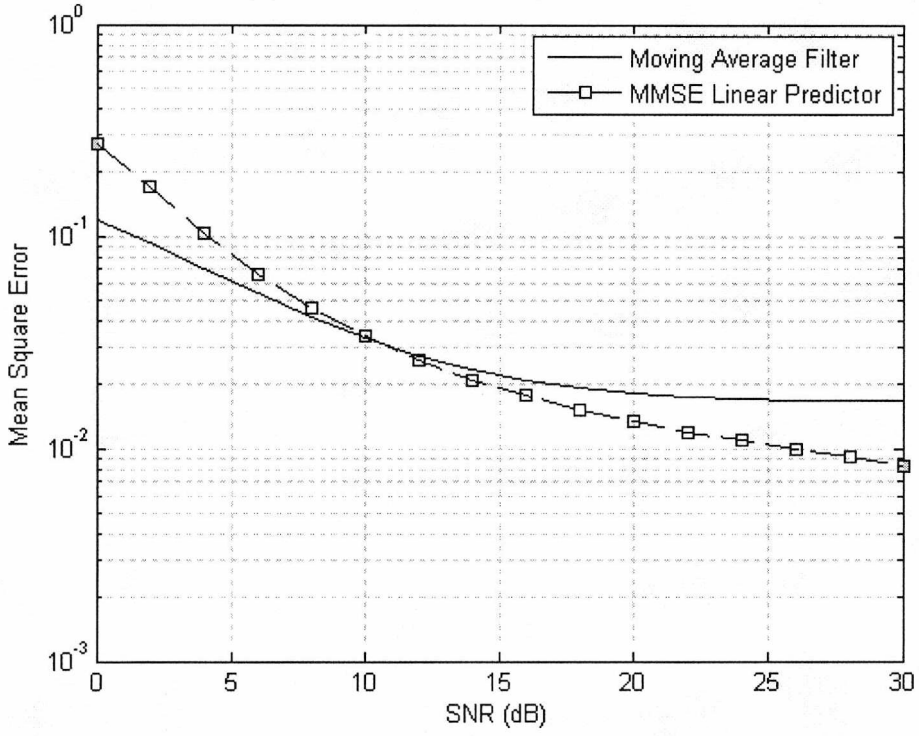

Fig. 3.8 The Mean Square Error Vs the single user channel SNR for a Vehicular A channel considering two channel estimators, namely the MMSE and Moving Average Filter.

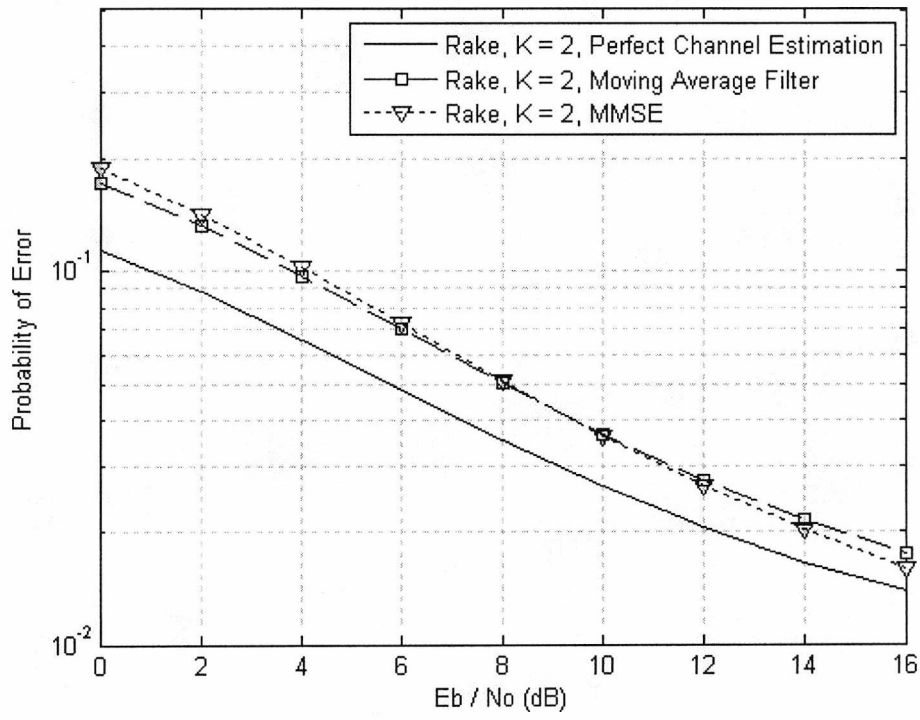

Fig. 3.9 The Probability of Error as a function of the single channel SNR considering two channel estimators, namely the MMSE and Moving Average Filter when implemented for a four finger Rake receiver.

3.4 DISCUSSION

Delay and channel acquisition with tracking are very important when defining diversity and optimum receivers in fading channels, particularly so when QOS requirements are stringent. Their relevance for optimum signal demodulation will be expatiated on in future chapters since delays and the fading parameters are expected to change during a transmission spanning more than a single radio frame[5]. For matrix level optimizations it is particularly important for defining the structure of the rows and columns in terms of where and when delays are included, otherwise the matrix inverse and pseudo-inverse will be ill-conditioned to the real sampled data. Hence it is imperative in a real time application that the delay and channel state information is decoupled into the demodulator to allow for one shot, finite window or sequential/recursive optimization with correct statistics. This problem is not so prevalent in adaptive filtering employing equalizers, where the only requirement for coherent reception is that a single delay path must be synchronized.

It is with clarity that sub-optimum detection of the delay paths are achievable utilizing correlation and/or matrix transformations based on a finite observation interval. The level of complexity from an implemental aspect varies according to the algorithm presented. It is fairly obvious that whitening requires that the statistics of the noise and interference are known or that at least the detector has the ability of obtaining the statistics from signaling and multiple code priori's. From a single user aspect, this is difficult to achieve practically, and the interference statistics would have to be estimated, either using feed-forward subtraction based on coarse decisions at the output of a correlation detector, or sampled matrix inversion rendering $\boldsymbol{L}^{-1} = \Sigma_{\mathrm{r}}^{-1/2}$ utilizing the desired signal + interference + noise space (where even the desired signal is treated as noise and thus the matched filter will be ill-balanced in terms of producing a statistically white interference solution). The aforementioned Minimum Variance delay estimator utilizes the sample covariance matrix (which must be estimated iteratively prior to applying matrix inversion), and while it is perfectly feasible for use in single user detection, the matrix size is prohibitively large for correlation windows expanding more than 3 Pilot symbols (as defined in current 3rd Generation networks), hence is of limited use if very long scrambling signatures are used. In such a case, it is suggested to truncate the size of the window by applying an observation length no greater than 3 equivalent symbols at the Pilot signaling data rate with one assigned symbol per cyclic code (allowing the receiver to capture all past, present

[5] The radio frame for UMTS spans one transmission time interval (TTI) defined as being 10ms.

and future timing delays). This is obviously impractical in long code non-cyclic CDMA downlink. A similar issue exists for subspace techniques, where matrix decomposition requires time-consuming iterations. Clearly the simplest delay estimator is the correlation receiver that actually requires no physical multiplication since the code-matched filters contain only unity weights plus a sign bit. The Table 3.1 shows a summary of the aforementioned delay path estimators and yields a brief account on the comparison between the algorithms in terms of performance, complexity, and practicality for long and short coding[6].

Delay estimation in WDCMA networks must be able to cope with moderate system loading to yield a desirable level of performance, yet also exhibit low complexity and fast acquisition to be realistic. Delay estimators must also be robust to different network impediments such as power imbalance, multiple access and narrowband interference. Estimators such as the MMSE and matched filter correlator (the conventional and whitening approach) require significant training in order to estimate the input and output statistics. While generation of sufficient training symbols is not a significant technical issue in the WCDMA downlink employing a common pilot channel, the acquisition time is fairly high when the system performance is interference limited. On the other hand, the complexity of correlation techniques is rather simple. Subspace and Minimum Variance delay estimators are blind and do not necessitate knowledge of the adjacent channel transmitted signatures and symbols (where interference whitening and the ideal MMSE solution requires this knowledge) and are interesting solutions to correlation based algorithms that are sensitive to interference and near-far effects. The acquisition time performance is very dependent on the number of users for the subspace delay estimator where high loading will make this receiver very inefficient (despite offering the best near-far resistance). In low SNR scenarios, the MUSIC subspace method does not perform well since the subspaces are not well separated and are limited to scenarios with low system throughput to allow fulfillment of the low rank signal assumptions employed in the derivation of the detector (subspace methods are generally derived based on the assumption of white Gaussian noise). Apposed to the subspace estimation procedure, the Minimum Variance estimator offers reasonable performance in a variety of near-far and loading situations exhibiting fairly low acquisition time compared to the correlator unless the number of users is very low.

---

[6] By short codes, it is not intuitive to consider the actual processing gain but rather whether the codes repeat on a symbol by symbol basis. Hence in this definition, short codes exhibit cyclostationary regardless of the length of code (which by convention is the processing gain as a non-decibel dimensionless metric).

Table 3.1 A brief comparison between the delay path estimators.

	Conventional Correlator	Whitening Correlator	Music Algorithm	Minimum Variance	MMSE
Training	None	Requires Priori	Blind	Blind	Pilot Signal
Performance	Near Optimum for Single User Channels in AWGN. High cell loading and NFR yields large performance degradation.	Exhibits some resistance to the number of users and NFR.	Fairly resistant to the NFR and Cell loading.	Good resistance to number of users and NFR.	More robust than correlator, but not Near-Far resistant. Performance depends on the number of users.
Complexity	Low	Greater complexity over conventional correlator.	Greater complexity over conventional correlator and Whitening solution.	Fairly high complexity of implementation.	Less complex than other techniques, more complex than correlator.
Implemental Aspect	Suitable for short and long codes.	Short codes only.	Short codes only.	Short codes only.	Mainly short codes. Long code application limited in terms of complexity and accuracy.

To this end, the Minimum Variance estimator is in some sense the most attractive alternative solution to the correlation-based detector[7] (although it offers a considerably higher complexity of implementation). The whitening and MMSE approaches yield some improvements in term of acquisition time and performance compared to the conventional correlation receiver; however they require long training windows and are subsequently more processing intensive. Subspace, MV and Maximum Likelihood (ML) methods deliver robust performance in near-far scenarios where theoretical results show that the performance bounds of these estimators are independent of the signatures and signaling powers of adjacent users. The ML estimators presented in [Bensley1996, Strom1996] yield far better performance in heavy loaded cells over all other "sub-optimum" schemes.

Traditional correlation based techniques may also be applied to long-code WCDMA. As in short-code systems, this technique is interference and the near-far limited where via the central limit theorem, the statistics of interference are near-Gaussian when a large number of users are active. An advanced statistical processing methodology can be applied to long code systems [Liu2002, Buzzi2003], although these generally invoke computationally complex algorithms that make practical implementation applying blind optimization or the likelihood principle rather questionable- particularly considering that a single user detector is blind to the code-orthogonal multi-user signatures. For this very reason, delay estimation for long-code

[7] The correlation/matched filtering based technique is used for delay estimation in the current UMTS downlink. This is chiefly due to the fact that the correlator is simple to implement and practical, while performance is also sufficient in the majority of realistic cases.

systems has not received much interest for active corporate Research and Development. A general conclusion of long-code estimation is that of greatly increased computational complexity since the time varying spreading codes lack sufficient statistics in relatively small time intervals due, in part to the cyclostationarity being destroyed when the spreading code is different for each information symbol. Hence general optimizations based on Bayesian or Likelihood theory for synchronization, delay tracking, data demodulation, and channel estimation (that are normally formulated for short-codes) yield no direct simplistic application in long-code systems. However, it was also stated in sections 3.1.1 – 3.1.5 that several of the more advanced processing methodology proposed for short code could also be applied in the long-code case. This of course relies on the gross assumptions that the channels and the number of users are completely stationary.

It was shown that channel estimation employing the moving average filter is perfectly acceptable for a standard rake diversity receiver employing long or short coding. For short code systems, the MMSE filter can be applied for the cases when the cell loading are not overly large and hence yield some improvement to the accuracy of the channel estimate. It is proposed in this thesis that the moving average filter definition is acceptable for the LMMSE rake receiver and adaptive forms of the LMMSE rake receivers. In the cases where an equalizer is implemented based solely on the channel estimates themselves, then the subtractive MMSE/Likelihood approaches would likely be required to prevent the filter being too divergent spectrally from the ideal inverse filter.

The standard receiver in WCDMA is the RAKE receiver, where the receiver multipath diversity is utilized by correlating the received signal with spreading codes that are ideally synchronized to different multipath delays assigned to different RAKE fingers. The Rake finger outputs are combined utilizing channel cophasing and a coarse estimate of the adjacent pilot channel power to achieve the maximum SNR at the receiver output before data detection (this of course is based on only a single channel assumption). The RAKE receiver is near optimum in a single-user point-to-point link, or in cases where multipath dispersion does not cause the multiple-access spreading codes to lack orthogonality in all delay paths. In real frequency selective channels, the multipath medium behaves equivalently to asynchronous transmission (as is the case in the uplink) and the receiver becomes vulnerable to the interference from the other users since it is highly difficult to design and implement spreading sequences that are orthogonal for all time offsets. Hence interference from adjacent users is unavoidable and the near-far problem can be particularly serious unless strict power control is invoked. However, in current WCDMA standards, this is not an easy problem to overcome if the number of users serviced in a

cell is large – since the geometry factor and received power per user exhibits rapid variations that are near impossible to overcome by this technique. An alternative approach for dealing with the far – near effect interference would be to consider near – far and multiple-access resistant receivers that do not necessitate strict power control.

CHAPTER 4
PERFORMANCE OF ADVANCED DUAL ANTENNA RECEIVERS FOR SINGLE USER DEMODULATION IN WCDMA CHANNELS

PREFACE

Chapter 2 investigated the performance of diversity combiners utilizing a dual antenna array. Chapter 3 explored different channel estimators for use in temporal/joint temporal-antenna diversity applications. This chapter explores more advanced diversity concepts for the WCDMA downlink, where adaptive and hybrid combining techniques are shown to significantly improve the performance of the downlink without having to resort to computationally exhaustive algorithms normally seen in the realm of optimum detection. Furthermore, the two-dimensional rake algorithm is extended in this chapter with decorrelating or interference whitening transforms forming a generalized broadband beamformer for combating doubly selective fading channels. This chapter is organized as follows: Section 4.1 overviews the 2D Rake receiver [Mostafa2004], where the contributions of this section involve an analytical approach to the idealized algorithm for flat fading channels, as well as a practical – analytical discrimination for multiuser temporally dispersive channels. A further contribution in this section is the derivation of the maximum ratio-combining rule for the rake receiver for improving the downlink performance over the traditional rake-combining rule (that being cophasing and equal gain combining). Section 4.2 presents an overview of the Rake-assisted beamformer [Song1999] giving a description of the numerical results obtained. Section 4.3 investigates the application of joint spatial – temporal receivers for decorrelating chip-level interference generated from a multipath-fading channel. This approach forms the structure of a broadband beamformer, where optimizations at chip or symbol rate can ensue to improve the downlink asymptotic efficiency in selective fading channels. The receivers developed in this section employing precise filter transformation can also be made adaptive to simplify the computational cost (and the requirement of exact knowledge of the channel).

4.1 THE TEMPORAL-SPATIAL DIVERSITY RECEIVER

The two-dimensional rake receiver consisting of a bank of chip-matched filters (after descrambling) assigned to resolvable multipath components utilizes an extra degree of freedom by exploiting the spatial selectivity of the channel with an extra antenna element separated by half a wavelength. The receiver (Fig. 4.1) symbol estimates (after CMF) are cophased and then input into a per-path spatial combiner to yield the decision statistic. The spatial combiner can be implemented according to any generalized diversity rule, where in this thesis rake finger level combining [Kohno1998] is utilized according to the EGC hypothesis assuming equal noise + interference variance on each antenna element for the L^{th} temporal diversity path. The outputs of all rake fingers are then optimally combined to generate the receiver decision statistic. The optimum combiner derived in Appendix F is given by (4.1), where the decision metric assuming antipodal symbols is

$$\Omega = \sum_{l=1}^{L} \frac{\sqrt{\hat{E}_b^l}}{\sqrt{\hat{E}_p^l}} \times \frac{\Re\{P_l^* Z_l\}}{\sigma_l^2} \tag{4.1}$$

with $Z_l = \sum_{i=1}^{A} \alpha_i^{(l)} \sqrt{E_b^l}\, b + \tilde{\eta}_d^{(l)}$ the l^{th} rake finger data output (where A = number of antennas) and $\alpha_i^{(l)}$ the channel coefficient for the i^{th} antenna l^{th} path. Similarly, the pilot channel rake output is $P_l = \sum_{i=1}^{A} \alpha_i^{(l)} \sqrt{\hat{E}_p^l}\, p + \tilde{\eta}_p^{(l)}$. $\tilde{\eta}_l$ and $\tilde{\eta}_p$ are the uncorrelated interference + noise sources, and $\sqrt{E_b^l}$ and $\sqrt{E_p^l}$ are the real amplitudes of the traffic and pilot channels. σ_l^2 is the interference + noise variance conditioned on the rake channel, l, and $\Re\{P_l^* Z_l\}$ the l^{th} spatial finger combining output for the traffic channel assuming channel estimation is applied with the common pilot channel.

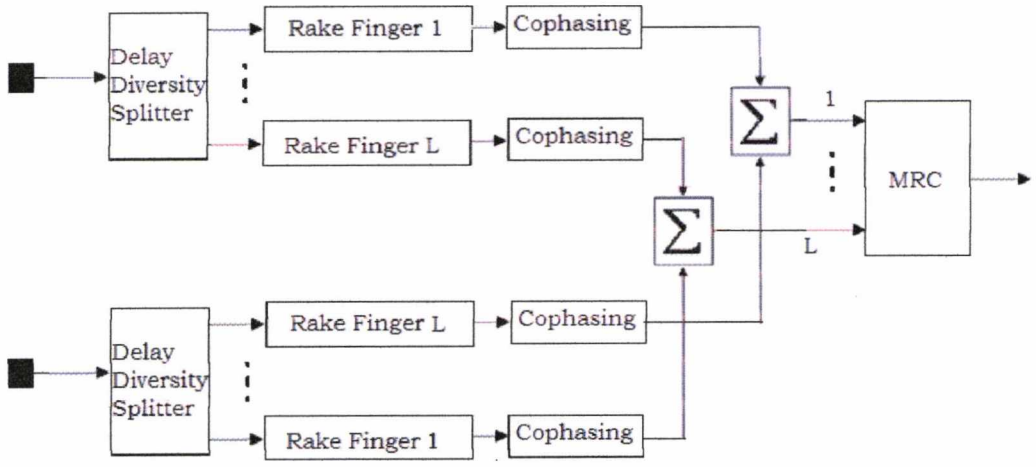

Fig 4.1 The 2D-Rake Receiver utilizing two antennas

4.1.1 The Ideal Rake Receiver for Spatial and Temporal Diversity Channels

Consider the case where "L" multipath channels with delay offset (forming the frequency selective fading channel) are somehow separated temporally where no adjacent channels colour the other after matched filtering (perfect synchronization and orthogonality between the code channels are assumed). This case then is very similar (or equivalent if all diversity branches have the same RMS fading parameter) to the spatial diversity combiner presented in Chapter 2 for optimum performance in flat fading channels. This therefore provides the asymptotic lower bounds for detection applying diversity that generally cannot be exceeded unless steps are undertaken to purposefully remove interference and fading from the system allowing the AWGN channel bound to yield the asymptote of the estimator. The real SNR asymptote is actually formed from the Cramer-Rao lower bound [Kay1993B] and is generally very close (if not identical) to the AWGN bound for uncoded information. A method of reaching this bound is achieved with the maximum likelihood sequence estimator for fading channels. It was discussed in Chapter 2 that likelihood sequence detection (and any other sequential decoder/estimator) are generally quite impractical when the transport information block is large (where deconvolving over all information symbols due to overlapping interference from previous and future samples is unrealistic in accordance to the estimation hypothesis).

4.1.1.1 L-FOLD DIVERSITY FOR A RAKE RECEIVER WITH UNEQUAL BRANCH SNR'S.

Assume that the noise at the output of the rake receiver is known and Gaussian, where the signal powers scattered over L paths are combined in an optimal manner such that the instantaneous SNR per symbol is maximized [Brennan1959]. The bit error probability of the Rake receiver applying a sign detector is given by (see also Appendix C, section C.4)

$$P_e = \frac{1}{2}\sum_{i=0}^{L-1}\left\{\prod_{\substack{k=0\\k\neq i}}^{L-1}\left(1-\frac{\bar{\gamma}_k}{\bar{\gamma}_i}\right)\right\}^{-1}\cdot\left(1-\sqrt{\frac{\bar{\gamma}_i}{2+\bar{\gamma}_i}}\right) \tag{4.2}$$

with $\gamma_i^{(n)} = \dfrac{\alpha_i^{(n)}\cdot\alpha_i^{(n)*}\cdot\varepsilon_b}{\sigma_{N,i}^2}$ the i^{th} diversity branch instantaneous SNR (where $\alpha_i^{(n)}$ is the instantaneous fading coefficient and $\sigma_{N,i}^2$ the variance of the noise floor) of first moment $\bar{\gamma}_i = \dfrac{E\left\{\alpha_i^{(n)}\cdot\alpha_i^{(n)*}\right\}\cdot\varepsilon_b}{\sigma_{N,i}^2}$.

4.1.1.2 M×L FOLD DIVERSITY FOR 2D RAKE RECEIVER WITH PARTIAL EQUALITY IN THE BRANCH SNR'S.

Assuming a M-antenna diversity assisted MRC system transmitting over Rayleigh flat fading channels, a closed form solution for the component BER can be obtained where (See [Proakis2001, pp. 781] for the derivation when all branches have equal SNR, and see Appendix C, section C.5 for the full derivation with unequal branch SNR's)

$$P_e = \sum_{d=1}^{M}\sum_{i=0}^{L-1}\left(\prod_{\underbrace{f=1}_{f\neq d}}^{M}\prod_{\underbrace{k=0}_{k\neq i}}^{L-1}\left(1-\frac{\bar{\gamma}_{k,f}}{\bar{\gamma}_{i,d}}\right)\right)^{-1}\left\{\frac{1-U^{(i)}}{2}\right\}^{d}\sum_{e=0}^{d-1}\binom{d-1+e}{e}\left\{\frac{1}{2}\left(1+U^{(i)}\right)\right\}^{e} \tag{4.3}$$

with $U^{(i)} = \sqrt{\dfrac{\bar{\gamma}_i}{2+\bar{\gamma}_i}}$, and $\binom{d-1+e}{e} = \dfrac{(d-1+e)!}{(d-1)!e!}$. This model assumes that the L Rake fingers on each diversity antenna branch are uncorrelated and have same mean SNR, i.e. $\bar{\gamma}_i = \bar{\gamma}_{i,d}\ \forall d$.

4.1.2 Diversity Combining with Cross Talk Between Channels

Having established some theoretical (lower limit) bounds for ideal diversity reception and the single user, single channel receiver, it would obviously be more practical to consider the channel-induced interference. The analysis thus far has of course assumed a non-interference scenario (i.e. assuming the Integrate Dump detector after despreading perfectly eliminates MAI) and that the data signalling energy was perfectly flat- i.e. constant. To account for the MAI + ISI[1], a unified theory was presented for the analysis of the rake receiver and any other linear detector in Appendix C, section C.1. The key to this analysis must first consider a method of generating the Gaussian approximation based on the measured SINR. Clearly the SINR will depend chiefly on a number of matters, namely the number of users accessing the channel, the distributions of their powers, the delay spread of the channel, and the processing gain of the desired user being demodulated (with the processing gains of adjacent users also factoring in the level of interference). Obviously a dynamic system theoretic with many variables lends towards making a number of assumptions that simply would not be true in real applications (i.e. assuming all diversity channels and codes are totally uncorrelated). Treating the MAI and IPI as random noise variables, the rake output SINR per symbol can be derived to form an analytical solution to the problem for Rake and 2D Rake receivers. If we assume that the i^{th} rake finger SINR per antenna is equivalent (which is highly likely), then we can treat the analysis in a unified manner. The i^{th} rake finger SINR is given by (see Appendix C, Section C.6. for the derivation)

$$\bar{\gamma}_i = \frac{\Theta_{\max}^2 G \mathrm{E}_1^{(i)}}{\sum_{k=1}^{K} \sum_{\substack{m=0 \\ m \neq i}}^{L} \sigma_{M,i(m)}^2 \mathrm{E}_k^{(m)} + \sigma_{RI,i}^2 + \Theta_{\max}^2 G \sigma_{\eta}'^2} \tag{4.4}$$

[1] For very high Processing Gain, MAI + ISI become negligible quantities due to random RSS codes between two propagation channels having normalized cross correlations approaching zero in the limit of G approaching infinity. This is particularly true if the dispersion is greater than the single chip period. Since this is only an approximation, one would realistically expect that increasing the processing gain of the desired channel with long RSS overlay would yield the contribution of MAI relative to the desired signal at the matched filter output to decrease.

with $\sigma^2_{M,i(m)} = \sum_{a=-N_c}^{N_c} \left| \boldsymbol{R}_a^T \boldsymbol{R}_{m-as} \right|^2$ and $\sigma^2_{RI,i} = \sum_{\substack{a=-N_c \\ a\neq 0}}^{N_c} \left| \boldsymbol{R}_i^T \boldsymbol{R}_{i-as} \right|^2 \mathrm{E}_1^{(i)}$. $\boldsymbol{R}_i$ is the i^{th} vector[2] of pulse shaping coefficients not accounting for the unit energy normalization $\Theta_{\max}^{-1}$. G represents the spreading factor, $\mathrm{E}_1^{(i)}$ represents the i^{th} finger desired user symbol energy accounting for the channel path loss and base station transmitter energy (including antenna gain) for the dedicated data channel. The model treats the CPICH interference in a joint fashion with self-interference and multiple access interference (with K representing the total number of transport channels including the desired user). N_c represents the number of chip intervals spanned either side of the pulse shaping filter axis of symmetry, where s is the number of samples per chip and L the total number of rake fingers. To calculate the analytical probability of error bounds, equation (4.2) or (4.3) can be used for the Rake or 2D-Rake receiver respectively.

4.1.3 NUMERICAL EXAMPLES

The analytical and Monte Carlo simulations for the 2D Rake receiver are presented in this section. The primary observations first consider the input SNR as an argument against the theoretical BER (depending of course on the mean output SINR of the detector). For purpose of comparison, all results are sectioned according to the number of simultaneously active users such that the Temporal, Spatial, and Temporal-Spatial diversity receiver performance can be evaluated. Furthermore, analytical and simulation results are included on each BER Vs SNR plots to determine the accuracy of the Gaussian approximation compared to Monte Carlo simulation estimates. The rake receiver was implemented with four diversity fingers for the Vehicular Channel A model, mainly due to the lower power (longer delay spread paths) not generally being captured by the temporal acquisition equipment. The channel was set for vehicular speed of 36Km/Hr with number of users treated as a variable. The user powers were set as a uniform random variable (relative to the desired channel being demodulated) within the limits –5(dB) < P(dB) < 5dB. The spreading gain was set to 32 and long duty cycle gold code scrambling signatures (common to all users) overlaid the information, control and pilot channels simulating a time variant spreading sequence (as is the case for the UMTS downlink). The first result (Fig. 4.2)

[2] The RRC vector of coefficients is partitioned into a long vector with zero padding to represent the i^{th} multipath echo component. This results in a chip-level interference model where all interference terms are due to the difference between the sampled delay vector, $\boldsymbol{R}_i$, and any other delay/future sampled vector $\boldsymbol{R}_{i\pm T}$.

indicates the performance bounds for the Spatial, Rake and 2D Rake for a single user channel. This is expanded for multiple access channels (Figs. 4.3 – 4.5) with K = 4, 8, and 16 users. No multicode transmissions were assumed and all access interference was variable spreading factor (VSF). The results show that the 2D Rake diversity offers superior performance to the spatial only and rake receiver but no significant improvement or contribution can be concluded since the performance gains are rather marginal where the receiver still has a relatively high asymptotic bound for multi-user channels. The analytical solutions utilizing the uncorrelated Gaussian interference + noise approximation yields quite accurate results (compared to simulation) for higher number of users, but yields more optimistic (i.e. it overestimates) performance for lower number of users. This has been reported in other journal publications when considering rectangular pulse shaping – see [Huang2005, Cheng2002] and [Cheun1997] where the authors also derived improved Gaussian approximations considering the correlations between interference.

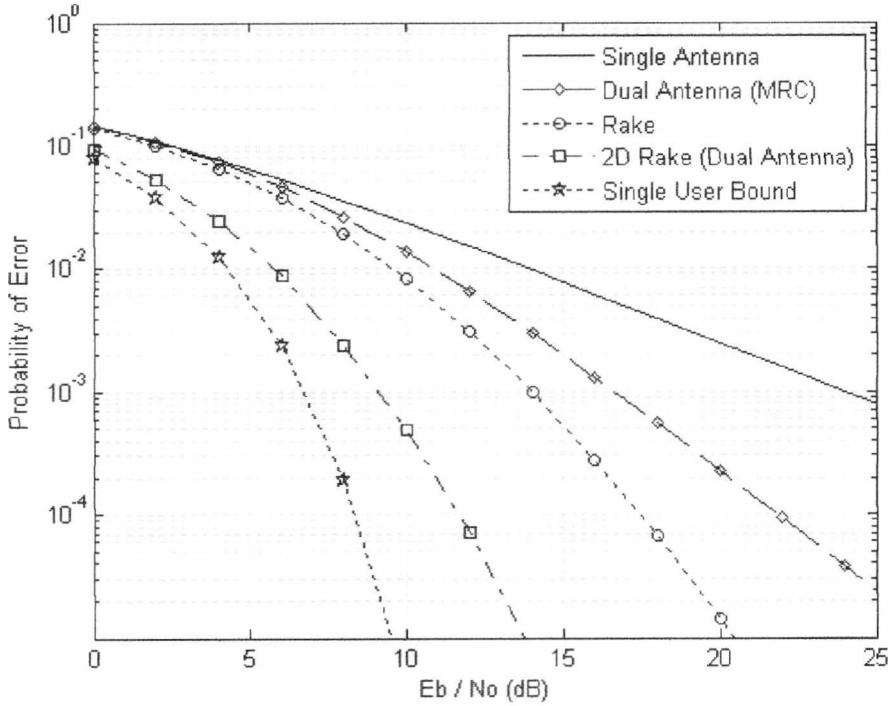

Fig. 4.2 Performance of Rake and 2D Rake for a single channel.

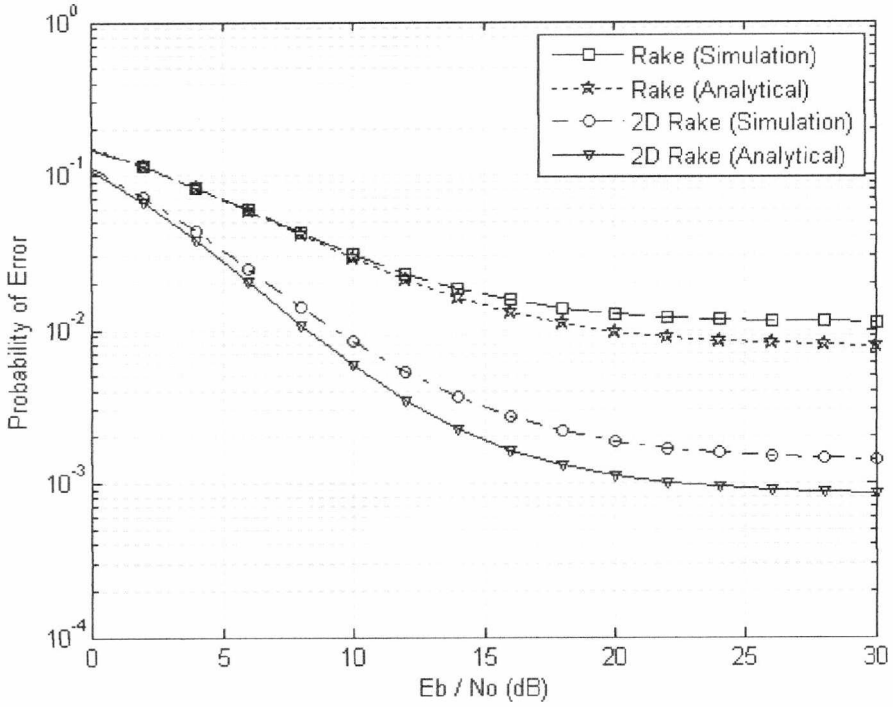

Fig 4.3 Performance of Rake and 2D Rake for K=4 users.

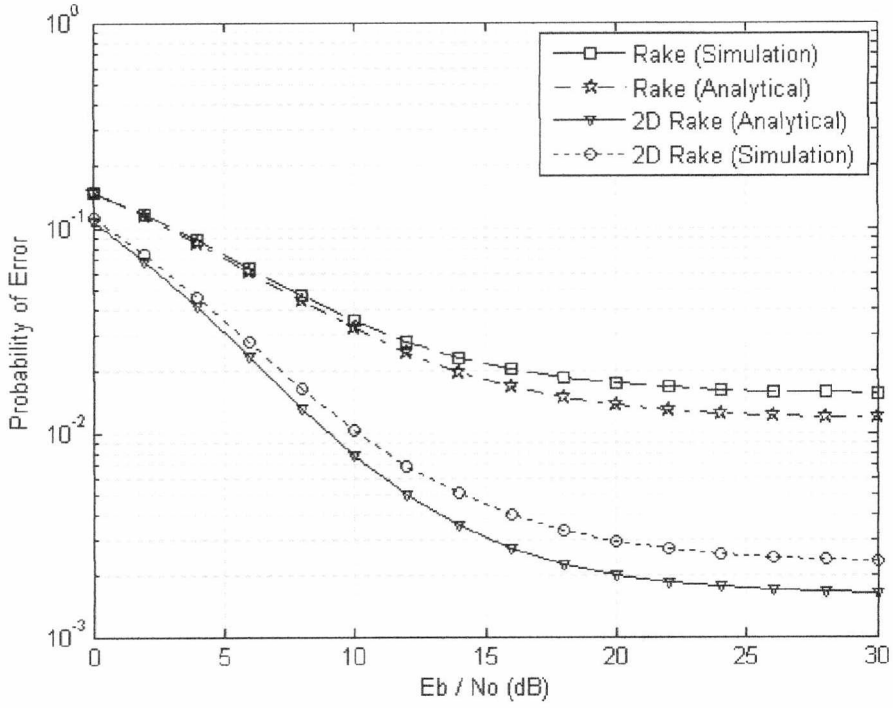

Fig 4.4 Performance of Rake and 2D Rake for K=8 users.

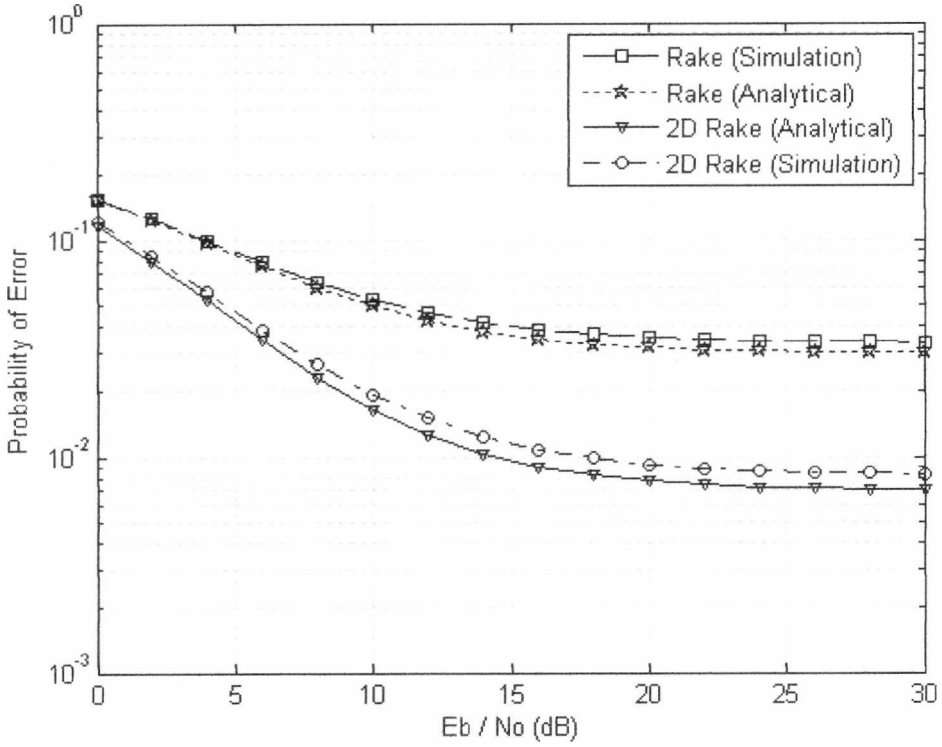

Fig 4.5 Performance of Rake and 2D Rake for K=16 users.

4.1.4 DISCUSSION

Diversity combining applying temporal and spatial-temporal algorithms are fairly well known techniques for mitigating the influence of nearly flat fading channels where the cross interference induced for the rake receiver by the delay paths are not particularly significant. This is more prevalent for narrow-band PCS systems (such as IS-95). Wideband systems like the UMTS employing shorter spreading codes yield the contribution of interference due to channel frequency selectivity to be more significant, particularly for any one single user channel employing moderate data rates. Investigations into voice traffic for the downlink employing a fixed 12.2Kbps dedicated data channel generated a somewhat less stringent criterion towards the interference effect due to higher spreading factor. This aspect has not been investigated for this thesis since the Chapter 2 highlighted the performance of the downlink for dual antenna diversity with various spreading factors plotted against the system loading. This result is fairly ubiquitous across many detection and estimation hypotheses (the performance of diversity enhanced estimators improve upon this result but still render similar behavioural characteristics). What this section shows is that for relatively moderate data rates employing a fixed spreading factor of 32, interference is quite considerable and the resultant diversity combiners yield asymptotic BER performance since interference was not

effectively cancelled. The reason that any performance gain was possible was purely down to the uncorrelated channel and interference assumptions, which is where diversity gain can improve the detection probability. It can be envisaged that closely correlated diversity channels will produce no significant effect. However, research undertaken in [Dolmans1999, Kim2000] indicated that dual antenna separations of even a quarter of wavelength gave enough diversity improvement to be useful for the WCDMA downlink in even noise and interference limited channels (where the receiver output SINR was low). This research concluded that quarter wavelength and half wavelength arrays gave fairly similar performance.

4.2 RAKE ASSISTED BEAMFORMING

Up to this point, brief considerations on the diversity applications for single user demodulation have been presented and it was found that interference from other users accessing the same channel is a problem that cannot be simply overcome. The degrading qualities of interference depend on the number of users and the power variations between all users relative to the path loss/fading parameters in a base-station coverage sector leading to the motivation towards the development of asymptotically efficient single/multi user receiver structures (even in the presence of disparate received power levels with non-orthogonal signalling formats and/or multipath channel induced asynchrony with/without initial synchronous multiplexing). A spatio-temporal receiver employing adaptive diversity combining is discussed in this section. Such receivers (termed as being two dimensional rake receivers) exploit the spatial correlations of fading (channel space-selectivity) as well as the temporal dependency of fading channels combined to form a frequency selective model. It is clear from (4.4) that traditional rake receiver asymptotic performance depends on the number of diversity paths, sensors, active users, and the far-near effect in Downlink power control scenarios (where for $A<L$, limitations on the probability of error are induced due to additive interference). In other words, large delay spreads; low number of sensors, and high number of active users presents a performance lower bound that is interference limited. To prevent multipath distortion in most situations, a mobile phone antenna diversity scheme could consider adaptive beamforming. Adaptive beamforming exploiting pattern diversity and directivity is of some interest in that for fading channels, antenna beam nulls could be placed in the direction of interference (that which causes significant degradation to the desired signal) with the antenna boresight pointed towards the signal of interest. However, as mentioned in Chapter 2, obtaining such information without priori knowledge on the

direction of arrival requires adaptive optimization and many antenna sensors in highly dispersive channels. Nevertheless, utilizing spatial-temporally derived diversity channels greatly increase the degrees of freedom for the beamformer, where large performance gains are possible in uplink and downlink scenarios – see [Song1999, Dell'Anna1999] and [Kim2001, Mostafa2004].

4.2.1 STRUCTURE OF THE RAKE ASSISTED BEAMFORMER

The receiver considered in this section uses dual spatial-temporal diversity (Fig. 4.6), where each antenna contains an individual rake diversity scheme. Symbol-level combining is proposed for single user detection applying a 2-element array due to simplicity of generating the required cost function. Hence this receiver is thus a post array MF combiner- i.e. a temporal-spatial receiver. A common implementation would be to apply beamforming/antenna combining prior to matched filtering with a rake receiver- i.e. a spatial-temporal receiver [Affes1998]. The theory to this approach considers the multi-element beamformer tracking the individual delay spread components of the multipath field for the desired user (assuming that each path has independent angular spread function), where each beamformer output is input to an individual rake processing finger prior to diversity combining. The problem with this method is one where optimization of the antenna weights are more difficult to achieve due to the higher modulated symbol rates and the issue of generating a cost function yielding the required optimization for a single user in WCDMA channels. Furthermore, the thesis considers the limitation of only two antenna elements hence presents a fairly major impediment to this technique. A comparison of spatial combining methods based on Wiener optimization and traditional MRC will be presented in the proceeding sections. No analytical results are presented since a detailed account and comparison for different diversity combining problems is somewhat exhaustive to include[3]. The receiver utilizes complex, adaptive combining, where each individual rake finger output, per path, per antenna is combined utilizing the MMSE algorithm (the NLMS implementation would be applied on a finger by finger basis, where the error signal is formed from the difference between the output of the finger-level spatial combiner for a delay path and the desired delay path signal). The outputs of the spatial combiner are then

[3] Work is proceeding on analytical results for publication in the future, since the author's other main project and interest is for Macrodiversity architectures in the current UMTS since space-time trellis coding and adaptive antennas form the backbone for near-optimum diversity reception. This topic is slightly off-scope for this thesis and hence is not considered further.

summed according to the MRC rule. The structure of the receiver is easily observed in Fig. 4.6.

Note that the finger-level adaptive combining utilizing the MMSE approach is identical to the method in Chapter 2; hence no algorithmic explanation is required. The RLS algorithm for a dual antenna receiver would be a common solution to the diversity combiner problem. Research conducted in [Kim2001] considered the NLMS algorithm. If a CPICH or suitably accurate decision directed training waveform is not available, the Minimum Variance or Blind MSINR algorithm could be used instead (where the receiver has added complexity of estimating the second order statistics of interference and the desired signal).

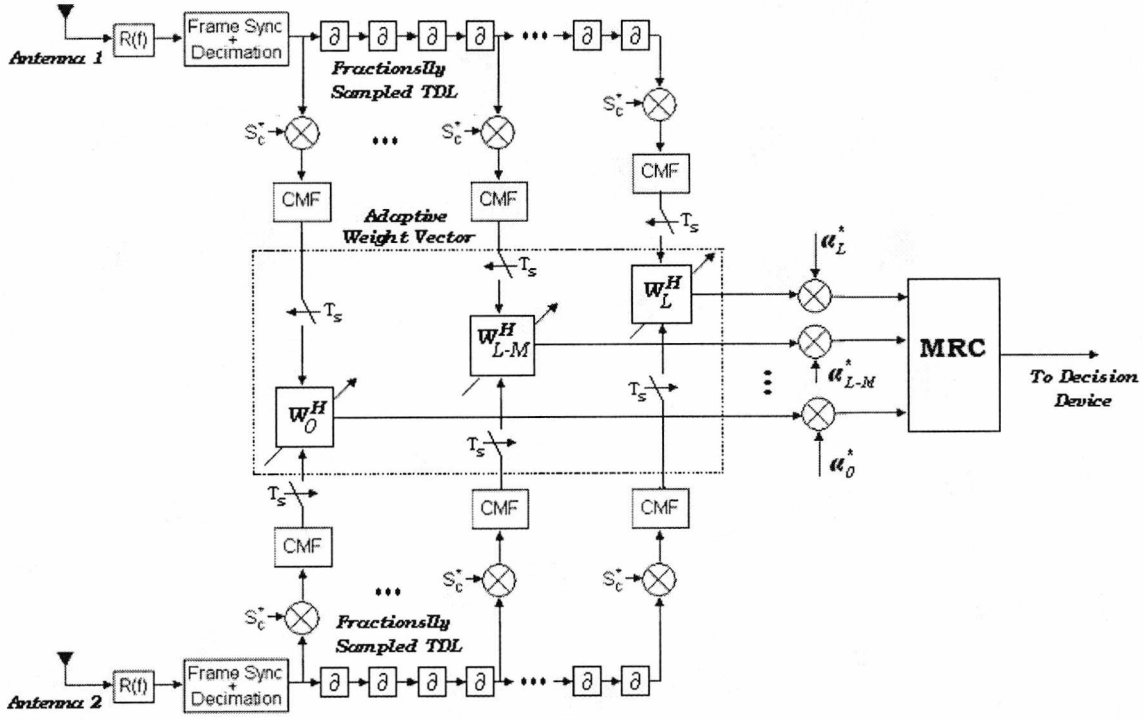

Fig 4.6 The 2D-Rake Receiver utilizing adaptive finger combining.

4.2.2 NUMERICAL RESULTS

The main results for this section will consider the measured BER for a variety of loading conditions. The number of spatial sensors = 2, and the fading channel is generated to incur the number of propagation paths to be far greater than the number of sensors, i.e. the propagation channel considered yields the six delay path Vehicular A model with four echo components constituting each wave bundle. This was invoked to overload the array where the limited degrees of freedom will burden the receiver in terms of spatial filtering of the interference waveforms. The purpose of this is to ensure that overly generous propagation conditions do not cause near optimum reception creating a false sense of perspective on the results were a real channel simulator be used. The Figs. 4.7 – 4.9 show the simulated bit error rates plotted against the symbol energy to noise ratio for K = 4, 8, and 16 users respectively. The results for the temporal-spatial diversity combiner and the Rake were included for purpose of comparison. The first observation that can be generated is that the adaptive 2D Rake receiver is interference limited, i.e. the adaptive combining algorithm does not fully initiate interference cancellation. The second observation of some importance is the full MMSE solution produces only marginally better performance than the implementation considering the RLS adaptive algorithm; hence the RLS method is perfectly valid for the combiner. The NLMS method was not considered since it was reasoned in Chapter 3 that for simplistic dual antenna diversity, the additional computational complexity of the RLS algorithm is affordable. It is clear from the results that adaptive combining produces superior performance to the traditional maximum ratio combining solution, although this performance gain is fairly marginal due to the limited number of spatial filtering elements. To initiate a superior performance, many more antenna sensors would have to be used resulting in complexity and integration cost since handsets are generally physically small and low power. The case for devices such as a Notebook PC offering connectivity to the radio network would yield greater potential in utilizing the antenna array space more optimally. The case for adaptive antenna combiners in the reverse link is stronger than the downlink case since limitations on array dimensionality are not as stringent.

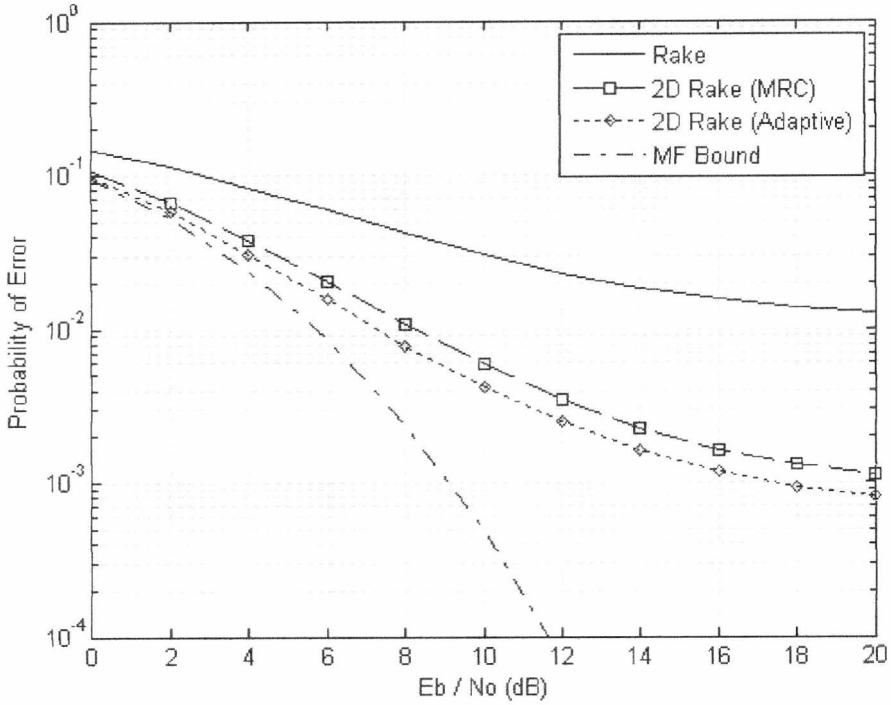

Fig 4.7 Performance of the adaptive Rake for K=4 users.

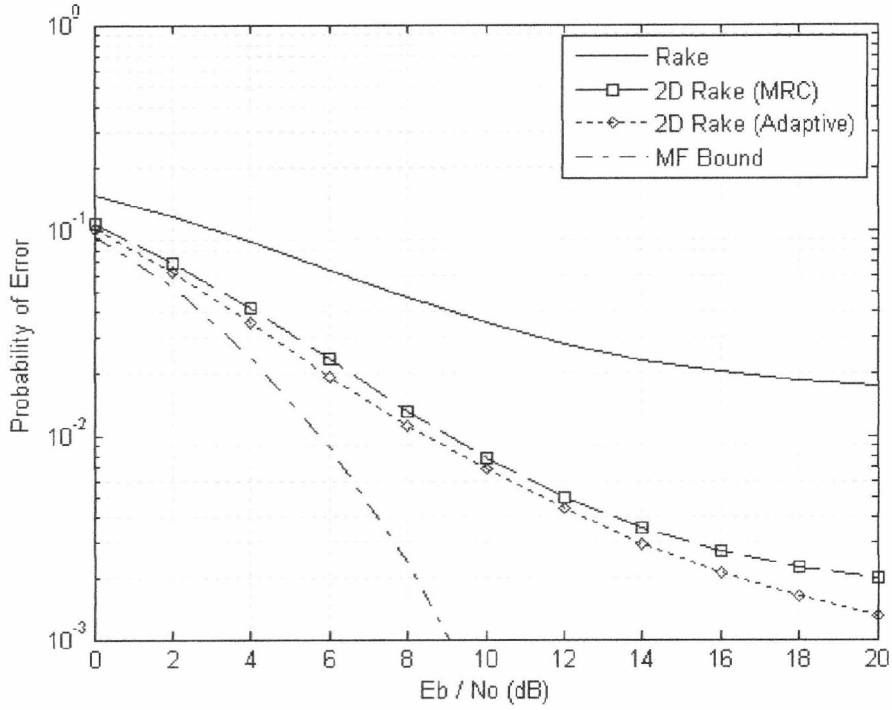

Fig 4.8 Performance of the adaptive Rake for K=8 users.

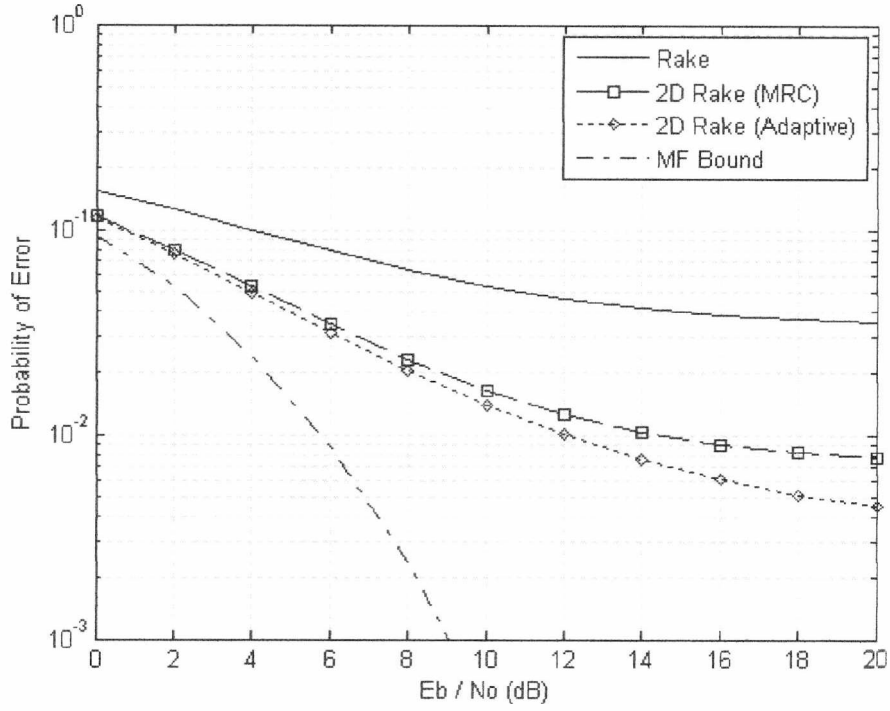

Fig 4.9 Performance of the adaptive Rake for K=16 users.

4.3 JOINT SPATIAL – TEMPORAL DIVERSITY FOR NEAR OPTIMUM BROADBAND BEAMFORMING

A pensive approach to advanced acquisition of the single user data channel is presented in this section considering the limitations of the mobile terminal in terms of knowledge of the multiple access interference and the channel itself. The generic receiver for uplink/downlink SISO and MISO channels is the multiuser receiver, which is centralized and attempts to obtain information of all received signals to improve performance via some optimization technique (i.e. like Decorrelation or Serial Interference Cancellation). Multiuser receivers require the so-called stationary information of the received signals from all users (in particular the multiple access codes assigned by the network and the relevant timings in multipath channels). This is of course considered a "bridge too far" in single-user detection. A very popular receiver mentioned in research journals for interference suppression (offering high asymptotic efficiency) is the maximum likelihood multi-user receiver where, in highly loaded channels, its implementation aspects prevent it from being no more than a hypothetically desired lower bound for fading channels. From a Single User perspective, an optimal maximum likelihood multi-user receiver is not only unfeasible by requiring joint estimation of channel parameters and multi-user modulation codes [Verdu1986, Forney1972,

Ungerboeck1974], but also far too complex for practical implementations where several suboptimal receivers [Duel-Hallen1995] for this detection problem have been proposed in the past 15 years. Most near-far/interference resistant receivers are centralized in that all multi-user signals are processed jointly in the receiver. When considering the downlink receiver, only the desired user signal should be demodulated while suppressing the interference due to other users. The widely acclaimed LMMSE, Decorrelating, Parallel/Serial interference cancelling and Maximum Likelihood estimators considered by other researchers for the mobile uplink are multiuser demodulation techniques introduced for DS-CDMA channels. These approaches are clearly unsuitable for applications in single user detection in fading channels since:

(1) Joint multi-user estimation requires knowledge of all active signature sequences.

(2) Maximum Likelihood in its present form has an exponential complexity relating to the number of channels requiring demodulation.

(3) Large-scale matrix inversions typical of Bayesian estimation require a high level of arithmetic complexity involving multiplication and large amounts of memory. Windowing and factorization simplifies arithmetic complexity at a cost to performance if the channel changes too rapidly.

(4) Mathematical solutions to generalized LMMSE estimators assume knowledge of all signalling parameters including transmitted powers, channel and delay variables and the additive noise moments. Clearly in a real solution, such parameters require estimation beforehand which therefore translates to a high latency in that the algorithms require reception of the entire signal prior to detection. Obviously this approach does not lend well to real time data/multimedia communications. An approach overcoming this involves forward and backward substitution of the correlation metrics within the signature covariance matrix- however the cost involved is that the filter may be unstable for uncorrelated noise [Verdu1998].

A dearth of information on the access channel parameters (such as the multipaths and the adjacent channel coding) for current WCDMA standards employed in the third generation yield such detectors as being largely impractical- since obtaining/estimating the adjacent user signatures represents a formidable challenge particularly when long, non-cyclic RSS codes overlay the channels. Hence near-optimum approaches like the Decorrelator and LMMSE estimator have limited practicality in downlink demodulation, but also the optimum receiver, i.e. the likelihood sequence detectors introduced in [Forney1972], and expanded for CDMA in [Verdu1986] require the whole radio frame to be received prior to demodulation, and is impractical considering the length of a UMTS radio frame. Overcoming the strict requirement of multi-channel knowledge is the Blind LMMSE (MOE) receiver and its subspace/constrained variants. These techniques developed by Honig [Honig1995] and other

researchers (note [Verdu1998, Wang1998, Wang2004] and the reference therein) offer identical solutions (in terms of performance SINR) to the classical LMMSE approach without necessitating knowledge of the active signatures. The principle complexity advantage of Blind detection manifests for both single and multi-user scenarios, although the subspace (utilizing the geometric/projection properties between signal and noise) and constrained optimization receivers only allow the algorithms be implemented when coding is short and exhibits cyclostationary. Since the downlink of WCDMA systems tends to be overlaid with longer PN sequences, blind single/multi user detection proposed in [Honig1995, Zhenhua1990, Tsatsanis1998] is largely impractical. This issue has been addressed considering an equalization methodology (i.e. decorrelating the channel induced interference without considering the adjacent user signatures) provided the multiple access is synchronous and exhibits orthogonal/Hadamard coding, see [Zecevic1997, Giannakis1997, Hooli2001, Heikkila2001, Chi2006] for a detailed account of blind equalization/system identification applying the MOE constraint, and blind adaptation techniques such as Griffiths or the Constant Modulus algorithm [Treichler1983] for the WCDMA downlink. This section expatiates upon the receivers investigated in Chapter 2 and prior sections of this chapter by considering the issue of downlink demodulation with a dual antenna broadband beamformer (formed by utilizing channel equalizers). It must be noted that the performance of the "ideal" rake receiver even in single user fading channels (where self interference is rather small for larger processing gains) is actually quite close to optimum if the diversity channels are mutually uncorrelated. Furthermore, due to the varying transmission conditions and dynamic channel allocations for wireless networks, popular single user matched filters such as adaptive equalizers or whitening transforms [Mirbagheri2002, Majmundar2000] may not be entirely necessary in all conceivable situations- i.e. there are cases where for low system loading the rake receiver may perform more than adequately.

4.3.1 2D-Rake Receiver with Uniformly Distributed Fingers: An Interference Whitening Criterion

The previous incarnations of the 2D Rake receivers assumed the All-Rake (ARAKE) property where each resolvable delay path was demodulated with the multiple finger structures coherently combined to generate a decision statistic. This approach generally causes the receiver to lose some diversity due to correlated (coloured) noise arising from multipath dispersion and pulse shaping. The usage of coding structures such as Walsh Hadamard orthogonal spreading sequences can be exploited to generate a post-matched filter maximum likelihood detector accounting for the noise correlations – particularly when

additional rake fingers are placed into the system to increase the degrees of freedom. From a more generic perspective, we can utilize as many degrees of freedom as possible without necessitating timing acquisition and recovery on a path-by-path basis. Hence this receiver is analogous to the symbol level equalizer (or GRAKE receiver) where extra diversity is offered in the form of oversampling with each rake finger time/scrambling code offset by a fraction of a chip [Bottomly2000]. The filter coefficients can be optimized according to the MMSE criterion – as was done in [Frank2002] forming the symbol equalizer. The symbol level equalizer is actually equivalent to the MMSE chip level equalizer (down to a scalar) with the added advantage of lower complexity (since the inclusion of "L" despreading devices prior to equalizer-symbol-projected combining instead of one despreader is not costly). The method used in this section is the likelihood optimization, where it can be shown that the likelihood approach and MMSE approach produce similar coefficients (differing by an inverse scalar). Assuming that additional rake fingers are assigned uniformly along the tap-delay line, the interference whitening solution can be applied considering a hypothesis test modelled with multivariate Gaussian likelihood functions [Kay1993B, pp. 385]:

$$\begin{aligned} H_1 &: p_1(\boldsymbol{\gamma}) = \frac{1}{(2\pi)^{0.5n}\left|\boldsymbol{\Sigma}_u\right|^{0.5}} exp\left[-0.5(\boldsymbol{\gamma}-\boldsymbol{h})^H \boldsymbol{\Sigma}_u^{-1}(\boldsymbol{r}-\boldsymbol{h})\right] \\ H_{-1} &: p_{-1}(\boldsymbol{\gamma}) = \frac{1}{(2\pi)^{0.5n}\left|\boldsymbol{\Sigma}_u\right|^{0.5}} exp\left[-0.5(\boldsymbol{\gamma}+\boldsymbol{h})^H \boldsymbol{\Sigma}_u^{-1}(\boldsymbol{r}+\boldsymbol{h})\right] \end{aligned} \tag{4.5}$$

where $\boldsymbol{\gamma}$ is the chip matched filter output vector of dimensionality = N_f with N_f the total number of rake fingers/taps. $\boldsymbol{\Sigma}_u$ represents the interference auto-covariance matrix and $\boldsymbol{h}$ the vector of first moments – which is (for the correlated Gaussian interference assumption) the complex channel coefficients weighted by the mean data channel amplitude.

The log-likelihood ratio is

$$\begin{aligned} log_e\left[\lambda(\boldsymbol{\gamma})\right] &= -0.5(\boldsymbol{\gamma}-\boldsymbol{h})^H \boldsymbol{\Sigma}_u^{-1}(\boldsymbol{r}-\boldsymbol{h}) + 0.5(\boldsymbol{\gamma}+\boldsymbol{h})^H \boldsymbol{\Sigma}_u^{-1}(\boldsymbol{r}+\boldsymbol{h}) \\ &= 2\boldsymbol{h}^H \boldsymbol{\Sigma}_u^{-1}\boldsymbol{\gamma} \end{aligned} \tag{4.6}$$

The test statistic for maximum likelihood detection is

$$2\boldsymbol{h}^H \boldsymbol{\Sigma}_u^{-1}\boldsymbol{\gamma} \geq log_e\left(\frac{P(H_{-1})}{1-P(H_{-1})}\right) \tag{4.7}$$

where for equiprobable hypotheses, $P(H_{-1}) = P(H_1)$ satisfying $P(H_{-1}) + P(H_1) = 1$ yields

$$\boldsymbol{h}^H \boldsymbol{\Sigma}_u^{-1}\boldsymbol{\gamma} \geq 0 \tag{4.8}$$

Assuming that $\boldsymbol{\Sigma}_u$ is positive definite, there exists a Cholesky decomposition $\boldsymbol{\Sigma}_u = \boldsymbol{L} \cdot \boldsymbol{L}^H$ with $\boldsymbol{L}$ a lower triangular matrix. Hence the decision variable becomes

$$\partial = \left(\boldsymbol{L}^{-1}\boldsymbol{h}\right)^{H} \boldsymbol{L}^{-1}\boldsymbol{\gamma} \tag{4.9}$$

resulting in the receiver given in Fig. 4.10. The matrix $\boldsymbol{L}^{-1}$ acts as a whitening transform that operates on the signal vector $\boldsymbol{\gamma}$ - see [Monk1994, Wei1996, Yoon1996, Sivenesan2005] for application of whitening matched filters in DS-CDMA. The weight vector $\boldsymbol{w} = \boldsymbol{L}^{-1}\boldsymbol{h}$ performs the matched diversity combining for the receiver. Note that the Rake solution is still desirable, hence $h_{i,j} = 0$ for all fingers not assigned to a real delay path.

FURTHER NOTES REGARDING THE ALGORITHM: The exact inverse transform $\boldsymbol{\Sigma}_u^{-1}$ commuting over all filter taps may be ill – conditioned due to $\boldsymbol{\Sigma}_u$ being sparse for long – code CDMA. It is therefore suggested to add a small fractional constant along the main diagonal of $\boldsymbol{\Sigma}_u$ prior to inversion. Alternatively, the entire matrix dimensions can be reduced to just the filter taps of interest (where zero padding on unused filter taps is not incurred). Statistically speaking, the filter taps centered on the conventional Rake delay channel (considering only the two or three adjacent taps yielding the strongest inverse solution) would result in a better and more practically viable receiver. Expatiating upon the sparse $\boldsymbol{\Sigma}_u$ matrix for long-code CDMA, the dual antenna receiver, for the same reason, would not be jointly optimized according the temporal and spatial signatures (the optimization for each filter will be individual).

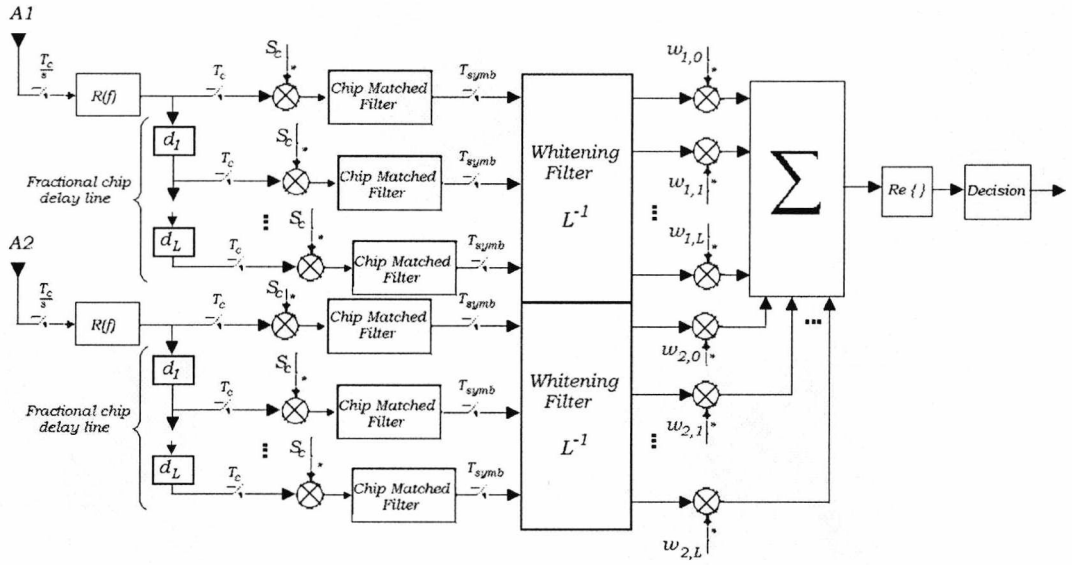

Fig 4.10 The Interference Whitening Rake Receiver utilizing Matched Filter combining.

4.3.2 LMMSE RAKE RECEIVER

When the scrambling codes are short or cyclic or both, then the traditional multi-user problem can be transferred to the single-user problem even if adjacent codes are unknown. The use of short codes make interference cancellation more feasible since equalizer structures utilizing the Blind MMSE [Honig1995] or LMMSE estimators [Honig1994] can be implemented as linear FIR filters to jointly equalize and decorrelate interference whilst simultaneously providing the detector with a sufficient unbiased decision statistic. These receivers can be seen as equalizers that decorrelate the channel and the multi-user signature correlations (at symbol level), and as such the LMMSE multi-user receiver requires knowledge of all the signature correlations to project interference away from each user. The single user LMMSE receiver can be implemented blindly (with the MOE optimization making use of Lagrange multipliers) or as a decision directed MMSE filter. In this thesis, the decision directed LMMSE multi-channel single-user receiver is considered which deems that no signature sequences are known other than the one preassigned from a Base Station to a particular user under investigation. Suitable estimators related to the rake receiver are the LMMSE interference-cancelling receivers derived from the pre-combining and post-combining LMMSE criterion presented in [Latva-Aho2000]. Rather than application of a front-end linear filter, decision directed Wiener estimators could be used to suppress interference. This has been applied for Post-Combining [Miller1995] and Pre-combining LMMSE [Latva-Aho1997] algorithms and shown to yield acceptable performance in relatively short code CDMA systems. The standard LMMSE receiver presented in [Latva-Aho2000] minimizes the mean squared error between the receiver output and the true transmitted data sequence and suppresses both inter-path and inter-channel interference under near-far situations. The coefficients of the aforementioned LMMSE receiver depend on the channel condition of all users; hence requiring continuous adaptation as the channel changes state. If the fade rate of the channel is rapid (i.e. of the order of the actual chip rates), the standard adaptive LMMSE receivers [Miller1995] need to be updated continuously and may have severe convergence problems where the adaptive filter will "see", or rather interpret the situation as being non-stationary. Furthering the scope within the statistical class of LMMSE estimators, a simple alteration to the optimization criterion (to overcome convergence problems of the standard adaptive LMMSE receiver) renders the Precombining LMMSE Receiver [Latva-Aho2000] minimizing the MSE between the receiver output and the channel coefficient data symbol product for each path. Hence, it is assumed that the channel parameters of the desired user are known or estimated, as is the case in the conventional coherent rake receiver. The Precombining LMMSE receiver

depends only on the normalized signature sequence cross-correlations and the average channel profiles of all active users. Since delays and the average channel profiles change slowly in Pedestrian and low-speed vehicular channels, the adaptation requirements of the Precombining LMMSE receiver are less stringent than those of the adaptive conventional LMMSE receivers. Again, as in the conventional LMMSE Receiver, the direct solution requires multiuser demodulation. A simple modification to the structure can yield a blind single user detector via a bank of Wiener filters trained by scaling the rake receiver hard decisions with the appropriate channel estimate. The algorithmic approach to this detector is actually one of the most well-researched and commonly known receivers in the field of single and multi-user demodulation for CDMA systems hence this area is not investigated in detail for the thesis. Applying the linear model $\boldsymbol{r} = \boldsymbol{H\theta} + \boldsymbol{\eta}$ (with $\boldsymbol{H}$ the observation matrix, $\boldsymbol{\theta}$ the vector to be estimated, and $\boldsymbol{\eta}$ the noise vector), the well-known LMMSE vector estimator yielding the Bayesian Gauss-Markov theorem [Kay1993A, page 391] is used to derive the LMMSE multi-user estimator (producing the soft information prior to applying a decision hypothesis/criterion), where

$$\hat{\boldsymbol{\theta}} = E(\boldsymbol{\theta}) + \boldsymbol{\Sigma}_{\theta}\boldsymbol{H}^{H}\left(\boldsymbol{H}\boldsymbol{\Sigma}_{\theta}\boldsymbol{H}^{H} + \boldsymbol{\Sigma}_{\eta}^{-1}\right)^{-1}\left(\boldsymbol{r} - \boldsymbol{H}E(\boldsymbol{\theta})\right) \tag{4.10}$$

If $\boldsymbol{\theta}$ is zero-mean, i.e. $E(\boldsymbol{\theta}) = 0$, and the noise uncorrelated Gaussian with covariance $\boldsymbol{\Sigma}_{\eta}^{-1} = \sigma_{\eta}^{2}\boldsymbol{I}$, then the estimator becomes $\hat{\boldsymbol{\theta}} = \boldsymbol{\Sigma}_{\theta}\boldsymbol{H}^{H}\left(\boldsymbol{H}\boldsymbol{\Sigma}_{\theta}\boldsymbol{H}^{H} + \sigma_{\eta}^{2}\boldsymbol{I}\right)^{-1}\boldsymbol{r}$ where using the ABCD Matrix inversion Lemma [Frank2002], it is easy to show that $\hat{\boldsymbol{\theta}} = \left(\boldsymbol{H}^{\mathrm{H}}\boldsymbol{H} + \sigma_{\eta}^{2}\boldsymbol{\Sigma}_{\theta}^{-1}\right)^{-1}\boldsymbol{H}^{\mathrm{H}}\boldsymbol{r}$. The signal covariance matrix is given by $\boldsymbol{\Sigma}_{\theta} = E\left(\boldsymbol{\theta}\cdot\boldsymbol{\theta}^{H}\right)$. Substituting the model 1 (from Chapter 2) denoting $\boldsymbol{H} = \boldsymbol{S}$ and $\boldsymbol{\theta} = \boldsymbol{F}\sqrt{\boldsymbol{E}}\boldsymbol{b}$, the classical LMMSE multi user estimator for fading channels becomes

$$\hat{\boldsymbol{\theta}} = \left(\boldsymbol{S}^{H}\boldsymbol{S} + \sigma_{\eta}^{2}\boldsymbol{\Sigma}_{\theta}^{-1}\right)^{-1}\boldsymbol{S}^{H}\boldsymbol{r} \tag{4.11}$$

consisting of a bank of chip matched filters where the outputs are decorrelated with the linear transform $\left(\boldsymbol{S}^{H}\boldsymbol{S} + \sigma_{\eta}^{2}\boldsymbol{\Sigma}_{\theta}^{-1}\right)^{-1}$. The problem from a single user aspect is that the inverse transform commutes over all correlation metrics within the multi-user signature matrix. A modification to this structure can be made applicable for single user scenarios where each chip-matched filter aligned temporally to the Rake delay path, p, is replaced by a Wiener estimator found by minimizing the quadratic form $\frac{\partial}{\partial \boldsymbol{w}_{p}} E\left\{\left(\theta_{p}(t) - \boldsymbol{w}_{p}^{H}\boldsymbol{x}_{p}(t)\right)^{H}\left(\theta_{p}(t) - \boldsymbol{w}_{p}^{H}\boldsymbol{x}_{p}(t)\right)\right\}$ yielding the continuous unbiased estimate $y_{p}(t) = \boldsymbol{w}_{p}^{H}\boldsymbol{x}_{p}(t)$, with

$$\boldsymbol{w}_p = \Sigma_{xx}^{-1} \boldsymbol{\Lambda}_{dx} \tag{4.12}$$

the vector of filter coefficients where $\Sigma_{xx} = E\{\boldsymbol{x}(t) \cdot \boldsymbol{x}^H(t)\}$, $\boldsymbol{\Lambda}_{dx} = E\{\theta_p(t)\boldsymbol{x}_p(t)\}$, and $\theta_p(t) = \alpha_p(t)\sqrt{E_1^{(p)}}b_1(t)$ the desired soft information sequence. In a practical adaptive filter implementation [Latva-Aho1998], we make a decision on $\sum y_p(t) \forall\, p$ with $\hat{b}_1(t) = \text{sgn}\left(\sum_{l=0}^{L-1} \hat{\alpha}_l^*(t)\hat{\theta}_l(t)\right)$ and use this to form the training sequence, i.e. $\hat{\theta}_p(t) = \hat{\alpha}_p(t)\sqrt{E_1^{(p)}}\hat{b}_1(t)$ with $\hat{\alpha}_p(t)$ the channel estimate for the p^{th} path. The filter regressor $\boldsymbol{x}_p(t)$ is stacked such that the middle portion of the window estimates the current sample $\hat{\theta}_p(t)$ when convolved with the weights $\boldsymbol{w}_p$. The length of $\boldsymbol{x}_p(t)$ > G, hence the side information contains past and future samples for applying the equalization projection to remove the effect of interference. For adaptive filtering applying the NLMS algorithm, it would be typical to initialise the weight vector as $\boldsymbol{w}_p = \left[0_{N(G-2)}^T, \boldsymbol{S}_{su}^{*T}, 0_{N(G-2)}^T\right]^T \in \boldsymbol{C}^{NG}$ where *N-G* is a scalar representing the excess length of the filter window. The single user structure utilizing decision directed Wiener estimators (where the rake hard decisions for the desired physical channel are scaled by an appropriate channel estimate) forms the classical LMMSE Rake receiver (Fig 4.11).

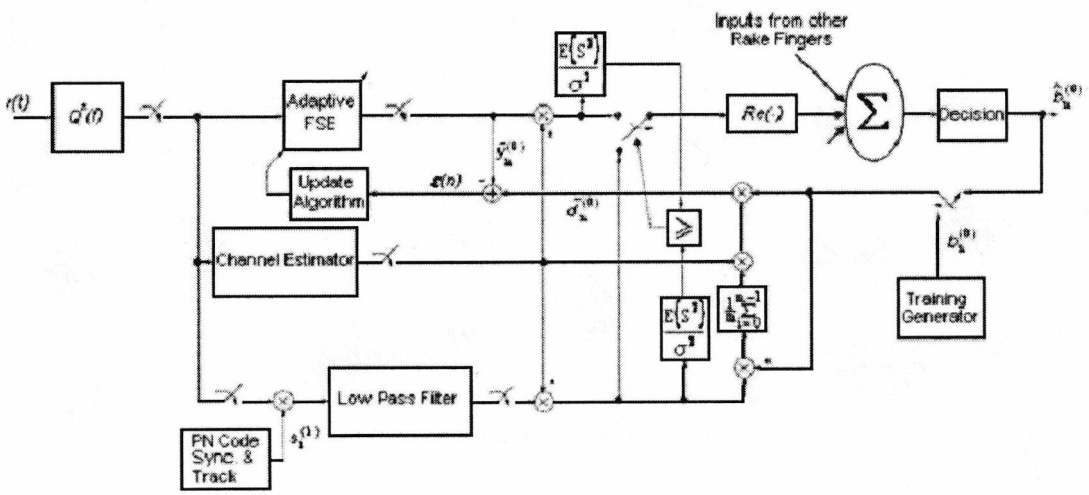

Fig 4.11 The Single User Adaptive LMMSE Rake Receiver. The additional control circuitry consisting of SINR estimation was utilized to direct training from a traditional rake receiver when the initial weights of the filter produce overly noisy outputs until convergence occurs. The combiner also associates the output rake fingers from other antenna elements.

4.3.3 Two Dimensional Chip Equalization

A conventional approach to downlink reception in WCDMA (i.e. consisting of the rake receiver) neglects multiple-access interference since the channel shared by the multi-user transmissions consists of a synchronous multiplex with each user-assigned code being orthogonal to all other codes. However, the fading channel generating multiple propagation paths with non-zero delay spread yields asynchrony and circumvention of the code orthogonality, thus posing limitations to the channel capacity. Furthermore, the Pilot Channel in WCDMA usually accompanies the data channel, where multipath fading obliterates this adjacent channel code orthogonality and renders an additive bias term that degrades performance- particularly when noting that the Pilot channel accounts for a large portion of the base-station transmission power. Clearly to improve downlink performance and capacity, an optimization must be applied to the detection problem for circumvention of the affects of fading. Techniques applying diversity but no specific interference cancellation technique were explored in Chapter 2 and found to be asymptotically bounded by additive interference rendering an irreducible noise floor in multi-user channels.

The LMMSE single-user criterion presented in the previous section is a very commonly referred algorithm for sub-optimum demodulation in the downlink, and is rather attractive in that it can be made adaptive requiring little more than a decision-generated training sequence (normally formed by making hard-decisions on the output of the rake receiver) and a linear channel estimate. However, this technique is generally not suited to long-code systems where the code duty cycle is either impermissibly longer than the temporal duration of the coded data symbol or virtually non-existent (i.e. Gold scrambling codes applied with generator polynomial $2^{41} - 1$ truncated to 38400 chips). In this case, channel equalization would appear to be the most logical solution to remove the channel induced asynchrony and allow interference suppression with a matched filter. Linear Equalization utilizing the zero-forcing optimization is an interesting, if primordial technique first developed in the 1960's [Lucky1966]. The main problem of Zero-forcing equalization [Quereshi1985] is that related to the filter coefficients where:

(A) Original equalizers proposed had priori information on the signalling medium (i.e. twisted pair/coaxial/optical fibre channel with prediction based on channel sounding) where in wireless, the channel is extremely variable and difficult to predict with any degree of accuracy – particularly when noting that channel sounding and/or overheads are very bandwidth inefficient. The UMTS employs a common access channel (the CPICH) to enable synchronization/tracking and channel phase estimation- however the problem with this channel is that it interferes

with adjacent channels due to multiple propagation delays reducing the accuracy of estimation. Alternative baseband coding techniques, separate RF channels (close to the carrier frequency for which information is modulated upon) and sounding pulses would generate superior channel estimation technique at a cost to complexity and spectral efficiency.

(B) The use of channel and delay acquisition techniques can render some information on the signalling medium if a pilot channel is transmitted either in the bit stream or in a synchronous adjacent channel. However, wireless channels change fairly rapidly, hence a continuous channel estimator is required and the zero-forcing equalizer has to adapt to these changes. If the channel were known for all time, the receiver structure can be optimized for the time variant (TV) channel. But this is not realistically applicable generally.

(C) Once the channel is known, the inverse filter representing the zero-forcing equalizer is not guaranteed to be stable in all known circumstances- even though an advantage of the inverse solution is a very simple recursion that can be applied to calculate the coefficients (this recursion is widely known in the deconvolution theorem where for a stable channel, the inverse solution is an infinite numeric series that should ideally decay – i.e. is asymptotic to zero). Generally this problem can also be solved in the frequency domain – note [Falconer2002] and the references therein.

(D) The truncation of the filter impulse response yields residue ISI since inverse filtering generates an infinite number of terms. Furthermore, the zero-forcing tap weights do not account for the additive noise in the desired channel, and hence such receivers are well documented to accentuate the noise particularly when deep spectral nulls are observed in the faded signal [Quereshi1985]. In low ISI/MAI generating channels, this can worsen performance even more so than a far simpler conventional receiver. For this reason, vector based LMMSE equalizer optimization is preferred due to the algorithm, statistically speaking, not generally increasing the moments of noise while also offering a "near ZF" solution in low additive noise channels. The asymptotic limits of the LMMSE channel equalizer are in fact the zero forcing equalizer.

Generic optimization approaches proposed for equalization in third generation mobile usually consider an adaptive/training FIR solution utilizing the Common Pilot Channel. While this approach has been shown [Chowdhury2002, Hooli2002] to yield impressive gains in performance, a problem not often mentioned is that of the generation of the "full" training sequence and whether the Bayesian "cost function" be implemented at the full channel baud rate or the raw data rates of the dedicated data channel. Clearly a chip rate solution would be immediately biased due to the receiver's inability to track and demodulate other users for

performing equalization with a perfectly regenerated training signal (since this training signal should be equivalent to the desired multiuser channel signals). Hence at chip level optimization, the receiver would "see" a rather high noise + interference floor. Of course, a symbol rate solution (applying the difference between the soft outputs of a despreading device and the receiver hard decisions) would offer a much lower noise floor particularly if the processing gain of the desired channel were rather high. However a conundrum with this technique occurs when the noise + interference floor is not overly high (compared to the CPICH) and hence will offer much slower convergence- particularly so in fast fading channels. Indeed, a symbol rate solution to the general serial equalization (and even decision feedback equalization) problem actually becomes analogous to the block linear equalizer such as those presented in [Klein1996].

4.3.3.1 The Broadband Beamformer Employing LMMSE Chip Equalization.

Consider a multiple input, single output (MISO) channel characterized with impulse response (conditioned on the receiver antenna, A) where

$$\boldsymbol{h}^{(A)}[\upsilon] = \sum_{l=0}^{L-1} \partial[\upsilon - l] \cdot h_l^{(A)} \tag{4.13}$$

with $\partial[\upsilon - l] = \begin{cases} 1, & \upsilon = l \\ 0, elsewhere \end{cases}$. A serial chip equalizer with truncated impulse response (and linear FIR filter definition), $\boldsymbol{f}^{(A)}[\upsilon]$ can be characterized with N_f taps (with $N_f > L$) where

$$\boldsymbol{f}^{(A)}[\upsilon] = \sum_{a=0}^{N_f} \partial[\upsilon - a] \cdot f_a^{(A)} \tag{4.14}$$

Since the chip equalizer is implemented for the multi user information stream with $\boldsymbol{\theta} = \sum_{k=1}^{K} \boldsymbol{S}_k \sqrt{\boldsymbol{E}_k} \boldsymbol{b}_k$, an estimate of $\boldsymbol{\theta}$, $\hat{\boldsymbol{\theta}}$ is obtained for the m^{th} chip interval (where $\hat{\boldsymbol{\theta}}$ is delayed by d and the model ignores the tails of transmission at the beginning and end of a radio frame) where

$$\hat{\boldsymbol{\theta}}[m-d] = \sum_{A=0}^{M-1} \sum_{a=0}^{N_f-1} f_a^{(A)} \cdot \gamma^{(A)}[m] \tag{4.15}$$

with $\gamma^{(A)}[m]$ the A^{th} antenna filter regressor (containing samples of the channel distorted multi user information stream with additive noise). This can be written as a vector dot product with

$$\hat{\theta}[m-d] = \boldsymbol{f}^{(A)H} \cdot \boldsymbol{\gamma}^{(A)}[m] \tag{4.16}$$

and $\boldsymbol{f}^{(A)} = \left[f_{N_f-1}^{(A)}, f_{N_f-2}^{(A)}, \cdots, f_0^{(A)}\right]^T \in C^{N_f \times 1}$,

$\boldsymbol{\gamma}^{(A)}[m] = \left[\gamma^{(A)}[m-N_f+1], \gamma^{(A)}[m-N_f+2], \cdots, \gamma^{(A)}[m]\right]^T \in C^{N_f \times 1}$. We can define a channel matrix (conditioned for a particular antenna) as

$$\mathcal{H}^{(A)} = \begin{bmatrix} h_{L-1}^{(A)} & h_{L-2}^{(A)} & \cdots & h_0^{(A)} & \cdots & 0 \\ 0 & h_{L-1}^{(A)} & h_{L-2}^{(A)} & \cdots & h_0^{(A)} \cdots & 0 \\ \vdots & \ddots & & & & \vdots \\ 0 & \cdots & h_{L-1}^{(A)} & h_{L-2}^{(A)} & \cdots & h_0^{(A)} \end{bmatrix} \in C^{N_f \times (N_f+L)} \tag{4.17}$$

which is precisely defined for the regressor of the equalizer. Note that $\mathcal{H}^{(A)}$ has Toeplitz structure and thus is positive semi definite. Denoting $\boldsymbol{\theta}^{(A)}[m]$ as the multi user sequence vector (unperturbed by the channel and noise), we can formulate

$$\boldsymbol{\gamma}^{(A)}[m] = \mathcal{H}^{(A)} \cdot \boldsymbol{\theta}^{(A)}[m] + \boldsymbol{\eta}^{(A)} \tag{4.18}$$

with $\boldsymbol{\theta}^{(A)}[m] = \left[\theta^{(A)}[m-N_f-L+2], \theta^{(A)}[m-N_f-L+3], \cdots, \theta^{(A)}[m]\right]^T \in C^{(N_f+L)\times 1}$ and $\boldsymbol{\eta}^{(A)}$ the additive noise with two sided PSD. Generally for the SIMO channel, the dependency of the multi user sequence vector on the antennas can be removed where $\boldsymbol{\theta}^{(A)} = \boldsymbol{\theta}\ \forall A$. The estimate, $\hat{\theta}[m-d]$ can be expressed in terms of (5.26) with $max(d) = m - N_f - L + 2$ and

$$\hat{\theta}[m-d] = \sum_{A=1}^{M-1} \boldsymbol{f}^{(A)H} \cdot \left\{\mathcal{H}^{(A)} \cdot \boldsymbol{\theta}[m] + \boldsymbol{\eta}^{(A)}\right\} \tag{4.19}$$

The model can be extended to account for sequential detection. Consider the chip level complex random information vector of dimensionality $z >> N_f + L$, where only $N - N_f$ ($N_f + L < N < z$) of the downlink chip rate symbols are estimated. In this case (provided the tails of transmission at the beginning and end of a radio frame are ignored), let the two dimensional vector denote the shifted time sequence of multi user chips[4] which is conveniently sized for the static channel matrix $\mathcal{H}^{(A)}$. Let $\boldsymbol{X}$ be given by

$$\boldsymbol{X} = [\boldsymbol{\theta}_{N_f+L-2}, \boldsymbol{\theta}_{N_f+L-3}, \cdots, \boldsymbol{\theta}_0]^T \in C^{(N_f+L)\times(N-N_f)} \tag{4.20}$$

[4] It is important to note that the WCDMA downlink is a multiple user shared synchronous channel. Hence the information vector contains the multiple summations of the different downlink transmissions from the base station to users undergoing coverage.

with $\boldsymbol{\theta}_n = \boldsymbol{D}_n \boldsymbol{\theta} \in C^{(N-N_f)\times 1}$ the vector consisting of the downlink channel information. Define $\boldsymbol{\theta} = [\theta_{(z)}, \theta_{(z-1)}, \cdots, \theta_{(0)}]^T \in C^{z\times 1}$ as the sequence column vector with $\boldsymbol{D}_n = \left[\boldsymbol{0}_{(N-N_f)\times(N_f+L-n)}, \boldsymbol{I}_{(N-N_f)}, \boldsymbol{0}_{(N-N_f)\times L}\right] \in C^{(N-N_f)\times(N+L)}$ where $\boldsymbol{0}_{(N-N_f)\times(N_f+L-n)}$ is the null matrix and $\boldsymbol{I}_{(N-N_f)}$ the identity matrix. The equalizer regressor matrix considering (5.28) can be given as

$$\boldsymbol{\Upsilon}^{(A)} = \boldsymbol{\mathcal{H}}^{(A)} \cdot \boldsymbol{X} + \boldsymbol{\eta}^{(A)} \in C^{N_f \times (N-N_f)} \tag{4.21}$$

where the estimated sequence is given by

$$\hat{\boldsymbol{\theta}}^T = \sum_{A=1}^{M-1} \boldsymbol{f}^{(A)H} \cdot \boldsymbol{\Upsilon} \in C^{(N-N_f)\times 1} \tag{4.22}$$

To derive the multi channel equalizer, consider jointly optimising the chip equalizer according to the spatial and temporal signatures, hence stack the channel matrix (becoming a tall matrix) and the filter regressor such that

$$\boldsymbol{\mathcal{H}} = \left[\boldsymbol{\mathcal{H}}^{(0)T}, \boldsymbol{\mathcal{H}}^{(1)T}, \cdots, \boldsymbol{\mathcal{H}}^{(M-1)T}\right]^T \in C^{MN_f \times (N_f+L)} \tag{4.23}$$

$$\boldsymbol{\Upsilon} = \left[\boldsymbol{\Upsilon}^{(0)T}, \boldsymbol{\Upsilon}^{(1)T}, \cdots, \boldsymbol{\Upsilon}^{(M-1)T}\right]^T \in C^{MN_f \times (N-N_f)} \tag{4.24}$$

with

$$\hat{\boldsymbol{\theta}}^T = \boldsymbol{f}^H \cdot \boldsymbol{\Upsilon} \in C^{(N-N_f)\times 1}. \tag{4.25}$$

where $\boldsymbol{f} = \left[\boldsymbol{f}^{(0)T}, \boldsymbol{f}^{(1)T}, \cdots, \boldsymbol{f}^{(M-1)T}\right]^T \in C^{MN_f \times 1}$. Hence a basis has been formed for deriving a linear channel equalizer utilizing an estimation hypothesis. The MMSE chip equalizer minimizing the quadratic form $\boldsymbol{J} = E\left\{\left\|\boldsymbol{\theta} - \hat{\boldsymbol{\theta}}\right\|^2\right\}$ yields the following quadratic MSE function

$$\boldsymbol{J} = \boldsymbol{f}^T\left(\boldsymbol{\mathcal{H}}\boldsymbol{\Sigma}_{XX}\boldsymbol{\mathcal{H}}^H + \boldsymbol{\Sigma}_\eta\right)\boldsymbol{f}^* - 2\Re\left(\partial^T \boldsymbol{\Sigma}_{XX}\boldsymbol{\mathcal{H}}^H \boldsymbol{f}^*\right) + \partial^T \boldsymbol{\Sigma}_{XX}\partial \tag{4.26}$$

with $\boldsymbol{\Sigma}_{XX} = E\left\{\boldsymbol{\theta}\cdot\boldsymbol{\theta}^H\right\} \in C^{(N_f+L)\times(N_f+L)}$ representing the true sequence covariance. $\boldsymbol{\Sigma}_\eta = E\left\{\eta\cdot\eta^H\right\}$ is the noise covariance matrix. $\partial \in C^{(N_f+L)\times 1}$ is the unit vector with a 1 in the position $N_f + L - d$. Obtaining the minimum MSE by solving $\frac{\partial \boldsymbol{J}}{\partial \boldsymbol{f}} = 0$ yields

$$\boldsymbol{f}_{MMSE}^T = \partial^T \boldsymbol{\Sigma}_{XX}\boldsymbol{\mathcal{H}}^H\left(\boldsymbol{\mathcal{H}}\boldsymbol{\Sigma}_{XX}\boldsymbol{\mathcal{H}}^H + \boldsymbol{\Sigma}_\eta^{-1}\right)^{-1} \tag{4.27}$$

Using the ABCD matrix inversion Lemma, we can obtain the standard form of the filter noting $(A+BCD)^{-1} = A^{-1} - A^{-1}B\left(DA^{-1}B+C^{-1}\right)^{-1}DA^{-1}$ with $\partial^T \boldsymbol{\Sigma}_{XX} \boldsymbol{\mathcal{H}}^H \left(\underbrace{\boldsymbol{\mathcal{H}}}_{B} \underbrace{\boldsymbol{\Sigma}_{xx}}_{C} \underbrace{\boldsymbol{\mathcal{H}}^H}_{D} + \underbrace{\boldsymbol{\Sigma}_{\eta}^{-1}}_{A} \right)^{-1}$ allowing the equivalent filter to be computed yielding

$$\boldsymbol{f}_{MMSE}^T = \partial^T \left(\boldsymbol{\mathcal{H}}^H \boldsymbol{\Sigma}_{\eta}^{-1} \boldsymbol{\mathcal{H}} + \boldsymbol{\Sigma}_{XX}^{-1} \right)^{-1} \boldsymbol{\mathcal{H}}^H \boldsymbol{\Sigma}_{\eta}^{-1} \tag{4.28}$$

If $\boldsymbol{\Sigma}_{\eta}$ is uncorrelated Gaussian Noise, i.e. $\boldsymbol{\Sigma}_{\eta} = \sigma_n^2 \boldsymbol{I}$, then

$$\boldsymbol{f}_{MMSE}^T = \partial^T \left(\boldsymbol{\mathcal{H}}^H \boldsymbol{\mathcal{H}} + \sigma_n^2 \boldsymbol{\Sigma}_{XX}^{-1} \right)^{-1} \boldsymbol{\mathcal{H}}^H \tag{4.29}$$

It can be immediately noted from (4.29) that this equalizer requires the $(N_f + L) \times (N_f + L)$ data covariance matrix to be known – which is one of the difficulties of the method since all multi user codes and channel powers must be known or estimated. It can also be noted that the channel matrix $\boldsymbol{\mathcal{H}}$ must be known or estimated. The zero forcing equalizer overcomes these preliminaries (other than knowledge of the channel) and is found when the channel SNR $\rightarrow \infty$, i.e. the asymptotic bound of the MMSE chip equalizer. In this case, $\sigma_n^2 \boldsymbol{\Sigma}_{XX}^{-1} = 0$ and

$$\boldsymbol{f}_{ZF}^T = \partial^T \left(\boldsymbol{\mathcal{H}}^H \boldsymbol{\mathcal{H}} \right)^{-1} \boldsymbol{\mathcal{H}}^H \tag{4.30}$$

4.3.3.2 The Adaptive 2D LMMSE Equalizer

Due to the limited practicality of (4.29) and (4.30), the multi channel serial chip equalizer can be implemented as an adaptive FIR filter utilizing the NLMS or RLS algorithm. Also in the WCDMA downlink considering pulse shaping, we can resort to the model in Chapter 2. In this case the dual antenna chip equalizer can be obtained by solving

$$\frac{\partial}{\partial \boldsymbol{f}} E\left\{ \left| \boldsymbol{f}^H \boldsymbol{r} - \left(\boldsymbol{S}_1 \xi_1 \mathrm{b}_1 + \sum_{i=2}^{K} \boldsymbol{S}_i \xi_i \mathrm{b}_i + \boldsymbol{P}_s \boldsymbol{\xi}_s \boldsymbol{p} \right) \right|^2 \right\}$$

element wise (leading to a block estimator), which yields

$$\boldsymbol{f} = \boldsymbol{\Sigma}_r^{-1} \boldsymbol{\Lambda}_{dr} \tag{4.31}$$

with $\boldsymbol{\Sigma}_r = E\left\{ \boldsymbol{r} \cdot \boldsymbol{r}^H \right\}$, $\boldsymbol{r} = \left[\boldsymbol{r}_1^T, \boldsymbol{r}_2^T \right]^T$ leading to the decomposition

$$\boldsymbol{\Sigma}_r = \boldsymbol{Q}\boldsymbol{F} \left\{ \sum_{k=1}^{K} \xi_k^2 \left[\boldsymbol{S}_k \boldsymbol{S}_k^H \right] \right\} \boldsymbol{F}^H \boldsymbol{Q}^T + \boldsymbol{\Sigma}_{\eta} \tag{4.32}$$

and $\Lambda_{dr} = E\left\{\left(\boldsymbol{S}_1\xi_1 b_1 + \sum_{i=2}^{K}\boldsymbol{S}_i\xi_i b_i + \boldsymbol{P}_s\boldsymbol{\xi}_s\boldsymbol{p}\right)\cdot\boldsymbol{r}\right\}$ with $\boldsymbol{r}$ given in Chapter 2 leading to

$$\Lambda_{dr} = \boldsymbol{QF}\left\{\sum_{k=1}^{K}\xi_k^2\left[\boldsymbol{S}_k\boldsymbol{S}_k^H\right]\right\} \tag{4.33}$$

The chip equalizer given in (4.31) is the general MMSE form of the filter where the model assumes that the multi channel information vector $\left(\boldsymbol{S}_1\xi_1 b_1 + \sum_{i=2}^{K}\boldsymbol{S}_i\xi_i b_i + \boldsymbol{P}_s\boldsymbol{\xi}_s\boldsymbol{p}\right)$ is known. Realistically for the WCDMA downlink, two cases can be made available to the filter for training, namely $\boldsymbol{S}_1\xi_1\hat{b}_1$ for decision directed adaptation, or $\boldsymbol{P}_s\boldsymbol{\xi}_s\boldsymbol{p}$ for CPICH adaptation. Since the pilot channel contains known symbols (exhibiting higher power than any corresponding physical data channel), then this is the most logical solution for training an adaptive equalizer whose coefficients will be used to equalize the corresponding data channel. Note that $\boldsymbol{P}_s\boldsymbol{\xi}_s\boldsymbol{p}$ will form the scrambled pilot symbols (formally set in UMTS with a constant symbol $1+j$) with $\boldsymbol{\xi}_s$ the received amplitude. This solution has been researched in [Petre2000] for DS-CDMA in general and [Hooli2002] as part of a generalized paper covering many different aspects of adaptive equalization in wireless mobile utilizing spread-spectrum multiple access. The NLMS algorithm is considered in this thesis for the adaptive filter due to simplicity. The general receiver structure is given in Fig. 4.12 for one diversity antenna. An adaptive fractionally spaced equalizer (FSE) considering an oversampling index of four is investigated in the thesis. The adaptive equalizer is proceeded by a diversity combiner and despreading devices (descrambling and integrate-dump detection/chip matched filtering).

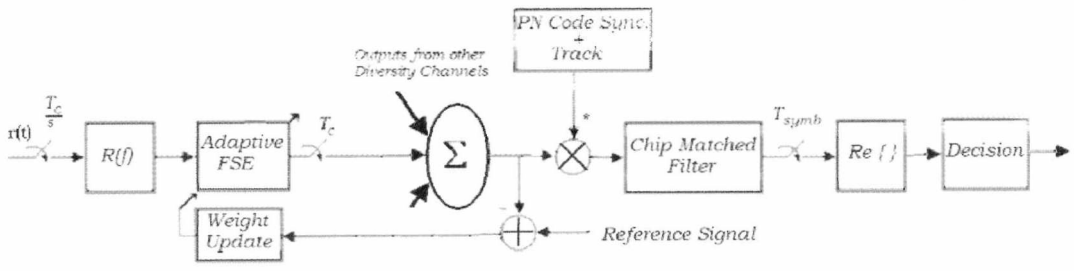

Fig 4.12 The Adaptive multi-channel chip equalizer employing training from the scrambled pilot channel. This diagram is symbolic and not a true reflection of implementation where the equalizer weights are "transferred" to a separate channel filter for demodulating the single user.

4.3.4 Approximate Relationships Between the Symbol Level Equalizer, LMMSE Post-Combining Rake receiver, and MMSE Chip Equalizer

The aforementioned receiver technologies are shown in this section to be somewhat similar to each other. We start with the decision variable of the chip equalizer, which is $\partial_{EQ} = \boldsymbol{S}_1^H \boldsymbol{f}^H \boldsymbol{r}$ (assuming $\boldsymbol{f}$ is a block transform) resulting in

$$\partial_{EQ} = \xi_1^2 \left(\boldsymbol{S}_1 \boldsymbol{F}\boldsymbol{Q}\right)^H \left[\left\{ \sum_{k=1}^{K} \xi_k^2 \left[\boldsymbol{S}_k \boldsymbol{S}_k^H\right] \right\} \boldsymbol{F}^H \boldsymbol{Q}^T + \boldsymbol{\Sigma}_\eta \right]^{-1} \boldsymbol{r} \tag{4.34}$$

The postcombining LMMSE Rake receiver utilizing $\boldsymbol{w} = arg\ min E\left\{ \left| \boldsymbol{w}^H \boldsymbol{r} - \mathrm{b}_1 \right|^2 \right\}$ results in the decision variable (after some linear algebra)

$$\partial_R = \xi_1 \left(\boldsymbol{S}_1 \boldsymbol{F}\boldsymbol{Q}\right)^H \left[\left\{ \sum_{k=1}^{K} \xi_k^2 \left[\boldsymbol{S}_k \boldsymbol{S}_k^H\right] \right\} \boldsymbol{F}^H \boldsymbol{Q}^T + \boldsymbol{\Sigma}_\eta \right]^{-1} \boldsymbol{r} \tag{4.35}$$

where comparing (4.34) and (4.35) yields $\partial_R = \frac{1}{\xi_1} \partial_{EQ}$, i.e. the postcombining LMMSE Rake receiver and the LMMSE chip equalizer produce the same decision statistic down to a scalar.

The WMF has coefficients given by $\boldsymbol{w}_{WMF} = \boldsymbol{\Sigma}_u^{-1} \boldsymbol{h}$. The MMSE chip equalizer has coefficient vector $\boldsymbol{f} = \boldsymbol{\Sigma}_r^{-1} \boldsymbol{\Lambda}_{dr} \approx \xi_1^2 \boldsymbol{\Sigma}_r^{-1} \boldsymbol{h}$ using a false assumption. Write $\Sigma_r = \Sigma_s + G \Sigma_u$ and hence $\Sigma_u = \frac{1}{G} \Sigma_r - \frac{\xi_1^2}{G} \Sigma_h$ with $\Sigma_h = E\left\{ \boldsymbol{h}\boldsymbol{h}^H \right\}$. Using the Matrix inversion Lemma we can show that

$$\boldsymbol{w}_{WMF} = G \left[\Sigma_r^{-1} - \frac{\Sigma_r^{-1} \Sigma_h \Sigma_r^{-1}}{\boldsymbol{h}^H \Sigma_r^{-1} \boldsymbol{h} + \frac{1}{\xi_1^2}} \right] \boldsymbol{h} \tag{4.36}$$

Equating (4.36) with $\boldsymbol{f} \approx \xi_1^2 \boldsymbol{\Sigma}_r^{-1} \boldsymbol{h}$ allows an approximate relationship to be developed noting

$$\psi = \frac{G\boldsymbol{\Sigma}_r}{\xi_1^2}\left[\Sigma_r^{-1} - \frac{\Sigma_r^{-1}\Sigma_h\Sigma_r^{-1}}{\boldsymbol{h}^H\Sigma_r^{-1}\boldsymbol{h} + \frac{1}{\xi_1^2}}\right] = G\left[\frac{-1}{\xi_1^4\boldsymbol{h}^H\Sigma_r^{-1}\boldsymbol{h} - \xi_1^2}\right] \quad \text{with } \psi \text{ a scalar of}$$

proportionality. Hence

$$\boldsymbol{w}_{WMF} = \left[\frac{G}{\xi_1^2\left(1 - \xi_1^2\boldsymbol{h}^H\Sigma_r^{-1}\boldsymbol{h}\right)}\right]\boldsymbol{f} \tag{4.37}$$

showing the WMF and MMSE equalizer produce similar coefficients differing by a scalar of proportionality. This is only an approximation due to the MMSE chip equalizer assumption that $\Lambda_{dr} \approx \xi_1^2\boldsymbol{h}$. This also does not mean that the interference whitening Rake and MMSE chip equalizer will perform similarly, since the relationship between the receivers as in (4.37) is only approximate. The Appendix H contains a derivation of the symbol level dual antenna receiver allowing for comparison with the chip level version in 4.3.3.1 for completeness.

4.3.5 SIMULATION EXAMPLES

Presented in this section are some simulation results for the Receiver techniques described in this section. The simulation parameters were set to those in Chapter 2 and preceding sections of this chapter to keep consistency with observations. The delay acquisition and tracking was assumed perfect unless stated otherwise. The multipath channel employed was the classical Rayleigh channel with parameters indicative of the Vehicular A channel. The vehicular speed was set to 36Km/Hr (unless explicitly stated for a simulation plot) simulating a fairly fast fading channel. The access channel considered variable number of users with Uniform random power distribution (simulating the power control considering that all users were scattered in the basestation transmission sector).

The LMMSE Rake receiver will not be considered since its performance is virtually identical to the ideal LMMSE Channel equalizer with short codes. The first result of this section (Fig. 4.13) compares the Rake, 2D Rake, the interference-whitening Rake, the Zero forcing and LMMSE Channel equalizer. This was done to give a clear sense of perspective as to the performance of the various algorithms for moderately loaded synchronous downlink channels (K = 16). This observation, and other general observations (conditioned on the system capacity) conducted by the author concur that the LMMSE dual channel equalizer greatly improves the downlink performance over the classical 2D Rake receiver. This is due

to the algorithm accounting for all temporal and spatial aspects of diversity allowing interference cancellation and optimum diversity combining for improving the SNR. The Zero forcing channel equalizer is similarly optimal except for cases when the channel SNR are low (since the ZF Channel equalizer generally increases the noise floor despite offering perfect channel decorrelation[5]). The Interference-Whitening Rake (analogous to the GRAKE) yields superior performance over the classical 2D Rake, but unsurprisingly was less optimal than the LMMSE channel equalizer (see section 4.3.4 where it was found the diversity weights are similar to an approximate rather than exact equalizer). The effect of channel estimation is included for the LMMSE channel equalizer where real channel estimates cause a quite significant degradation to the performance. The next set of results (Figs. 4.14 – 4.17) investigates the performance of the adaptive channel equalizer employing the NLMS algorithm[6] (using the common pilot channel for applying the adaptation). This was conducted for K = 4, 8, 16 and 30 users. The first observation is that the exact MMSE solution is nearly interference resistant (with the only difference in performance due to the excess MSE incurred from the tails generated due to the truncated impulse response of the filter). The case for the adaptive NLMS channel equalizer is not so ideal. For low channel loading (K = 4 and K = 8), the channel equalizer yields significantly improved performance over the 2D Rake receiver (although this performance is significantly degraded compared to the full MMSE implementation). However, for moderate to high channel loading conditions, the performance improvement over the 2D Rake receiver is not so significant. In fact, for K = 30 users (based on the uniform distribution of user powers) the performance of the adaptive channel equalizer is almost the same as the 2D Rake receiver except for SNR < 6dB where the adaptive equalizer performed worse. This is not surprising since the adaptive solution utilizing the CPICH will "see" an exceedingly low SNR when many users are multiplexed into the synchronous downlink. For lower numbers of users assuming that the Pilot channel accounts for a larger portion of the base station transmitted power (in this thesis $10\log_{10}\left(\frac{\xi_p^2}{\xi_d^2}\right) = 10dB$), the $10\log_{10}\left(\frac{\xi_p^2}{\sum_{k=1}^{K}\xi_k^2}\right)$ > 0dB. However for significantly larger number of users, this ratio is less than 0dB. This causes slow convergence of the adaptive filter and greater misadjustment due to the larger eigenvalue spread of the signal

[5] We assume that the FIR equivalent of the Zero forcing and LMMSE channel equalizer is sufficiently long such that the tails of interference due to the finite length deconvolution are much smaller than the background noise.

[6] We don't consider the RLS scheme due to the far higher complexity over the NLMS.

covariance matrix. If the $10\log_{10}\left(\frac{\xi_p^2}{\sum_{k=1}^{\kappa}\xi_k^2}\right)$ is too low, convergence of the adaptive filter may not be realizable. This is an aspect that has some considerable limitations with dynamic network user allocations, hence blind adaptive MOE [Honig1995] or Prefiltering algorithms (such as the adaptive rake prefilter investigated in [Hooli2001, Hooli2002]) may be more suitable. The adaptive MOE equalizer circumventing specific training sequences was also investigated in these papers. This technique utilizes the CPICH for channel estimation where the equalizer is decomposed into a channel constrained fixed component and an adaptive component. Blind equalization applying the MOE, subspace, Griffith's, or the constant modulus algorithm was investigated in [Heikkila2001, Zecevic1997, Giannakis1997, Xu1995]. Blind equalization techniques do not generally improve upon the chip equalizer employing the CPICH, but some advantage can be gained in particularly noisy channels. We can ensure convergence of the adaptive CPICH trained equalizer by dynamically adjusting the adaptive step size according to the eigenspread of the covariance matrix, but this is a significant extra complexity component[7]. The adaptive chip equalizer was also tested for different vehicular channel speeds when K = 16 (Fig. 4.18). The results show that increasing vehicular speed (creating a channel with large Doppler spread) increases the probability of symbol error. This was an expected result since the higher Doppler spread increases the fading rate causing the filter to never properly converge and track the varying conditions. Hence the adaptive CPICH trained chip equalizer has implemental/adaptive constraints in fast fading channels. This problem is not easily overcome unless a more advanced adaptation scheme is used (such as the RLS) normally incurring a significantly enhanced computational cost.

[7] Dynamically adjusting the step size can result in significant performance gain for adaptive filters– see [253]. However this does not ensure convergence in all conceivable scenarios.

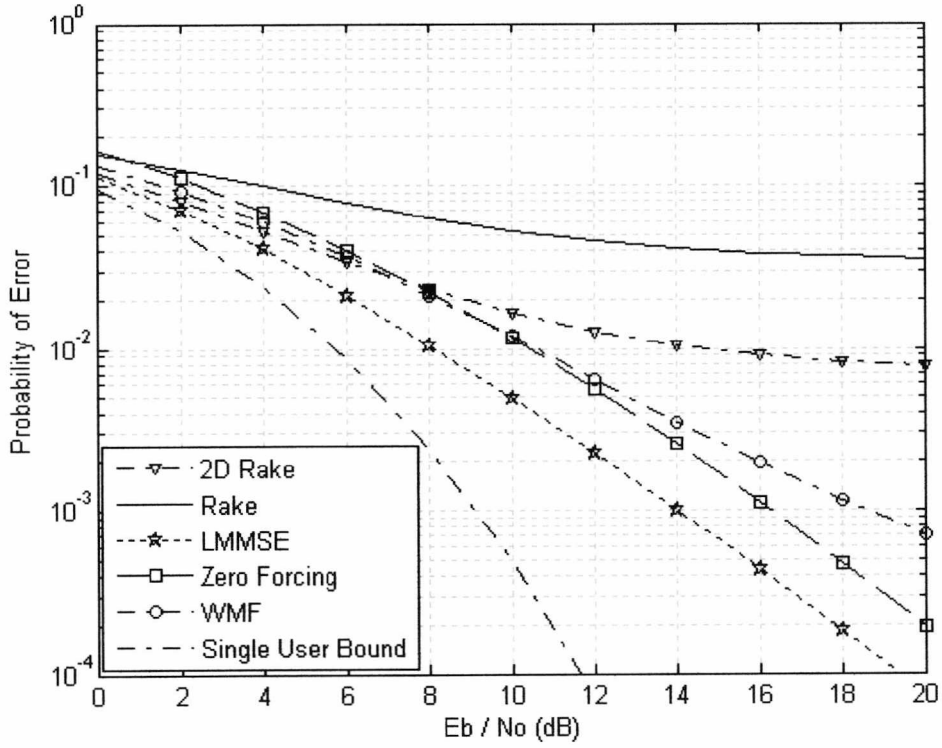

Fig 4.13 Performance of the advanced diversity receivers for K=16 users.

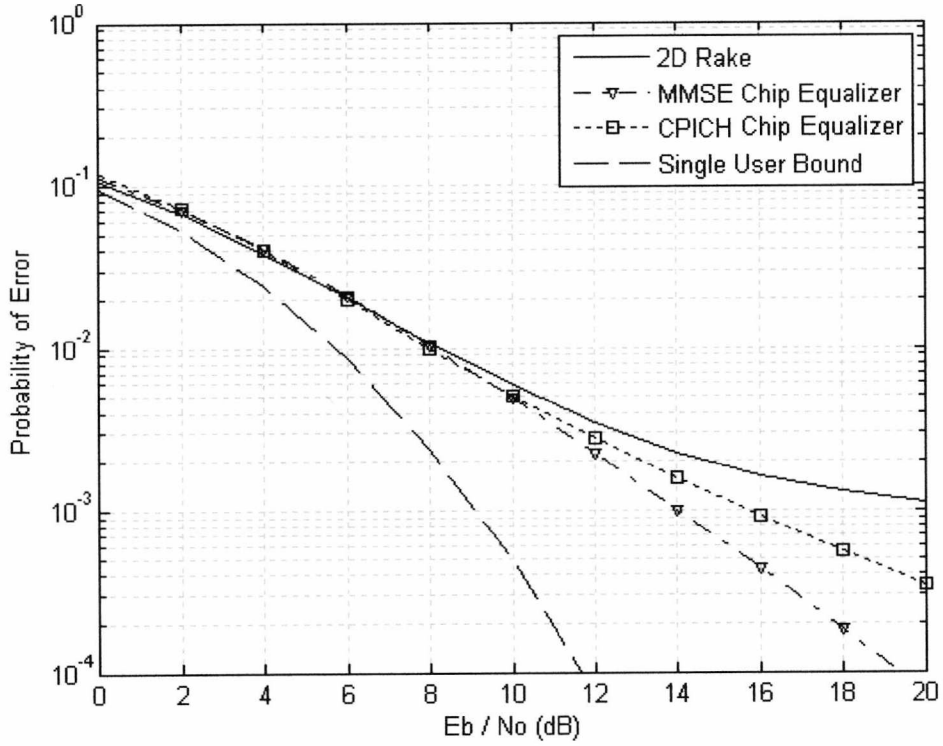

Fig 4.14 Performance of the adaptive chip equalizer for K=4 users.

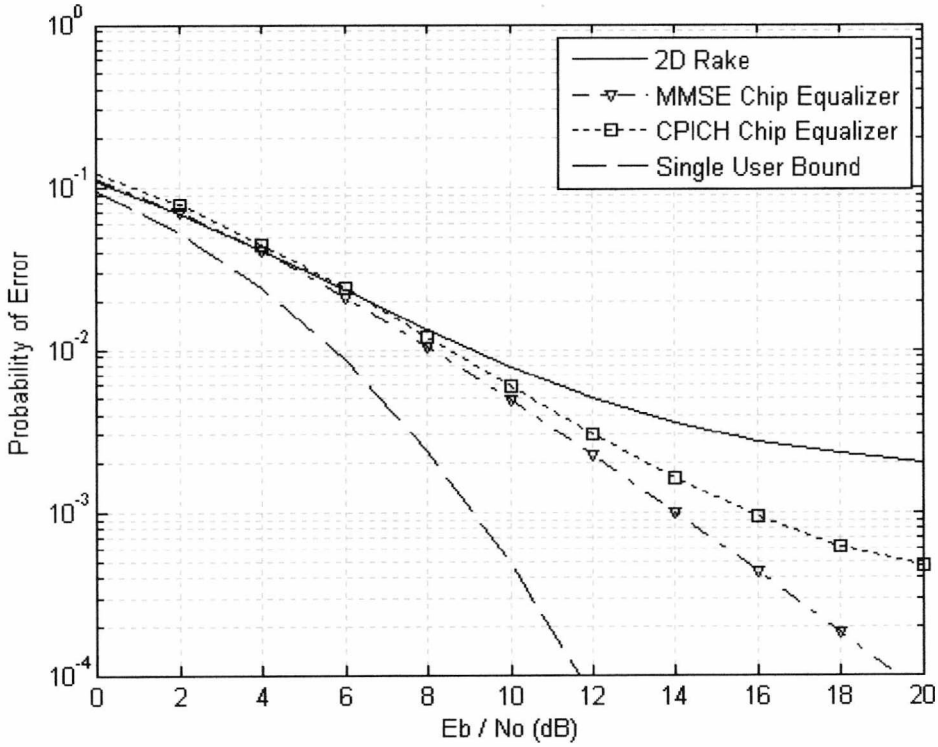

Fig 4.15 Performance of the adaptive chip equalizer for K=8 users.

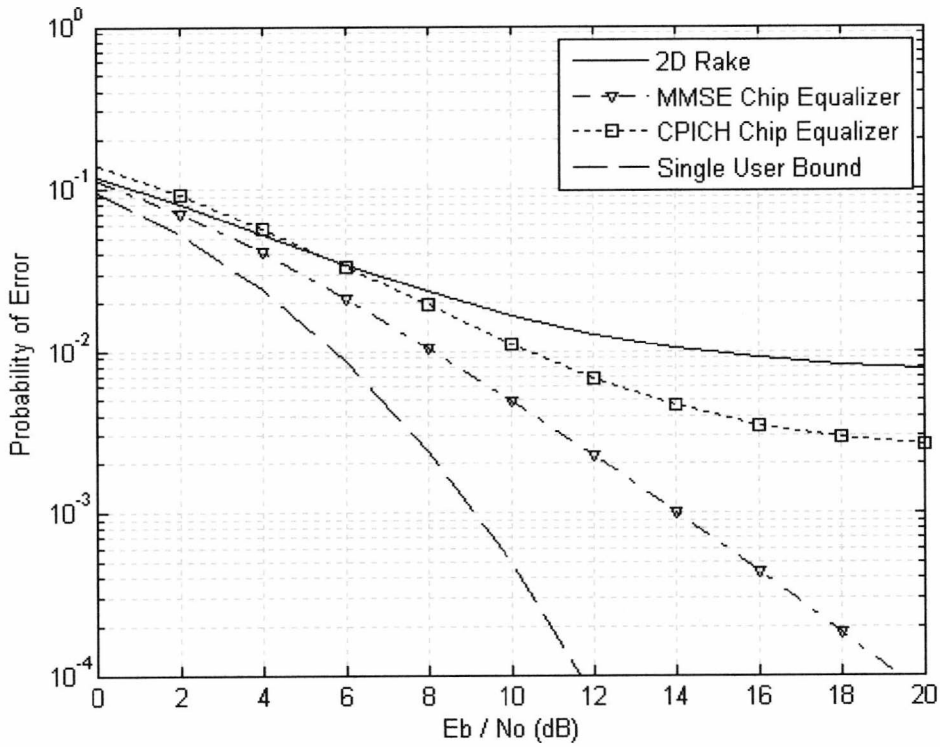

Fig 4.16 Performance of the adaptive chip equalizer for K=16users.

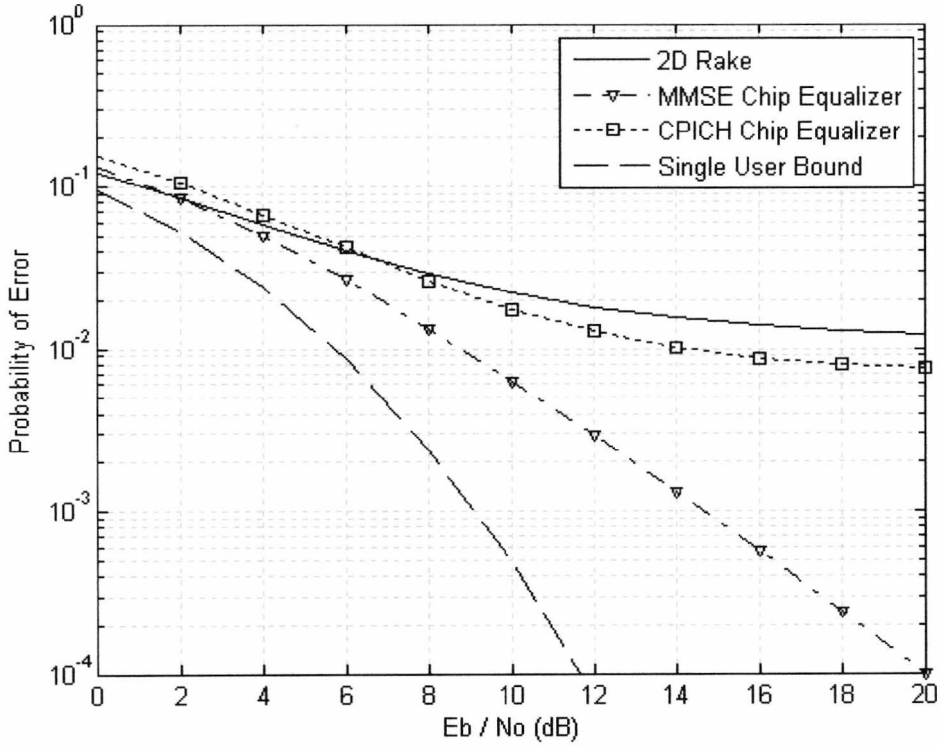

Fig 4.17 Performance of the adaptive chip equalizer for K=30 users.

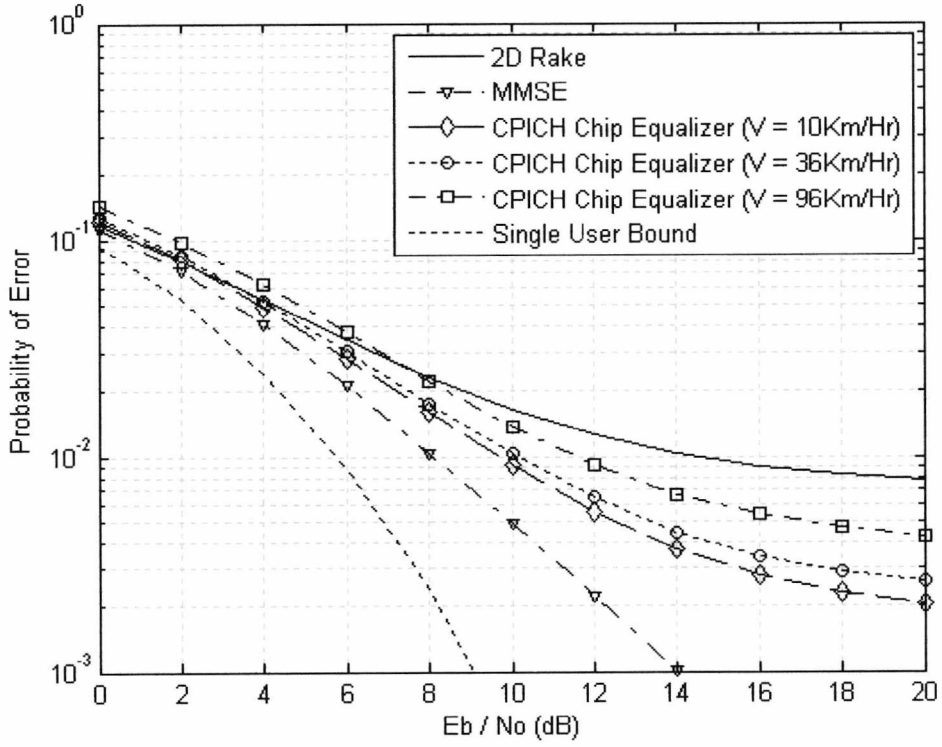

Fig 4.18 Performance of the adaptive chip equalizer for different vehicular speeds when K=16.

4.4 DISCUSSION

The performance of the Adaptive 2D Rake receiver and multi-channel chip equalizers were analyzed for the WCDMA downlink and shown to yield significant improvements in the probability of detection. However, the implemental complexities and practicality of the different receiver devices require some consideration. The interference Whitening solution requires that the second order statistics of interference are known or estimated. However, accurate estimation of the multivariate interference is a non-trivial process and the receiver cannot be assumed to have this knowledge. A crude estimation methodology can be applied utilizing the technique employed in Chapter 2 for the MSNIR beamformer (see Proposition E.1 in Appendix E). However, upon estimation of the interference statistics, the non-trivial matrix inversion is a major impediment to this method. The use of Cholesky factorization can significantly reduce this complexity, although this solution can still be quite costly to implement. The case for the chip equalizer employing MMSE or zero-forcing optimization requires that the channel is known over the transmission interval. Realistically, this channel must be estimated employing the methods in Chapter 3 for the rake receiver. Since channel estimation is noisy, this effect will transfer to the performance of the equalizer in question. The simplest solution is the adaptive channel equalizer incurring a cost to performance. The main drawback to using the common pilot channel as the statistical regressor (and training based on the chip rate pilot signal formed by scrambling the known symbols) is that the channel SINR (i.e. the pilot chip to interference + noise ratio) will inevitably be low for all cases other than for single user channels and low noise scenarios. Overcoming the excess MSE by applying chip rate adaptation would be symbol level or hybrid symbol/chip training [Bastug2005]. However, the cost of symbol level training can be very slow convergence [Krauss2000]. The use of more advanced adaptation schemes utilizing the structure of the received signal auto-covariance would be required for near-optimum equalization. Such a structure utilizing the block Toeplitz structure of the inverse auto-covariance matrix was researched in [Hooli2002], where the equalizer was decomposed into a pre-filter (with coefficients set to the middle row of the inverse matrix) and a Rake combiner. The adaptation of the equalizer was employed using the Householder RLS algorithm. The receiver was shown to significantly outperform the adaptive chip equalizer (using the pilot channel), but the argument against this algorithm is its computational complexity. Overall the adaptive chip equalizer employing the NLMS algorithm appears the most logical solution for the downlink detection problem since performance is satisfactory at minimal complexity for a wide variety of cases. The big question mark is very high system capacity and fast fading channels causing significant degradation to the filter performance.

Any realistic implementation for a diversity receiver in current and future mobile wireless systems will need to cope with high and variable data rates transmitted through a channel employing long or short codes. In current WCDMA systems, the data rate can be increased without bandwidth expansion via reduction of the spreading factor (denoted variable spreading factor). Another technique regularly mentioned is called multicode where data rates can be dynamically adjusted by the allocation of several parallel spreading codes on separate data channels of fixed spreading factor. In the UMTS-FDD forward link, the diversity receiver employed is based on the conventional RAKE receiver. The multi-rate techniques proposed and employed in WCDMA yield rather different receivers – where the multicode case requires separate integrate-dump filters per data channel, per path. Furthermore, multirate transmissions in dispersive fading channels incur an additional interference term- namely the interference between adjacent code channels of the single users "own data". This is quite different to the ISI generated in low processing gain variable spreading factor or IPI when the coding is longer or non-cyclic (or when propagation delays cause correlation between the direct and reflected path yielding an effective single path channel with no ISI but no diversity gain). In fact, this technique is more analogous to the interference mechanism denoted as MAI, hence will present an asymptotic bound on the Rake receiver performance even in single-user data channels (i.e. K=1). Channel equalization has been shown to remove the asymptotic bound on interference due to parallel user/data channels sharing the downlink channel, hence any optimum/sub-optimum synchronous detection problem in the WCDMA downlink will start and end with adaptive equalization. Alternative techniques that are blind to the channel allocations by other users are scarce (particularly for long-code CDMA), although one researcher published a paper proposing interference cancellation for the downlink by noticing that the OSVF Walsh Hadamard codes have repeatability – i.e. the first few chips within a code are shared by many other codes in the sequence (particularly the children codes exhibiting some sequence repetition with parent codes). This research contribution [Dahlhaus1997] showed that some downlink interference cancellation is possible. Poor and Verdu proposed the classic paper for optimum single user demodulation in multiple access channels in 1988 [Poor1988], but this technique required explicit knowledge of the access codes.

CHAPTER 5
NUMERIC CODING FOR SINGLE USER TERMINALS IN WCDMA CHANNELS

PREFACE

Chapters two through four focused exclusively on the optimisations and implementations of various diversity and matched filter algorithms to improve the quality of detection in the WCDMA downlink. The effect of arithmetic imprecision was neglected during analysis of the performance for a fixed or adaptive filter at circuit and/or system level when implemented as part coherent receiver in wireless communication. It cannot be assumed that the fairly high precision generated from floating point calculations in computer simulation would be immediately transferable to a practical receiver. Constraints regarding the size and the available power on a mobile handset (for instance) generate a requirement to circumvent, as far as possible, the complexity of the receiver integration onto ASIC, FPGA or DSP technologies. Approaches for computational reduction either incur tradeoffs in algorithmic complexity (i.e. removing matrix level operators and replacing with adaptive FIR filters if permissible by the algorithm), diminution in the filter length (by truncating the impulse response) or application of a performance-enhancing filter away from the receiver front end (where the baud rate is much higher). Leading examples of algorithmic approaches to complexity reduction in WCDMA systems include the rake/array receiver with power savings and reduced diversity order [Eng1996], chip-level equalization with finite memory [Petre2000], finite windowed Decorrelation and LMMSE interference suppressing filters [Wijayasuriya1996], equalization applied at symbol level [Krauss2000], and adaptive least squares versions of the generic LMMSE diversity receiver [Barbosa1998]. On this note, it is very commonly observed that applying approximations or hardware saving algorithms to any filtering device reduces the net system performance. It is the objective of this chapter to generalize a matched filter and rather than reduce its order or apply some form of approximation, the system and filter level aspect for investigation is the numeric precision. It is well known that reduction of the amount of area and power consumption is proportional to the number of bits encoded to each real number. Clearly, reduction in the number of bits preferably to a fixed-point representation would reduce the overall complexity of the arithmetic units. Multipliers are generally arithmetic devices that have a hardware

complexity (number of gates/switching devices) that grows exponentially with the number of fractal bits encoded for each quantized number. Techniques to reduce the arithmetic complexity at gate level include the Canonical Signed Digit and Residue number systems [Cavanagh1984]. However, reduction in the arithmetic precision leads to obviously undesirable effects such as round-off and quantization errors degrading the signal to noise ratio at the output of a matched filter. Finite precision effects also yield noticeable errors in a digital filter's frequency response and may result in digital filters behaving as non-linear systems. Therefore, a method based on observational and analytical techniques would be useful to determine the acceptable limits of the arithmetic precision such that the receiver performance is not degraded to an extent that can be considered unacceptable. The lack of dynamic range and truncated word length for conventional fixed-point arithmetic can yield a large performance loss particularly when a low number of bits are encoded per number. This can be compensated by utilizing a floating-point representation with truncated mantissa at a cost to the computational load. Therefore, for this reason alone, the logarithmic number system is proposed in this chapter to carry the burden of performing high speed, accurate multiplications for matched filters used/proposed for the WCDMA downlink. The logarithmic number system has certain advantages over fixed-point number systems in that the dynamic range is usually far greater, where multiplication in the logarithmic domain can be controlled (and made equivalent to the floating point multiplication with truncated word length) and executed using look up tables (for lower precision application) or Lagrange interpolators with relatively small fixed multipliers. This chapter is broken down as following: Section I introduces the concept of binary coding and statistical modelling of the errors due to multiplication and MAC operations. Section II describes the logarithmic number system and the various linear-logarithmic and logarithmic-linear coding methodologies important for application in digital filters. Error modelling and an important criterion for equivalent floating point resolution are introduced to ensure that logarithmic arithmetic does not degrade the net accuracy when executing logarithmic domain multiplication. Section III yields an investigation of uniform and logarithmic coding for the Root Raised Cosine Matched Filter and the Adaptive Equalizer presented in Chapter 5. The system level performance is expatiated for fixed precision application and compared with the double-precision floating point used by default in Matlab.

5.1 Fixed-Precision Arithmetic Employing Uniform Binary Coding

This section presents an overview of fixed-point arithmetic as employed in the majority of digital signal processing applications. Due to the popularity of digital filtering techniques over analogue counterparts, real analogue numbers/samples require some form of coding prior to being manipulated by a digital processor. Since uniform radix 2 coding is by far the most conventional method for representing analogue numbers (which may be a quantity representing an actual potential difference or any other physical process interpreted as a voltage by a transducer), the concept of infinite numeric precision is idealistic rather than practical. Numbers in communication systems are typically represented in real or complex format with finite numeric precision [Cavanagh1984]. The usual approach in computer simulation would be to assume that numbers are of infinite precision[1] and thus in practical hardware design/simulation, a discrepancy may occur between simulated and ideal performance. Quantization is the process of converting a continuous signal into a discrete signal. The actual accuracy of the quantization process depends chiefly on coding used, the number of bits encoded, and whether the coding is of fixed or floating-point representation. Quantization in this thesis considers a uniform quantizer of fixed bin width [Bennett1948]. A quantizer need not be constrained in such a manner since techniques like companding and dithering are well known uses of non-linear quantization for certain types of signals (i.e. non-uniform statistical signals like voice where fixed networks generally employ non-linear quantization). The non-faded WCDMA signal without interference and noise is "nearly" uniformly distributed – although in the presence of fading, interference and noise, this distribution at the receiver front end usually is approximately Gaussian. In such an environment with variable statistics (depending on loading and fading conditions), a non-uniform quantizer may only offer marginal improvements over uniform quantization (with a cost of complexity), hence is not considered further for analysis.

Traditional FIR filtering algorithms compute digital convolution via a multiply accumulate process, hence for finite precision quantization; it would be useful to model the quantization and truncation errors. The difficulty of determining the level of quantization and round off error arises due to the actual acceptable dynamic range of the receiver. The mobile receiver consists of a hybrid of analogue and digital signal processing components, where the

[1] The default double precision floating point representation used in many software programs yields sufficient numeric accuracy for the vast majority of scientific applications, hence the numeric imprecision can be ignored if base 10 numbers are not rational or recurring.

analogue interface generally concentrates on the carrier down-conversion and low noise (often assumed linear) amplification of a low power QPSK modulated RF signal. The amplifier forms part of a super heterodyne receiver. The first assumption of this section presupposes that the amplifier with automatic gain control (AGC) is non-existent, as is the demodulating circuitry (employing mixers, phase locked loops, low pass and anti aliasing filters) for the RF carrier. While strictly not true, if the demodulation/mixing and amplifier processes are assumed perfect, their impact can be neglected for simplicity of analysis. Based on this supposition, the received signal after multipath fading must be normalized to its mean envelope power yielding a maximum signalling amplitude swing no greater than 5V (the additive noise statistically speaking may add a spurious spike greater than this level although this is highly improbable). Hence the quantizer with 1 sign and 3 integer bits will never (unless the SNR << 0dB) suffer from the severe spectral regrowth that occurs with amplitude clipping. The second assumption considers scaling the input and output of filters to prevent overflow causing large errors. This is chiefly for the fixed-point filter representation where scaling by a number > 2^3 should prevent or negate arithmetic overflow. The Floating-point number systems (which includes the logarithmic number system) utilize normalizations creating a mantissa and exponent, where logarithmic arithmetic for the signed exponent part of the number incurs during multiplication; hence overflow is only an issue when extremely large dynamic ranges are encountered (which wont happen due to clipping of any spurious emission by the quantizer in any case).

5.1.1 Fixed and Floating-point Representation

Any number using a base "a" can be represented with

$$\left(\ldots b_2 b_1 b_0 . b_{-1} b_{-2} \ldots\right)_a = \ldots + b_2 a^2 + b_1 a + b_0 + b_{-1} a^{-1} + b_{-2} a^{-2} + \ldots \tag{5.1}$$

where the b are the digits (for radix 2 coding the digits are referred to as bits). Base 2 coding is by far the most conventional approach for representing numbers within digital devices and thus is quantized in binary form [Cavanagh1984]. Binary number systems can be further broken into two classes: Fixed and Floating Point. The fixed-point representation, as the namesake implies, refers to a number quantized with fixed precision, and fixed decimal point. This number format takes the generic form

S	$\ldots IIII$	.	$FFFFFFFFFFFFFFF\ldots$

where I represents the integer digits of the number, $S \in \{1, \ 0\}$ the sign bit, and F the fractional digits. Mathematically, any number can be represented in fixed point as

$N = (-1)^S \sum_{i=-f}^{I} c_i 2^i$ with $c_i \in \{1, \ 0\} \ \forall \ i$. Generally, fixed-point numbers are treated either as integers or fractals in hardware. In this thesis, the fixed-point representation is numerically scaled (by a fixed scalar $\geq 2^{\text{MSB}}$) such that $-1 < N < 1$. The floating-point representation is somewhat different, where a fixed quantized number is converted into an exponent (which is stored by the processor as a logarithmic quantity) and normalized mantissa bounded by $1 \leq \Lambda < 2$. Mathematically, this is represented as $N = (-1)^S \cdot 2^E \cdot (1 + \Lambda)$ and hence $N = (-1)^S \cdot 2^E \cdot \sum_{i=0}^{F} c_i 2^{-i}$ with $c_0 = 1$. The number format takes the generic form

S	***... E E E***	***1.***	***F F F F F F F F F F F F F F F ...***

where E represents the exponent digits. The differences between the floating and fixed-point representation manifest themselves when implementing a practical digital filter. A floating-point number yields a greater complexity due to the conversion process, where this thesis uses a leading one detector [Lee1998] (to obtain the most significant digit stored as the exponent) and a barrel shifter (with truncation at the output) for obtaining the mantissa. Numeric operations such as multiplication and addition are generally more difficult to implement with floating-point numbers. The fixed-point representation yields lower complexity implementation where numerical scaling (via a shift) of the quantized number is conducted to prevent arithmetic overflow due to multiplication and addition. On the downside, fixed-point number representation suffers from poor dynamic range and is generally more sensitive to numeric error. The advantages and disadvantages of fixed and floating-point numbers are well known and wont be discussed further in this thesis – for further detail refer to [Eng1996] which contains a detailed account of binary number systems for general micro-computer application. There are several different forms of representing a binary number, the most common of which is two's complement. For an infinite number of bits, a real number N can be perfectly represented using fractional two's complement notation as

$$N = 2^E \cdot \left(-c_0 + \sum_{i=1}^{\infty} c_i 2^{-i} \right) \tag{5.2}$$

where c_0 defines the direction of the number. If $c_0 = 1$, the number is negative, and if $c_0 = 0$ the number is positive.

5.1.2 NUMERIC ERRORS FOR GENERIC FIR FILTERS

The transversal FIR filter is the most commonly encountered filter architecture for DSP application. The generic form consists of a tap delay line where quantized input signal samples are stored, shifted, scaled by the filter coefficients, and accumulated to yield the desired response. Since the digital convolution performed by the filter is memoryless, stability is always guaranteed. The transversal filter is the basic structure of the equalizers, rake receivers, and interference-canceling receivers presented in chapters 2 and 4. This section explores the modeling assumptions and difficulties of obtaining analytical solutions for the second order statistics of numeric error. The numeric errors in digital filters arise due to a variety of reasons that all relate to finite quantization. The most difficult aspect of modeling the effects of quantization transpires when multiplication occurs between two discrete random variables, where the probabilistic nature of error is actually somewhat dependent on the density functions of the input samples, filter coefficients, and the quantization noise itself. This section is therefore partitioned into three parts where 5.1.2.1 evaluates the quantization error incurred in data acquisition, 5.1.2.2 evaluates the error generated during a multiplication process, while 5.1.2.3 investigates the bulk errors created for a generic FIR filter based on deterministic and random coefficients.

5.1.2.1 QUANTIZATION NOISE

The most basic quantizer [Bennett1948] is shown in Fig. 5.1, where x is the input and x_e the quantized output. For simplicity of presentation, only 8 bins are included. The quantization steps are considered to be uniform meaning all parts of the signal range will be represented equally with same general rounding errors (assuming x is uniformly distributed). The probability density function for the quantizer is uniform and discrete, where

$$p(x_e) = \sum_{\substack{i=-n \\ i\ odd}}^{n} \left(\frac{1}{n}\right) \partial\left(x - \frac{iq}{2}\right) \tag{5.3}$$

with $\partial(\bullet)$ the Dirac function and $q=2^{-m}$ the LSB of the quantization process.

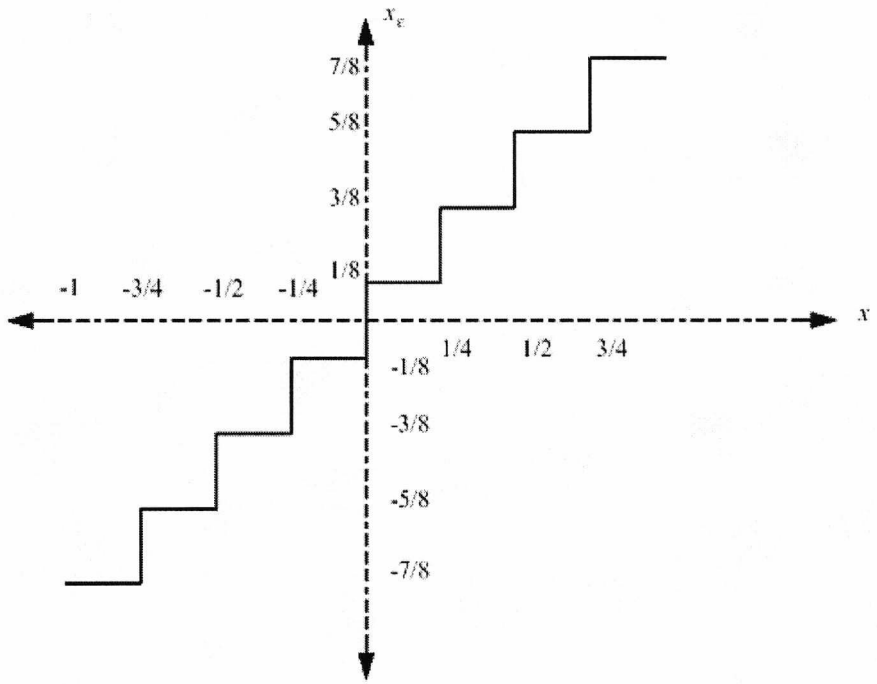

Fig 5.1 General depiction of the quantization function with uniform bin width.

Since real WCDMA communication systems utilize simultaneous multiple access, the signals received will exhibit random properties, thus rendering a deterministic analysis of quantization error inappropriate. To this end, the stochastic model first proposed by Bennett [Bennett1948] will be considered. In this model, the sampled signals are treated as random variables, where a single port circuit (Fig. 5.2) is used to develop a quantization error criterion. This circuit, consisting of a single adder, treats the round-off errors incurred for a binary coded number as being an additive noise source. For a quantizer employing a rounding function, this noise source will usually be correlated with the input signal (but not generally share statistical properties with the original source). The quantization error, e is given by

$$e = x - Q(x) \tag{5.4}$$

with $Q(x)$ the quantization function. The first assumption that will be applied for the following model is that x is uniform and independent of $p(x_e)$, hence yielding e as being uniformly distributed where

$$p(e) = \begin{cases} \frac{1}{q} & -\frac{q}{2} \le e < \frac{q}{2} \\ 0 & elsewhere \end{cases} \tag{5.5}$$

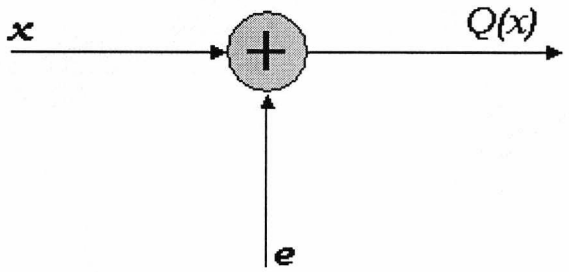

Fig 5.2 General Quantized signal model.

The variance of the quantization noise is $\sigma_q^2 = \int_{-\infty}^{\infty} e^2 p(e)\, \partial e = \frac{1}{q}\int_{-\infty}^{\infty} e^2\, \partial e$ giving

$$\sigma_q^2 = \frac{q^2}{12} \tag{5.5}$$

The mean of the quantization noise can be easily shown to be zero. [Sripad1977] presented a paper that provided a necessary and sufficient condition for modeling quantization noise with a uniform noise model. The probability density function of the quantization error was shown to be

$$p(e) = \begin{cases} \frac{1}{q} + \frac{1}{q}\sum_{n\neq 0} \varphi_x\left(\frac{2\pi n}{q}\right) \cdot \exp\left(\frac{-j2\pi ne}{q}\right), & -\frac{q}{2} \le e < \frac{q}{2} \\ 0 & elsewhere \end{cases} \tag{5.6}$$

with $\varphi_x\left(\frac{2\pi n}{q}\right) = E\left\{exp\left(j\frac{2\pi nx}{q}\right)\right\}$ the characteristic function of the continuous random variable x. $E[\bullet]$ is the expectation given by $E[y] = \int_{-\infty}^{\infty} yp(y)\, \partial y$. It was shown that $\varphi_x\left(\frac{2\pi n}{q}\right) = 0 \;\forall\, n \neq 0$ holds only when $p(e)$ is uniform, i.e. given by (5.3). The error introduced to the uniform quantization model if x is not uniform is, of course $\frac{1}{q}\sum_{n\neq 0} \varphi_x\left(\frac{2\pi n}{q}\right) \cdot \exp\left(\frac{-j2\pi ne}{q}\right)$ for $-\frac{q}{2} \le e < \frac{q}{2}$.

For Gaussian signals, i.e. exhibiting density function $p(x) = \frac{1}{\sigma_x\sqrt{2\pi}} exp\left(-\frac{x^2}{2\sigma_x^2}\right)$, the density function of the quantization error can be shown to be

$$p(e) = \begin{cases} \frac{1}{q}\left[1 + 2\sum_{n\neq 0} cos\left(\frac{2\pi ne}{q}\right) \cdot exp\left(\frac{-j2\pi^2 n^2 \sigma_x^2}{q^2}\right)\right], & -\frac{q}{2} \le e < \frac{q}{2} \\ 0 & elsewhere \end{cases} \tag{5.7}$$

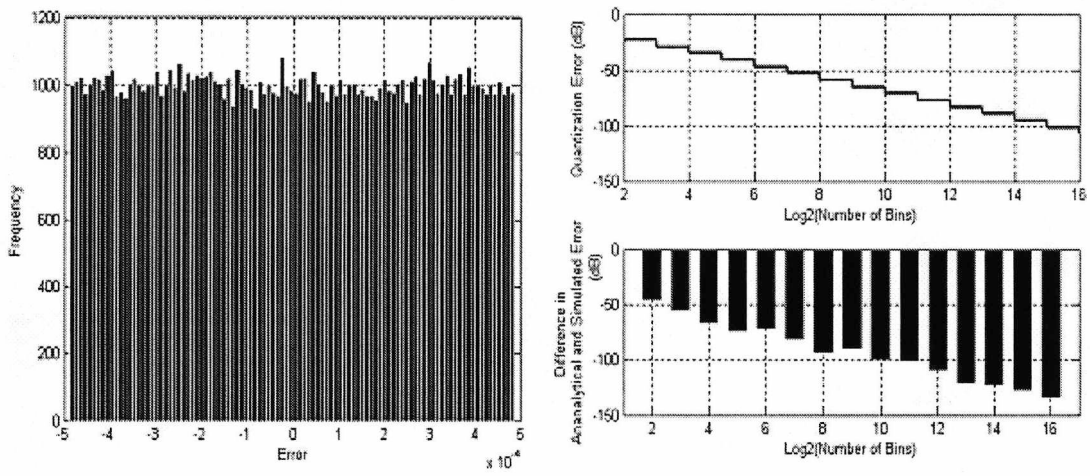

(A) (B)

Fig 5.3 (A) The histogram of the quantization error for a Gaussian source. Number of bins = 2^{11}. **(B)** The absolute error between the modeled and simulated variance.

with mean = 0 and variance

$$\sigma_q^2 = \frac{q^2}{12}\left[1 + \frac{12}{\pi^2}\sum_{n=1}^{\infty}\frac{(-1)^n}{n^2}exp\left(\frac{-2\pi n^2\sigma_x^2}{q^2}\right)\right] \tag{5.8}$$

Generally, for $\sigma_x >> q$ as is generally practical, then $\sigma_q^2 \rightarrow \frac{q^2}{12}$ hence the uniform quantization model usually holds. Consider the Fig. 5.3, which shows the validity of the uniform error model when the source is white Gaussian noise. As seen, the histogram (and hence PDF) for a 10-bit quantizer is nearly uniform for the simulation containing a million samples– thus confirming the approximation that the quantization error is uniform for white Gaussian noise. The error in the expected and simulated variance for a variety of quantization levels is extremely low.

5.1.2.2 Multiplication Errors for Binary Coding

A typical FIR filter is required to perform the vector inner product to yield the desired response. Therefore, the effect of round-off error and quantization noise for a single filter unit is the subject of interest. In general, an FIR filter consists of a number of complex scalar multipliers and an adder, where the error generated for a single multiplication process is dependent on the number coding format, i.e. floating point and fixed-point arithmetic produce very different results. The filter coefficient can be treated as being fixed or random, where the random case is a crude model for diversity receivers employing phase tracking or filters exhibiting adjustable properties (as is the case for adaptive filters excited with non-stationary regressor). The Transversal FIR filter can be modeled as a concatenation of basic

units consisting of a single multiplier[2] (Fig. 5.4). The output of this unit would be input to an accumulator. In this section, the multiplier, w is fixed and we consider the worst-case quantization error as $q/2$. The work conducted by [Barnes1985], analyzed the statistics of round-off error and the conditions for which the correlated, uniform white noise model was appropriate. The first assumption made in this model was that the constant, w, can be expressed by equating an odd integer N being divisible by a scalar fractal $M \propto 2^{-m}$, i.e. $w = N/M$. It was assumed that N was already discretized. The round-off error statistics was derived in this paper where the second moment of error was

$$\sigma_{re}^2 \approx \frac{q^2}{12}\left[1+\frac{1}{M^2}\right] \tag{5.9}$$

and the first moment given by $\mu_{re} \approx \frac{q}{2M}$, where the round-off error sequence was modeled as uniformly distributed white noise. The conditions upon which the white noise model is appropriate is based on the provision the standard deviation of the regressor satisfies $\sigma_x \geq \frac{Mq}{2}$, which is usually met in practical applications. [Tokaji1987] expanded the initial research by Barnes, where conditions for which the error statistics were uniform and white was derived when the multiplier coefficient was a continuous random variable. However, the problems with the modelling approach in [Barnes1985] and [Tokaji1987] were that the key analysis considered just the round-off (or rather, the truncation) error incurred when two discrete (and already quantized) variables were multiplied. No consideration was given to the total error inclusive of numeric quantization at the inputs. [Wong1990] addressed this issue and developed the statistical models when both the input signal and multiplier coefficient were continuous random variables prior to quantization and scaling. The analysis is far too complex for inclusion in the thesis, where no direct solution was yielded on the moments of this additive noise source (which is what this chapter primarily addresses for making a Gaussian/Uniform approximation for the additive error).

[2] This model is treated as an equivalent mathematical interpretation rather than a practical implementation, which would only consider a single scale and quantization process for a filter implemented with tap-delay line.

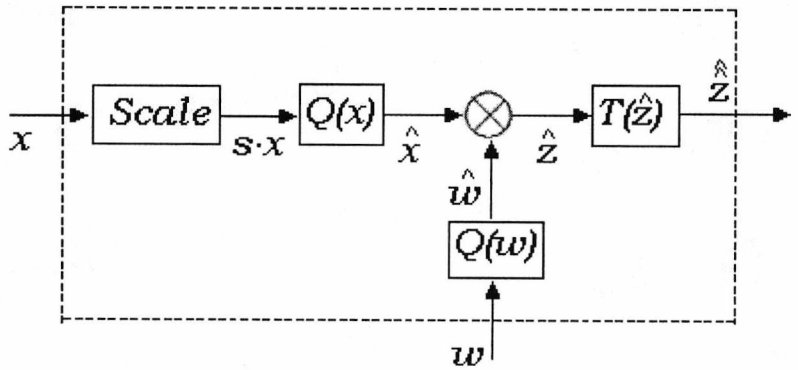

Fig 5.4 The basic unit for a fixed-point FIR filter

The second order statistics when w is fixed (or a random variable) is the topic of investigation. Based on the variable assignment in Fig. 5.4, the product $\hat{z}$ can be given by

$$\begin{aligned}\hat{z} &= Q(swx)\cdot Q(w) \\ &= (sx + n_x)\cdot(w + n_w) \\ &= swx + sn_w x + wn_x + n_w n_x\end{aligned} \tag{5.10}$$

with error given by

$$\hat{z}_e = sn_w x + wn_x + n_w n_x \tag{5.11}$$

where w and n_w are fixed quantities (where n_w is the quantization error associated with w), $n_x \sim U\left(0, \frac{q^2}{12}\right)$ and x the random variable. The effect of truncation is not modelled in this section- this will be explored in the sequel and considered at the output of a generic FIR filter. The problem with characterizing $\hat{z}_e$ is due to the statistical dependence on x when n_x is modelled as uniform noise – i.e. we treat $\hat{z}_e$ as being equated with the sum of two independently realized random variables[3]. However, close inspection of (5.11) reveals that the contribution of $n_w n_x$ can be considered negligible. Furthermore, if w is a scalar close to 1 and s a relatively small fractal constant, then the wn_x term will tend to dominate $sn_w x$. Hence $\hat{z}_e$ can be quite closely approximated with uniform distribution, i.e. $\hat{z}_e \sim U(\mu_E, \sigma_E^2)$. The second moments of error, assuming mutually independent random variables, can be expressed as

[3] Mathematically speaking this problem is not profound since the sum of two random variables and its higher order moments can be solved quite trivially using analytical methods. The problem is the solution is conditioned entirely on the characterization of x where the Gaussian approximation for WCDMA signals is not entirely accurate. The uniform approximation for the numerical errors of a fixed multiplier can be shown to be quite appropriate.

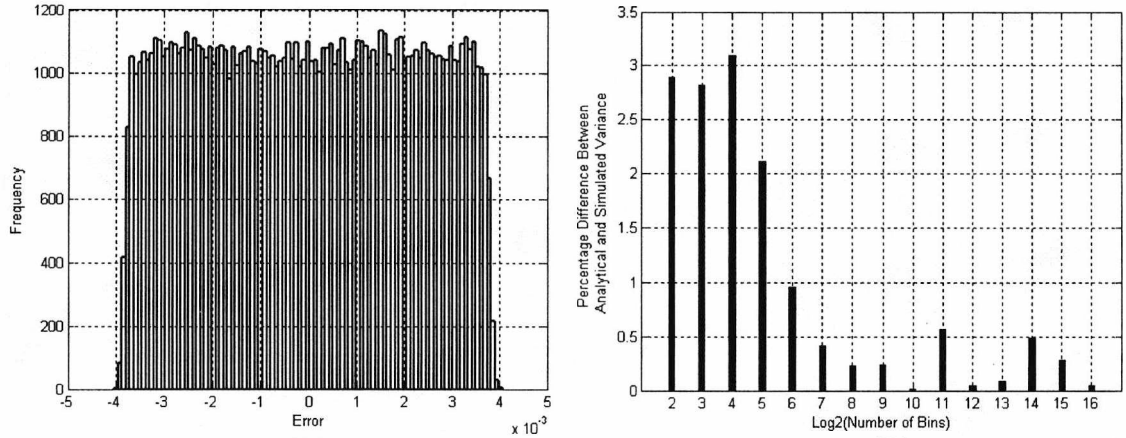

Fig 5.5 (A) The histogram of the multiplication error for a Gaussian source. Number of bins = 2^{11}. **(B)** The percentage error between the modeled and simulated variance.

$$\sigma_E^2 = n_w^2\sigma_x^2 + \left[w^2 + n_w^2\right]\frac{q^2}{12s^2} \tag{5.12}$$

The validity of the uniform approximation and the accuracy of (5.12) are shown in Fig. 5.5. In this simulation, w was treated for simplicity as a single random sample and $x \sim N(0,1)$. As can be seen, the Uniform noise approximation is fairly good, while the variance model (5.12) produces a fairly close match to the simulated variance with maximum deviation of approximately 3%.

The floating-point multiplier implementation utilizing the basic unit (Fig. 5.6) is rather more difficult to analytically solve. The main issue centralizes around the truncated mantissa having a non-trivial characteristic function when the variables being quantized are random (due to the discrete density function of the exponent). If we treat x as a uniformly distributed random variable (or if Gaussian, treating x for $x \geq 2$), a simple probability of truncation can be formulated where assuming Gray coding,

$$P(Tr) = 2 \cdot \sum_{k=1}^{N}\left(\frac{1+2^{k+1}}{2^k}\right) \cdot P\left(2^k \leq x < 2^{k+1}\right). \tag{5.13}$$

For a numerical example, if x is uniformly distributed in the range $-5 \leq x \leq 5$, then $P(Tr) = \frac{7}{20}$. Hence even though this is quite significant (although less so for a Gaussian signal), the effect of truncation errors and therefore scaling will be ignored for the model. The second moments of error, assuming mutually independent random variables, can be expressed as

$$\sigma_E^2 = n_w^2\sigma_x^2 + \left[w^2 + n_w^2\right]\frac{q^2}{12}. \tag{5.14}$$

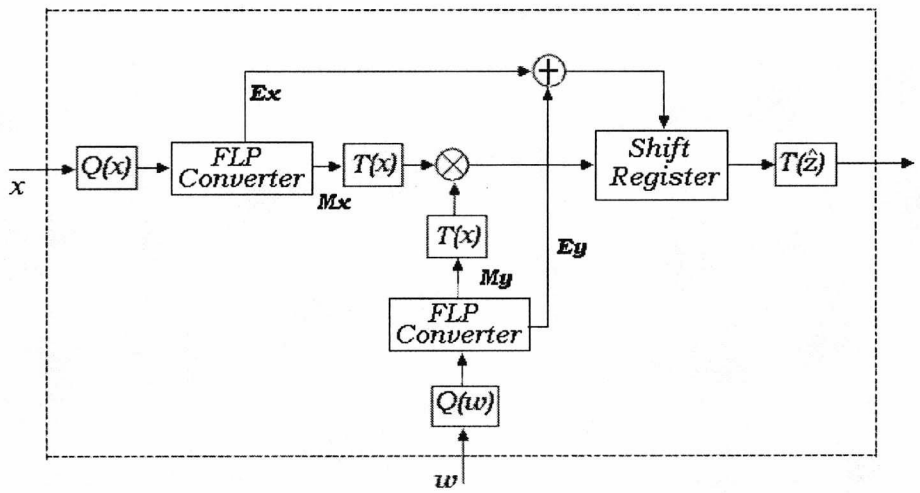

Fig 5.6 The basic unit for a floating-point FIR filter

It was shown in [Barnes1985] and for the fixed-point case that the multiplication error is uniform with second moment modelled quite accurately with (5.13). The case for floating point is not so clear, as the following simulation examples show. The Monte Carlo simulations for a Uniform random multiplier and Gaussian Signal were used to conduct a number of examinations such that the floating-point and fixed-point solutions can be compared. The first result (Fig. 5.7 A) shows that the floating-point solution yields about 5dB less numeric RMS error over the fixed-point multiplier, where the difference in error is independent of the quantization. The Fig. 5.7 B shows the average histogram of error for floating point when x is Gaussian. It is fairly obvious that the uniform noise approximation is not applicable for floating-point arithmetic, where the real characteristic function for Gaussian signals is not trivial to obtain – see [Wong1990] for the proofs and probability density functions for the fixed-point case when the quantized signal is Gaussian or Uniform. The validity of (5.13) and (5.14) was tested utilizing the Monte Carlo simulation to obtain the expected error difference between the analytical and simulated RMS error results – Fig. 5.8. The application of (5.14) is seen to yield less than 1% modelling error for the fixed-point solution, therefore validating this equation. The case for floating-point arithmetic is far less optimistic, where the modelling error is significantly larger at about 5 - 11% (depending on quantization). This simply means that for a reasonable approximation, (5.14) is validated. Exact solutions would require the methods undertaken in [Wong1990].

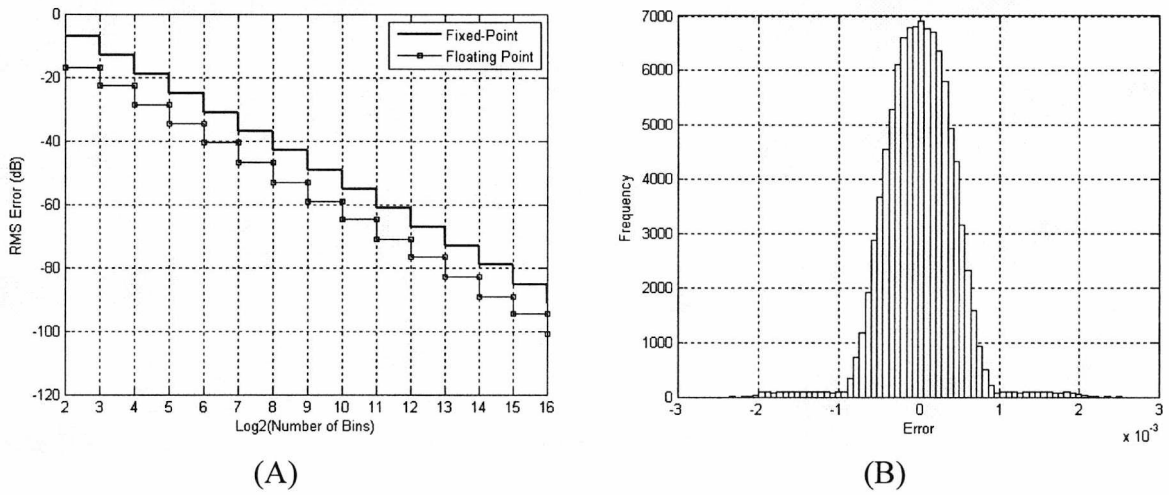

(A) (B)

Fig 5.7 (A) RMS error for Fixed and Floating-point arithmetic.
(B) The histogram of the multiplication error for a Gaussian source. Number of bins = 2^{11}.

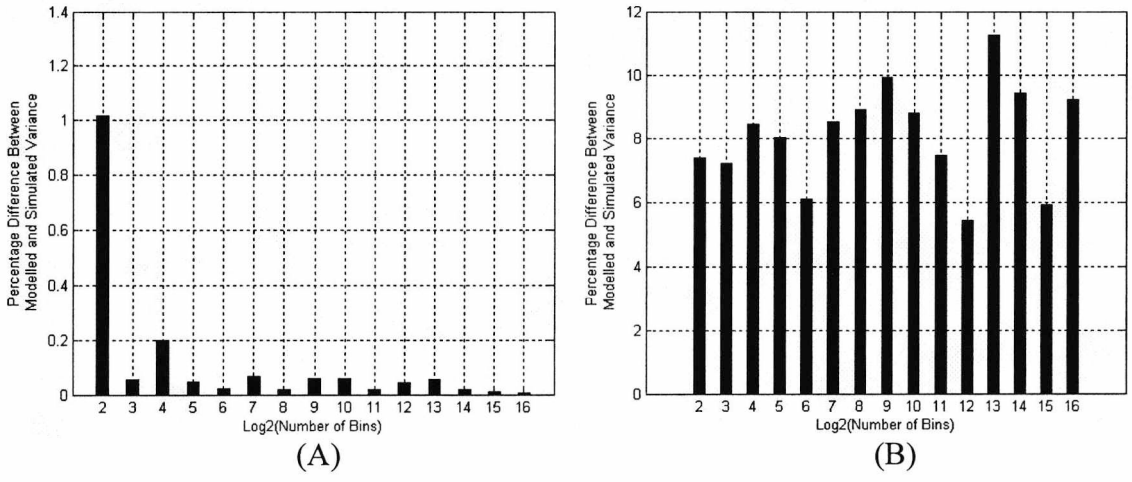

(A) (B)

Fig 5.8 (A) Percentage difference between analytical and simulated RMS error for fixed-point.
(B) Percentage difference between analytical and simulated RMS error for floating-point.

5.1.2.3 ROUND-OFF ERROR FOR A GENERIC FIR FILTER

Consider a forward LTI filter with response given by

$$y[n] = \sum_{i=1}^{L} w_i \cdot x[n-i]. \tag{5.15}$$

For the diversity receivers presented in Chapter 4, three key processing blocks are ubiquitous – namely the front end pulse shaping matched filter, the spread-spectrum matched filter/Decorrelator, and diversity combining utilizing the channel phase/envelope information. If the entire receiver were to be integrated onto a single silicon ship, one would duly expect the multiplier to be of fixed word length. Hence the outputs of the digital

processing blocks at the receiver front end would have to be truncated (or numerically fixed with faithful rounding). In this case, the output of a single FIR filter can be given as

$$y[n] = T\left(\sum_{i=1}^{L} w_i \cdot x[n-i]\right) \tag{5.16}$$

with $T(\bullet)$ the truncation function. The round-off error at the filter output can be given as

$$\varepsilon[n] = \varepsilon_T[n] - \varepsilon_q[n] \tag{5.17}$$

with $\varepsilon_T[n] = \sum_{i=1}^{L} \hat{w}_i \cdot \hat{x}[n-i] - T\left(\sum_{i=1}^{L} \hat{w}_i \cdot \hat{x}[n-i]\right)$ the truncation error and $\varepsilon_q[n] = \sum_{i=1}^{L} w_i \cdot n_x[n-i] + \sum_{i=1}^{L} n_w[i] \cdot x[n-i] + \sum_{i=1}^{L} n_w[i] \cdot n_x[n-i]$ the multiplier errors. The terms $\hat{w}_i$ and $\hat{x}[n-i]$ represent the already quantized multiplier variables. For a fixed-point solution, the individual tap multiplication error is approximated as uniform distributed with mean μ_e and standard deviation σ_e. Since the filter output is assumed to be the sum of "L" mutually independent uniformly characterized random variables, the statistics of ε_q will be Gaussian by virtue of the central limit theorem provided L is quite large- see Fig. 5.9. The truncation error is uniform, i.e. $\varepsilon_T \sim U\left(0, \frac{q_T^2}{3}\right)$. Using the same assumptions presented in section 5.1.2.2, the RMS error at the output of a generic FIR filter is given as

$$\begin{aligned} \text{Fixed Point}: \quad \sigma_E^2 &= L \cdot \left(\overline{n}_w^2 \sigma_x^2 + \left[\sum_{i=1}^{L} w_i^2 + \overline{n}_w^2 \right] \frac{q^2}{12s^2} \right) + \frac{q_T^2}{3} \\ \text{Floating Point}: \quad \sigma_E^2 &= L \cdot \left(\overline{n}_w^2 \sigma_x^2 + \left[\sum_{i=1}^{L} w_i^2 + \overline{n}_w^2 \right] \frac{q^2}{12} \right) + \frac{q_T^2}{3} \end{aligned} \tag{5.18}$$

The validity of the Gaussian Noise assumption and the variances presented in (5.18) for fixed and floating-point arithmetic is shown in Fig 5.10 and Fig 5.11 respectively. The length of the filter was set to 127 and the coefficients were set to RRC response with normalization applied such that the filter autocorrelation function yielded a maximum of unity. The input to the filter was the WCDMA signal presented by the "model 1" in Chapter two, with sixteen additive users. The user powers were random with 10000 realizations. The variance of error was averaged over different power distribution and channel states with Monte Carlo simulation. As can be seen, the theoretical Gaussian noise models with variances given in (5.18) agree well for both cases (the approximation is slightly better for fixed point arithmetic). The noise expectation is given as $\mu_{re} \approx -L\frac{q}{sM}$ and is generally close to zero. The Fig 5.11 indicates that the floating-point implementation yields

considerable lower RMS error than the fixed-point version (by nearly 10dB). An important observation is that for low fixed-precision (i.e. 4 bits), the numeric errors for a practical filter are significant. It will be seen later that matched filters in WCDMA channels operate poorly (using scaled fixed point arithmetic) with such low precision. The modelling errors (using 5.18) are also shown, where the fixed-point solution yields errors potentially as high as 5%. The floating-point model gives approximately double this error. It is clear that the model is only an approximation.

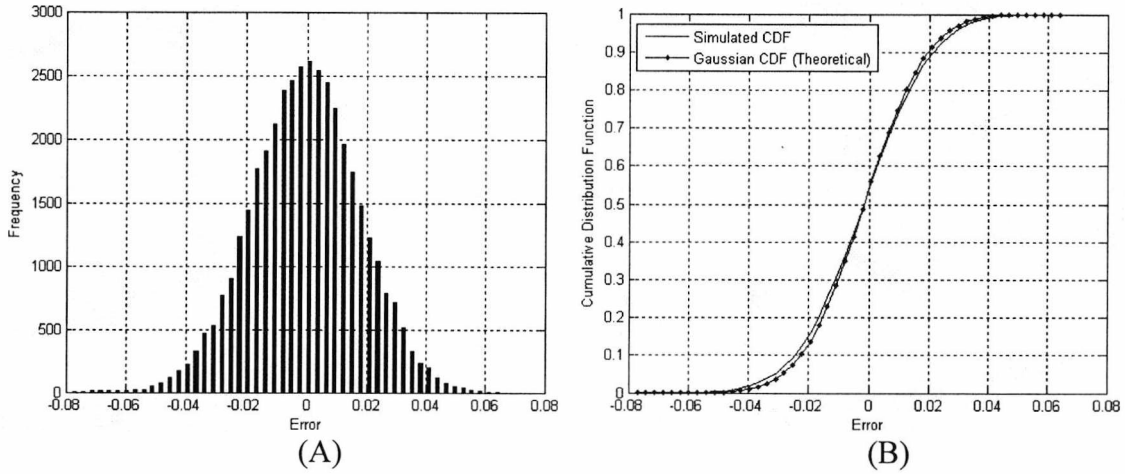

Fig 5.9 (A) Histogram of the fixed-point round-off error for a Gaussian source. No. bins = 2^{11}.
(B) The cumulative distribution function of simulated error Vs the Gaussian Model CDF.

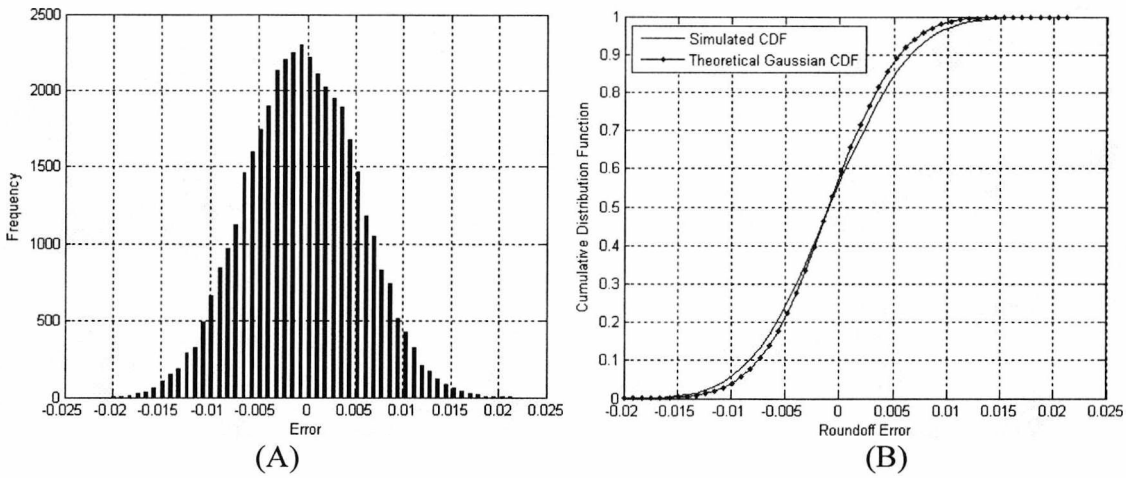

Fig 5.10 (A) Histogram of the floating-point round-off error for a Gaussian source. No. bins = 2^{11}.
(B) The cumulative distribution function of simulated error Vs the Gaussian Model CDF.

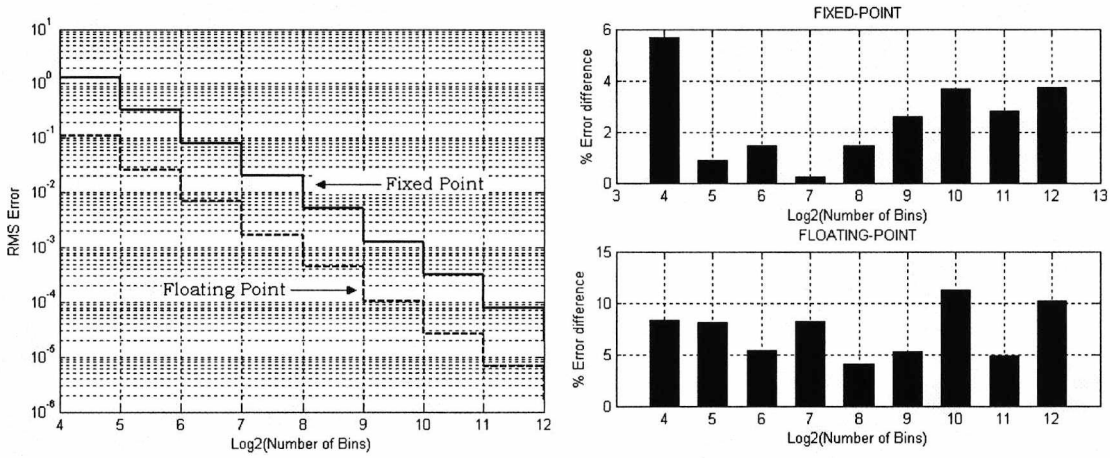

Fig 5.11 (A) RMS round-off error for the floating and fixed-point filter.
(B) Difference between analytical and simulated RMS error for floating and fixed-point.

5.2 Hybrid Logarithmic Arithmetic for Digital Filters

Conventional implementations of canonical FIR filters employ fixed or floating-point binary arithmetic for generating the multiply-accumulate (MAC) operations to execute digital convolution. Matched filters like the Root Raised Cosine matched filter or LMMSE Chip Equalizer are implemented near the analogue/digital interface at the receiver front-end and hence would yield a quite considerable number of MAC operations due to the high bandwidth of multi/single-user signals (and hence high sampling rate). This naturally incurs a large number of calculations utilizing hardware array multipliers. Widely used filter structures such as the lattice and the symmetric linear phase filter can at best reduce half the number of multiplications required to compute the filter output but do not circumvent multiplication. A useful property of binary arithmetic is that multiplication between a set of real numbers encompasses an addition when considering the base 2 logarithm. Accurate conversion of a number into a base 2 logarithm is not a trivial process, however for a floating-point binary number, the translation is simplified somewhat since the integer part is already a logarithmic quantity. The structures of all filters discussed here-forth are based on transversal tap delay line. Unlike the Symmetric and Lattice structures, the transversal tapped delay line requires no addition prior to the multiply-accumulate operation for convolution. This generally enables easier implementation of multiplierless filters invoking the Logarithmic Number System (LNS). The LNS has many useful properties that supplement the application of enabling arithmetic products being performed with linear addition. This, for many filter applications in a dynamic CDMA receiver, can be

advantageous in reducing the overall hardware complexity and power, and allow for integration on cheaper, more efficient devices.

5.2.1 INTRODUCTION

The uses of logarithms in signal processing applications have been investigated since the early 1950's. Binary logarithms augment many useful properties that include compressing large dynamic ranges into much smaller word sizes and offering a low power, high-speed alternative to multiplication since logarithmic multiplication is implemented simply with an addition [Swartzlander1975]. This section focuses mainly on the application and conversion of linear numbers into logarithms for FIR filter structures used in matched filtering and equalization. The conversion of a number into the non-linear logarithmic format has been quite an active research subject for computer applications. The difficulty with the subject is that logarithmic coding is inefficient when high numerical precision is required since techniques generally employ large look up table structures and regression – e.g. see [Coleman2000]. However, for lower precision signal processing applications, logarithmic coding can be efficiently applied with a wide range of methods. Logarithmic conversion for lower precision applications are most commonly implemented using simple look up table structures, which may either be full-dynamic range addressable [Swartzlander1975] or partitioned into smaller parts where the conversion would require linear regression or polynomial expansion [Mclaren2003, Lewis1990, Lai1991]. It should be noted that far more accurate and expensive methods are available for approximating logarithms and its related functions. These involve either time consuming iterative techniques [Kostopoulos1991] or large look up table sizes and interpolations of either first or higher orders such as quadratic or Chebychev methods [Lewis1994, Huang1996, Coleman1995]. Despite recent advances in the extension of very high precision logarithms [Lewis1990, Arnold1992], low precision logarithmic applications have been found from the authors research to offer either equivalent or slightly impaired performance in fixed and dynamic filter applications in CDMA receivers. Much recent interest in low-precision logarithmic arithmetic is not only related to its dynamic range or speed of logarithmic multiplication, but also the compression offered in custom chips which can significantly reduce the power consumption. Less switching is required for the higher order bits in the logarithmic number system than a uniform number system during the multiplication process. Logarithmic arithmetic also produces filters that are more tolerant to the round-off and relative errors that are introduced by the equivalent sized uniform representation, and generally fewer bits are required to represent a number

range with similar precision to the uniform representation [Barlow1985]. There are essentially two main classes of logarithmic arithmetic calculations in multiply-accumulate operations. The first class executes an algorithm such as a FIR filter entirely in the logarithmic domain (where high non-linear calculations are introduced into the system due to the logarithmic equivalent of linear addition). The second-class associate's logarithmic arithmetic with multiplication and standard linear arithmetic with addition – referred to in the text and this thesis as Hybrid-Logarithmic arithmetic [Lai1991, Lee1995]. The work conducted in this chapter focuses exclusively on the application of Hybrid-Logarithmic arithmetic in FIR filters to bypass the further complexity of logarithmic addition/subtraction (which requires table lookups). This chapter also discusses one prominent form of the LNS, (which generically can be defined as unsigned, signed, and dual redundant LNS) called the Signed-LNS (SLNS) [Swartzlander1975]. Most applications suitable for the LNS need less precision than the IEEE-754 floating-point standard provides. Thus, table-based codecs are economical for small fixed-point word sizes, making the SLNS a natural choice for devices such as FPGAs.

5.2.2 PRELIMINARIES

Any real quantized number, N for radix 2 coding can be represented by

$$N = (1 - Z)(-1)^S 2^{\varepsilon} \prod_{i=-m}^{-1} 2^{C_i 2^i} \tag{5.19}$$

with m the number of fractal bits and $\varepsilon = floor(\log_2|N|)$ for $N \neq 0$. Let $\log_2 \left| \frac{N}{2^{\varepsilon}} \right| = \sum_{i=-m}^{-1} C_i 2^i$ bounded by $0 \leq \log_2 \left| \frac{N}{2^{\varepsilon}} \right| \leq 1$ represent the base 2 logarithmic conversion where $C_i \in \{1, 0\} \forall i$ symbolizes the binary digit at the i^{th} bit. $S \in \{1, 0\}$ and $Z \in \{1, 0\}$ are the sign and zero flag bits conditioned where $S = 1$ for $N < 0$ and $Z = 1$ for $N = 0$. The goal of the logarithmic codec is to approximate the logarithm with sufficient accuracy such that the square difference between (5.19) and the actual value of N is not so large that numerical errors cause large misadjusment and hence low efficiency. The SLNS was proposed to overcome the computational difficulties of fixed and floating-point multiplications in DSP arithmetic. The Sign/Logarithm number consists of a sign flag bit immediately followed by the logarithm of the absolute number (since the log of a negative number $\propto \pm j$). Consider a

number χ with arbitrary base λ, $\chi > 0$, where $\chi = \lambda^{Lx}$, and $L_x = \frac{1}{2}log_\lambda(\chi^2)$. This system can be altered to consider a zero flag bit, due to the $log(0) = -\infty$. To avoid the log of zero, let $L_x = \frac{1}{2}log_\lambda(\chi^2 + \partial(\chi))$, where $\partial(\chi) = 1$ for $\chi = 0$, and $\partial(\chi) = 0$, for all other real positive values of χ. Hence any real number can be realized by:

$$\chi = (-1)^{1-\mu(\chi)} \cdot (1-\partial(\chi)) \cdot \lambda^{\left(\frac{1}{2}\cdot log_\lambda(\chi^2+\partial(\chi))\right)} \tag{5.20}$$

with $\mu(\chi) = 1, \chi \geq 0$. $\mu(\chi) = 0, \chi < 0$. Using $\lambda = 2$ as the radix for the LNS, consider the arbitrary number χ represented by the 4-tuple $\{Z(\chi), S(\chi), I(\chi), L(fr(\chi))\}$, where $Z(\chi)$, $S(\chi)$, $I(\chi)$, $L(fr(\chi))$ represent the zero flag bit, sign flag bit, integer part and the absolute base 2 logarithm of the normalized fractional part respectively. It is common to represent the logarithmic number in a floating point format, where χ can be modified such that:

$$x = 2^{\varepsilon}(1+\Lambda) \tag{5.21}$$

where ε is an integer ≥ 0 and $1 > \Lambda \geq 0$ the normalized fractional part of χ. Hence χ can be represented as

$$\chi = (-1)^{S(\chi)} \cdot (1-Z(\chi)) \cdot 2^{\varepsilon} \cdot 2^{L(1+\Lambda)} \tag{5.22}$$

where $Z(\chi) = \partial(\chi), S(\chi) = 1-\mu(\chi)$, and $L(1+\Lambda) = log_2(1+\Lambda)$. The main advantage of representing numbers as binary logarithms is that multiplication arithmetic becomes addition in the SLNS domain. If $c = a \times b$, then $C = Z_c \cdot S_c \cdot 2^{(\varepsilon_c + I(L_c))} \cdot 2^{fr(L_c)}$, where $L_c = L_a + L_b$, and $L_a = log_2(1+\Lambda_a)$, $L_b = log_2(1+\Lambda_b)$, $\varepsilon_c = \varepsilon_a + \varepsilon_b$, where $I(L_c)$ and $fr(L_c)$ are the integer and fractional parts of L_c, and $Z_c = (1-Z(a)) \bullet (1-Z(b)) = \overline{Z(a) \mid Z(b)}$, $S_c = S(a) \oplus S(b)$. The $\oplus$ operator is the logical XOR. Linear addition in the logarithmic domain is highly non-linear and far more complicated to perform, where if $c=a+b$, then $L_c = L_a + log_2\left(1 + 2^{L_b - L_a}\right)$. It is common to use a look up table (LUT) to evaluate this expression, where it is generally considered practical for numerical applications with less than 16-bit precision. An alternative solution is Hybrid Linear-Logarithmic arithmetic (H-LNS). This can be used to overcome difficulties of linear addition with logarithms by converting between the logarithmic and linear domain to perform the operation. If the advantages of using the Hybrid-LNS are to be realized, it is essential that log and antilog conversion be achieved quickly with sufficient accuracy. Lin/Log and Log/Lin conversion with look up tables is proposed for this thesis, where the address range

and the numerical accuracy impose limitations in terms of practical application. The table becomes prohibitively large when high precision and very accurate approximations are required. For applications using lower accuracy, as is the case for this thesis, look up tables for Log/Antilog conversions of the mantissa/fractal quantities become more practical and relatively inexpensive. Fig. 5.12 outlines the main elements used in Lin/Log and Log/Lin conversion. The number, χ is first converted into a suitable floating-point form by use of a leading-zero detector. The LUT contains a predetermined, small number of addresses with fractal logarithmic entries of fixed precision. These entries are pre-calculated according to the values in the address range. Log/Lin conversion is basically the reverse operation of the Lin/Log process except the look up table for exponential conversion uses the fractal component of the logarithm in its address range.

The use of complex numbers somewhat further complicates the architecture of the receiver. Complex number multiplications require four multiplies and two additions to produce the cross products, which results in one real and one imaginary term. In the logarithmic domain, this translates to four summations and two antilog look up table conversions to adequately replace complex number inner products with logarithmic arithmetic. Compared to standard floating point number systems, the SLNS has similar dynamic range and similar accuracy [Brent1973] for the same word size. In fact, the overall precision for the SLNS is better than the equivalent floating point implementation due to the uniform geometric error characteristics over the entire range of values since log-domain addition incurs no rounding error. Compared to fixed-point binary, where the relative precision fluctuates drastically as a function of the numeric value, similar average relative precision with greater dynamic range can be encoded using the SLNS using fewer bits with the advantage that the higher order bits in the LNS alter less frequently than those in comparable fixed-point systems resulting in power saving.

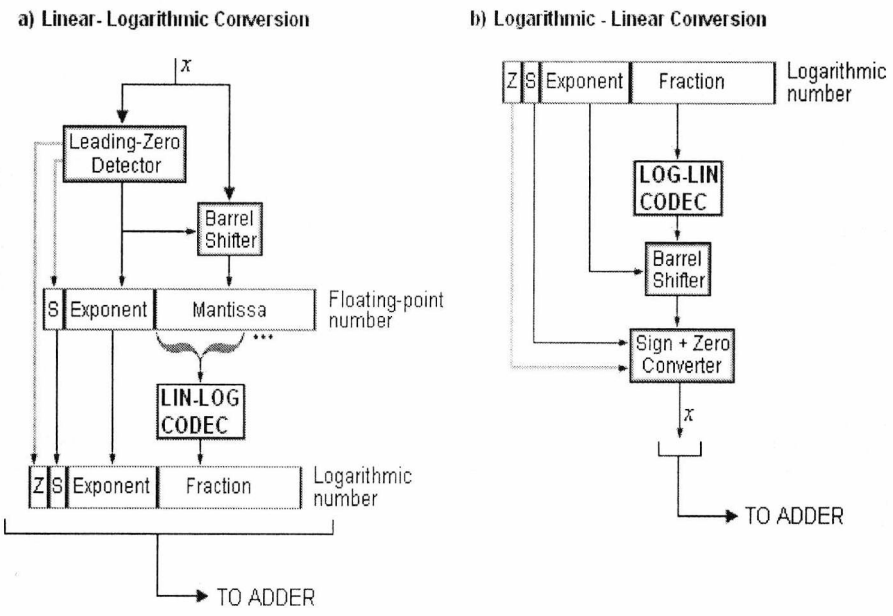

Fig 5.12 Log-Lin and Lin-Log conversion for the H-LNS

5.2.3 LOGARITHMIC CODECS

5.2.3.1 DIRECT LOOK UP TABLE CONVERSION

The direct LUT codec maps a quantized value of N, $Q(N)$ to an address corresponding to a pre-assigned logarithmic fraction where

$$log_2\left|\frac{N}{2^{\varepsilon}}\right| \approx \left\{Q\left(\frac{N}{2^{\varepsilon}}\right) \longrightarrow log_2\left|Q\left(\frac{N}{2^{\varepsilon}}\right)\right|\right\} \tag{5.23}$$

and 2^{ε} is a normalizing factor constraining the input for logarithmic conversion to be in the interval $1 \le \frac{N}{2^{\varepsilon}} < 2$. The accuracy of the logarithmic conversion is proportional to the number of address bits. For example, an 8-bit truncated mantissa could be mapped to a 255-element look up table with stored logarithmic fraction. Due to the exponential rise in required memory per bit increase; direct LUT conversion alone does not generally incur the computational burden for codecs employing more than 16-bit fractional word lengths. An example of the approximate logarithmic function employed by the codec is shown in Fig 5.13. Similarly, an anti-logarithmic codec utilizing the direct LUT approach could be employed. The coefficients are simply the inverse logarithm (an exponential function) tabulated for every numeric logarithmic value. For brevity, the antilogarithmic codec is assumed to employ one extra address bit (i.e. twice as large as the logarithmic codec). The

reason for this (Proposition 5.1) is to ensure that the accuracy of Lin → Log → Lin process yields more or less the same accuracy as the stand-alone floating-point representation (with fixed and truncated mantissa). This is of course not absolutely necessary, but for analytical solutions, it at least allows a practical numeric model to be applied if this condition is met. Without this condition, applying a numeric model for the round-off error is exceedingly difficult due to the logarithmic and exponential functions being non-linear.

PROPOSITION 5.1:

The exponential conversion, utilizing a LUT based codec where

$$2^{\log_2\left|\frac{N}{2^{\varepsilon}}\right|} \approx \left\{ \log_2\left(Q\left|\frac{N}{2^{\varepsilon}}\right| \right) \longrightarrow 2^{Q\left[\log_2\left(Q\left|\frac{N}{2^{\varepsilon}}\right|\right)\right]} \right\} \tag{5.24}$$

has accuracy dependent on the rounding of the logarithm returned from the Lin-Log codec. If we assume the logarithmic fraction is encoded with more digits than the input to the conversion in (5.24), then the overall rounding $Q\left[\log_2\left(Q\left|\frac{N}{2^{\varepsilon}}\right|\right)\right]$ is important to consider-particularly noting that the logarithm $\log_2\left(Q\left|\frac{N}{2^{\varepsilon}}\right|\right)$ is scaled by two to prevent arithmetic overflow during addition. A sufficient criterion for ensuring the practical LUT method does not degrade the Lin → Log → Lin process by faithful rounding is given here-with: Assuming the maximum rounding error T of the binary logarithm is $T = 2^{-b-1}$ (b is LSB of the logarithmic fraction), the worst-case Lin-Log conversion is $\log_2(|x|)+\log_2\left(1+\left|\frac{n_x}{x}\right|\right)+T$ where $N = x + n_x$. In the linear domain, the total conversion error can be easily shown to be $e_T = x\left(2^T - 1\right)+ n_x 2^T$. Let $e_K = x\left(2^K - 1\right)+ n_x 2^K$ denote the acceptable error incurred by conversion, where equating the two terms making b the argument yields $b = -\log_2(K)-1$. If K is chosen such that $x\left(2^K - 1\right)+ n_x 2^K - n_x$ yields a maximum error ½ a LSB of the floating point value, then $K = \log_2\left(1+\frac{2^{-m}}{2\cdot(x+n_x)}\right)$ with m the number of fractal bits for the equivalent floating point number. Hence $b = \left\lceil -\log_2\left(\log_2\left(1+\frac{2^{-m}}{2\cdot(x+n_x)}\right)\right)-1 \right\rceil$ with $\lceil\bullet\rceil$ the ceiling

function. The maximum error occurs when $x + n_x = 1 + 2^{-L}$ where L is the number of fractional bits for the Lin-Log conversion, where assuming $m = L$, we can state with no loss of generality that $b = \left\lceil -log_2\left(log_2\left(1 + \frac{1}{2 \cdot (1 + 2^m)} \right) \right) - 1 \right\rceil$. Making the small number approximation for the logarithm, $log_2\left(1 + \frac{1}{2 \cdot (1 + 2^m)} \right) \approx \frac{1}{2 \cdot (1 + 2^m)}$ and also that $log_2\left(\frac{1}{2 \cdot (1 + 2^m)} \right) \approx -\left\{ 1 + m + log_2\left(1 + \frac{1}{2^m} \right) \right\}$, the number of fractional bits for the logarithm (and hence the exponential LUT address) is given by

$$b = \left\lceil m + log_2\left(1 + \frac{1}{2^m} \right) \right\rceil = \mathrm{m} + 1 \tag{5.25}$$

thus validating why an extra bit precision is required for the Lin-Log mapping in (5.24).

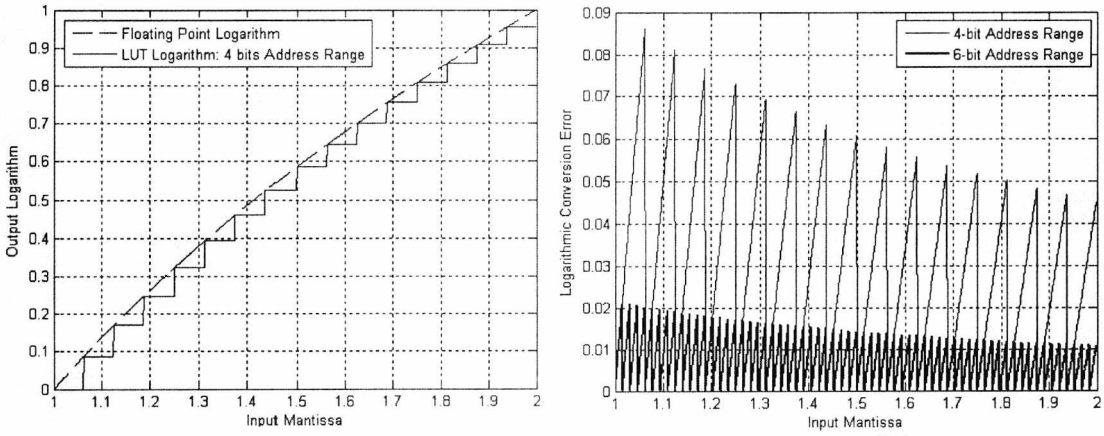

Fig 5.13 (A) Lin-Log codec showing the double precision logarithm and 4-bit truncated LUT address.
(B) Logarithmic conversion error for 4-bit and 5-bit address range.

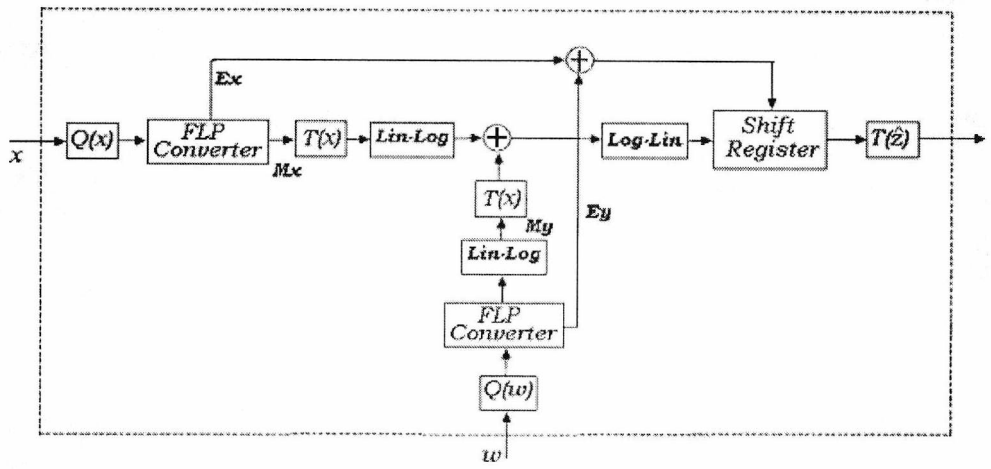

Fig 5.14 The basic unit for a floating-point FIR filter utilizing the Hybrid-Logarithmic approach.

5.2.3.1.1 ERROR ANALYSIS DUE TO ROUNDING

For the Logarithmic sum (see Fig 5.14 showing the basic unit), $Z = X + Y$, the linear domain error is

$$Z_e = 2^{L(Q(X))+L(Q(Y))} - 2^{log_2|X|+log_2|Y|} \tag{5.26}$$

where $L(\bullet)$ is the logarithmic codec function and $Q(\bullet)$ the quantization/rounding function. Note this analysis ignores the effect of truncation on the exponential function. The logarithmic domain error is

$$\varepsilon = \{L[Q(X)] + L[Q(Y)]\} - (log_2|X| + log_2|Y|) \tag{5.27}$$

where equating (5.26) with (5.27) yields the following error function

$$Z_e = 2^{log_2|X|+log_2|Y|}\left(2^{\varepsilon} - 1\right). \tag{5.28}$$

Let the relative logarithmic error be given by $\lambda = 2^{\varepsilon} - 1$. If the error, ε is introduced due to rounding, then it can be treated as a uniformly distributed RV [Bennet1948] with CDF

$$F_{\varepsilon}(\varepsilon) = \frac{\varepsilon}{2T} + \frac{1}{2}, \quad -T < \varepsilon \le T \tag{5.29}$$

where $T = 2^{-b-1}$ with b the LSB digit of the logarithmic fraction (stored in memory). However, for fairly low precision logarithms, we include the fact that a significant error can be generated due to faithful rounding of the number prior to LUT conversion. If an assumption is made such that $L(Q(X))$ is uniform (which is a good approximation provided

that the logarithmic rounding in the LUT is smaller than the input quantization bin-width and Y is a constant) then (5.29) holds provided the range of ε is altered. Hence

$$F_{\varepsilon}(\varepsilon)=\frac{\varepsilon}{2T}+\frac{1}{2},\quad -T_1<\varepsilon\le T_2 \tag{5.30}$$

where $T_1=log_2\left(1+2^{-m-1}\right)+2^{-b-1}$ and $T_2=log_2\left(\frac{1+2^m}{0.5+2^m}\right)+2^{-b-1}$ with m the LSB digit of the input linear number to the codec. Generally we can equate $T=T_1=T_2$ for most cases when $m > 4$. Furthermore, λ is related to ε via $\varepsilon=log_2(1+\lambda)$ where converting the variables of (5.30) to λ yields

$$F_{\lambda}(\lambda)=\frac{log_2(1+\lambda)}{2T}+\frac{1}{2},\quad 2^{-T}-1<\lambda\le 2^{T}-1 \tag{5.31}$$

The PDF is given by $P_{\lambda}(\lambda)=\frac{\partial}{\partial\lambda}F_{\lambda}(\lambda)$, where

$$P_{\lambda}(\lambda)=\frac{log_2 e}{2T}\left(\frac{1}{1+\lambda}\right) \tag{5.32}$$

with e = 2.718... the base of the natural logarithm. The mean, μ_e, can be obtained taking the expectation of (5.31) where $\mu_e=\int_{2^{-T}-1}^{2^{T}-1}\lambda\cdot P_{\lambda}(\lambda)\partial\lambda$ giving rise to the following expression

$$\mu_e=\frac{log_2 e}{T}\left(\textbf{\textit{sinh}}\left\{T-T\left(1-\frac{1}{log_2 e}\right)\right\}-\left\{\frac{log_e\left(2^{T}\right)-log_e\left(2^{-T}\right)}{2}\right\}\right) \tag{5.33}$$

where ***sinh(•)*** is the hyperbolic sine function. The mean square error (MSE) is given by the second moment of the PDF, where $\sigma_e^2=\int_{2^{-T}-1}^{2^{T}-1}\lambda^2\cdot P_{\lambda}(\lambda)\partial\lambda$. Solving this problem yields

$$\sigma_e^2=\frac{log_2 e}{T}\left(\textbf{\textit{sinh}}\left\{T-T\left(1-\frac{1}{log_2 e}\right)\right\}\cdot\left[\textbf{\textit{cosh}}\left\{T-T\left(1-\frac{1}{log_2 e}\right)\right\}-2\right]-\left\{\frac{log_e\left(2^{T}\right)-log_e\left(2^{-T}\right)}{2}\right\}\right) \tag{5.34}$$

where ***cosh(•)*** is the hyperbolic cosine function. Note that (5.34) is denoted with the variance syntax since the MSE and variance are almost identical when the mean is small. This model is suitable for describing the statistics of round off provided the truncation of the mantissa is ignored (as in the floating point case) or non-existent. Including the effects of truncation for a floating-point number is a non-trivial process since the scaling for the random data is also probabilistic and dependent on the sample distribution. Therefore this is

omitted for brevity. The effect of antilogarithmic coding is ignored where we assume Proposition 5.1 and that the LUT coefficients for this codec are of infinite precision (i.e. we do not consider truncating the output which would usually be done in practice). Equation (5.34) is for the relative error variance. For the true variance, we can first rewrite (5.28) as $Z_e = X \cdot Y \cdot \left(2^{\varepsilon} - 1\right) = X \cdot Y \cdot \lambda$. Since X is a random variable and Y fixed, we can rewrite (5.34) as $\sigma_E^2 = \sigma_x^2 Y^2 \sigma_e^2$ assuming uncorrelated variables. The validity of the model will be tested in the next section with Monte Carlo simulation of an FIR filter. The Fig. 5.15 compares the results of the H-LNS multiplier implementation with the floating-point multiplier and fixed-point multiplier for various precisions. It is clear that the logarithmic implementation yields lowest RMS error out of all the schemes.

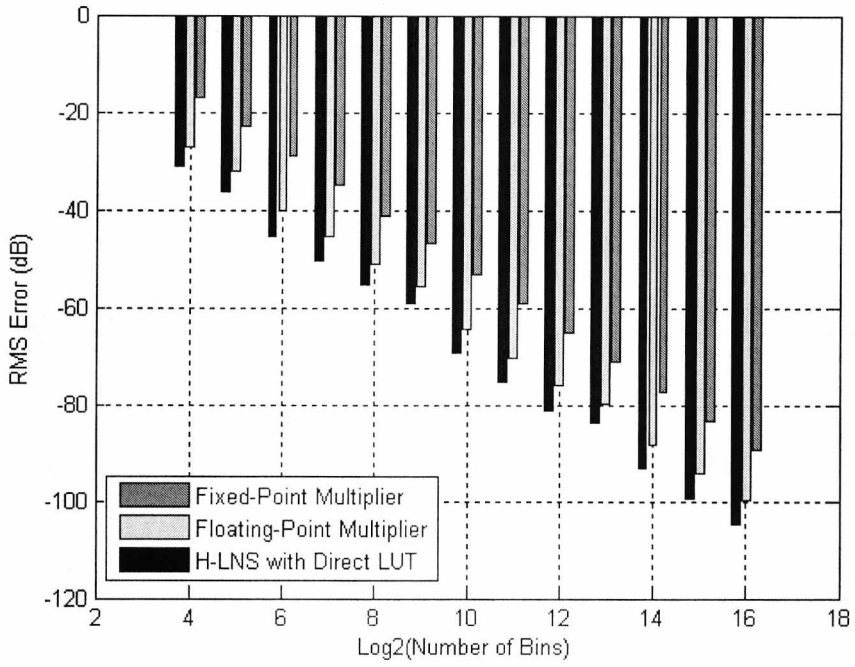

Fig 5.15 The RMS Error for a single multiplier for the H-LNS, floating-point, and fixed-point.

5.2.3.1.2 ERROR ANALYSIS FOR AN FIR FILTER

One practical advantage of using a Lin-Log codec instead of performing linear addition in the logarithmic domain is that for large filter lengths employing a successive addition scheme, the error does not accumulate multiplicatively as in [Koike2002]. The disadvantage is that for relatively small FIR filters, the error will generally be larger. The output of a single FIR filter can be given with (5.18). The round-off error at the filter output can be expressed as

$$\varepsilon[n] = \varepsilon_T[n] - Z_q[n] \tag{5.35}$$

with $\varepsilon_T[n] = \sum_{i=1}^{L} \hat{w}_i \cdot \hat{x}[n-i] - T\left(\sum_{i=1}^{L} \hat{w}_i \cdot \hat{x}[n-i]\right)$ the truncation error (at the FIR filter output) and $Z_q[n] = \sum_{i=1}^{L} w_i \cdot x[n-i] \cdot \lambda_i$ the logarithmic rounding errors. Since the filter output is assumed to be the sum of "L" mutually independent random variables, the statistics of Z_q will be approximately Gaussian provided L is quite large. The truncation error is uniform where $\varepsilon_T \sim U\left(0, \frac{q_T^2}{3}\right)$. The RMS error at the output of a generic FIR filter is therefore given as

$$\sigma_E^2 = L \cdot \sigma_x^2 \cdot \sigma_e^2 \cdot \left[\sum_{i=1}^{L} w_i^2\right] + \frac{q_T^2}{3} \tag{5.36}$$

with σ_e^2 given in (5.34). Repeating the simulation from section 5.1.2.3, the table 5.1 compares the simulated and analytical variances for the floating-point and Logarithmic implementations of the 127-tap RRC filter. This was conducted for 8, 9, 10, 11, and 12-bit precision where the word truncation at the output of the filter was set to be equivalent. It is clear that the analytical and simulated variances compare well. It is also clear that the H-LNS implementation yields lower overall error compared to floating-point solution. The Fig 5.16 compares the simulated error statistics with a Gaussian approximation based on the model (5.36). It can be seen for 10-bits of precision, the overall filter error can be modelled accurately as a Gaussian random variable of certain variance σ_E^2 given in (5.36), and mean given in (5.33).

Table 5.1 A comparison between the theoretical and simulated variances of round off error for the H-LNS and Floating Point number systems

b	Floating-Point Experimental ($\times 10^{-3}$)	Floating-Point Theoretical ($\times 10^{-3}$)	Logarithmic Experimental ($\times 10^{-3}$)	Logarithmic Theoretical ($\times 10^{-3}$)
8	0.4405	0.4469	0.4084	0.3894
9	0.1238	0.1139	0.1013	0.0964
10	0.0323	0.0307	0.0262	0.0239
11	0.0066	0.0069	0.0058	0.0056
12	0.0018	0.0018	0.0016	0.0015

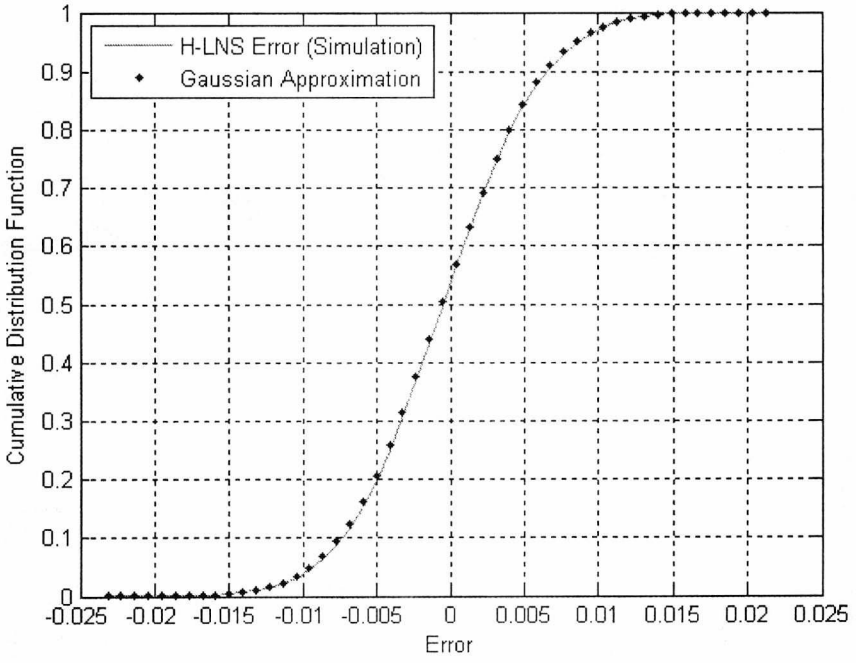

Fig. 5.16 The cumulative distribution function of simulated error (for 10-bit quantization) Vs the Gaussian Model CDF.

5.2.3.2 INTERPOLATION

For larger word sizes, the direct ROM approach is not economical and techniques such as interpolation employing smaller look up tables can be used [Arnold2001]. There are many variations of interpolation for approximating the logarithmic function- i.e. a linear Chebychev method was presented in [Lewis1994], a linear-Taylor method in [Arnold2003] and a quadratic-Lagrange method in [Coleman1995]. All of the aforementioned implementations partition the logarithmic/non-linear addition function where the distance

between tabulated points is non-uniform in order to achieve precision similar to the IEEE-754 floating-point standard. However, the work conducted in this thesis for a practical WCDMA receiver showed that this level of precision is not absolutely necessary. Generally, practical receivers require no more than 15-bits equivalent fixed-point precision for executing most digital algorithms associated with WCDMA networks. Hence, in this thesis, only relatively simple codecs are considered and therefore the linear-Lagrange method with uniform spacing between tabulated points will be investigated. The utilization of a direct LUT conversion for the address range $1 \le Q(N) < 2^m$ renders accurate, but memory limited solutions when $m > 15$. An alternative approach, employing smaller look up tables at a cost of a small fixed-point multiplier (an 8-bit multiplier is considered in this paper), is Lagrange interpolation. In this case, the logarithm can be approximated by

$$log_2\left|\frac{N}{2^{\varepsilon}}\right| \approx \Delta^{-1}\left\{\left\langle L\left(Q\left(\frac{N}{2^{\varepsilon}}\right)+\Delta\right)-L\left(Q\left(\frac{N}{2^{\varepsilon}}\right)\right)\right\rangle \cdot \left\langle \frac{N}{2^{\varepsilon}}-Q\left(\frac{N}{2^{\varepsilon}}\right)\right\rangle\right\}+L\left\{Q\left(\frac{N}{2^{\varepsilon}}\right)\right\} \quad (5.37)$$

where Δ is the LSB of the LUT addresses (assuming they are uniformly spaced) and $L(U)$ is the logarithmic conversion function returned from the table. Referring to Fig 5.17, the function is approximated with a straight line where Δ is the spacing between tabulated points. Due to the uniform spacing, $\Delta = 2^{-M}$, i.e. a constant power-of-two. For larger M the approximation becomes more accurate at the cost of increased memory requirement (and also size of the multiplier if this accuracy is to be exploited). The actual H-LNS algorithm presented in the previous section is exactly the same, except this time the codec employs linear regression. Linear regression is applied for the mantissa of the floating-point number (ensuring the logarithm always will return a real positive scalar), although this need not be the case – i.e. the logarithmic function could be implemented for $N > 2$.

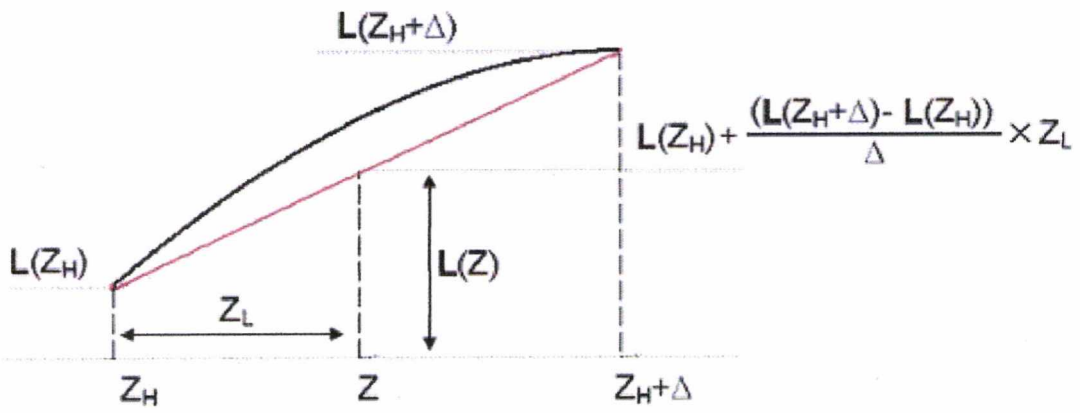

Fig. 5.17: A diagrammatic example of estimating the a non-linear function (in this case the logarithm) with linear regression. In this case, Z_H and $Z_H + \Delta$ are the upper and lower limits of linear interpolation. Z represents the number being approximately mapped by the function.

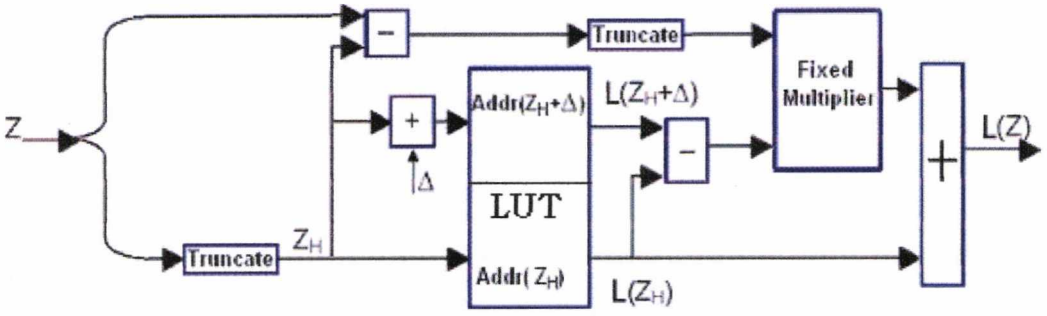

Fig. 5.18 The Linear-Lagrange Interpolator

The Fig. 5.18 shows a block diagram for a linear-Lagrange interpolator that implements the approximation (5.37). This design uses a LUT (either a dual-port memory/interleaved ROM or two separate LUT's) to obtain $L(Z_H + \Delta)$ and $L(Z_H)$ simultaneously. The contents of the LUT are the rounded values of $Log_2(Z_H) = L(Z_H)$ at all multiples of Δ within the range. One of the addresses input to the memory must be incremented by Δ. The largest-cost component in the circuit is a fixed-point multiplier. This may appear to somewhat "undo" the principal point of logarithmic arithmetic (which is to build simple arithmetic circuits with improved accuracy), however, if one considers that a 12 bit LUT with the direct approach contains 55,535 words, a linear-Lagrange interpolator could exponentially reduce the table size while providing a similar accuracy even with a relatively small multiplier. The size of the multiplier therefore becomes the critical component in determining whether or not this approach is viable (particularly over the fixed-point multiplier solution).

5.2.3.2.1 THE APPROXIMATE LOGARITHMIC CODEC

For the Logarithmic interpolator, the simplest approximation that can be made is where a straight line is fitted between $Z_L = 1$ and $Z_H = 2$. Substitution of $\Delta = Z_H - Z_L = 1$ into (5.37) yields the logarithmic codec being defined with function

$$log_2\left|\frac{N}{2^{\varepsilon}}\right| \approx Q\left(\frac{N}{2^{\varepsilon}}\right) - 1 \tag{5.38}$$

where $1 \le \left|\frac{N}{2^{\varepsilon}}\right| < 2$, and $log_2\left|\frac{N}{2^{\varepsilon}}\right| = log_2(1+\Delta) \approx \Delta$ which is a good Taylor series approximation if Δ is a small valued fraction. For Δ a larger fraction, this approximation is far less accurate – see Fig. 5.19 showing the logarithmic curve for $\log_2(1+x)$, its linear approximation $x-1$ and the resulting error $\log_2(1+x)-x+1$. The antilogarithmic conversion could also be approximated in a similar manner with the function

$$2^{\log_2\left|\frac{Q(N)}{2^{\varepsilon}}\right|} \approx \log_2\left|\frac{Q(N)}{2^{\varepsilon}}\right| + 1 \tag{5.39}$$

where $0 \le \log_2\left|\frac{Q(N)}{2^{\varepsilon}}\right| < 1$. An advantage of this technique is that it is extremely simple to implement, where the logarithmic and antilogarithmic codecs require no multiplication, and no ROM. A numeric example of the algorithm is now presented. Consider a binary number $1101 = 13_{Dec}$. The exponent of this number is 3 (the MSB is at the digit representing 2^3). The mantissa, $x = 1.101 = 1.525_{Dec}$. Now, $\log_2(13) \approx 3 + 1.525 - 1$ which equates to $\log_2(13) \approx 3.525_{Dec} = 11.101_{BIN}$. The real logarithm should be $\log_2(13) = 3 + \log_2(1.525) = 3.70043$. The error for this example is relatively large. The error for the approximate logarithmic conversion is now the subject of interest.

1. Error Due to the Approximation of the Logarithm

The error due to logarithmic approximation can be easily shown to be

$$E_L = \log_2(1+\Lambda) - \Lambda \tag{5.40}$$

and is independent of the exponent of the number. The maximum error can be found from differentiating E_L with respect to Λ and setting to zero. Hence

$$\frac{\partial E_L}{\partial \Lambda} = \frac{1}{(1+\Lambda)\log_e 2} - 1 = 0 \tag{5.41}$$

where solving yields the maximum error occurring when $\Lambda = 0.44269$. The maximum error, $E_L(\max) = 0.0861$ at this point, thus the error will be confined in the range $0 \le E_L \le 0.0861$.

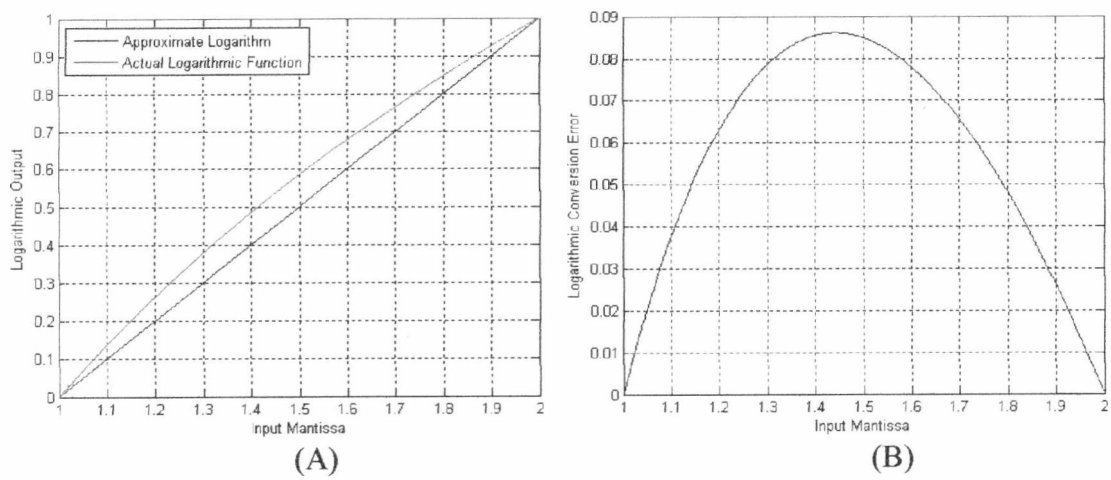

Fig 5.19 (A) Lin-Log codec showing the double precision logarithm and approximate logarithm. **(B)** Logarithmic conversion error for the approximate logarithm.

2. Error Resulting from the Approximate Logarithmic Domain Multiplication

The logarithmic multiplier is simply conducted by converting two numbers into the logarithmic domain via the codec described by (5.38), adding the two logarithmic numbers, and then converting the sum into the linear domain by using the antilogarithmic codec described in (5.39). With no approximation, the product $Z = X \times Y$ can be presented in the logarithmic domain as

$$log_2(Z) = \{\varepsilon_X + log_2(1 + \Lambda_X)\} + \{\varepsilon_Y + log_2(1 + \Lambda_Y)\} \tag{5.42}$$

and in the linear domain as

$$Z = 2^{\varepsilon_X + \varepsilon_Y} \{(1 + \Lambda_X) \times (1 + \Lambda_Y)\}. \tag{5.43}$$

From (5.38), the approximate logarithmic sum is represented as

$$log_2(Z) \approx \{\varepsilon_X + \Lambda_X\} + \{\varepsilon_Y + \Lambda_Y\}. \tag{5.44}$$

We now consider the case where the sum $\Lambda_X + \Lambda_Y < 1$. If this condition is met, the linear number Z is approximated (after utilizing the antilogarithmic codec) with

$$Z \approx 2^{\varepsilon_X + \varepsilon_Y} \{1 + \Lambda_X + \Lambda_Y\} \tag{5.45}$$

where the overall proportional error is given as

$$\xi = \frac{2^{\varepsilon_X + \varepsilon_Y} \{1 + \Lambda_X + \Lambda_Y\} - 2^{\varepsilon_X + \varepsilon_Y} \{(1 + \Lambda_X) \times (1 + \Lambda_Y)\}}{2^{\varepsilon_X + \varepsilon_Y} \{(1 + \Lambda_X) \times (1 + \Lambda_Y)\}} \tag{5.46}$$

yielding

$$\xi = \frac{1 + \Lambda_X + \Lambda_Y}{(1 + \Lambda_X) \times (1 + \Lambda_Y)} - 1. \tag{5.47}$$

For the case where the sum $\Lambda_X + \Lambda_Y > 1$, we have a carry where (5.44) develops into

$$log_2(Z) \approx \underbrace{\{1 + \varepsilon_X + \varepsilon_Y\}}_{\text{int } eger} + \underbrace{\{\Lambda_X + \Lambda_Y - 1\}}_{fraction} \tag{5.48}$$

and hence (5.47) becomes

$$\xi = \frac{2 \cdot (\Lambda_X + \Lambda_Y)}{(1 + \Lambda_X) \times (1 + \Lambda_Y)} - 1 \tag{5.49}$$

Differentiating ξ with respect to Λ_X or Λ_Y and equating to zero, it is relatively easy to show that the maximum multiplication error occurs at $\Lambda_X = \Lambda_Y = 0.5$, which yields $\xi = 0.11$ (or about 11%). If would be useful to use a computer simulation to determine for a wide range of numbers where the approximate logarithmic technique becomes equivalent to the direct LUT codec in terms of RMS error. The Fig 5.20 gives a good example for the mean square error of the direct LUT codec and the approximate logarithm when executing

the product between two Gaussian random variables. The logarithmic product errors were averaged over 100000 independently distributed samples, where the direct LUT approach was iterated between 2 and 10 address bits.

The approximate logarithm was fixed in precision to 14 bits. This result shows that the approximate logarithm yields a MSE similar to a table look up with 4 address bits. The advantage of course is that no ROM or multiplier is required for the codec. The reduction of the relatively large error due to the approximate logarithmic codec was investigated by [Combet1965] whom partitioned the range of x into four parts and used a piece-wise linear approximation. The absolute maximum error was reduced by a factor of 5. This improvement requires two sums and an extension of decisional electronics for the determination of the correction and it also required the storage of the correction factors. [Hall1970] defined coefficients for a linear least squares fit of the function $\log_2(1+x)$ by partitioning the range of x into four intervals. The maximum error was reduced by a factor of 1.3 but four additional sums were required. Marino [1972] used a parabolic approximation requiring the same number of additions where the precision was improved by a factor of 2.5.

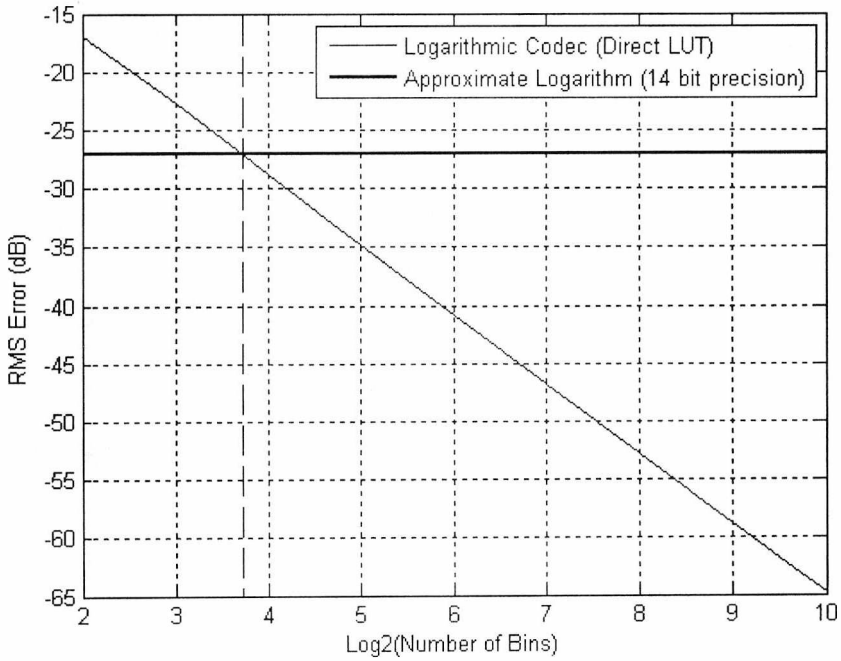

Fig 5.20 A comparison between the MSE for the direct LUT logarithmic codec and the approximate Logarithm.

5.2.3.2.2 THE LINEAR-LAGRANGE CODEC WITH MULTIPLE TABULATED POINTS

The Linear-Lagrange Codec is algorithmically simple (5.37), but includes a multiplier as part of the domain conversion. The object of this section is to compare the performance of the Linear-Lagrange Codec with the direct LUT Codec for different ROM and Multiplier sizes and hence determine where the two approaches yield the same second order statistics. To get an insight into the logarithmic conversion applying the Lagrange Piece-wise model, consider the Figs 5.21 and 5.22 showing the conversion for three and six tabulated points where the multiplier is fixed for 12-bit and 5-bit numbers. It can be seen that the 5-bit multiplier yields a significant conversion error compared with the 12-bit multiplier.

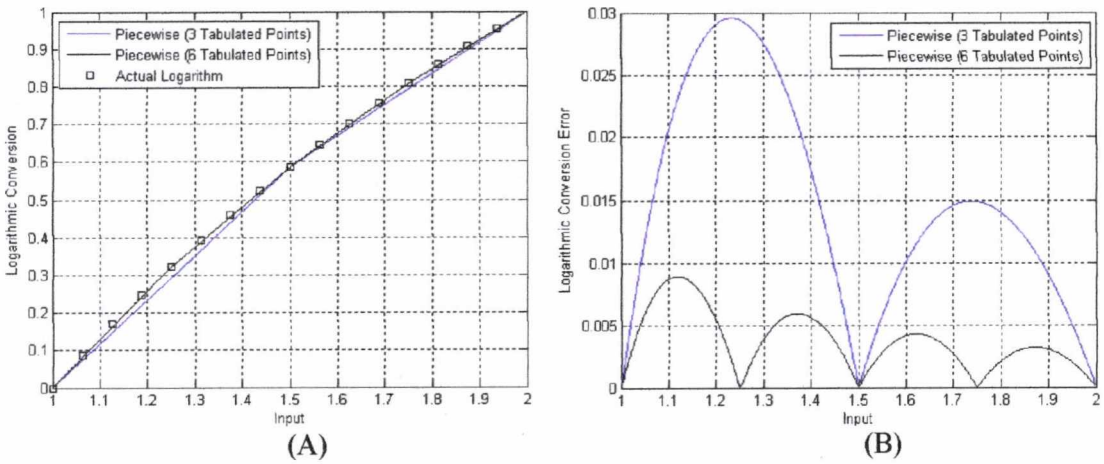

Fig 5.21 (A) Lin-Log codec showing the double precision logarithm and Piece-wise logarithm for 3 and 5 tabulated points.
(B) Logarithmic conversion error for Piece-wise logarithm with 3 and 5 tabulated points.

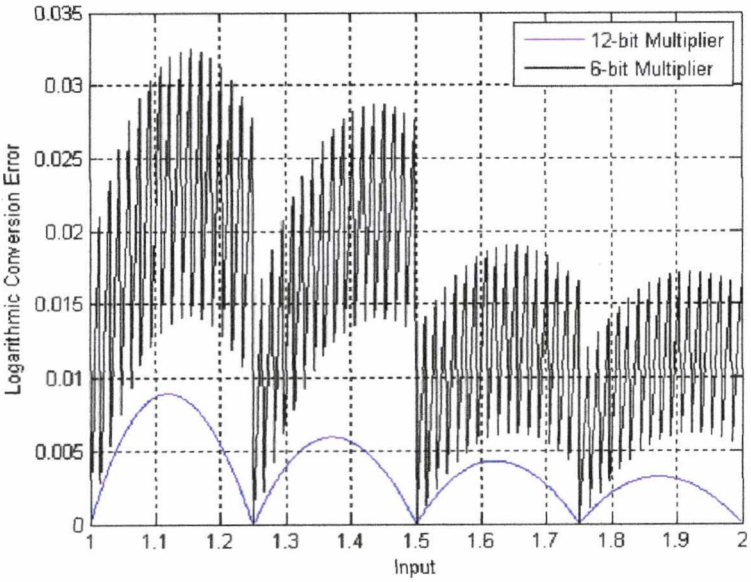

Fig 5.22 A comparison between the Piece-wise logarithm with 5 tabulated points for a 12-bit and 5-bit multiplier

In order to compare the Linear-Lagrange and Direct LUT Codecs, consider executing the product between two Gaussian random variables (of unity variance). The logarithmic product mean square error (averaged over 100000 independently distributed samples) is the topic of investigation for different ROM and multiplier sizes. The first simulation (Fig. 5.23) conducted yields the MSE for the Linear-Lagrange interpolator for various address precisions against the length of the multiplier. It is assumed the logarithmic sum is converted back into the linear domain according to Proposition 5.1. It can be seen that the MSE exhibits asymptotic behaviour when the range of the LUT is fixed. For the case where $m = 1$ (where the number of addresses in ROM = $2^m + 1$), a fixed multiplier greater than 9-bits gives little performance advantage. For $m = 2$, a multiplier > 10-bits is not necessary to improve performance. Generally we can write that the length of the multiplier (provided $m < 8$) for acceptable performance $\approx 8 + m$. The Fig. 5.24 shows a comparison of various Linear-Lagrange codecs (with different fixed-precision multiplier) with the direct LUT codec. The numbers prior to logarithmic conversion were quantized to 15-bits (and the LUT coefficients were also 15-bit fractal numbers). It can be concluded (or rather, generalized) that if the argument of performance is the number of address bits, the Linear-Lagrange codec always outperforms the direct LUT until the number of address bits $\approx$ the multiplier length. For the notion of equivalence, a 2-bit LUT Linear-Lagrange codec with 5-bit multiplier offers similar performance to a direct LUT codec employing 5 address bits. A 4-bit LUT Linear-Lagrange codec with 12-bit multiplier offers similar performance to a direct LUT codec employing 11 address bits. It can be concluded that for low-precision applications, the Linear-Lagrange codec is more complicated than the direct LUT approach, simply because if one wants to achieve superior accuracy with this technique with relatively small memory, the fixed-point multiplier must be 8-bits (or greater) to be comparable with the direct LUT approach utilizing far more LUT elements. Hence, for low-precision application, the Linear-Lagrange codec does not appear to offer any significant advantage in terms of complexity. However, if significant accuracy is required, the direct LUT approach is impractical, and hence the Linear-Lagrange codec is one method for generating the solution practically. For example, a 7-bit address LUT with 15-bit multiplier will generate an equivalent performance to a direct LUT approach with 17-bit address. This statement is based on the presumption that the codec stores the preassigned logarithmic fraction with 15-bits precision. Also it is also worth mentioning that the products were between two Gaussian variables, thus yielding truncation (prior to number conversion) an issue.

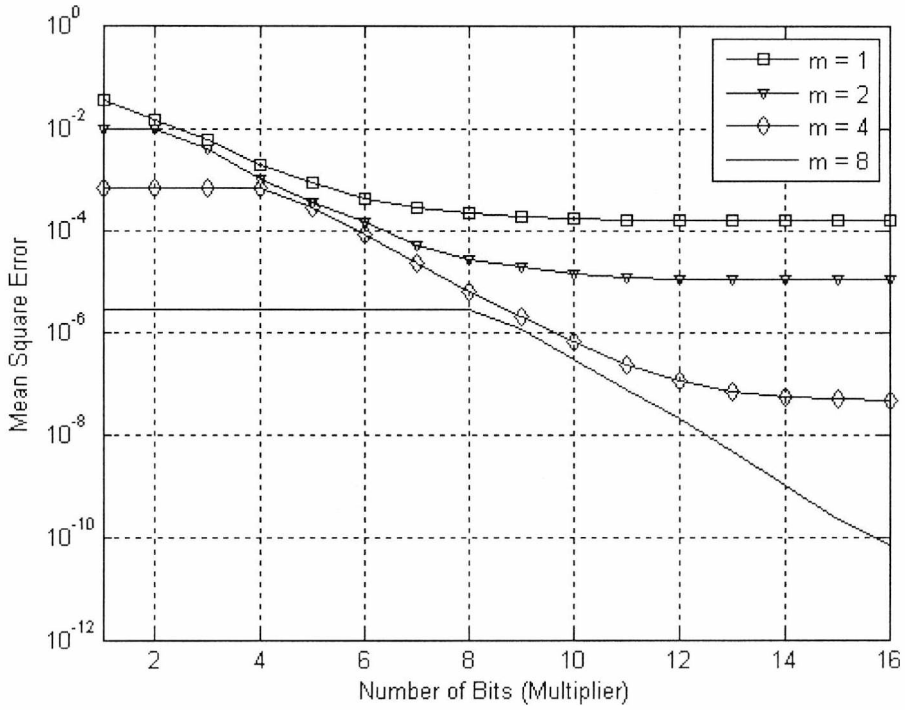

Fig 5.23 A comparison of the MSE Vs Number of multiplier bits for different address exponents, m.

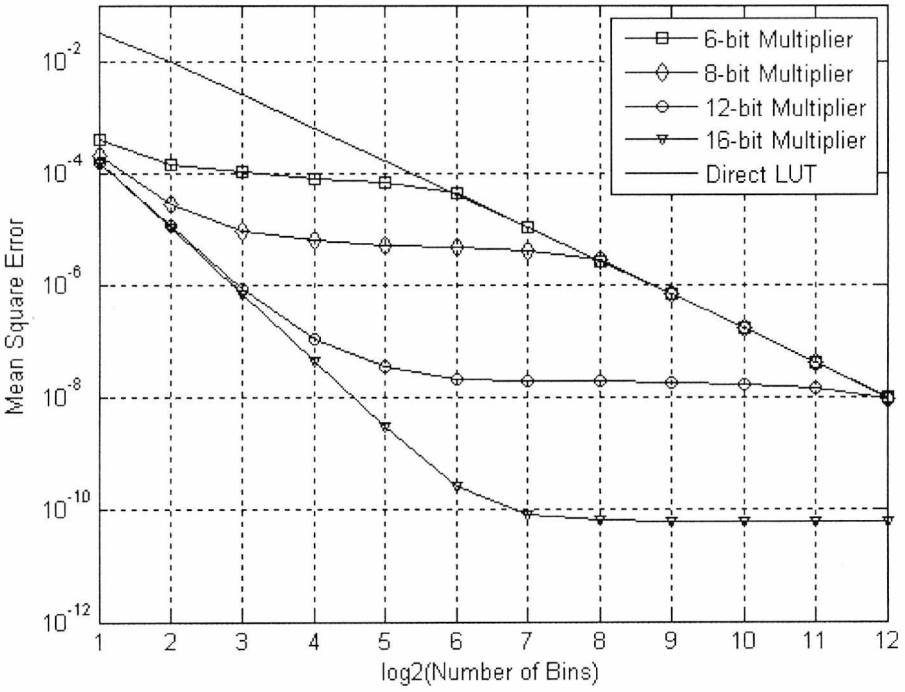

Fig 5.24 A comparison of the MSE Vs number of address bits for different fixed-precision multipliers.

5.2.3.3 Performance Comparison of Hybrid Logarithmic Codecs for a Root-Raised Cosine Matched Filter

This section expatiates on the previous work by considering a digital FIR matched filter employed at the receiver front end for rake receivers and equalizers. The performance of the filter with simulated multi-channel data will be considered where the approximations presented in the previous sections will treat the additive error as Gaussian noise. This is in fact not trivial, since equalizers (or other channel matched filters such as the LMMSE Rake receiver) will see this error as partially correlated noise. As such the performance of adaptive equalizers can deteriorate significantly due to finite precision arithmetic – where errors can be quite large for the RRC filter due to the length of the filter impulse response. This error for Rake receivers is not quite as significant- since the rake algorithm is normally followed with a NP-hard detector- i.e. it is a detector rather than estimator. Of course, the overall round-off error can be circumvented entirely (or at least reduced significantly) by employing large word size – which is not considered in thesis. This chapter (and section) concentrates solely on relatively low precision arithmetic (< 16 bits). The Hybrid-Logarithmic implementation of the RRC filter at the front end of a Rake Receiver, Channel Equalizer or LMMSE Interference suppressing filter is shown in Fig. 5.25. The input to the filter is the oversampled (8 samples per chip) demodulated RF signal consisting of the desired faded channel (with chips shaped with RRC filter by the transmitter) with the multiuser overlay. The linear samples are converted into the logarithmic domain with the Log-Lin codec prior to filtering, and back to the linear-domain after summation with the filter coefficients. Note that the D/A converter in the diagram represents the simulation approach (i.e. all numbers are represented as binary digits which much be converted back to analogue quantities for purpose of simulation). Practically, the output of the FIR filter will be decimated and/or down sampled for further processing by devices such as equalizers and/or integrate dump (i.e. despreading) detectors.

The first investigation is observant rather than numerical where the power spectral density (PSD) of the RRC filter is modelled in simulation for various logarithmic codecs with address precisions of 8 and 12-bits. For the receiver filter, the coefficients were stored as preassigned logarithmic fractals (quantized to 9 or 13 bits precision). The input to the filter was a set of pulses exhibiting RRC spectrum (no additive interference was modelled), thus the overall spectrum at the filter output should be raised cosine (RC). For purpose of comparison, the equivalent precision fixed-point uniform implementation is given in Fig. 5.26. It can be seen the Direct LUT codec (Fig. 5.27) produces a superior response compared with the equivalent 8 and 12-bit fixed-point implementation. The Linear-Lagrange codec (with fixed 8-bit multiplier and 3 or 5 tabulated points) similarly

outperforms the fixed-point implementation (see Fig. 5.28), although the overall accuracy is slightly worse than the Direct LUT codec. It is worth noting that with fixed multiplier of 8-bits, increasing the number of tabulated points does not overly affect the filter response. The Fig. 5.29 shows the filter response when the Log-Lin conversion is performed with the approximate logarithmic algorithm (with fixed 12-bit precision). It is seen that the approximation yields a filter response that is quite reasonable, although obviously degraded compared to the other schemes.

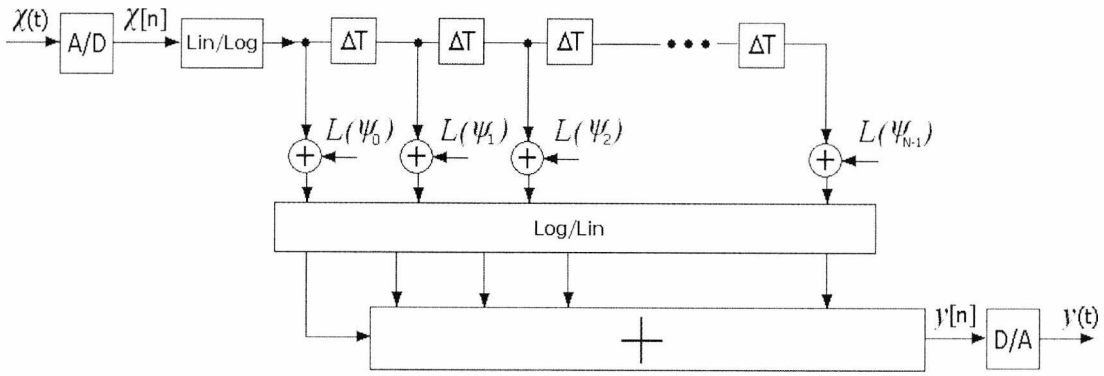

Fig 5.25 Hybrid Logarithmic implementation of the RRC filter

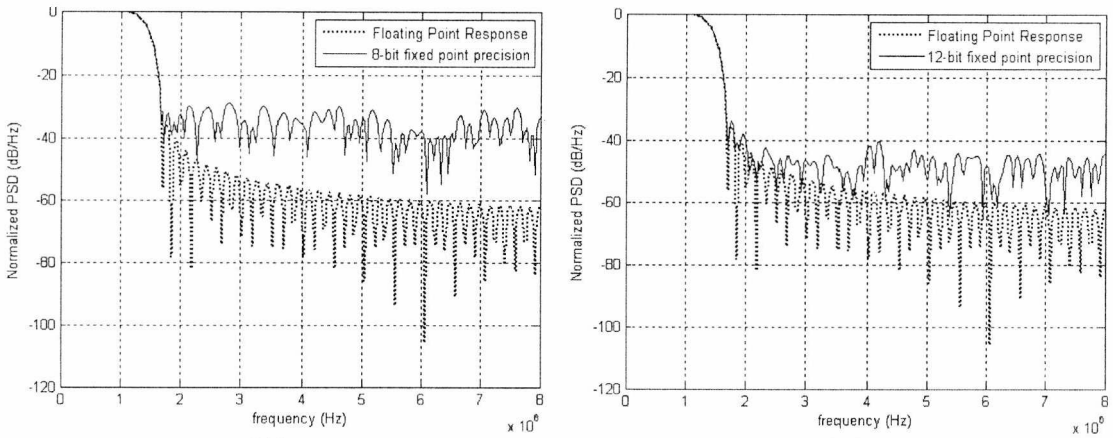

Fig 5.26 (A) RRC PSD with 11-bit fixed-point arithmetic (precision = 8 bits).
(B) RRC PSD with 15-bit fixed-point arithmetic (precision = 12 bits).

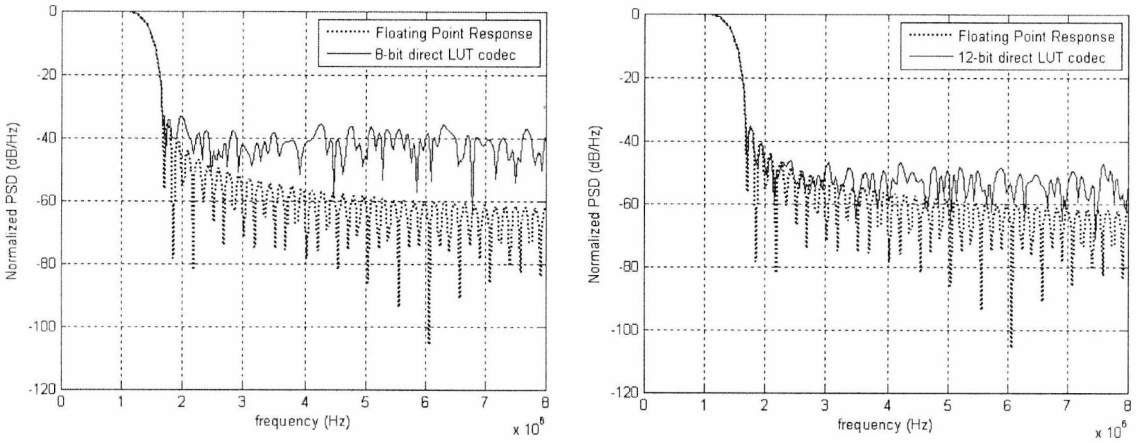

(A) (B)

Fig 5.27 (A) RRC PSD with 11-bit H-LNS arithmetic (Direct LUT = 8 bits address, 13-bit coefficient).
(B) RRC PSD with 15-bit H-LNS arithmetic (Direct LUT = 12 bits address, 17-bit coefficient).

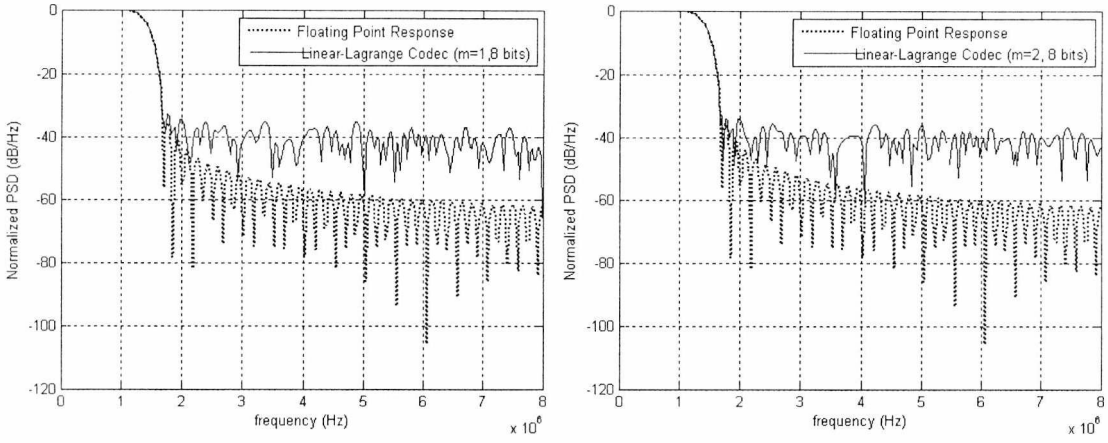

(A) (B)

Fig 5.28 (A) RRC PSD with 11-bit H-LNS arithmetic (Linear-Lagrange, 8-bit multiplier, 3 Tabulated points, 13-bit coefficient).
(B) RRC PSD with 11-bit H-LNS arithmetic (Linear-Lagrange, 8-bit multiplier, 5 Tabulated points, 13-bit coefficient).

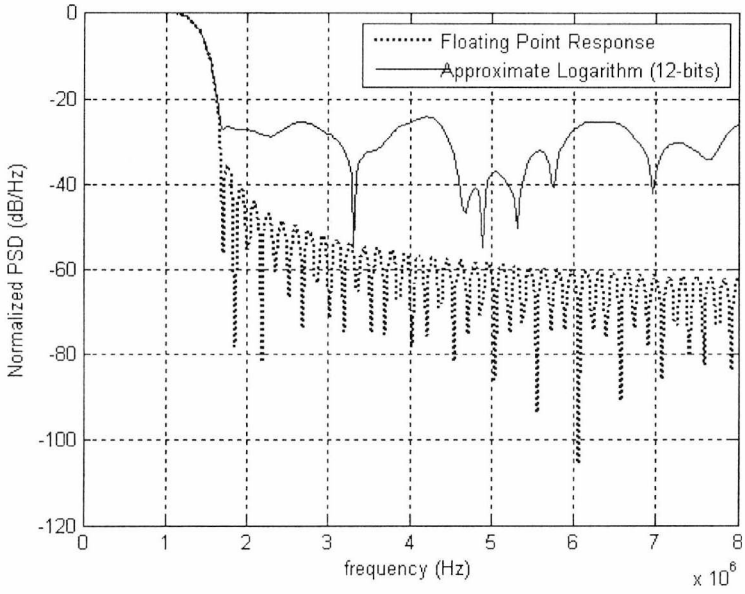

Fig 5.29 RRC PSD with 15-bit H-LNS arithmetic (12-bit precision) employing approximate logarithmic codec.

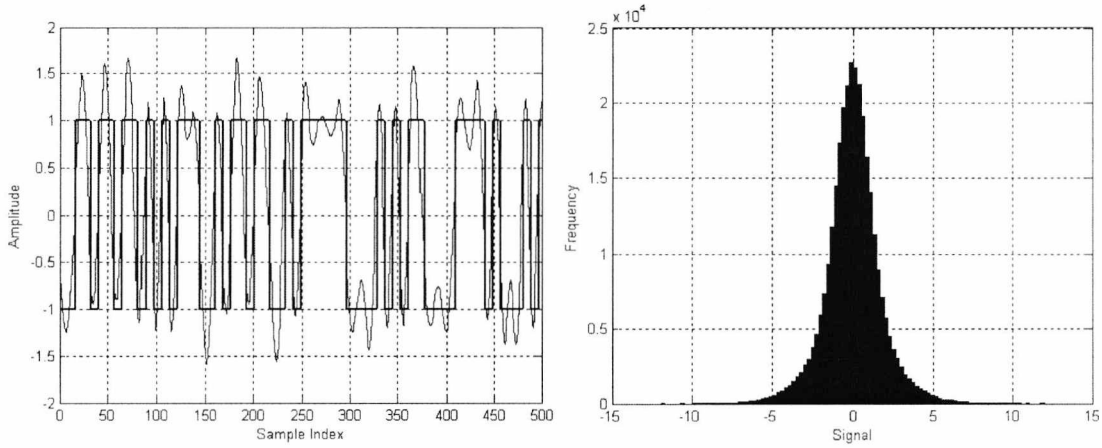

Fig 5.30 (A) A slice of the RRC waveform for the desired channel (no fading considered).
(B) The histogram of the input multiuser signal after demodulation.

The second investigation considers the mean square noise (variance) at the output of the RRC filter when the regressor consists of a simulated WCDMA downlink waveform. In this model, the number of users was K = 16 with random amplitudes where at least one user has RMS amplitude 5dB greater than the desired user (which, for convenience had amplitude = 1). We consider a low noise channel for this investigation where the AWGN had variance = -10dB (i.e. the CNR = 10dB). The unfaded desired single user waveform (see Fig. 5.30A) of unit energy was transmitted with RRC pulse shape. The interference + desired signal (at chip level) is approximately Gaussian (Fig. 5.30B) where the bulk of the signal occupies the $-5V < A < 5V$ interval after a low noise amplifier. Based on the desire to model the total error at the output of the RRC filter as uncorrelated AWGN of certain variance σ_N^2, the Fig. 5.31 and Table 5.2 contain the measured/simulated variances for a range of input signal precisions. For brevity, it was assumed the filter coefficients were represented with identical precision. The Fig. 5.31A compares the error performance of the filter for the fixed-point multiplier (employing two's complement numeric coding) and the H-LNS with direct LUT codec, with approximate codec (employing 16-bits numeric precision), and with the Lagrange-Linear codec (employing a 4-bit address LUT, 12-bit numeric precision and a 12-bit multiplier). Due to the large range of error for different precisions, the units of error were made decibel metrics for visual purposes. It can be seen that the Direct LUT outperforms all the aforementioned codecs (at the higher end of numeric precision), where the relative performance improvement over the two's complement number system is particularly important at low precision (< 5 bits) since the variance of the Gaussian approximation is actually very large for uniform coding. This relevant improvement is about -10dB. In comparison to the uniform codec, the approximate logarithm performs surprisingly well appearing to contrast the result in Fig. 5.20 for a fixed multiplier. This discrepancy is due to

the FIR filter coefficients being fixed fractals rather than random. For the specific implementation, the approximate algorithm performs about as well as the Direct-LUT codec employing 5-bits address precision. The Table 5.2 shows a couple of numeric examples when the mantissa of the input is fixed to 4 and 8 bits of precision. The Lagrange-Linear Codec was adjusted to this precision as well. Of particular note, the Direct-LUT codec offers about ten times lower MSE over the uniform counterpart. The next section will concentrate on the Rake receiver and adaptive LMMSE Rake receiver to yield observations on how the numeric precision and coding affects the receiver performance in frequency selective fading channels, particularly if the receiver algorithms are implemented after the RRC filter.

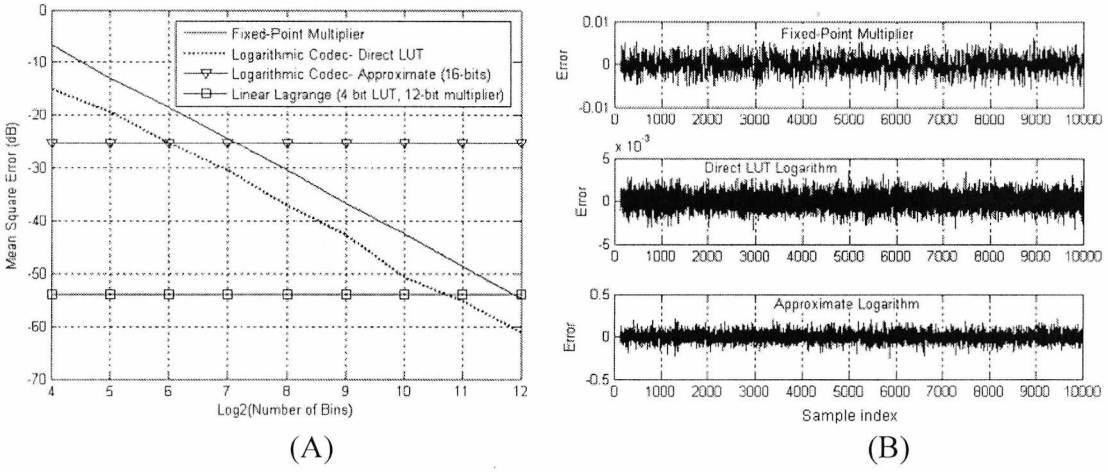

Fig 5.31 (A) The MSE as a function of the numeric precision for the fixed-point twos-complement, Direct LUT, Approximate Logarithm, and Linear-Lagrange Codec.
(B) Example error waveforms for the fixed-point twos-complement, Direct LUT, and Approximate Logarithm for 12-bits numeric precision.

Table 5.2 A comparison between the fixed-point twos-complement, Direct LUT, Linear-Lagrange Codec and Approximate Logarithm MSE for 4 and 8 bits numeric precision.

b	Fixed-Point Multiplier (MSE)	Logarithmic Direct-LUT (MSE)	Logarithmic Interpolative (MSE)
4	0.2118	0.0310	0.0310
8	8.9295×10^{-4}	1.9463×10^{-4}	2.0046×10^{-4}
Approximate Logarithm (16-bits)		30.13×10^{-4}	

5.2.3.4 SUMMARY

The Hybrid-Logarithmic number system implemented with direct LUT, Linear-Lagrange, and approximate codecs was investigated for both product generation and a fixed-point 127-tap RRC filter with multi-channel WCDMA data. The results show that the logarithmic codec employing direct LUT produced more accurate product generation with lower net round off error than an equivalent fixed-point binary implementation for the RRC filter. It was also shown by simulation that the modelled errors at the output of an RRC filter with Gaussian signals (which is a crude model of the WCDMA signal with many users) agreed well with the simulated errors in terms of the second order statistics. It was also discussed that although Linear-Lagrange codecs offered great potential in terms of offering very accurate solutions, the cost is relatively expensive multiplication requiring 12 to 16 bit fixed multipliers to be effective. However, the growth in FPGA devices with relatively low memory resources but built in multiplier may make the Linear-Lagrange codec a more suitable conversion method over the direct LUT case. The simplest codec employing the Lagrange method with no tabulated points (i.e. the approximate logarithm) is by far the simplest technique at a cost to the net performance. This method may not be suitable for implementation within long tap-delay line filters due to the error accumulation (see Fig. 5.31B). Overall, it is clear from the results that the Linear-Lagrange codec and Direct LUT codec offer superior error performance compared to the equivalent fixed precision twos-complement number system.

5.3 PERFORMANCE OF RAKE AND LMMSE RECEIVERS EMPLOYING LOGARITHMIC CODECS

The previous investigations into the performance of the logarithmic codecs with WCDMA signals for a RRC matched filter actually fulfil an important investigation into the net performance of a Rake receiver (or adaptive interference suppressing filters) with finite precision coding. Using the analytical methods presented in section 5.2 and 5.3 and the uncorrelated Gaussian assumption, we can model the noise (caused by round off) input to the rake receiver for any signal quantized to "m" bits. This can permit for relatively simple SINR or BER models for the receiver and also allow a minimum precision bound to be attained for near-optimum performance.

An issue to be addressed in this section is the problem for a Logarithmic implementation of an adaptive filter being dependent on the adaptation criterion. For the

least squares algorithms, the generic formulae involve multiplication and summation terms to update the filter coefficient. This requires (for the H-LNS implementation) that the filter coefficients be stored in memory as Linear quantities necessitating conversion to the Logarithmic domain. The actual NLMS update can be made simpler (requiring no multiplication or Log-Lin, Lin-Log conversion) via the signed-regressor [Eweda1990], signed-signed [Dasgupta1986], or signed-error [Claasen1981] LMS algorithms – where the cost incurred is that the MSE and convergence are degraded. An alternative approach can be employed where the filter coefficients do not have to be stored as linear quantities. In this case, the NLMS update is performed in the logarithmic domain utilizing a third LUT for performing linear addition. It can be shown that the logarithmic domain addition can use sensible approximations for small or large number arithmetic, while employing a very small LUT for intermediate numbers. This approach is quite efficient for integrating the NLMS adaptive filter logarithmically since provided the filter is converging, the small number approximations usually hold and thus addition can be implemented using the already available antilogarithmic codec (provided the small number is scaled to fall in "range" and rescaled after conversion).

5.3.1 Performance of the Rake Receiver Employing Finite Precision Logarithmic Coding

This section analyses the effect of numeric precision on the performance of the Rake receiver for the WCDMA downlink employing RRC pulse shaping. The performance of the rake will be investigated via simulation and analytical models.

5.3.1.1 Analytical Model

For simplicity, the rake receiver analytical model assumes to incur no truncation, scaling, or arithmetic round-off error due to the diversity combining coefficients. This effect can be modelled and observed with simulation. For a single rake finger synchronized to the L^{th} delay path, the mean "finger" SINR is derived accounting for numeric error prior to diversity combining. If we denote the single variable, $\partial_L[T]$ as the desired rake finger soft information sequence (weighted by the channel phase coefficient), the total interference inclusive of arithmetic round off is

$$\begin{aligned}\xi^{(L)}_{ro+MAI}[T] &= S_c^H[T]\cdot\left\{\xi^{(L)}_{MAI}[T]+\eta_{(L)}[T]+\varepsilon_r^{(L)}[T]+\chi_d^{(L)}[T]\right\}-\partial_L[T]\\ &= S_c^H[T]\cdot\left\{N^{(L)}[T]+\varepsilon_r^{(L)}[T]\right\}\end{aligned} \tag{5.50}$$

where T is a temporal sampling variable, $\chi_d^{(L)}[T]$ the desired spreaded signal, $S_c^H[T]$ the time variant scrambling + spreading sequence (modelled as a complex Bernoulli multivariate sequence), $N^{(L)}[T]=\xi_{MAI}^{(L)}[T]+\eta_{(L)}[T]$ the multiple access interference + noise, and $\varepsilon_r^{(L)}[T]$ the additive correlated round-off noise term (given analytically for fixed-point, floating-point, and logarithmic number systems presented earlier in this chapter). For simplicity, denote $\beta^{(L)}[T]=S_c^H[T]\cdot N^{(L)}[T]$ and $E^{(L)}[T]=S_c^H[T]\cdot\varepsilon_r^{(L)}[T]$. The MSE of $\xi_{ro+MAI}^{(L)}[T]$ is hence given as

$$\begin{aligned}E\left\{\left|\xi_{ro+MAI}^{(L)}[T]\right|^2\right\}&=E\left\{\beta^{(L)}[T]^2+\left|E^{(L)}[T]\right|^2+2\beta^{(L)}[T]\cdot E^{(L)}[T]\right\}\\&=\sigma_{M+\eta,(L)}^2+\sigma_{\varepsilon r,(L)}^2+2\phi_{(L)}\end{aligned}\tag{5.51}$$

with $\phi_{(L)}=\rho_\phi[b]\sqrt{\sigma_{M+\eta,(L)}^2\times\sigma_{\varepsilon r,(L)}^2}$ where $\rho_\phi[b]$ is the correlation factor conditioned on the number of bits, b and is denoted as $\rho_\phi[b]=\dfrac{E\left(\beta^{(L)}[T]\cdot E^{(L)}[T]\right)}{\sqrt{\sigma_{M+\eta,(L)}^2\times\sigma_{\varepsilon r,(L)}^2}}$. This correlation factor (Fig. 5.32 and Fig. 5.33) can be calculated and tabulated for different precisions to be used in the analytical model. Therefore the p^{th} rake finger mean SINR (Applying the Chapter 5 model and denoting $\mathrm{E}_1^{(p)}=\mathrm{E}_b^{(p)}$) is given as:

$$\bar{\gamma}_p=\frac{\Theta_{\max}^2 G\mathrm{E}_1^{(L)}}{\left\{\sum_{k=1}^{K}\sum_{\substack{m=0\\m\neq p}}^{L}\sum_{i=-N_c}^{N_c}\left|\boldsymbol{R}_p^T\boldsymbol{R}_{m-is}\right|^2\mathrm{E}_k^{(m)}+\Theta_{\max}^2\left[\sigma_{\varepsilon r,(p)}^2+\sigma_{cr,(p)}^2\right]\right\}+\sum_{\substack{i=-N_c\\i\neq 0}}^{N_c}\left|\boldsymbol{R}_p^T\boldsymbol{R}_{L-is}\right|^2\mathrm{E}_1^{(p)}+\left(\Theta_{\max}^2 G\sigma_\eta'^2\right)}\tag{5.52}$$

with

$$\sigma_{cr,(p)}^2=2\rho_\phi[b]\sqrt{\sigma_{\varepsilon r,(p)}^2\left(\sum_{k=1}^{K}\sum_{\substack{m=0\\m\neq p}}^{L}\sum_{i=-N_c}^{N_c}\left|\frac{\boldsymbol{R}_L^T\boldsymbol{R}_{m-is}}{\Theta_{\max}}\right|^2\mathrm{E}_k^{(m)}+G\sigma_\eta'^2\right)}\tag{5.53}$$

The density function of the rake output SINR is given as

$$f(\gamma_{out})=\sum_{d=1}^{M}\sum_{i=0}^{L-1}\left((d-1)!\bar{\gamma}_i^d\left\{\prod_{\underbrace{f=1}_{f\neq d}}^{M}\prod_{\underbrace{k=0}_{k\neq i}}^{L-1}\left(1-\frac{\bar{\gamma}_{k,f}}{\bar{\gamma}_{i,d}}\right)\right\}^{-1}\cdot\left(\gamma_{out}^{d-1}\cdot\left[exp\left\{-\frac{\gamma_{out}}{\bar{\gamma}_i}\right\}\right]\right)\right)\tag{5.54}$$

with conditional probability of error given by:

$$P_e(\bar{\gamma})=\int_0^\infty Q\left(\sqrt{\gamma_{out}}\right)\cdot f(\gamma_{out})\,\partial\gamma_{out}\tag{5.55}$$

Note that $\sigma_{\eta}'^{2}$ will represent the two-sided noise density for the single user channels (i.e. a baseband symbol level noise source) in the probability of error measurements. The quantity $\left(\Theta_{\max}^{2} G\sigma_{\eta}'^{2}\right)$ is a measure of the effective noise (i.e. the input noise density at chip rather than symbol level). To obtain the probability of error bound, we simply add the conditional BER over all diversity channels, where the BER per channel is obtained by calculating (5.55) numerically on a channel-by-channel basis. It is important to note that the model is in fact a Gaussian approximation (formed by the false assumption that all noise and interference is Gaussian). More exacting analytical techniques can be used, i.e. by calculating the density functions of interference, noise, etc considering the SIMO channel model more precisely. This of course incurs a far greater cost in terms of mathematical complexity. The author of this thesis initially tried to derive a more accurate model, but it was found that several integrals involving estimation of statistical products and summations yielded no closed loop solutions resulting in this work being placed on hold. In the near future, these models will be re-examined.

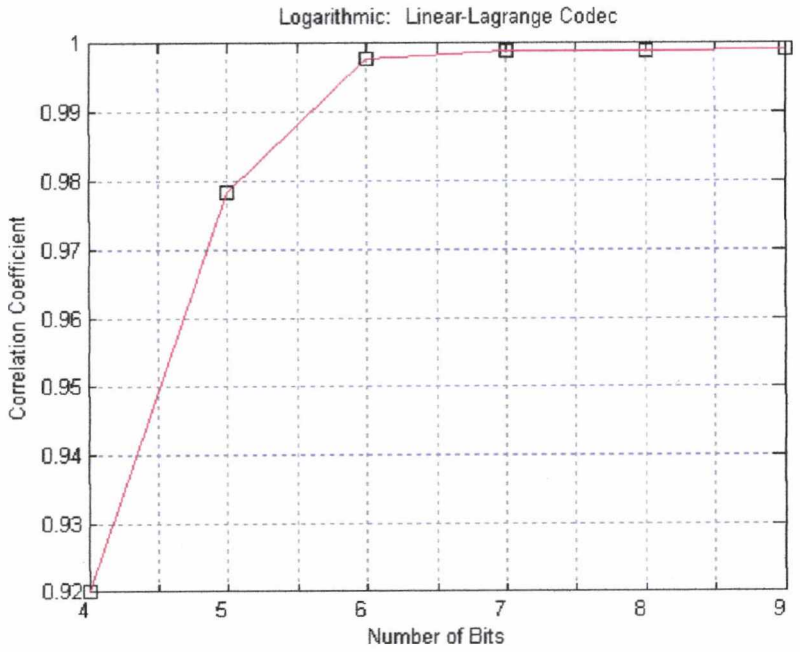

Fig 5.32 The correlation coefficient, $\rho_{\phi}[b]$ for Logarithmic Linear-Lagrange Codec obtained with simulation.

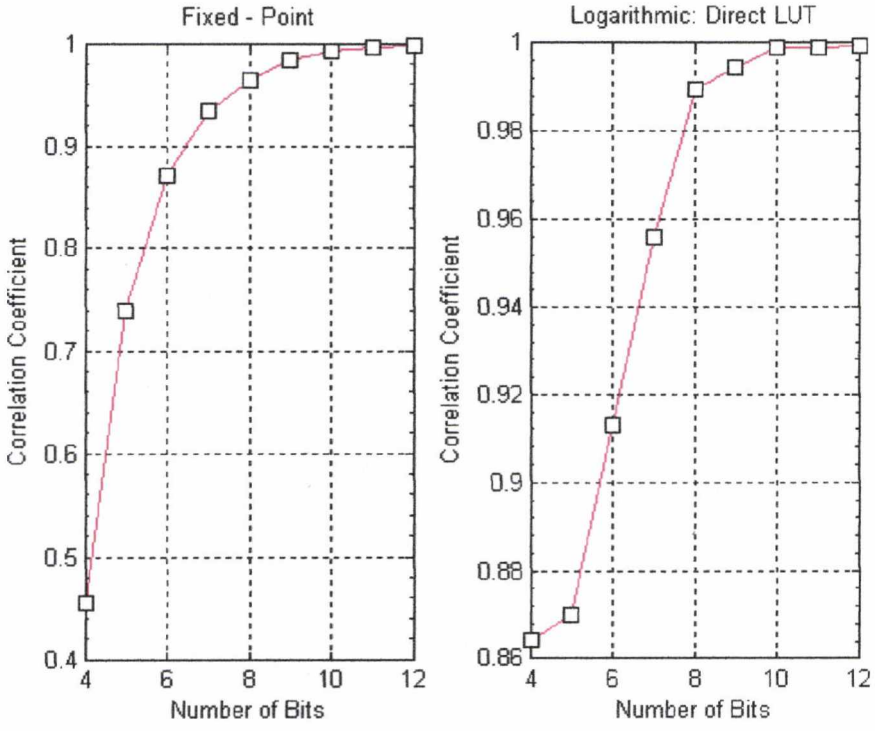

Fig 5.33 The correlation coefficient, $\rho_{\phi}[b]$ for the LUT based Logarithmic Codec and Fixed-Point Binary solution. These were conducted with analytical methods using the variance models presented in Section 5.2.

5.3.1.2 NUMERICAL EXAMPLES

This section presents the numerical results of the Rake receiver employing finite precision logarithmic arithmetic. A comparison between the analytical methods and Monte Carlo simulation are shown along with the double precision floating-point bound. The key observation (Fig. 5.35) will attempt to find a lower bound of arithmetic precision such that the performance of the Rake receiver is not significantly degraded compared to the ideal bound of double precision arithmetic (which we take to be the infinite precision model since this is the maximum achievable accuracy used by default in the Matlab simulator). The fixed-point twos-complement implementation will also be included for point of comparison with the logarithmic performance. The logarithmic conversion methodology considers the direct LUT codec. The first result (Fig. 5.34) considers the performance of the rake receiver under various loading conditions when only a 4-bit address range LUT is used. The quantization effect of channel estimation is included in the result. It is clear that a 4-bit address range LUT gave a perfectly acceptable performance. The next result (Fig. 5.35) expatiates by considering a range of address precisions between 4 and 12 bits for both fixed-point and logarithmic implementation for an 8-user channel. For purpose of comparison, the analytical results are also shown. The analytical and simulation results assume perfect

combining where the effect of channel cophasing and MRC coefficient (due to estimation in noisy channels) errors are ignored. The first observation concurs with the discussion in Chapter 5 (section 5.1) that the analytical solution based on the Gaussian approximation over-estimates the performance of the receiver. The second observation is that the probability of error (conditioned on the number of bits for the particular channel realization) for number of bits > 8 with both uniform and logarithmic implementation are very close to asymptotic bound (provided by DFLP precision). Hence increasing the numeric precision beyond about 9 bits will not offer any significant performance gain. Finally, it is clear from the observation that the H-LNS offers superior performance particularly when the quantizer encodes a lower number of bits precision.

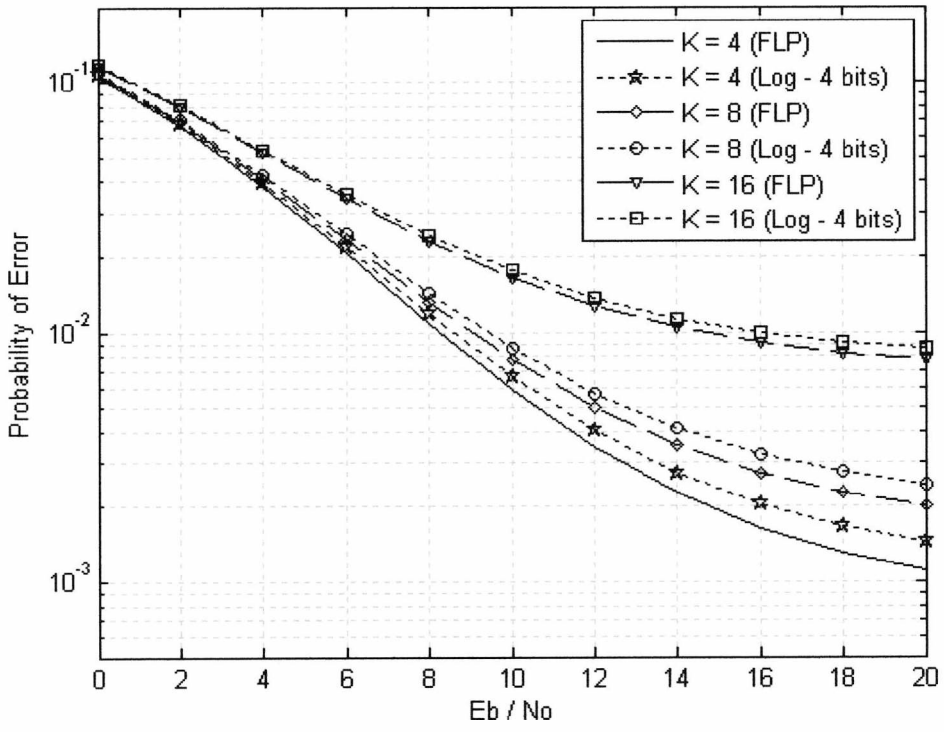

Fig 5.34 Performance of the Rake receiver employing 4-bit quantization.

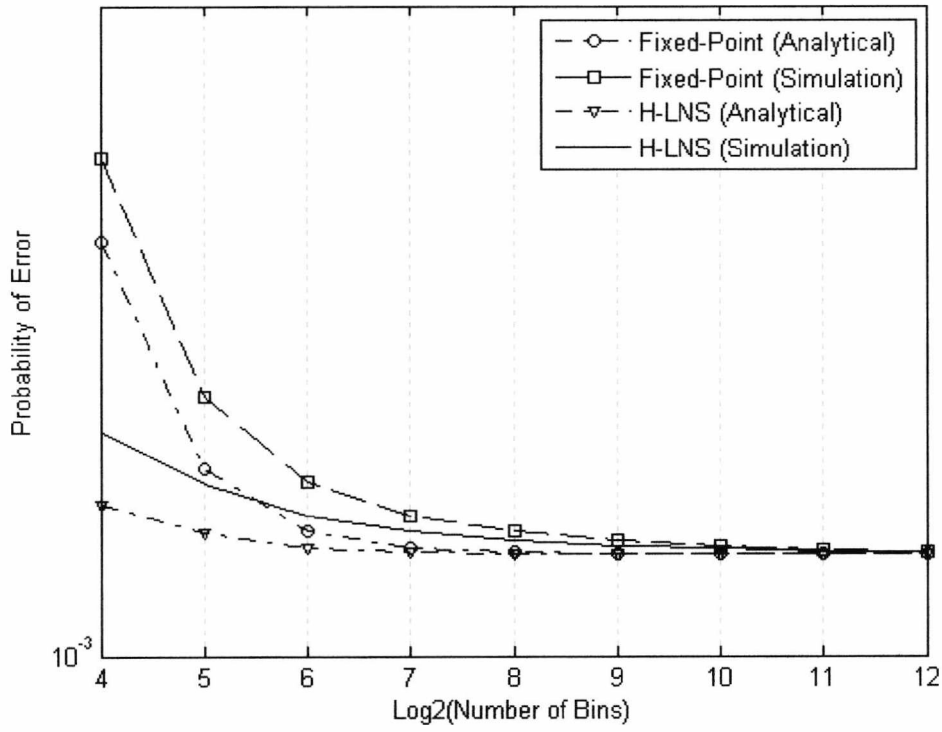

Fig 5.35 Performance of the Rake Vs numeric precision.

5.3.2 Performance of the Adaptive LMMSE Receiver Employing Finite Precision Logarithmic Coding

This section explores the performance of the adaptive LMMSE Rake/Equalizer employing finite precision logarithmic coding. The reasons for adaptive solutions to the generic LMMSE optimisation applying linear data/chip estimation[4] (via the second order statistics) are due, in principle, to complexity and non-stationary environments. The MMSE implementation of the linear serial chip equalizer, for instance, has a serious drawback in that the channel must be estimated/known prior to projection of the aforementioned algorithm. The accuracy of the channel estimation, particularly for time-variant channels, would naturally incur the main cost of the equalizer performance in fading channels. The foremost complexity issue for the equalizer arises due to calculation of the matrix inverse-particularly when filters ideally should be optimised for processing windows up to 3-5 times the channel delay spread [Treichler1996]. For the Vehicular A channel, this would translate to a nominal filter length covering approximately 50 chips. For fractionally spaced equalizers, the number of taps could be as high as 400 if 8 samples per chip are used. This makes matrix inversion extremely costly to undertake and also has the disadvantage that for

[4] Translated to essentially a finite windowed, causal and stable filter/filter bank realization.

a Wiener filter realization, the auto covariance matrix requires estimation via averaging at least 100 data symbols (ignoring all the tails in the transmission). This would provide a real time receiver with a high latency/lag in demodulation. Adaptive filtering takes care of all these issues by removing the constraint of matrix inversion and essentially the requirement of explicit channel estimation or statistical priories. However, adaptive filters have the disadvantage that near-optimum performance is difficult to achieve and such filters are usually biased estimators (i.e. the filters converge and "rattle" around a nominal misadjustment). Consequently, analysing the performance of an adaptive receiver generally requires the convergence behaviour of the filter to be investigated. This is not an entirely trivial process, particularly when initiating finite numeric precision, signed-regressor or "heavily quantized/truncated" adaptive filtering algorithms. For this reason alone, analytical methods and solutions are ignored, where this section focuses exclusively on results from simulation. A paper submitted for publication (Paper IV) performed a study of the analytical performance bounds utilizing logarithmic coding, but this was for a fixed equalizer in a fixed channel with known impulse response. This paper investigated the ideal/upper-bound performance of a precise equalizer (rather than adaptive), hence analytical solutions presented here are of limited practical use for adaptive equalizers employing training waveforms (which may be decision directed or use the noisy pilot channel). It is noteworthy to mention that significant contributions have appeared in publications for the behaviour and convergence of a wide range of adaptive filtering algorithms including the LMS and NLMS [Haykin1996, Slock1993], signed regressor/error LMS [Eweda1990], LMS with leakage [Nascimento1999], and the signed-signed LMS. The analysis for the majority of papers considered the adaptive filters being excited with Gaussian regressor. The behaviour of adaptive filters with finite precision arithmetic was researched in [Nascimento1999, Caraiscos1984]. The convergence behaviour of generic LMS adaptive filters are difficult to translate to a probability of error bound, where some useful contributions from Barbosa and Miller [Barbosa1990] and Juntti and Latva-aho [Junnti1999] analysed the error performance from the *H-infinity* perspective – i.e. using the excess MSE (or rather the filter misadjustment) in steady state where the assumption was made that the filter converged to a global minimum. However, this steady state MSE is dependent on the actual signal itself and thus the eigenspread of the regressor auto covariance matrix. What this entails is that for a useful investigation, the error performance for the LMMSE Rake receiver was explored with a semi-analytical solution.

The ubiquitous performance metric investigated in the thesis thus far is the decision probability of error (assuming a maximum likelihood detector for binary antipodal signalling over an AWGN channel). This section primarily addresses the implemental aspects of the adaptive receiver with logarithmic coding and attempts (with reasonable assumptions and

observations from simulation) to gather a sufficient, low cost implementation that performs with similar probability of error as a filter built with full double-precision floating point arithmetic. The novelty behind this approach is that fully integrated multiplierless receivers can yield superior performance to traditional implementation, but be somewhat cost effective and also result in significant power savings. This is useful for industrial application since real handset devices are equipped with rather limiting rechargeable batteries where cost effective receiver solutions on programmable logic devices are currently (and for the foreseeable future) incurring bottlenecks for statistical signal processing application in current and future mobile networks.

5.3.2.1 The Hybrid-Logarithmic Adaptive Filter Architecture

Much akin to the RRC filter employing hybrid-logarithmic architecture, the adaptive equalizer is built on exactly the same principle. The difference here is that the filter weights are time variant, and indeed, made time variant by the adaptive algorithm in question. For the NLMS algorithm, the weights are updated according to the cost function (i.e. the error) and the regressor forming the instantaneous and noisy gradient estimate. This is an extra processing nuisance that in some way circumvents the logic behind applying look-up-table based codecs (and the SLNS in general). The reason for this is purely down to the update requiring a minimum of three independent Log-Lin and Lin-Log conversions (and all numeric conversions dealing with carry bits from log-domain multiplication and linear-domain addition) to convert the coefficient update into a logarithmic value. This is made even more costly when the coefficients are complex (where in this thesis the filter coefficients are always complex). A low-precision uniform/twos-complement implementation (at least for the weight update unit) may well be more efficient despite offering relatively poorer performance (this will be seen in latter sections). As discussed already, the filter lengths will be inherently long (> 50 chip intervals) hence the approximate logarithm presented in section 5.2 will be basically useless. Note the performance of the approximate logarithm was only reasonably good for the RRC filter when the filter weights were already initialised accurately as logarithmic values. In the case of the adaptive filter, this is not so and despite initial research in [El-Eraki2003], the approximate codecs for WCDMA offered poorer performance than that of a digital FM radio receiver for vehicles. This is simply explained by the fact that the adaptive update (and error) either "stalls" or yields reverse polarity gradient estimates causing catastrophic divergence since too many Lin-Log and Log-Lin conversions generate unacceptable numeric error. Preliminary

research into this aspect concluded that the update part of the filter behaved similarly to the Signed-Signed LMS algorithm with fixed step size where this implementation rarely converges to any global minima with WCDMA signals (the approximate Log gave equivalent accuracy of only 1-2 bits with three conversion processes). The key to the adaptive filter implementation rests on how the coefficient is updated during the filter training. The proceeding sections focus entirely on the implemental aspect of this unit (where the rest of the filter is basically simple). The Fig. 5.36 yields a diagrammatic interpretation of the adaptive multiplierless equalizer employing the H-LNS.

5.3.2.2 The NLMS Update Unit With No Approximation

The architecture for the weight computational unit in this set up (Fig. 5.37) considers numeric conversions between logarithmic and linear domain to perform multiplication and addition. This results in the requirement of three table look ups (or alternatively three sub-routines in the DSP program memory initiating the Log-Lin and Lin-Log codecs). This approach incurs a complication that should ideally be avoided if possible since the time for coefficient calculation in a numeric processor is at least doubled over a fixed-point uniform implementation.

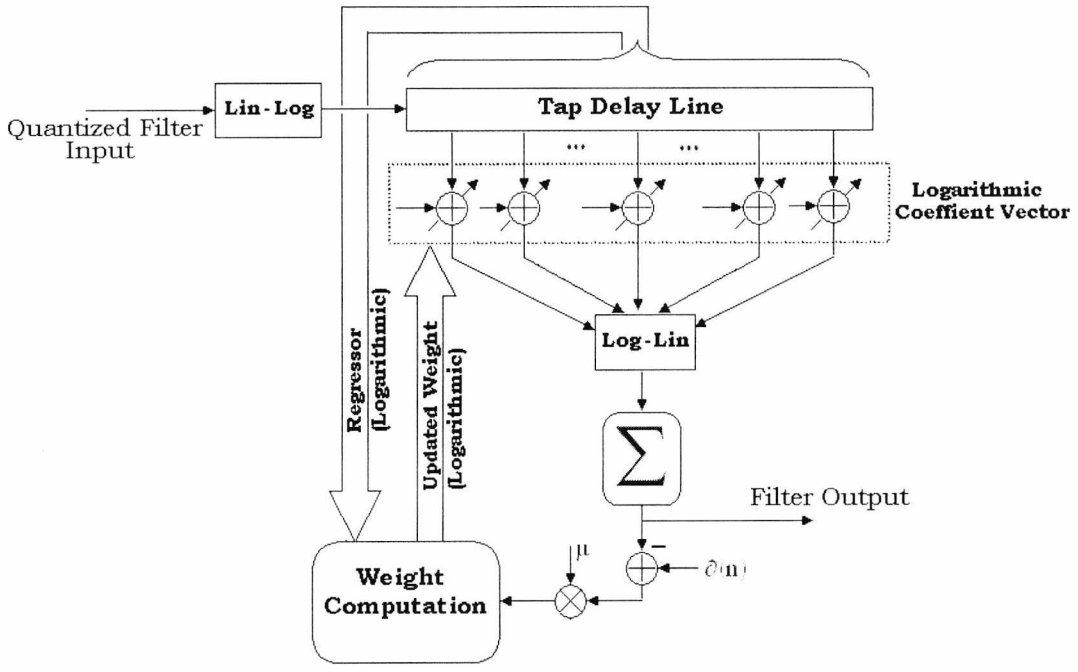

Fig 5.36 A generalized diagram of the adaptive filter architecture utilizing the H-LNS.

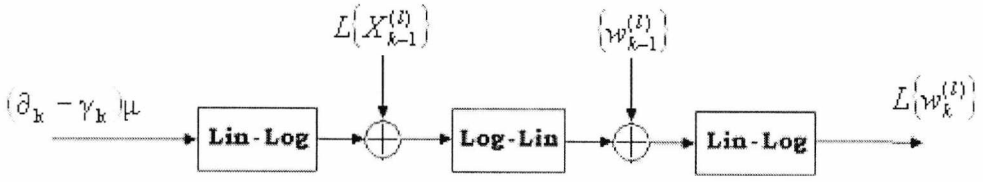

Fig 5.37 The architecture of the NLMS update employing the H-LNS

This is an important issue since for chip-rate equalizers, the processing speed would require all filter computations (including the update term for the next sample) to be executed in a fraction of a chip period. In other words, if the oversampled chip period is 0.25μs, the filter may be required to perform over 1500 inner products, additions and shifts in this time span (assuming a fractionally sampled 400-tap transversal equalizer). It is quite obvious that this approach pushes the limits of current DSP technology, where the additional complexity of three codec operations just to perform the coefficient update is one that must be circumvented if at all possible.

5.3.2.3 THE NLMS UPDATE UNIT WITH QUANTIZED APPROXIMATION

Simply stated, this section considers that the largest computational load is the product between the scaled error and regressor. If the regressor is "heavily quantized or rounded", this product term could at worst involve a couple of shift and summation terms requiring no fixed multiplier, and even better, requiring no Lin-Log and Log-Lin conversion. This approach (Fig. 5.38) effectively removes two codec operations and is thus far more attractive complexity-wise. However, what is not so clear is the scientific foundation for allowing such gross simplifications to the filter update – i.e. it would be rather pointless to initiate simplification at a large cost to filter performance. This is mathematically explored in the Appendix B for the Signed Regressor LMS algorithm. What is shown here is that the convergence in the MSE metric is slower than the corresponding NLMS with equal step size, but the excess convergence MSE can be made similar to the NLMS provided the step size is proportionate to the NLMS step size by a factor $\sqrt{\frac{2}{\pi}} \cdot \sigma_{xx}$ with σ_{xx} the regressor standard deviation. If this is not met reliably, the excess MSE will be greater. The general truncated NLMS algorithm is given as:

$$\boldsymbol{w}_k^{(n)} = \boldsymbol{w}_k^{(n-1)} + \left(\frac{\mu}{f\left\{ \rho + \left\| \boldsymbol{\chi}_{(n)}^H \boldsymbol{\chi}_{(n)} \right\| \right\}} \right) \cdot e_{(n)}^* \cdot f\left\{ \boldsymbol{\chi}_{(n-1)} \right\} \qquad (5.56)$$

where $f\{\bullet\}$ is the truncation function. $e^*_{(n)}$ is the conjugate error term defined as $e^*_{(n)} = \left(d_{(n)} - \mathbf{w}^H_{(n-1)}\boldsymbol{\chi}_{(n)}\right)^*$. This can be defined for any implemental aspect dependent on complexity, as the following two cases indicate.

i) For 1 bit truncation, the MSB of the number χ is taken – this being the sign bit. Hence $f\{\chi\} = sgn\{\chi\} \in \{1, 0, -1\}$. *sgn(*)* is the Signum function, and the NLMS update is commonly known as the Signed-Regressor (SR) LMS [Eweda1990]. This causes the update to be multiplierless (even in the linear domain) and all that is required is Lin-Log conversion for the adaptive filter coefficients.

ii) Since χ is stored in the processor as a logarithmic quantity, a simple implementation could consider that $f\{\chi\} = T\{\chi, e+1\} \in \{\Im\}$ with $\Im$ the set of signed integers where e is the number of exponent bits. This translates for the numeric processor as a real shift $\propto 2^m$, $m \in \{\Im\}$. This will be called the Signed-Exponent-Regressor (SER) algorithm. The algorithm is still multiplierless in the sense that a fixed multiplier is not required to perform numerical switching of the lower order bits.

The complexity of the algorithm is quite significantly enhanced if $f\{\chi\} = T\{\chi, M\}$ for $M>e+1$ requiring antilogarithmic conversion and floating point multiplication. Hence only the SR and SER LMS cases will be considered.

5.3.2.4 THE NLMS UPDATE UNIT WITH LOG-DOMAIN ADDITION

This approach considers that the logarithmic coefficient update is desired; hence one way of removing the constraint of three LUT conversions is to employ a Logarithmic domain adder (Fig. 5.39) requiring a separate codec to evaluate the adjustment function. This adjustment function [Arnold2001] is given here-with:

Consider the relation Z = X + Y. Logarithmically we may represent this as

$$Log_2|Z| = Log_2|X| + Log_2\left|1 + \frac{Y}{X}\right| \tag{5.57}$$

If X and Y are represented as logarithmic quantities $L\{X\}$ and $L\{Y\}$, the expression becomes

$$Log_2|Z| = Log_2|X| + Log_2\left|1 + 2^{L\{Y\}-L\{X\}}\right| \tag{5.58}$$

where $Log_2\left|1+2^{L\{Y\}-L\{X\}}\right|$ is the adjustment function that must be evaluated.

The proper and highly accurate implementation of this function would be with a LUT, or a LUT based mapping employing piece-wise approximation with linear or polynomial functional. The current bottlenecks for evaluating the adjustment function incur for IEEE-754 floating-point precision. However, this level of precision (23 bits) is not part of the thesis objective hence only very basic conversion methods are explored. The methods explored consider large and small number approximations, and linear regression or direct LUT evaluation for intermediary numbers. The only system level complexity disadvantage occurs when the sign and zero flags of the overall conversion $Log_2|Z|$ must be encoded. This means that we deal with subtraction – i.e. the adjustment function becomes $Log_2\left|1-2^{L\{Y\}-L\{X\}}\right|$ which has singularity around $2^{L\{Y\}-L\{X\}}=1$. Consequently, this function cannot be easily implemented with linear regression around this region. Small and large number approximations still hold. For convenience, the logarithmic adjustment function is shown in Fig. (5.40) for addition and subtraction. This is quite insightful since it is fairly obvious that for $L\{Y\} - L\{X\} > 5$, the adjustment function is approximately linear, and for $L\{Y\} - L\{X\} < -5$, the function is exponential. Note that if two numbers are negative when added, we use the addition-based function (and reverse the sign of the total). Similarly, if X is negative but Y positive (rather than Y negative and X positive), we can still use the subtraction-based function and flip the sign of the total (after conversion) provided |X| > |Y|. The methodology of evaluating the logarithmic adjustment function is now explored.

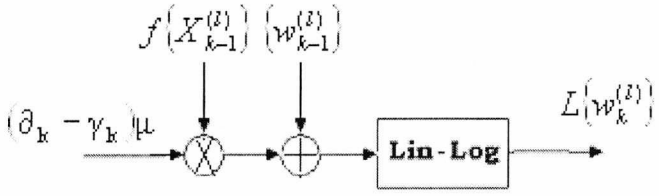

Fig 5.38 The architecture of the NLMS Update with regressor approximation.

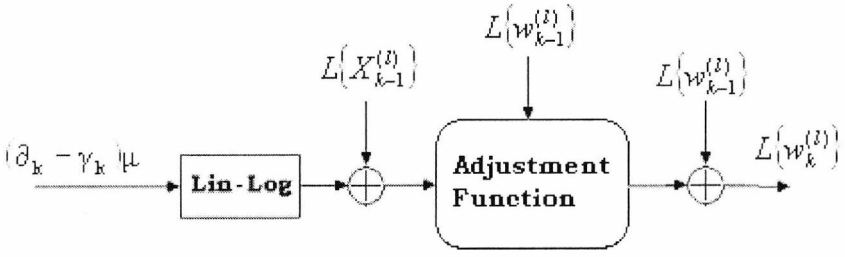

Fig 5.39 The architecture of the NLMS update with logarithmic domain addition

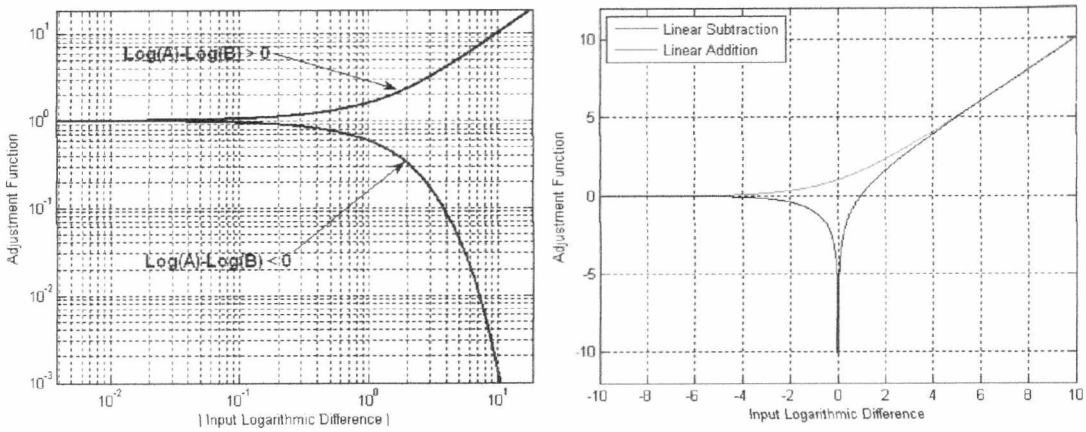

Fig 5.40 (A) The logarithmic adjustment function for addition.
(B) The logarithmic adjustment function for subtraction.

5.3.2.4.1 THREE PIECE MODEL UTILIZING THE UPPER AND LOWER BOUNDS OF THE LOGARITHMIC ADJUSTMENT FUNCTION

The simplest method of evaluating the adjustment function for addition or subtraction is to make the small and large number approximation. We start with the upper bound.

Upper Bound: Figuratively speaking, the adjustment function is approximately linear for larger numbers, hence equating $A = L\{Y\} - L\{X\} >> 0$, we make the approximation (with B any scalar)

$$\begin{aligned} Log_2\left|1+2^A\right| &\approx A \quad \left|A \geq B \quad (addition)\right. \\ Log_2\left|1-2^A\right| &\approx A \quad \left|A \geq B \quad (subtraction)\right. \end{aligned} \tag{5.59}$$

The choice of B for the desired accuracy of conversion is now the topic of investigation. Let the logarithmic adjustment error be denoted by the following inequality where

$$\begin{aligned} \varepsilon &= Log_2\left|1+2^B\right| - B \leq \frac{1}{2}2^{-b} \\ &= Log_2\left|\frac{1+2^B}{2^B}\right| \leq \frac{1}{2}2^{-b} \end{aligned} \tag{5.60}$$

with b the least significant digit representing the desired error bound. Performing some simple algebra allows a relation between b and B to be formulated where

$$B \geq \left\lfloor Log_2\left|\frac{-1}{1-2^{\left(\frac{1}{2}2^{-b}\right)}}\right| \right\rfloor \tag{5.61}$$

This relationship is linear (due to the ceiling function) and requires that for desired fractional equivalent precision of at least "b" bits, then $B \geq b+1$.

Lower Bound: The adjustment function is approximately exponential for $A << 0$, hence make the estimation

$$\begin{aligned} Log_2\left|1+2^A\right| &\approx 2^A \quad |A \leq C \quad (addition) \\ Log_2\left|1-2^A\right| &\approx -2^A \quad |A \leq C \quad (subtraction) \end{aligned} \tag{5.62}$$

This lower bound can be implemented with the already existent antilogarithmic codec. Note that this codec employed fixed range of $0<L\{Z\}<1$ while A is essentially a negative number. To make this LUT available, some numeric fixing is required. The number A is logarithmic hence has an integer and fractional part. We then can write with no loss of generality that $2^A = 2^{-(e+f)} = 2^{-e} \cdot 2^{-f}$. While $0 < |f| < 1$ with $f < 0$, we can add a 1 to this result and guarantee the range of the LUT is satisfied. The number conversion is satisfied where $2^A = 2^{-(e+f)} = 2^{-e} \cdot \left(2^{-1} \cdot \left\{2^{1-f}\right\}\right)$ with 2^{1-f} executed by the LUT (or even an approximate antilogarithmic codec requiring a simple add by one, i.e. equate the conversion as $f+2$) with the resultant right shifted by one digit (to satisfy the practical logarithmic fraction requirement). Let the logarithmic adjustment error be denoted by the following inequality where

$$\begin{aligned} \varepsilon &= Log_2\left|1+2^C\right| - 2^C \leq \frac{1}{2}2^{-b} \\ &= Log_2\left|\frac{1+2^C}{2^{2^C}}\right| \leq \frac{1}{2}2^{-b} \end{aligned} \tag{5.63}$$

This problem is not so easily solved, but a solution can be obtained if b is mapped to C (with C taking on the role as the predetermined scalar) hence,

$$b \geq -\left\lceil Log_2\left\{\frac{1}{2 \times Log_2\left[\left|\frac{1+2^C}{2^{2^C}}\right|\right]}\right\}\right\rceil \tag{5.64}$$

The best way of dealing with this approach is to map b to C for a variety of negative scalars and either tabulate or graphically represent results to choose the appropriate lower bound for the approximation. This is an approximately linear function, where for desired fractional equivalent precision of at least "b" bits, then $C \leq -(b-1)$.

Intermediary Bound: For a number, A which falls between C and B, the logarithmic adjustment function must be determined with a LUT or linear regression (for logarithmic addition only). We consider two specific cases:

i) When the range is $0 < A < 4$ allowing a simple codec to be implemented with linear relation $f(A) = \frac{3}{4}A + 1$. The multiplication can be performed with two shifts and additions. This is for the addition-based function only. The subtraction function is difficult to interpolate simply.

ii) A LUT is applied between the range $-5 < A < 7$ for application of the algorithm. This keeps the error sufficiently low if a minimum of 5 bits of equivalent precision is required for the lower and upper bounds.

5.3.2.4.2 METHOD UTILIZING A SINGLE LOOK UP TABLE

If we observe the $Log_2|1+2^A|$ function, it is possible to apply a single LUT by denoting that $Log_2|1+2^A| = A + Log_2|1+2^{-A}|$. It should be obvious that for A $\geq$ 0, the $Log_2|1+2^{-A}|$ function has clear boundaries where $0 < Log_2|1+2^{-A}| \leq 1$. Hence we can apply a look-up table to evaluate this function where the algorithm becomes:

If X and Y are represented as logarithmic quantities $L\{X\}$ and $L\{Y\}$ with $Z = X + Y$ the desired arithmetic computation, then noting $A = L\{Y\} - L\{X\}$,

$$Log_2|Z| = Log_2|X| + A + \underbrace{Log_2|1+2^{-A}|}_{LUT\ Evaluation} \tag{5.65}$$

provided $L\{Y\} > L\{X\}$, i.e. A $\geq$ 0. Similarly, the subtraction-based algorithm is implemented (i.e. Z = Y - X) with

$$Log_2|Z| = Log_2|X| + A + \underbrace{Log_2|1-2^{-A}|}_{LUT\ Evaluation} \tag{5.66}$$

and the same condition that $L\{Y\} > L\{X\}$, i.e. A $\geq$ 0. With this LUT evaluation, if $A = 0$, we simply bypass the LUT and assign a false mantissa value (and set the zero flag bit) or denote the overall result as a string of zeros (setting the zero flag bit in the process).

However, what if the conditional bound on A $\geq$ 0 is not realized? If A < 0, it is clear the LUT would be required to have far greater dynamic range. This is even more of a

mathematical limitation for subtraction where the logarithm of a negative number ($1-2^{-A}<0$) is complex. A simple way around this problem would be to condition the addition/subtraction such that A ≥ 0 always. This is achieved by this simple pseudo code:

$$A = Log_2|Y| - Log_2|X|;$$
$$if \quad sign(A) \neq -1$$
$$\quad Log_2|Z| = Log_2|X| + |A| + Log_2\left[1 \pm 2^{-|A|}\right];$$
$$else \quad Log_2|Z| = Log_2|Y| + |A| + Log_2\left[1 \pm 2^{-|A|}\right];$$
$$end\ if$$

In other words, the sign of A is used for the conditional test statement. Hence if the number is negative, we simply use the LUT as before (taking the absolute value of A) except the difference is the largest value (in this case, Y) is used as the summation term.

5.3.2.4.3 Comparison of the Logarithmic Addition Techniques

The total conversion error employing the adjustment function will not be investigated statistically for what is an approximate algorithm (making it somewhat difficult to analyse due to non-linear functions). However, consider the Fig (5.41A) and Fig (5.41B) showing the adjustment error and relative adjustment error over a relatively small range of A. It can be seen that the LUT approach improves the error performance over the Linear-Lagrange approximate method. It can also be noted that the asymptotic limits of the error is zero for the small and large number approximation. However, the relative error does not behave in such an idealistic manner where it can be seen that this error is asymptotic (around 0.3) as the number decreases (i.e. increases in magnitude for A < 0). This roughly translates to about 30% numeric error in this range. This is fairly typical for small number approximations and this error remains uniform (unless at infinity where this error is in fact zero) no matter how large the magnitude of A. If the number is quantized below 15 bits, this error obviously increases. Note the relative error and actual error are completely different metrics, where in the range $A < 0$, the actual error decreases while the relative error increases thus the relation is inversely proportional. The Figs (5.42) and (5.43) show the conversion error and relative error for the LUT only evaluation (the example considered 8-bit LUT address range when the difference contained three integer bits). It is clear from the results that the direct-LUT only evaluation generated superior performance over the three-piece model despite the necessity of the extra memory required to generate the logarithmic domain addition.

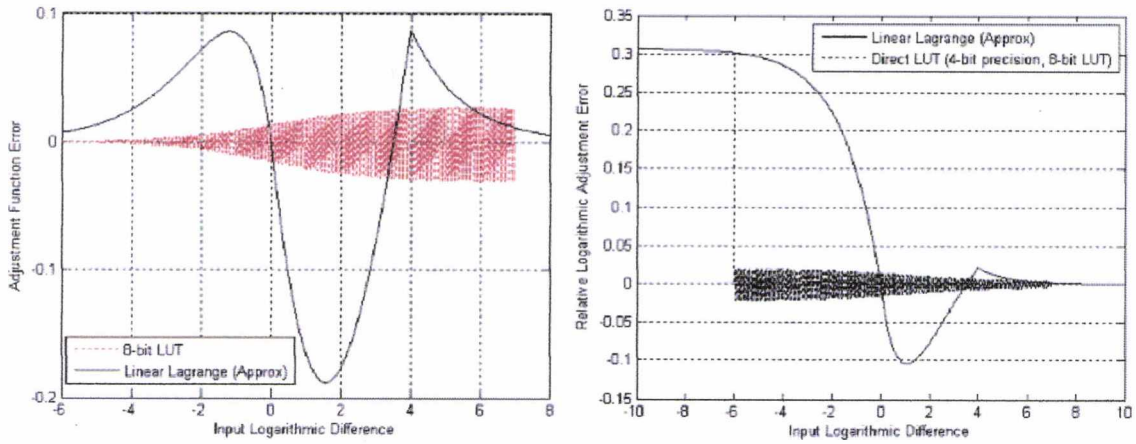

(A) (B)

Fig 5.41 (A) The logarithmic adjustment function error for the three-piece model.
(B) The relative logarithmic adjustment function error for the three-piece model.

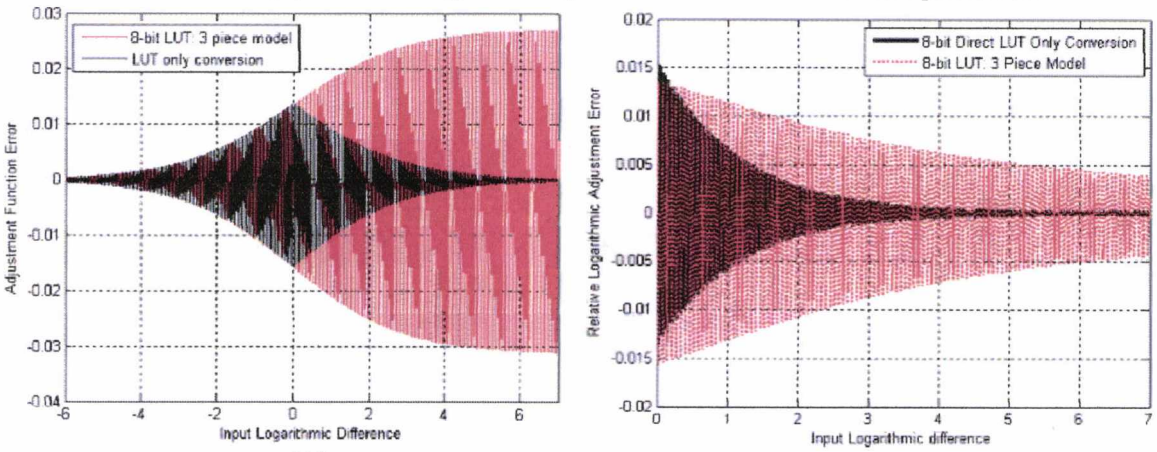

(A) (B)

Fig 5.42 (A) The logarithmic adjustment function error for the direct LUT conversion with 8-bit address.
(B) The relative logarithmic adjustment function error for the direct LUT conversion with 8-bit address.

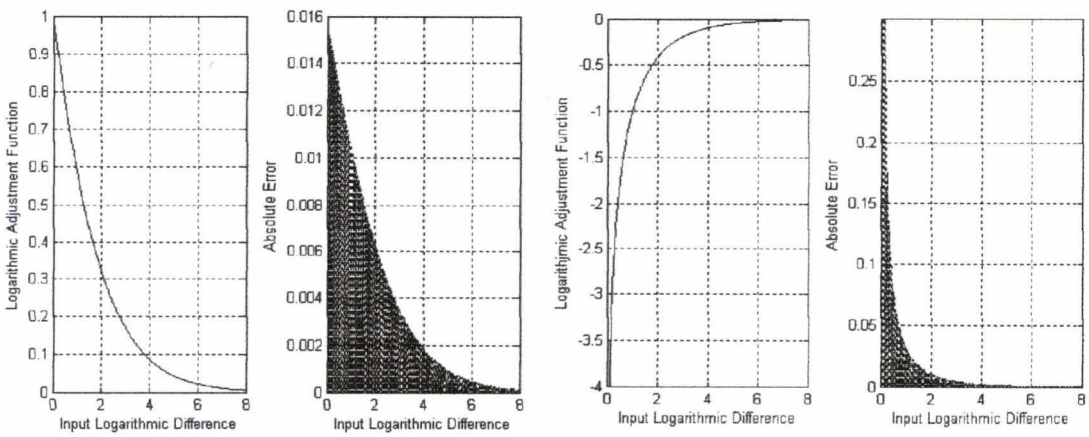

(A) (B)

Fig 5.43 (A) The logarithmic addition adjustment function and error for the direct LUT conversion with 8-bit address.
(B) The logarithmic subtraction adjustment function and error for the direct LUT conversion with 8-bit address.

5.3.2.5 NUMERICAL EXAMPLES

The adaptive channel equalizer is analyzed in this section employing three different NLMS update methodologies utilizing the H-LNS and/or the S-LNS. The first result (Fig. 5.44) shows the convergence of the filter in the MSE metric for 8 additive uniformly distributed users for the WCDMA downlink modelled with Vehicular A Channel with vehicular speed of 20Km/Hr. The results were generated for the NLMS, SR-LMS and SER-LMS considering the double precision floating point number system. The purpose of this simulation is to indicate the convergence of the schemes rather than the effect of arithmetic precision. It is clear from the simulation that the NLMS offers the best performance, although the SER-LMS gave a comparable result. As expected, the SR-LMS performed least effectively. This can be noted by approximately double the convergence time when the step size was altered to speed up convergence at a cost to greater misadjustment. The next result (Fig. 5.45) considered the probability of error for an 8-user channel when the channel equalizer was built with the H-LNS architecture utilizing the Direct LUT codec and the truncated word length adaptive LMS methods. The look up tables for the codec employed 9-bit address resolution for this example. The SER-NLMS implementation offered reasonable performance in comparison to the NLMS for this particular channel. The SR-LMS on the other hand performed significantly worse due to slower convergence and larger misadjustment. The implemental aspect for this approach is rather questionable for the WCDMA downlink channel equalizer; hence it is proposed that the SER-NLMS is given consideration for adapting the filter coefficients. The technical difference between the SER-NLMS and SR-NLMS is only the additive complexity of a single shift operation, which is quite affordable. The NLMS scheme operating in a fixed 8-user channel with SNR of 20dB (Fig. 5.46) is the next topic of investigation, where the number of address bits for the logarithmic codecs were varied from 4-bits to 12 bits (no comparison with the truncated word length NLMS was offered in this section). For comparison, the uniform fixed-point number system was included. The Linear-Lagrange method considered a 12-bit fixed multiplier. It is clear that the best performance is offered by the Linear-Lagrange codec where the NLMS algorithm had full H-LNS architecture (the direct LUT Codec offered similar performance in the asymptotic limits when the number of bits > 7). In conclusion to these observations, it is clear that for numeric accuracy > 9 bits, the performances of the uniform and logarithmic implementations are very similar considering the probability of error metric. Where the performance advantage of H-LNS arithmetic manifests is in the lower precision bounds. It is in these bounds where the Linear-Lagrange codec built with fixed 12-bit multiplier offers the best performance. The H-LNS implementation with log-domain addition for the update part of the filter performed extremely well, offering superior

filter response to the fixed-point solution. This technique could be made as accurate as the "full H-LNS" architecture if the LUT contained more tabulated points. In general, if the adjustment function was conducted applying 9-bits of resolution (i.e. a 12 bit address range LUT considering 3-bit integer), the performance would be identical to the full H-LNS application (built with a 9-bit logarithmic conversion LUT) applying direct LUT only conversion. The cost of the Linear-Lagrange codec is the additional complexity of a fixed-point multiplier hence the case for the Direct LUT implementation is stronger, where the performance is basically identical to Linear-Lagrange codec for number of bits > 7. It can also be concluded that the logarithmic domain adder for the NLMS filter gave perfectly adequate performance in comparison to the full H-LNS implementation.

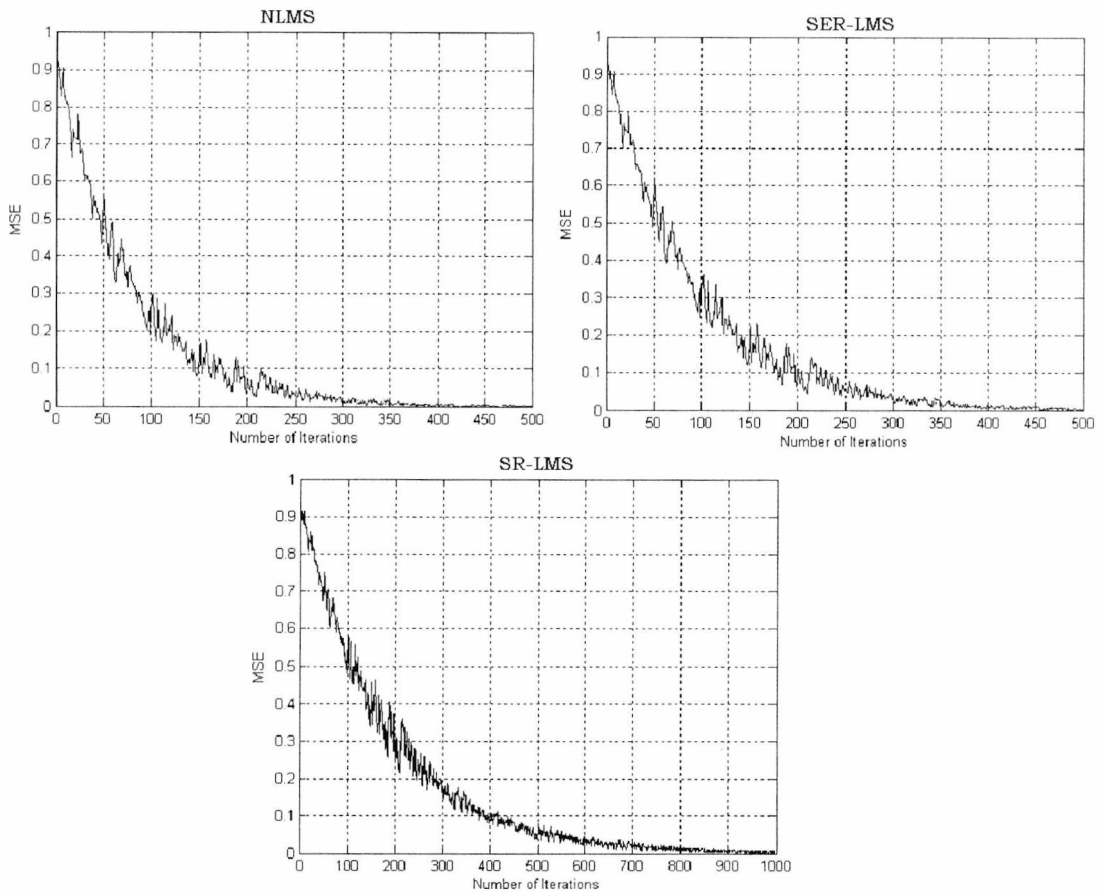

Fig 5.44 Convergence of the adaptive equalizer with NLMS, SR-LMS, and SER–LMS.

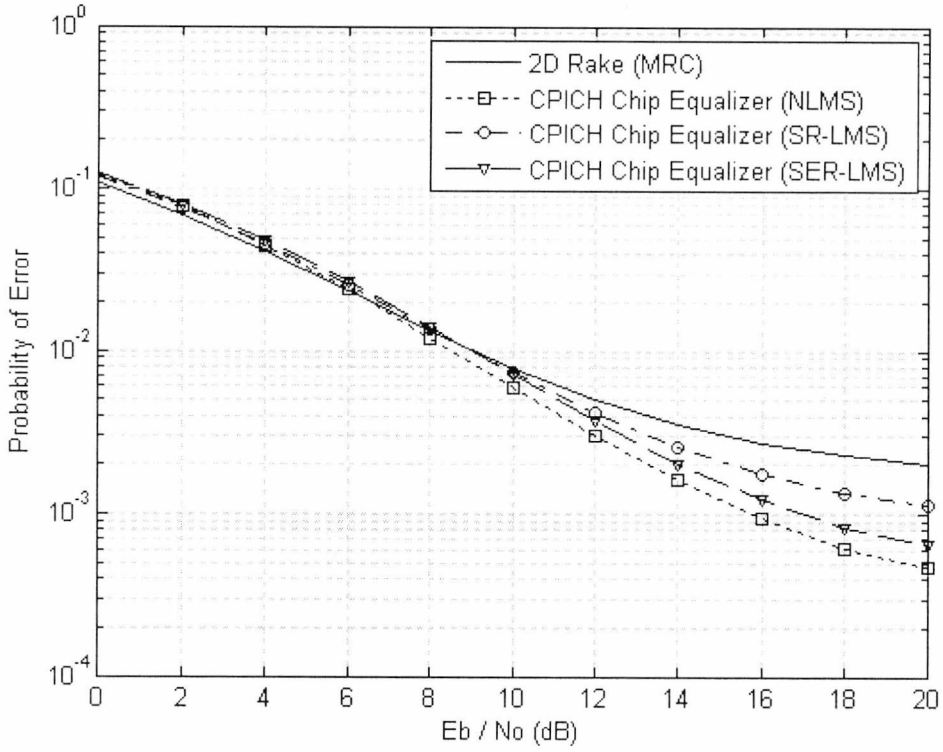

Fig 5.45 Performance of the adaptive equalizer with H-LNS arithmetic.

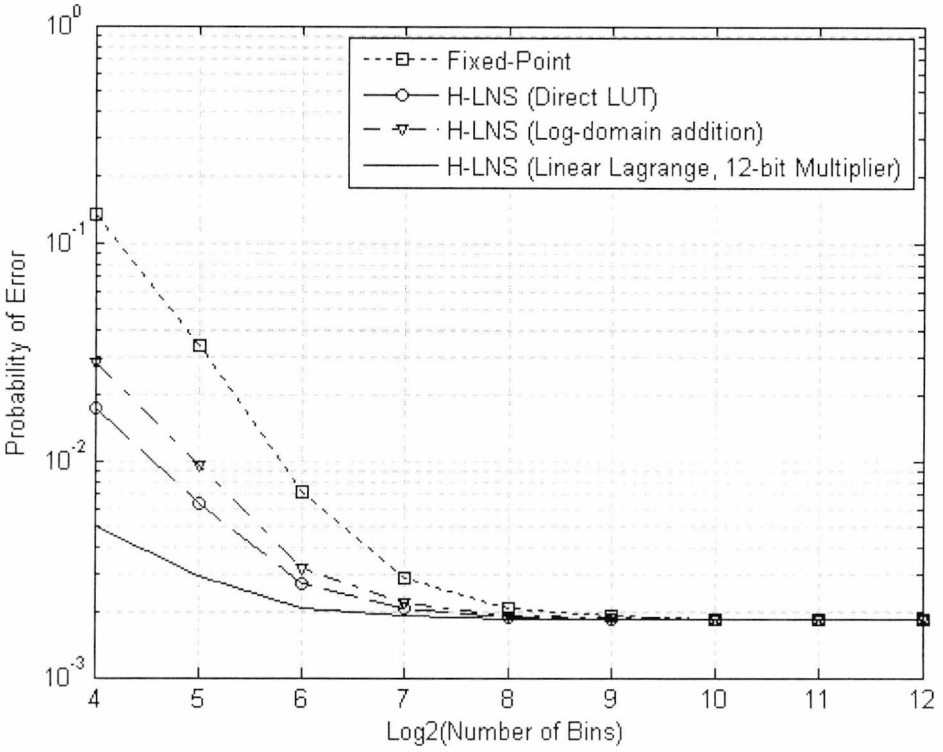

Fig 5.46 Performance of the adaptive equalizer Vs numeric precision.

In summary, all logarithmic schemes (not including the approximate adaptation algorithms) outperformed the fixed-point uniform implementation. This is relevant since (apart from the Linear-Lagrange codec) the H-LNS filter implementation yields superior product computations over the fixed-point binary case, but does not necessitate hardware level multiplication where only basic addition units and small amounts of memory are required to compute the filter response. The important contributions of this section include:

I) H-LNS arithmetic yields superior filters to the corresponding uniform fixed-point binary arithmetic.

II) H-LNS arithmetic employing Linear-Lagrange codecs with 12-bit multiplier does not offer any significant performance advantage over the direct LUT codec for numeric precision > 9 bits.

III) The NLMS update term does not require the full H-LNS solution yielding three LUT conversions. Results show that logarithmic domain addition employing a simple LUT for calculating the adjustment function results in filters with similar numeric accuracy. The performance disadvantage of log-domain addition is not noticeable for numeric precision > 9 bits.

IV) The approximate NLMS update terms employing heavily trucated regressor offer reasonable performance particularly for the SER-LMS case. The case of initiating a proposal based on the SER-LMS for adaptive equalization is a topic requiring review since theoretical results would be required to fully appraise this technique. Initial investigations into this simple technique are promising. In future it is planned to expatiate upon the analysis of this filter applying theoretical modelling.

V) The H-LNS implementation of the adaptive equalizer does not require extremely large resolution. The results show that 9 to 12 bit address look up tables yield no significant degradation compared to the floating-point implementation. Hence a proposal that can be generated based on the observational models is that an adaptive channel equalizer built with 9-bit H-LNS architecture is sufficient.

CHAPTER 6
CONCLUSIONS AND FUTURE WORK

6.1 CONCLUSIONS

This thesis investigated the subject of receiver diversity for the WCDMA downlink and the effect of finite precision logarithmic coding for the Rake and LMMSE Channel equalizer. The performance of dual antenna array receivers with adaptive diversity combining and temporal-spatial equalization was analyzed for a variety of channel and interference conditions. Results indicate that significant performance improvement could be obtained with only marginally increased computational complexity. The application of adaptive channel equalizers (a well researched subject for SISO channels) in the context of downlink diversity yielded highly promising performance and is a viable technical alternative to the rake receiver. The investigations into the numeric coding aspect found that 8-bits numeric precision applying the H-LNS gave perfectly acceptable performance for the Rake receiver. The LMMSE Channel equalizer applying adaptive filtering was found to give perfectly adequate performance for 9-bits numeric precision with the only moderately increased complexity (over the most simple signed-regressor adaptive filter) of entirely logarithmic domain addition for the recursive element of the filter. It was found in all cases of direct equivalence that the logarithmic coding implementations outperformed the uniform fixed-point counterpart. It may then be concluded that logarithmic domain filter computations are affordable and superior to utilizing the standard binary arithmetic units employed currently in most commercial programmable logic devices and DSP chips.

The chapters are summarized in terms of technical content and important results obtained:

Chapter 1: This chapter highlights relevant background information. In conclusion to the investigation, the many optimum multi-user demodulation techniques are not transferable to the WCDMA downlink. This immediately constrains the downlink to only a few logical algorithms – namely transmitter diversity, adaptive antennas, equalization, and temporal-spatial filtering algorithms.

Chapter 2: The WCDMA downlink models were presented. The performance of dual antenna receivers composed of integrate-dump estimators was investigated. The research considered maximum ratio combining solutions and adaptive combining solutions for interference scenarios. It was found that employing the MRC technique for two antennas yielded superior performance over the single antenna case for mutually uncorrelated diversity branches, where the performance metric decreased significantly when antennas were placed closer together. However, the case of interference suppression remained unsolved. The case was extended for two antenna beamforming algorithms that attempted to obtain sufficient statistics to mutually decorrelate interference according to the spatial signatures of the incident signals. It was found that some improvement was yielded by the MMSE and MSINR optimizations, but this improvement was marginal due to the low number of sensors and sheer number of paths incident to the array. Adaptive solutions found that both NLMS and RLS schemes offered reasonable performance. The RLS adaptation scheme was clearly superior to the NLMS, but came with greater computational cost. The blind adaptive SINR algorithm was found to offer fairly impaired performance, and hence it's implemental aspect is not generally considered further in the thesis. Proposals by other researchers, i.e. [Kwon1999, Choi2000, Choi et. al. 2002], for similar algorithms concluded significant performance gain for large number of sensors as in the uplink. The blind MSINR beamformer appears to be more practical in terms of performance in this type of scenario with greater degrees of freedom. In conclusion, adaptive beamforming appears quite promising, but limitations incurred by interference are not removed, and the overall detection problem essentially remained unresolved up to this point.

Chapter 3: This chapter investigated the performance of the Rake receiver considering the effect of delay acquisition and channel estimation on the device. It was found that delay acquisition applying correlation, subspace, and statistical techniques generally yielded sufficient performance in the WCDMA downlink provided the coding was short and cyclic. Long codes only generated the correlation technique; hence current WCDMA standards will not generally support the subspace and minimum variance technique. The subspace technique lacked the full rank assumptions to fully apply interference resistant delay acquisition for large numbers of users, despite have huge relevance and optimality in traditional antenna array and multi-user delay acquisition. An alternative channel estimation scheme was presented using an adaptive filter and found to improve the accuracy of phase acquisition for the downlink. This is based on the presumption that the base-station specific scrambling code exhibited cyclostationary of the order of the symbol period. Since this is not generally the case for the current UMTS downlink, its aspect is more powerful for uplink

receivers applying the LMMSE Rake receiver, for instance. The UMTS supports both long and short codes for the downlink, although the general consensus is that long codes are used on the downlink, and short codes for the uplink.

Chapter 4: This chapter investigated many aspects of diversity for the WCDMA downlink. Of the noteworthy techniques, temporal-spatial rake receivers with adaptive and maximum ratio diversity combining were initially investigated. The results obtained using simulation and analytical techniques indicated significantly enhanced performance over the classical rake receiver and dual antenna combiner. A performance improvement was noted utilizing adaptive combining over hybrid combining, although the margin of improvement was not overly significant in Vehicular A channels. The RLS adaptation algorithm was implemented since rake level finger combining does not yield large array structures (i.e. the inputs to the adaptive combiner were bivariate and not multivariate) – hence it is preferable to trade-off performance for complexity enhancement in this case. The next step in the receiver design considered the equalization methodology with the interference whitening, MMSE equalizer, and Zero Forcing channel equalizers integrated into the antenna array (forming a broadband beamformer). Research results confirmed the performance of perfect and imperfect channel equalizers (formed from noisy channel estimates) and compared the resulting detectors with the temporal-spatial diversity combiner. It was found that the equalization methodology even with relatively inaccurate channel estimates significantly outperformed the diversity combiner. The case for adaptive equalization using the NLMS algorithm (where the RLS algorithm yielded too high a complexity to be considered viable) found that acceptable performance could be obtained for fairly low system loading. When the number of adjacent users became too large, the performance gain over the standard 2D combiner was marginal.

Chapter 5: This chapter expanded the detection problem to the more realistic case where receiver would be integrated with a the numeric constraints of a digital signal processor. For low cost, low power solutions, the computer arithmetic employed would likely be low precision fixed or floating-point. Hence quantization and multiplication errors will incur product-accumulation numeric round-off errors for digital filtering algorithms. The purpose of this section was to investigate the effect of computer arithmetic on the performance of the rake receiver and adaptive LMMSE channel equalizer. To overcome the problem of applying fixed hardware multipliers, the hybrid logarithmic number system was proposed to incur the computational burden of performing the filter inner products. The results show that the Hybrid logarithmic number system gave superior multiplier round-off error performance since product are replaced by simple full adders built with very simple logic. The implemental aspects for various codecs were explored since some logarithmic conversion

units are quite significantly simpler than others. It was found that the Linear-Lagrange codec offered potentially the best performance with the cost of a fairly high precision multiplier. This approach would be more suited to programmable devices with existing on-board multiplier and relatively low read only memory. The case of the adaptive channel equalizer yielded three possible implementations utilizing logarithmic codecs. It was argued that employing successive codec operations for computing the filter update yielded too high a complexity – i.e. this part of the filter was computationally cumbersome. Further arguments were generated for the case of the filter coefficient update unit implemented with heavily quantized regressor allowing a fully multiplierless update in the linear domain with only Lin – Log conversion for converting the weight into a logarithmic quantity for the filter Multiply-Accumulation operations. However, this technique came at a cost to performance, although the signed-exponent-regressor LMS did not yield significant degradation. Finally, a moderately complex technique was investigated applying fully logarithmic-domain addition. The additional component is a look up table and some additional logic circuitry for calculating the sign and zero flag bits. The results indicate near identical performance to the most complicated logarithmic implementation, and for logic devices employing reasonable amounts of memory, the additional cost appears to be affordable.

6.2 Future Work

6.2.1 Future Work related to WCDMA

The work considered in this thesis primarily investigated the performance of diversity receivers for uncoded transmissions. The information contained in the dedicated data and control channels will be coded either applying rate 1/2 or 1/3 convolutional or turbo codes. The rationale behind investigating uncoded transmissions was the difficulty of estimating the probability of error using fairly standard Monte Carlo techniques – this difficulty was only due to the unreasonable simulation times. The work in the initial development of the WCDMA simulation models applied channel and space-time coding (such as the Alamouti scheme) but results for even the rake receiver with moderate interference levels naturally incurred relatively low probability of errors. This automatically made simulation times span several days/weeks. This is an aspect for further consideration – particularly for integrating dual antenna beamforming receivers when the transmitting base station incurs space – time codes and/or channel coding schemes.

The problem of detection and finite precision numeric coding in the WCDMA downlink applying diversity is largely solved. However a few absolutely crucial issues pertain not

only for this thesis, but also for the scope and current state of affairs in WCDMA downlink detection: .

i) Equalizers applying the full MMSE optimization in time or frequency domains are problematic since accurate channel and timing knowledge is required by the receiver to initiate a useful diversity algorithm. Clearly, errors in estimated channel impulse responses and timing will gravely affect the receiver's performance. Adaptive schemes are useful but also susceptible to convergence problems in rapidly varying channels with high system loading (creating higher interference floor). Alternative blind solutions can be tested for the downlink – such as the adaptive MOE receiver or the maximum SINR algorithm. The application of these algorithms for broadband beamforming remains uninvestigated at the time of the thesis conception.

ii) Diversity combining solutions applied simplistic channel models that ignored the aspect of real antennas – i.e. Patch, Helix, Microstrip, and Dipole antennas are not isotropic devices hence the half a wavelength antenna separation can no longer be assumed to offer two diversity channels that are somewhat uncorrelated. Furthermore, the channel model did not consider the narrow angle of arrival (low angular spread) possibility where diversity gain would be compromised in such a scenario.

An interesting development in the author's research, not mentioned in this thesis, was the application of a near-optimum integer constrained maximum likelihood estimator [Duel-Hallen1995] for the downlink utilizing only knowledge of the timing and pulse shaping spectra. This allowed interference to be projected away from the desired signal at chip rather than symbol level with the bonus that channel estimation could occur post-filtering for increased accuracy. However a few problems were encountered in performance. The first issue is the filter gave near equivalent asymptotic MMSE equalizer performance provided the channel impulse response yielded lags that were spaced in proportion to approximately half a chip period. For channels where even one delay component aligned close to the chip boundary, the receiver became unstable and basically useless. Furthermore, the receiver generally did not cope well with high levels of uncorrelated additive noise, where the resulting output noise often increased by up to 10dB. The problem identified was that of the pulse shaping and group delay of the transmitter filter, where altering the pulse shapes and this group delay could significantly enhance performance even when the channel delay components aligned approximately to the chip boundary. The only criterion for successful chip acquisition and estimation was that the multipath delay spread did not reflect perfectly onto the chip boundary (which is the transient where the chip changes from one symbol to

another). However, the issue with this technique applying different chip pulses is that the adjacent channel leakage even with perfect transmit amplifiers did not conform to the UMTS downlink spectral emissions mask. Hence this technique would not be conformant with the specifications supplied by the 3GPP. Work is ongoing on this technique where a trade-off or rather "halfway house" is initiated where perfect decorrelation is compensated for useable filters given the limitations of the 3GPP proposals.

The author of this thesis initially conducted a large survey of multi-user detection techniques and found that for networks with Macrodiversity, some multi-user detection problems are transferable to the WCDMA downlink scenario even with long non-cyclic spreading signatures. One such detector offering near optimum performance is the multi-user 2D Rake receiver [Brunner2000] where all channel diversities, correlations, and spatial signatures can be used to eradicate multi-user interference at Macro and Micro scale. The author currently is supervising an MSc student studying the aspect of WCDMA downlink diversity combining for Macrodiversity networks applying radio over fibre. It is hopeful that this project and proposals can generate enough interest to receive recognition and possible expansions for future research at Micro, Macro, and system level.

6.2.2 FUTURE WORK RELATED TO WIRELESS MOBILE

In this thesis, the tasks undertaken no more than scratch the surface of the in-depth scope of estimation and detection in wireless mobile. This thesis only investigated the prerogative that is Downlink WCDMA detection with simplistic diversity algorithms utilizing dual antenna arrays. However, future mobile systems, concentrating on delivering broadband information (along with high quality voice) and interactive real time services are open to a plethora of technical proposals. Several open-ended criterion exist:

1) Multiple access and modulation techniques for consideration in the forth generation: Current proposals include Multi-Carrier CDMA, OFDM, OF-CDMA, and hybrids of these technologies with traditional TDM.
2) Diversity Transmission and coding: MIMO appears to be the most consistent technology for enabling high quality information to be transmitted over fading channels. The question mark occurs in frequency selective channels. This has been largely addressed considering an equalization/projection filtering methodology for single and multi-user terminals.

3) Narrow-band multi-carrier overlay techniques are efficient for implementing PCS systems within the same spectral band as other services such as Blue tooth, GSM etc. The performance of such systems employing frequency hopping (as an example of diversity) is constrained – i.e. techniques such as equalization and linear Multi-user detection are difficult to implement. Accurate timing acquisition is also very difficult to implement in multi-carrier CDMA and is a current bottleneck.
4) Coding techniques: The use of Turbo or LDPC codes can deliver near optimum performance in a variety of channels – particularly when used in conjunction with equalization / linear multi-user detection scenarios. The problem with channel coding occurs for high information rate bottlenecks where insertion of parity bits (increasing the effective data rate) and de-interleaving / decoding algorithms generally require large amounts of data to yield sufficient statistics for optimum decoding. Clearly, with the proposals circulating in conference proceedings and journals as to the achievable data rates in future (approaching the Radio over Fibre rates), a large burden will be placed on the receivers in terms of processing power.

The scope for estimation and detection is basically the same in all communication systems, where the information limits are essentially decided by the noise and interference within the system. Overcome noise (where interference will appear as inclusive noise whether correlated / uncorrelated), and the information limits will be boundless. However, completely eradicating noise is, and never has been, a method that has ever been practically obtainable. The author of this thesis has every intention of being involved in this subject, which in large part is a unified topic across all areas of communication, image processing, medical / biometrical instrumentation, and many other scientific fields. The author has actively researched the topic of estimation in the presence of noise and has some extremely novel ideas relating to this interesting topic – most of which are completely in its infancy.

REFERENCES

3rd Generation Partnership Project (2001); Technical Specification Group Radio Access Network UTRA (BS) FDD; radio transmission and reception (3G TS 25.104 version 5.0.0). Tech. rep. 3rd Generation Partnership Project (3GPP).

3rd Generation Partnership Project (2002); Technical Specification Group Radio Access Network Spreading and modulation (FDD) (3G TS 25.213 version 5.0.0). Tech. rep. 3rd Generation Partnership Project (3GPP).

Adachi, F., Sawahashi, M. and Suda, H. (1998). "Wideband DS-CDMA for Next-Generation Mobile Communications Systems", *IEEE Communications Magazine*, Sept, pp. 56-69.

Affes, S. and Mermelstein, P. (1998). "A New Receiver Structure for Asynchronous CDMA: STAR- The Spatio-Temporal Array-Receiver," *IEEE Journal on Selected Areas in Communications*, Vol. 16, No. 8, pp. 1411-1422, October.

Alamouti, S. (1998). "A simple transmit diversity technique for wireless communications", *IEEE Journal on Selected Areas in Communications,* Vol. 16, No. 8: pp. 1451-1458.

Al-Dhahir, N. and Cioffi, J. M. (1995). "MMSE Decision-Feedback Equalizers: Finite-Length Results", *IEEE Transactions on Information Theory*, Vol. 41, No. 4, pp. 961-975.

Alexander, P. D. and Rasmussen, L. K. (1998). "On the Windowed Cholesky Factorization of the Time-Varying Asynchronous CDMA Channel", *IEEE Transactions on Communications*, Vol. 46, No. 6, pp.735-737.

Arnold, M. G. (2001). "Design of a Faithful LNS Interpolator", *Euromicro Digital System Design, Warsaw,* pp. 336-344.

Arnold, M., Bailey, T. and Cowles, J. (2003). "Error Analysis of the Kmetz/Maenner Algorithm", *Journal of VLSI Signal Processing*, pp. 33, 37-53.

Arnold, M., Bailey, T. and Cowles, J. (1992). "Comments on An Architecture for Addition and Subtraction of Long Word Length Numbers in the Logarithmic Number System", *IEEE Transactions on Computers,* Vol. 41, No. 6, pp. 786-787.

Arnold, M. G. and Winkel, M. D. (2001). "A Single-Multiplier Quadratic Interpolator for LNS Arithmetic", *International Conference on Computer Design*, pp. 178-183.

Aulin, T. (1979). "A Modified Model for the fading signal at a mobile radio channel", *IEEE Transactions on Vehicular Technology*, Vol. 28, No. 3, pp. 182-203.

Balaban, P. and J. Salz, J. (1992). "Optimum Diversity Combining and Equalization in Digital Data Transmission with Applications to Cellular Mobile Radio- Part I: Theoretical Considerations", *IEEE Transactions on Communications*, Vol. 40, No. 5, pp. 885-907.

Barbosa, A. and Miller, S. (1998). "Adaptive Detection of DS/CDMA signals in fading channels", *IEEE Transactions in Communications*, Vol. 46, No. 1, pp. 115-124.

Barhumi, I., Leus, G. and Moonen, M. (2003). "Time-varying FIR equalization of Doubly-Selective Channels", *Proceedings of the IEEE International Conference on Communications.*

Barlow, J. L. and Bareiss, E. H. (1985). "On Roundoff Error Distributions in Floating Point and Logarithmic Arithmetic', *Computing*, Vol. 34, pp. 325-347.

Barnes, C. W., Tran, B. N. and Leung, S. H. (1985). "On the statistics of fixed-point roundoff error", *IEEE Transactions on Acoustics, Speech, and Signal Processing*, Vol. ASSP-33, No. 3, pp. 595-606.

Bastug, A. and Slock, D. (2005). "Downlink WCDMA receivers based on combined chip and symbol level equalization", *European Transactions on Telecommunications*, Vol. 16, pp. 51-63.

Bauer, M., Schefczik, P., Soellner, M., and Speltacker, W. (2003). "Evolution of the UTRAN architecture", *4th International Conference on 3G Mobile Communication Technologies*, pp. 244 - 248.

Belfiore, d. (1979). "Decision Feedback Equalization", Proceedings of the IEEE, Vol. 67, No. 8, pp. 1143-1156.

Bello, P.A. (1963). "Characterization of Randomly Time-Variant Linear Channels", *IEEE Transactions on Communications Systems*, Dec, pp. 360-393.

Bennett, W. R. (1948). "Spectra of quantized signals", Bell System Technical Journal, Vol.27, pp. 446-472.

Bensley, S. and Aazhang B. (1996). "Maximum-likelihood synchronization of a single user for codedivision multiple-access communication systems", *IEEE Transactions on Communications*, Vol. 44, No. 6, pp. 302-319.

Bensley, S. and Aazhang B. (1996). "Subspace-Based Channel Estimation for Code Division Multiple Access Communication Systems", *IEEE Transactions on Communications*, Vol. 44, No. 8, pp. 1009-1019.

Bernstein, V. and Haimouch, A. M. (1996). "Space-time optimum combining for CDMA Communications", *Wireless Personal Communications*, Vol. 3, No. 1-2, pp. 73-89.

Berrou, C., Glavieux, A. and Thitimajshima, P. (1993). "Near Shannon Limit Error-Correcting Coding and Decoding: Turbo Codes, Vol. 1, IEEE International Conference on Communications, pp. 1064-1070.

Bertoni, H. L. (2000). "Radio Propagation for Modern Wireless Systems", New Jersey: Prentice Hall.

Blaunstein, N. and Bach Andersen, J. (2002). "Multipath phenomena in cellular networks", Artech House Publishers.

Bottomley, G. (1993). "Optimizing the RAKE receiver for the CDMA downlink", *Proceedings of the IEEE Vehicular Technology Conference (VTC)*, pp. 742-745.

Bottomley, G. E. and Wang, Y. E. (2000). "A Generalized Rake Receiver for Interference Suppression", IEEE Journal on Selected Areas in Communications, Vol. 18, No. 8, pp. 1536-1545.

Bravo, A. (1997). "Limited linear cancellation of multiuser interference in DS/CDMA asynchronous system", *IEEE Transactions on Communications*, Vol. 45, No. 11, pp. 1435-1443.

Brennan, D. (1959). "Linear diversity combining techniques", *Proceedings of IRE*, Vol. 47, No. 47, pp. 1075-1102.

Brent, R. (1973). "On the Precision Attainable with Various Floating-Point Number Systems", *IEEE Transactions on Computers*, pp. 601-607.

Brunner, C., Hammerschmidt, J. S. and Nossek, J. A. (2000). "Downlink eigenbeamforming in WCDMA", *Proceedings of the European Wireless Conference*, pp. 195-200.

Brunner, C., Hammerschmidt, J. S., Seeger, A. and Nossek, J. A. (2000). "Space-time eigenrake and downlink eigenbeamformer: Exploiting long-term and short-term channel properties in WCDMA", *Proceedings of the Global Telecommunications Conference (GLOBECOM)*, pp. 138-142.

Buehrer, R.M., Kaul, A., et al. (1996). "Analysis of DS-CDMA parallel interference cancellation with phase and timing errors", *IEEE Journal on Selected Areas in Communications.*, Vol. 14, No. 8, pp. 1522-1535.

Buzzi, S. and Poor, H. V. (2003). "On Parameter Estimation in Long-Code DS/CDMA Systems: Cramer-Rao Bounds and Least-Squares Algorithms", *IEEE Transactions on Signal Processing*, Vol. 51, No. 2, pp. 545-559.

Caraiscos, C. and Liu, B. (1984). "A Roundoff Error Analysis of the LMS Adaptive Algorithm", *IEEE Transactions on Acoustics, Speech and Signal Processing*", Vol. ASSP-32, No. 1, pp. 34-41.

Capon, J. (1969). "High resolution frequency-wave number spectrum analysis", *Proceedings of the IEEE*, Vol. 57, No. 8, pp. 1408-1418.

Cavanagh, J. F. (1984). "Digital Computer Arithmetic: Design and Implementation", McGraw-Hill Book Company, New York.

Chan, N.L. (1994). "Multipath Propogation Effects on a CDMA Cellular System", *IEEE Transactions on Vehicular Technology*, Vol. 43, No. 4, November, pp. 848-855.

Chang, P. S. and Wilson, Jr, A. N. (1995). "A Roundoff Error Analysis of the Normalized LMS Algorithm", *Proceedings of ASILOMAR Conference on Signals, Systems and Computers*, Vol. 2, pp. 1337-1341.

Cheng, J. and Beaulieu N. C. "Accurate DS-CDMA Bit-Error Probability Calculation in Rayleigh Fading", *IEEE Transactions on Wireless Communications*, Vol. 1, No. 1, pp. 3-14, 2002.

Cheun, K. (1997). "Performance of Direct-Sequence Spread-Sprectrum RAKE Receivers with Random Spreading Sequences", *IEEE Transactions on Communications*, Vol. 45, No. 9, pp. 1130-1143.

Chi, C. Y., Feng, C. C., Chen, C. H. and Chen, C. Y. (2006). "Blind Equalization and system identification: Batch Processing Algorithms, Performance and Applications", Springer.

Choi. J. (2004). "Receivers with Chip-Level Decision Feedback Equalizer for CDMA Downlink Channels", IEEE Transactions on Wireless Communications, Vol. 3, No. 1, pp. 300-314.

Choi, S., Choi, J., Im, H. and Choi, B, (2002). "A Novel Adaptive Beamforming Algorithm for Antenna Array CDMA Systems with Strong Interferers", *IEEE Transactions on Vehicular Technology*, Vol. 51, No. 5, pp. 808-816.

Choi, S. and Shim, D. (2000). "A novel adaptive beamforming algorithm for a smart antenna system in a CDMA mobile communication environment", *IEEE Transactions on Vehicular Technology*, Vol. 49, No. 5, pp. 1793 -1806.

Chowdhury, S., Zoltowski, M. and Goldstein, S. (2002). "Reduced-rank chip-level MMSE equalization for the 3GCDMA forward link with code-multiplexed pilot", *EURASIP Journal on Applied Signal Processing*, Vol. 8, pp. 757-770.

Chowdhury, S., Zoltowski, M. (2000). "Combined MMSE equalization and multi-user detection for high-speed CDMA forward link with sparse multipath channels", *Proceedings of the Asilomar Conference on Signals, Systems and Computers*, Vol. 1, pp. 389-393.

Claasen, T. M. and Mecklenbrauker, W. G. (1981). "Comparison of the Convergence of Two Algorithms for Adaptive FIR Digital Filters", *IEEE Transactions on Acoustics, Speech and Signal Processing*, Vol. 29, No. 3, pp. 670-678.

Clarke, R. H. (1968). "A Statistical Theory of Mobile-Radio Reception," *The Bell System Technical Journal*, Vol. 47, No. 6, pp. 957-1000.

Colburn, J. S., Rahmat-Samii, Y., Jensen, M. A. and Pottie, G. J. (1998). "Evaluation of Personal Communications Dual-Antenna Handset Diversity Performance", *IEEE Transactions on Vehicular Technology*, Vol. 47, No. 3, pp. 737-746.

Coleman, J. N. (1995). "Simplification of Table Structure in Logarithmic Arithmetic", *Electronic Letters*, Vol. 31, No. 22, pp. 1905-1906.

Coleman, J. N., Chester, E. I., Softley, C. I. and Kadlec, J. (2000). "Arithmetic on the European Logarithmic Microprocessor", *IEEE Transactions on Computers*, Vol. 49, No. 7, pp. 702-715.

Combet, M., Van Zonneveld, H. and Verbeek, L. (1965). "Computation of the Base Two Logarithm of Binary Numbers", *IEEE Transactions on Electronic Computers*, Vol. FE-11, No. 6, pp. 863-865.

Dahlhaus, D. and Jarosch, A., et al. (1997). "Joint Demodulation in DS/CDMA Systems Exploiting the Space and Time Diversity of the Mobile Radio Channel", *Proceedings of the 8th International Symposium on Personal, Indoor and Mobile Radio Communications*, Vol. 1, pp. 47-52.

Dahlman, E., Bemming, P. and Knutsson, J. (1998). "WCDMA- The Radio Interface for Future Mobile Multimedia Communications", *IEEE Transactions on Vehicular Technology*, Vol. 47, No. 4, pp. 1105-1117.

Dahlman, E., Gudmundson, B. and Nilsson, M. (1998). "UMTS/IMT-2000 Based on Wideband CDMA", *IEEE Communications Magazine*, Sept 1998, pp. 70-80.

Darwood, P., Alexander, P. and Oppermann, I. (2001). "LMMSE chip equalisation for 3GPP WCDMA downlink receivers with channel coding", *Proceedings of the IEEE International Conference on Communications (ICC)*, Vol. 5, pp. 1421-1425.

Dasgupta, S. and Johnson, C. R. (1986). "Some comments on the behavior of sign-sign adaptive identifiers", *Systems and Control Letters*, pp. 75-82.

Dell'Anna, M. and Aghvami, A. H. (1999). "Performance of Optimum and Suboptimum Combining at the Antenna Array of a W-CDMA System," *IEEE Journal of Selected Areas in Communications*, Vol. 17, No. 12, pp. 2123-2137, December.

Derryberry, R.T., Gray, S.D., and Ionescu, D.M. (2002). "Transmit Diversity in 3G CDMA Systems", *IEEE Communications Magazine*, Apr, pp. 68-75.

Dietrich, C. B., Dietze, K., Nealy, J. R. and Stutzman, W. L. (2001). "Spatial, Polarization, and Pattern Diversity for Wireless Handheld Terminals," *IEEE Transactions on Antennas and Propagation*, Vol. 49, No. 9, pp. 1271-1281.

Divsalar, D., Simon, M. K. and Raphaeli, D. (1998). "Improved Parallel Interference Cancellation for CDMA", *IEEE Transactions on Communications*, Vol. 46, No. 2, pp. 570-574.

Dolmans, G. and Leyten, L. (1999). "Performance Study of an Adaptive Dual Antenna Handset for Indoor Communications," *IEE Proceedings of Microwaves, Antennas and Propagation*, Vol. 146, No. 2, pp. 138-1444.

Duel-Hallen, A. (1993). "Decorrelating decision-feedback multiuser detector for synchronous CDMA", *IEEE Transactions on Communications*, Vol. 41, No. 2, pp. 285-290.

Duel-Hallen, A. (1995). "A family of multiuser decision-feedback detectors for asynchronous code-division multiple-access channels", *IEEE Transactions on Communications* Vol. 43, No. 2/3/4, pp. 421-434.

Duel-Hallen, A., Holtzman, J. and Zvonar, Z. (1995). "Multiuser detection for CDMA systems", *IEEE Personal Communications,* Vol. 2, No. 2, pp. 46-58.

El-Eraki, S. M., Batchelor, J. C., and Langley, R. J. (2003). "FM signal multipath reduction using multiplier-less digital adaptive filters", *Microwave and Optical Technology Letters*, Vol. 38, pp. 1-3.

El-Tarhuni, M. G. and Sheikh; A. U. H. (1998). "Performance Analysis for an Adaptive Filter Code-Tracking Technique in Direct-Sequence Spread-Spectrum Systems", *IEEE Transactions on Communications*, Vol. 46, No. 8, pp. 1058-1064.

Eng, T., Kong, N. and Milstein, L. B. (1996). "Comparison of Diversity Combining Techniques for Rayleigh-Fading Channels," *IEEE Transactions on Communications*, Vol. 44, No. 9, pp. 1117-1129, September.

Eweda, E. (1990). "Analysis and Design of a Signed Regressor LMS Algorithm for Stationary and Nonstationary Adaptive Filtering with Correlated Gaussian Data," IEEE Transactions on Circuits and Systems, Vol. 37, No. 11, pp. 1367-1374.

Falconer, D., Ariyavistakul, S. L. and Benjamin-Seeyar, A. (2002). Edison; B. "Frequency Domain Equalization for Single Carrier Broadband Wireless Systems", *IEEE Communications Magazine*, pp. 58-66.

Fan, H. H. and Li, X. (2000). "Linear prediction approach for joint blind equalization and blind multiuser detection in CDMA systems", *IEEE Transactions on Signal Processing*, Vol. 48, No. 11, pp. 3134-3145.

Fantacci, R. and Maranissi, D. (2005). "A Low Complexity Pilot Aided Channel Estimation Method for WCDMA Communication Systems", *IEEE Transactions on Vehicular Technology*, Vol. 54, No. 5, pp. 1739-1746.

Fawer, U. and Aazhand, B. (1995). "A Multiuser receiver for code-division multiple-access communications over multipath channel", *IEEE Transactions on Communications*, Vol. 43, No. 2/3/4, pp. 1556-1565.

Flikkema, P.A. (1997). "Spread-Spectrum Techniques for Wireless Communication", *IEEE Signal Processing Magazine*, May, pp. 26-35.

Forney, G.D. (1972). "Maximum-likelihood sequence estimation of digital sequences in the presence of intersymbol interference", *IEEE Transactions on Information Theory*, Vol. 18, No.3.

Forney, G. D. (1973). "The Viterbi algorithm", *Proceedings of the IEEE*, Vol. 61, No. 3, pp. 268-278.

Frank, C. D. and Visotsky, E. (1998). "Adaptive interference suppression for direct-sequence CDMA systems with long spreading codes". *Proceedings of the Allerton Conference on Communications, Control, and Computing*, pp. 411-420.

Frank, C. D., Visotsky, E. and Madhow, U. (2002). "Adaptive interference suppression for the downlink of a direct sequence CDMA system with long spreading sequences", special issue on Signal Processing for Wireless Communications: Algorithms, Performance, and Architecture, *Journal of VLSI Signal Processing*, vol. 30, no. 1, pp. 273-291.

Fukasawa, A., Sato, T. and Takizawa, Y. (1996). "Wideband CDMA System for Personal Radio Communications", *IEEE Communications Magazine*, pp. 116-123.

Giannakis, G., Tepedelenlioglu, C. and Liu, H. (1997). "Adaptive blind equalization of time-varying channels", *Proceedings IEEE International Conference on Acoustics, Speech and Signal Processing (ICA SSP)*, pp. 4033-4036.

Ghauri, I. and Slock, D.M. (1998). "Linear receivers for the DS-CDMA downlink exploiting orthogonality of spreading sequences", *Proceedings of the Asilomar Conference on Signals, Systems and Computers*, pp. 650-654.

Ghosh, M. (2001). "Adaptive chip-equalizers for synchronous DS-CDMA systems with pilot sequences", *Proceedings of the IEEE Global Telecommunications Conference*, Vol. 6, pp. 3385-3389.

Gilhousen, K.S., Jacobs, I.M. and Padovani, R. (1991). "On The Capacity of a Cellular CDMA System", *IEEE Transaction on Vehicular Technology*, Vol. 40, No. 2, pp. 303-311.

Glance, B. and Greenstein, L.J. (1983). "Frequency-Selective Fading Effects in Digital Mobile Radio with Diversity Combining", *IEEE Transactions on Communications*, Vol. 31, No. 9, pp. 1085-1094.

Glisic, S.G. and Vucetic, B. (1997). "Spread spectrum CDMA systems for wireless communications", Artech House, London, UK.

Godara, L.C. (1997). "Applications of Antenna Arrays to Mobile Communications, Part I: Performance Improvement, Feasibility, and System Considerations", *Proceedings of the IEEE*, Vol. 85, No. 7, pp. 1031-1360.

Godara, L. C. (1997). "Applications of Antenna Arrays to Mobile Communications, Part II: Beam- Forming and Direction-of-Arrival Considerations," *Proceedings of the IEEE*, Vol. 85, No. 8, pp. 1195-1245.

Gooch, R. and Lundell, J. (1986). "The CM Array: An Adaptive Beamformer for Constant Modulus Signals," *Proceedings of the IEEE ICASSP*, pp. 2523-2526.

Griffiths, L. J. (1969). "A simple adaptive algorithm for real-time processing in antenna arrays", *Proceedings of the IEEE*, Vol. 57, No. 10, pp. 1696-1704.

Hall, E. L., Lynch, D. D. and Dwyer, S. J. (1970). "Generation of Products and Quotients Using Approximate Binary Logarithms for Digital Filtering Applications", *IEEE Transactions on Computers*, Vol. C-19, No. 2, pp. 97-104.

Hamid, K. and Viberg, M. (1996). "Two Decades of Array Signal Processing Research", *IEEE Signal Processing Magazine*, pp. 67-94.

Hanly, S.V. and Tse, D.N. (1999). "Power Control and Capacity of Spread Spectrum Wireless Networks", *Automatica*, Vol. 35, pp. 1987-2012.

Hanzo, L., Liew, T., and Yeap, B. (2002). "Turbo Coding, Turbo Equalisation and Space-Time Coding for Transmission over Fading Channels", John Wiley and Sons.

Hara, S. and Prasad, R. (1997). "Overview of Multicarrier CDMA", *IEEE Communications Magazine*, Dec, pp. 126-133.

Haykin, S. (1996). "Adaptive Filter Theory", Prentice Hall, Upper Saddle River, USA, 3rd Edition.

Heikkilä, M. (2001). "A novel blind adaptive algorithm for channel equalization in WCDMA downlink", *Proceedings of the IEEE International Symposium on Personal, Indoor, and Mobile Radio Communications (PIMRC)*, Vol. 1, pp. 41-45.

Heikkila, M. J., Komulainen, P. and Lilleberg, J. (1999), "Interference suppression in CDMA downlink through adaptive channel equalization", *Proceedings of the IEEE Vehicular Technology Conference (VTC)*, Vol. 2, pp. 978-982.

Hooli, K., Juntti, M., Heikkilä, M. J., Komulainen, P., Latva-aho, M. and Lilleberg; J. (2002). "Chip-Level Channel Equalization in WCDMA Downlink", *Eurasip Journal on Applied Signal Processing*, Vol. 8; pp. 757-770.

Hooli, K., Latva-aho, M. and Juntti, M. (1999). "Comparison of LMMSE receivers in WCDMA downlink", *Procedings of the . ACTS Mobile Communications Summit*, Vol. 2, pp. 649-654.

Hooli, K., Latva-aho, M. and Juntti, M. (2001). "Performance Evaluation of Adaptive Chip-Level Channel Equalizers in WCDMA Downlink", *Proceedings of the IEEE International Conference on Communications (ICC)*, Vol. 6, pp. 1974-1979.

Hooli, K., Latva-aho, M. and Juntti M. (1999). "Multiple access interference suppression with linear chip equalizers in WCDMA downlink receivers", *Proceedings of the IEEE Global Telecommunications Conference (GLOBECOM)*, Vol. 1, pp. 467-471.

Hong, S. C., Choi, I. K., Jung, H., Kim, S. R., and Lee, Y. H. (2004). " Constrained MMSE Receivers for CDMA Systems in Frequency-Selective Fading Channels", IEEE Transactions on Wireless Communications, Vol. 3, No. 5.

Honig, M.L., and Madhow, U. (1994). "MMSE Interference Suppression for Direct-Sequence Spread-Spectrum CDMA", *IEEE Transactions on Communications*, Vol. 42, No. 12, pp. 3178 - 3188.

Honig, M.L., Madhow, U., and Verdu, S. (1995). "Blind adaptive multiuser detection", *IEEE Transactions on Information Theory*, vol. 41, no. 4, pp. 944-960.

Huang, K., Adachi, F. and Chew, H. (2005). "A More Accurate Analysis of Interference for Rake Combining on DS-CDMA Forward Link in Mobile Radio", *IEICE Transactions on Communications*, Vol. E88-B, No. 2, pp. 654-663.

Huang, S., Chen, L. and Chen, T. (1996). "A 32-bit Logarithmic Number System Processor", *Journal of VLSI Signal Processing*, 14, pp. 311-319.

Iltis, R. A. (1998). "Performance of constrained and unconstrained adaptive multiuser detectors for Quasi-synchronous CDMA mobile radio systems", *IEEE Transactions on Communications*, Vol. 46, No. 1, pp. 135-143.

ITU-R (1997). Recommendation ITU-R M.1225, guidelines for evaluation of radio transmission technologies for IMT-2000. Tech. rep. International Telecommunication Union (ITU).

Jakes, W. C. (1993). Microwave Mobile Communications, *IEEE press*, Piscataway, N. J.

Jeruchim, M. C., Balaban, P. and Shanmugan, K. S. (1994). "Simulation of Communication Systems", Plenum Press, New York.

Johnson, D. H. and DeGraaf, S. R. (1982). "Improving the Resolution of Bearing in Passive Sonar Arrays by Eigenvalue Analysis", *IEEE Transactions on Acoustics Speech and Signal Processing*, Vol. ASSP-30, No. 4, pp. 638-647.

Jung, P., Baier, P.W. and Steil, A. (1993). "Advantages of CDMA and Spread Spectrum Techniques over FDMA and TDMA in Cellular Mobile Radio Applications", *IEEE Transactions on Vehicular Technology*, Vol. 42, No. 3, pp. 357-363.

Jung, P. and Blanz, J. (1995). "Joint Detection with coherent receiver antenna diversity in CDMA mobile radio systems", *IEEE Transactions on Vehicular Technology*, Vol. 44, No. 1, pp. 76-88.

Juntti, M. J. and Aazhang, B. (1997). "Finite memory-length linear multiuser detection for asynchronous CDMA communications", *IEEE Transactions on Communications*, Vol. 45, No. 5, pp. 611-622.

Juntti, M. J. and Latva-aho, M. (1999). "Bit error probability analysis of linear receivers for CDMA systems in frequency-selective fading channels", *IEEE Transactions on Communications*, Vol. 47, No. 12, pp. 1788-1791.

Kalman, R. E. (1960). "A New Approach to Linear Filtering and Prediction Problems", *Transactions of the ASME-Journal of Basic Engineering*, 82 (Series D), pp. 35-45.

Kay, S. M. (1993). "Fundamentals of Statistical Signal Processing: Estimation Theory", Prentice-Hall, Englewood Cliffs, USA.

Kim, J.Y., Stuber, G.L., and Akyildiz, I.F. (2002). "A Simple Performance/Capacity Analysis of Multiclass Macrodiversity CDMA Cellular Systems", *IEEE Transactions on Communications*, Vol. 50, No. 2, pp. 304-308.

Kim, S. R., Jeong, Y. G. and Choi, I. K. (2000). "A Constrained MMSE Receiver for DS/CDMA Systems in Fading Channels", IEEE Transactions on Communications, Vol. 48, No. 11, pp. 1793-1793.

Kim, S. W., Ha, D. S. and Kim, J. H. (2000). "Performance Gain of Smart Dual Antennas at Handsets in 3G CDMA System," *The 5th CDMA International Conference*, Vol. 2, pp. 223-227, November.

Kim, S. W., Ha, D. S., Kim, J. H. and Kim, J. H. (2001). "Performance of Smart Antennas with Adaptive Combining at Handsets for the 3GPP WCDMA System," *The IEEE Vehicular Technology Conference*, pp. 2048-2052, October.

Klein, A. (1997). "Data detection algorithms specially designed for the downlink of CDMA systems with long spreading codes", *Proceedings of the IEEE Vehicular Technology Conference*, pp. 203-207.

Klein, A. and Baier, P. (1993). "Linear unbaised data estimation in mobile radio systems applying CDMA", *IEEE Journal in Selected Areas of Communications*, Vol. 11, 1993, pp. 1058-1066.

Klein, A., Kaleh, G. K. and Baier, P. (1996). "Zero-forcing and Minimum mean-square-error equalization in code-division-multiple-access channels", *IEEE Transactions on Vehicular Technology*, Vol. 45, No. 2, pp. 276-287.

Koetter, R., Singer, A. C. and Tuchler, M. (2004). "Turbo Equalization", IEEE Signal Processing Magazine, January, pp. 67-80.

Koike, S. (2002). "A Class of Adaptive Step-Size Control Algorithms for Adaptive Filters", *IEEE Transactions on Signal Processing*, Vol. 50, No. 6, pp. 1315-1326.

Kohno, R. (1998). "Spatial and Temporal Communication Theory Using Adaptive Antenna Array," *IEEE Personal Communications*, pp. 28-55.

Kohno, R. and Hatori, M. (1983). "Cancellation techniques of co-channel interference in asynchronous spread spectrum multiple access systems", *Electronics and Communications in Japan*, Vol. 66-A, No. 5, pp. 20-29.

Kohno, R. Imai, H. and Hatori, M. (1983). "Cancellation technique of co-channel interference in asynchronous spread-spectrum multiple-access systems", *IEICE Transactions on Communications*, 65-A, pp. 416-423.

Kohno, R., Meidan, R. and Milstein, L.B. (1995). "Spread Spectrum Access Methods for Wireless Communications", *IEEE Communications Magazine*, Jan, pp. 58-67.

Komulainen, P., Heikkila, M. J., and Lilleberg, J. (2000). "*Adaptive channel equalization and interference suppression for CDMA downlink*", IEEE 6th International Symposium On Spread-Spectrum Techniques and Applications, vol. 2, pp. 363-367.

Komulainen, P. and Heikkilä, M. (2001). "Adaptive channel equalization based on chip separation for CDMA downlink", *Proceedings of the IEEE International Symposium on Personal, Indoor, and Mobile Radio Communications (PIMRC)*, Vol. 3, pp. 1114-1118.

Kong, N., Riphagen, I., Lotter, M. and vanRooyen, P. (2005). "An Optimum Interference Mitigating Combing Scheme for the CDMA Downlink With the Same Complexity as MRC", *IEEE Transactions on Wireless Communications*, Vol. 4, No. 3, pp. 866-871.

Konhauser, W. (1998). "Applications and Services from 2nd to 3rd Generation", ICCT, pp. S22-08-1-S22-08-4.

Kostopoulos, D. (1991). "An Algorithm for the Computer of Binary Logarithms", *IEEE Transactions on Computers*, Vol. 40, No. 11, pp. 1267-1270.

Krauss, T. P., Hillery, W. J. and Zoltowski, M. D. (2000). "MMSE equalization for the forward link in 3G CDMA: Symbol-level versus chip-level", *Proceedings of the IEEE Workshop on Statistical Signal and Array Processing*, pp. 18-22.

Krauss, T. P., Hillery, W. J. and Zoltowski, M. D. (2002). "Downlink Specific Equalization for Frequency Selective CDMA Cellular Systems", *Journal of VLSI Signal Processing*, Vol. 30, pp. 143-161.

Krauss, T. P., Zoltowski, M. D. and Leus, G. (2000). "Simple MMSE equalizers for CDMA downlink to restore chip sequence: Comparison to zero-forcing and rake", *Proceedings of the IEEE International Conference on Acoustics, Speech, and Signal Processing*, pp. 2865-2868, June 5-9.

Krauss, T. P. and Zoltowski, M. D. (2000). "Oversampling diversity versus dual antenna diversity for chip-level equalization on CDMA downlink", *Proceedings IEEE Sensor Array and Multichannel Signal Processing Workshop*, pp. 47-51.

Kwon, S., Oh, I. and Choi, S. (1999). "Adaptive Beamforming from the Generalized Eigenvalue Problem with a Linear Complexity for a Wideband CDMA Channel", *Proceedings of the IEEE Vehicular Technology Conference*, pp.1890-1894.

Kuo, W. Y. (2001). "Improved Rake Receiver using finger Variance Weight", *Proceedings of the IEEE International Conference on Vehicular Technology"* pp. 1163-1167.

Lai, F. and Wu, C.E. (1991). "A Hybrid Number System Processor with Geometric and Complex Arithmetic Capabilities", *IEEE Transactions on Computers*, Vol. 40, No. 8, pp. 952-959.

Lamarca, M. and Vazquez, G, (1997). "Diversity techniques for blind channel equalization in mobile communications", *The 8th IEEE International Symposium on Personal, Indoor and Mobile Radio Communications*, Vol 3, 1-4 Sept. pp. 1079 - 1083.

Latva-Aho, M. (1998). "Bit error probability for analysis for FRAMES WCDMA Downlink Receivers", *IEEE Transactions on Vehicular Technology*, Vol. 47, No. 4, pp. 1119-1133.

Latva-aho M, (1998). "Advanced Receivers for Wideband CDMA Systems", *Acta Universitatis Ouluensis C 125*, University of Oulu Press, Oulu, Finland.

Latva-Aho, M. and Juntti, M. (1997). "Modified adaptive LMMSE receiver for DS-CDMA systems in fading channels", *Proc. IEEE International Symposium on Personal, Indoor, and Mobile Radio Communications (PIMRC)*, Vol. 2: p 554-558.

Latva-aho, M. and Juntti, M. (2000). "LMMSE detection for DS-CDMA systems in fading channels", *IEEE Transactions on Communications*, Vol. 48, No. 2, pp. 194-199.

Lee, P. (1995). "An FPGA Prototype for a Multiplierless FIR Filter Built Using the Logarithmic Number System", *5th International Workshop on Field-Programmable Logic and Applications*, pp. 303-310.

Lee, P. and Sartori, A. (1998). "Modular Leading One Detector for Logarithmic Encoder", *Electronic Letters*, Vol. 34, No. 8, pp. 727-729.

Lee, W. Y. C. (1998). "Mobile Communication Engineering", New York:McGraw Hill, 1985.

Lehnert, J. S. and Pursley, M. B. (1987). "Multipath diversity reception of spread spectrum multiple-access communications", *IEEE Trans. Communications*", Vol. COM-35, pp. 1189-1198.

Lenardi, M. and Slock, D. (2000). "SINR maximizing equalizer receiver for DS-CDMA", *Proceedings on European Signal Processing Conference (EUSIPCO)*.

Lenardi, M., Medles, A. and Slock, D. (2001). "Comparison of downlink transmit diversity schemes for RAKE and SINR maximizing receivers", *Proc. IEEE International Conference on Communications (ICC)*, Vol 6, pp. 1679-1683.

Lenardi, M., Medles, A. and Slock, D. (2000). "A SINR maximizing RAKE receiver for DS-CDMA downlinks", Proceedings of Asilomar Conference on Signals, Systems and Computers, Vol 2, pp. 1283-1287.

Leus, G, Barhumi, I. and Moonen, M. (2003). "MMSE Time-Varying FIR Equalization of Doubly Selective Channels", *Proceedings of the IEEE International Conference on Communications*.

Leus, S.M. and Paulraj, A. (2004). "An interference-suppressing RAKE receiver for the CDMA downlink", IEEE Signal Processing Letters, Vol. 11, No. 5, pp. 521 - 524.

Lewis, D. (1990). "An Architecture for Addition and Subtraction of Long Word-Length Numbers in the Logarithmic Number System", *IEEE Transactions on Computers,* Vol. 39, No. 11, pp. 1323-1336.

Lewis, D. M. (1994). "Interleaved Memory Function Interpolators with Application to an Accurate LNS Arithmetic Unit", *IEEE Transactions on Computers,* Vol. 43, No. 8, August, pp. 974-982.

Li, K. and Liu, H. (1999). "A new blind receiver for downlink DS-CDMA communications", *IEEE Communications Letters,* Vol. 3, No. 7: pp. 193-195.

Litva, J. and Yeung, T. K. (1996). "Digital beamforming in wireless communications", Artech House, Boston, USA.

Liu, H and Xu, G. (1996). "A Subspace Method for Signature Waveform Estimation in Synchronous CDMA Systems", *IEEE Transactions on Communications*, Vol. 44, No. 10, pp. 1346 - 1354.

Liu, P. and Xu, Z. (2002). "Channel Estimation and Multiuser Detection for Long Code CDMA", *Proceedings of the 36th Asilomar Conference on Signals, Systems and Computers,* Vol. 2, pp. 1453-1457.

Lorenz, R. and Boyd, S. (2005). "Robust Minimum Variance Beamforming", *IEEE Transactions on Signal Processing*", Vol. 53, No. 5, pp. 67-94, pp. 1-15, May.

Lucky, R. (1966). "Techniques for Adaptive Equalization of Digital Communication Systems", *The Bell System Technical Journal*, pp. 255-286.

Lupas, R. and Verdu, S. (1990) "Near-Far Resistance of Multiuser Detectors in Asynchronous Channels", *IEEE Transations on Communications*, Vol. 38, No. 14, pp. 496-508.

Lupas R. and Verdu, S. (1989). "Linear Multiuser Detectors for Synchronous Code-Division Multiple-Access Channels", *IEEE Transactions on Information Theory*, vol. 35, No.1, Jan, pp. 123-136.

Madhow, U. (1998). "MMSE Interference Suppression for Timing Acquisition and Demodulation in Direct-Sequence CDMA Systems", *IEEE Transactions on Communications*, vol. 46, no. 8, pp. 1065-1075.

Madhow, U. (1998). "Blind Adaptive Interference Suppression for Direct-Sequence CDMA", *Proceedings of the IEEE*, Vol. 86, No. 10, pp. 2049-2069.

Majmundar, M., Sandhu, N. and Reed, J. (2000). "Adaptive Single-User Receivers for Direct-Sequence Spread Spectrum CDMA Systems", *IEEE Transactions on Vehicular Technology*, Vol. 49, No. 2, pp. 379-388.

Mailaender, L. (2002). "Low-complexity implementation of CDMA downlink equalization", *Proceedings of the IEEE International Conference on 3G Mobile Communication Technologies*, London, UK, p 396-400.

Marino, D. (1972). "New Algorithms for the Approximate Evaluation in Hardware of Binary Logarithms and Elementary Functions", *IEEE Transactions on Computers,* pp. 1416-1421.

McLaren, D. J. (2003). "Improved Mitchell-Based Logarithmic Mutiplier for Low-Power DSP Applications", *IEEE International SOC Conference*, pp. 53-56.

Miller, S. (1995). "An adaptive direct-sequence code-division multiple access receiver for multi-user interference rejection", *IEEE Transactions on Communications*, Vol. 43, pp. 1746-1755.

Miller, S. (1996). "Training Analysis of adaptive interference suppression for direct-sequence code-division multiple-access systems", *IEEE Transactions on Communications*, Vol. 44, No. 4, pp. 488-495.

Milstein, L.B. (2000). "Wideband Code Division Multiple Access", *IEEE Journal on Selected Areas In Communications*, Vol. 18, No. 8, pp. 1344-1354.

Mirbagheri, A. and Yoon, Y. C. (2002). "A Linear MMSE Receiver for Mulitpath Asynchronous Random-CDMA with Chip Pulse Shaping", *IEEE Transactions on Vehicular Technology*, Vol. 51, No. 5, pp. 1072-1086.

Mitra, U. and Poor, H.V. (1995), "Adaptive receiver algorithms for near-far resistant CDMA", *IEEE Transactions on Communications*, Vol. 43, No. (2/3/4), pp. 1713-1724.

Monk, A. M. Davis, M. Milstein, L. B. Helstrom, C. W. (1994). "A noise whitening approach to multiple access noise rejection - part I: Theory and background", *IEEE Journal on Selected Areas in Communications*, Vol. 12, No. 5, pp. 817-827.

Moshavi, S. (1996). "Multi-user detection for DS-CDMA communications", *IEEE Communications Magazine*, Vol. 34, No. 10, pp. 124-137.

Mostafa, R., Khanna, P., Chung, W., Heo, J,. Reed, J. and Ha, D. (2004). "Performance Evaluation of 2D Rake Algorithms for WDCMA-DL Applications at the Handset", *IEEE Radio and Wireless Conference*, pp. 367-370.

Mudulodu, S. and Paulraj A. (2000). "A blind multiuser receiver for the CDMA downlink", *Proceedings of the IEEE International Conference on Acoustics, Speech, and Signal Processing (ICASSP)*, Vol. 5, pp. 2933-2936.

Naguid, A. F. and Paulraj, A. (1994). "A base-station antenna array receiver for cellular DS/CDMA with M-array orthogonal modulation", *Proceedings of the 28th Asilomar Conference on Signals, Systems and Computing*, pp. 858-862.

Nascimento, V. H. and Sayed, A. H. (1999). "Unbiased and stable leakage-based adaptive filters. IEEE Transactions on Signal Processing", Vol. 47, No. 12, pp. 3261-3276.

Noneaker, D. L. (1998). "Optimal Combining for Rake Reception in Mobile Cellular CDMA Forward Links", *IEEE Military Communications Conference*.

Opperman, I and Latva-Aho, M. (1997). "Adaptive LMMSE receiver for wideband CDMA systems", *Proc. IEEE Global Telecommunications Conference*, pp. 133-138.

Patel, P. and Holtzman, J. (1994). "Analysis of a simple successive interference cancellation scheme in a DS/CDMA system", *IEEE Journal on Selected Areas in Communication*, Vol. 12, No. 10, pp. 796-807.

Petre, F. and Moonen, M. et al. (2000). "Pilot-aided adaptive chip equalizer receiver for interference suppression in DS-CDMA forward link", *Proceedings of the IEEE Vehicular Technology Conference*, Vol. 1, pp.303-308.

Petre, F., Leus, G. and Engels, M., et al. (2001). "Semi-blind space-time chip equalizer receivers for WCDMA forward link with code-multiplexed pilot", *Proceedings of the IEEE International Conference on Acoustics, Speech, and Signal Processing*, Vol. 4, pp. 2245-2248.

Petrus, P., Reed, J. H. and Rappaport, T. S. (1997). "Effects of directional antennas at the base station on the Doppler spectrum", *IEEE Communications Letters*, vol. 1, No:2, pp. 40-42, March.

Pickholtz, R.L., Milstein, L.B. and Schilling, D.L. (1991). "Spread Spectrum for Mobile Communications", *IEEE Transactions on Vehicular Technology*, Vol. 20, No. 2, 1991, pp. 313-321.

Pickholtz, R.L., Schilling, D.L. and Milstein, L.B. (1982). "Theory of Spread-Spectrum Communications- A Tutorial", *IEEE Transactions on Communications*, Vol. 30, No. 5, pp. 855-884.

Polydoros, A. and Glisic, S. (1994). "Code Synchronization: A Review of Principles and Techniques", *IEEE 3rd International Symposium on Spread Spectrum Techniques and Applications*", Vol. 1, pp. 115-137.

Poor, H. V. and Verdu, S. (1998). "Single-user detectors for multiuser channels. *IEEE Transactions on Communications*", Vol. 36, No. 1, pp. 50-60.

Poor, H. V. and Verdú, S. (1997). "Probability of error in MMSE multiuser detection" *IEEE Transactions on Information Theory*, Vol. 43, No. 3, pp. 858-871.

Prasad, R., Mohr, and Konhauser, W. (2000). "Third Generation Mobile Communication System", Universal Personal Communications, Artech House Publishers.

Prasad, R., Mohr W. and Konhauser, W. (2000). "Third Generation Mobile Communication Systems", Artech House Publishers, ISBN 1-58053-082-6.

Proakis, J. and Magee, F. (1973). "Adaptive Maximum Likelihood Sequence Estimation for Digital Signalling in the Presence of Intersymbol Interference", *IEEE Transactions on Information Theory*, pp. 120 - 124.

Proakis, J. and Shamai, S. (1998). "Fading Channels: Information Theoretic and Communication Aspects", *IEEE Transactions on Information Theory*, pp. 2619-2692.

Proakis, J. (2001). "Digital Communications", 4th Edition, Mcgraw Hill.

Pursley, M. (1977). "Performance Evaluation for Phase-Coded Spread-Spectrum Multiple-Access Communication-Part I: System Analysis", *IEEE Transactions on Communications*, Vol. 25, No. 8, pp. 795-799.

Qureshi, S. (1985). "Adaptive equalization", Proceedings of the IEEE, Vol. 73, No. 9, pp. 1349-1387.

Rapajic, P. B. and Vucetic, B. S. (1995), "Linear adaptive transmitter-receiver structures for asynchronous CDMA systems", *European Transactions on Telecommunications*, Vol. 6, No. 1, pp. 21-27.

Rapajic, P. B. and Vucetic, B. S. (1994). "Adaptive receiver structures for asynchronous CDMA systems". *IEEE Journal on Selected Areas in Communications*, Vol. 12, No. 4, pp. 685 - 697.

Razavilar, J. Rashid-Farrokhi, P. and Liu, K. (1999). "Software Radio Architecture with Smart Antennas: A Tutorial on Algorithms and Complexity", *IEEE Journal of Selected Areas in Communications*, Vol. 17, No. 4, pp. 662-676.

Richardson, K.W. (2000). "UMTS overview", *Electronics & Communication Engineering Journal*, Volume 12, Issue 3, pp. 93 - 100.

Roy, D. S. (1994). "An adaptive multiuser receiver for CDMA systems", *IEEE Journal on Selected Areas in Communications*, Vol. 12, No. 6, pp. 808-816.

Roy, R. and Kailath, T. (1989). "ESPRIT-Estimation of Signal Parameters via Rotational Invariance Techniques," *IEEE Transactions on Acoustics Speech and Signal Processing*, vol. ASSP-37, pp. 984-996.

Samukic, A. (1998). "UMTS Universal Mobile Telecommunications System: Development of Standards for the Third Generation", *IEEE Transactions on Vehicular Technology*, Vol. 47, No. 4, pp. 1099-1104.

Saunders, S. R. (1999). "Antennas and Propagation for Wireless Communication Systems", New York: John Wiley & Sons.

Schlegel, C. and Wei, L. (1997). "A simple way to compute the minimum distance in multiuser CDMA systems", *IEEE Transactions on Communications*, Vol. 45, No. 5, pp. 532-535.

Schmidt, R. O. (1986). "Multiple Emitter Location and Signal Parameter Estimation," *IEEE Transactions on Antennas and Propagation*, Vol. AP-34, pp. 276-280.

Schneider, K.S. (1979). "Optimum detection of code division multiplexed signals", *IEEE Transactions on Aerospace and Electronic Systems*, 15(1), pp. 181-185.

Schodorf, J. B. and Williams, D. B. (1997). "A constrained optimization approach to multiuser detection", *IEEE Transactions on Signal Processing*, Vol. 45, No. 1, pp. 258-262.

Scholtz, R.A. (1977). "The Spread Spectrum Concept", *IEEE Transactions on Communications*, Vol. 25, No. 8, pp. 748-755.

Simon, M. and Alouini, M. (1998). "A Unified Approach to the Performance Analysis of Digital Communication over Generalized Fading Channels", *Proceedings of the IEEE,* Vol. 86, No. 9, pp. 1860-1876.

Simon, M. K., Omura, J.K., Scholtz, R.A. and Levitt, B.K. (1994). "Spread Spectrum Communications Handbook", McGraw-Hill, New York, USA.

Simeone, O., Bar-Ness, Y., and Spagnolini, U. (2004). "Linear and Nonlinear Preequalization/Equalization for MIMO Systems with Long-Term Channel State Information at the Transmitter", *IEEE Transactions on Wireless Communications*, Vol. 3, No. 2. pp. 373-378.

Sivanesan, K. and Beaulieu, N. C. (2005). "Interference Whitening Receivers for Bandlimited DS-CDMA Systems In Nakagami Fading", *IEEE Wireless Communications and Networking Conference.*

Slock, D. (1993). "On the convergence behavior of the LMS and the normalized LMS algorithms", *IEEE Transactions on Signal Processing*, Vol. 41, No. 9, pp. 2811-2825.

Slock, D. and Ghauri, I. (2000). "Blind maximum SINR receiver for the DS-CDMA downlink", *Proceedings of the IEEE International Conference on Acoustics, Speech, and Signal Processing (ICASSP)*, Vol 5, pp. 2485-2488.

Smith, R. F. and Miller, S. L. (1994). "Code timing estimation in a near-far environment for direct-sequence code-division multiple-access", *Proceedings of the IEEE Military Communications Conference*, pp. 47-51.

Song, Y. S. and Kwon, H. M. (1999). "Analysis of a Simple Smart Antenna for CDMA Wireless Communications," *IEEE Vehicular Technology Conference*, pp. 254-258, May.

Sripad, A. B. and Snyder, D. L. (1977). "A necessary and sufficient condition for quantization errors to be uniform and white", *IEEE Transactions on Acoustics, Speech, and Signal Processing*, Vol. ASSP-25, No. 5, pp. 442-448.

Steele, R, (1992). "Mobile Radio Communications", Pentech Press London.

Stein, S. (1987). "Fading Channel Issues in System Engineering", *IEEE Journal on Selected Areas in Communications*, Vol. 5, No. 2, 1987, pp. 68-88.

Stoica, P. and Nehorai, A. (1989). "MUSIC, Maximum Likelihood, and Cramer-Rao Bound", *IEEE Transactions on Acoustics, Speech and Signal Processing*, Vol. 37, No. 5, pp. 720-741.

Ström, E. G. and Malmsten, F. (1998). "Maximum Likelihood Synchronization of DS-CDMA Signals Transmitted over Multipath Channels", *IEEE International Conference on Communications*, Vol. 13, pp. 1546-1550.

Ström, E. G., Parkvall, S., Miller, S. L. and Ottersten, B.E. (1996). "Propagation delay estimation in asynchronous direct-sequence code-division multiple access systems", *IEEE Transactions on Communications*, Vol. 44, No. 1, pp. 84-93.

Swartzlander Jr., E. E. and Alexopoulous, A. (1975). "The Sign/Logarithm Number System", *IEEE Transactions on Computers,* pp. 1238-1242.

Tokaji, I. and Barnes, C. W. (1987). "Roundoff error statistics for a continuous range of multiplier coefficients", *IEEE Transactions on Circuits and Systems*, Vol. 34, No. 1, pp. 52-59.

Treichler, J. R. and Agee, B. G. (1983), "A New Approach to Multipath Correction of Constant Modulus Signals," *IEEE Transactions on Acoustics, Speech, and Signal Processing*, Vol. 31, No. 2, pp. 459-472.

Treichler, J. R. and Larimore, M. G. (1996). "Fractionally Spaced Equalizers: How long should they really be?" *IEEE Signal Processing Magazine*, Vol. 13, pp. 65-81.

Trees, L.V. (1971). "Detection, Estimation, and Modulation Theory Part III", Wiley, New York.

Tsatsanis, M. K. (1997). "Inverse filtering criteria for CDMA systems", *IEEE Transactions on Signal Processing*, Vol. 45, No. 1, pp. 102-112.

Tsatsanis, M. K. and Giannakis, G. B. (1996). "Optimal Decorrelating Receivers for DS-CDMA systems: A Signal Processing Framework", *IEEE Transactions on Signal Processing*, Vol. 44, No. 12, pp. 3044-3055.

Tsatsanis, M. K. and Xu, Z. (1998). "Performance Analysis of Minimum Variance CDMA Receivers", *IEEE Transactions on Signal Processing"*, Vol. 46, No. 11, pp, 3014-3022.

Turin, G.L. (1980). "Introduction to Spread Spectrum Antimultipath Techniques and their Application to Urban Digital Radio", *Proceedings of the IEEE*, vol. 68, no. 3, pp. 328-353.

Turin, G.L. (1984). "The effects of Multipath and Fading on the Performance of Direct-Sequence CDMA Systems", *IEEE Journal on Selected Areas in Communications*, Vol. 2, No. 4, pp. 597-603.

Ungerboeck, G. (1974). "Adaptive Maximum-Likelihood Receiver for Carrier-Modulated Data-Transmission Systems", *IEEE Transactions on Communications*, Vol. COM-22, No. 5, 624-636.

Vanghi, V. and Vojcic, B. (1996). "Soft interference cancellation in multiuser communications", Wireless Personal Communications, Kluwer, Vol. 3, No. 1-2, pp. 111-128.

Van Veen, B. D. and Buckley, K. M. (1988). "Beamforming: A Versatile Approach to Spatial Filtering", *IEEE ASSP Magazine*, pp. 4-24.

Varanasi, M. (1999). "Decision Feedback Mulituser Detection: A Systematic Approach", IEEE Transactions on Information Theory, Vol. 45, No. 1, pp. 219-240.

Varanisi, M. K. (1993). "Noncoherent detection in asynchronous multiuser channels", IEEE Transations on Information Theory, Vol. 39, No. 1, pp. 157 - 176.

Varansi, M. K. and Aazhang, B. (1990). "Multistage detection in asynchronous code-division multiple-access communication", *IEEE Transactions on Communications*, Vol. 38, No. 4, pp. 509-519.

Varanasi M. K. and Aazhang, B. (1991). "Near-optimum detection in synchronous code-division multiple-access systems", IEEE Trans. Commun., Vol. 39, No. 5, pp. 725- 736.

Vaughan, R. and Bach Anderson, J. (2002). "Channels, Propagation and Antennas for Mobile Communications", The IEE Electromagnetic Wave Series 50, ISBN 0 85296 084 0.

Vaughan, R. G. (1988). "On optimum combining at the mobile", *IEEE Transactions on Vehicular Technology*, Vol. 37, No. 4, pp. 181 - 188.

Verdu, S. (1989). "Computational Complexity of Optimum Multiuser Detection", *Algorithmica*, pp. 303-312.

Verdu, S. (1986). "Minimum Probability of Error for Asynchronous Gaussian Multiple-access Channels", *IEEE Transactions on Information Theory*, Vol. 32, No. 1, pp. 85-96.

Verdu, S. (1998). "Multiuser Detection", Cambridge University Press, ISBN 0-521-59373-5.

Verdu, S. (1986). "Optimum Multiuser Asymptotic Efficiency", *IEEE Transactions on Communications*, Vol. Com-34, No. 9, pp. 890-897.

Viterbi, A.J. (1979). "Spread Spectrum Communications- Myths and Realities", *IEEE Communications Magazine*, Vol. 17, No. 3, pp. 11-18.

Viterbi, A. J. (1967). "Error Bounds for Convolutional Codes and an Asymptotically Optimum Decoding Algorithm", IEEE Transactions on Information Theory, Vol. IT-13, No. 2, pp. 260-269.

Viterbi, A. J. (1971). "Convolutional Codes and Their Performance in Communication Systems", IEEE Transactions on Communications Technology, Vol. COM-19, No. 5, pp. 751-772.

Whalen, D. (1971). "Detection of Signals in Noise", New York: Academic.

Wang, X, and Poor, H. V. (1998). "Blind equalization and multiuser detection in dispersive CDMA channels", *IEEE Transactions on Communications*, Vol. 46, No. 1, pp. 91-103.

Wang, X. and Poor, H.V. (1999). "Iterative (turbo) soft interference cancellation and decoding for coded CDMA", *IEEE Transactions on Communications*, Vol. 47, No. 7, pp. 1046-1061.

Wang, X., and Poor, H. V. (2004). "Wireless Communication Systems: Advanced Techniques for Signal Reception", Prentice Hall, ISBN 0-13-021435-3.

Wax, M. and Kailath, T. (1985). "Detection of signals by information theoretic criteria" *IEEE Transactions on Acoustics, Speech, and Signal Processing*, Vol. 33, No. 2, pp. 387 - 392.

Weber, C. L. and Polydoros, A. (1984). "A Unified Approach to Serial-Search Spread-Spectrum Code Acquisition, Part I: General Theory", *IEEE Transactions on Communications*, pp. 542-549.

Weber, C. L. and Polydoros, A. (1984). "A Unified Approach to Serial-Search Spread-Spectrum Code Acquisition, Part II: A Matched Filter Receiver", *IEEE Transactions on Communications*, pp. 550-560.

Wei, F. and Rasmussen, L.K. (1996). "A near ideal noise whitening filter for an asynchronous time-varying CDMA system", *IEEE Transactions on Communications*, Vol. 44, No. 10, pp. 1355-1361.

Welburn, L. R., Cavers, J.K., and Sowerby, K. W. (2004). "Multiuser Macrodiversity Detection in Asynchronous DS-CDMA Systems", *IEEE Transactions on Wireless Communications*, Vol. 3, No. 2, pp. 544-554.

Werner, S. and Lilleberg, J. (1999). "Downlink channel Decorrelation in CDMA systems with long codes", *Proceedings of the IEEE Vehicular Technology Conference*, pp. 1614-1617.

Werner, S., de Campos, M. and Apolinario, J. (2000). "Kalman-filter based chip estimator for WCDMA downlink detection", *Proceedings of the European Signal Processing Conference (EUSIPCO)*.

Wijayasuriya, S. S. H. and Norton, G. H. (1996). "A sliding window Decorrelating Receiver for multiuser DS-CDMA radio networks", *IEEE Transactions on Vehicular Technology*, Vol. 45, No. 3, pp. 503-521.

Windrow, B. and McCool, J. (1976). "A Comparison of Adaptive Algorithms Based on the Methods of Steepest Descent and Random Search", *IEEE Transactions on Antennas and Propagation*, Vol. AP-24, No. 5, 615-637.

Widrow, B., McCool, J. M., Larimore, M. G. and Johnson, C. R. (1976). "Stationary and nonstationary learning characteristics of the LMS adaptive filter", *Proceedings of the IEEE,* Vol. 64, No. 8, pp. 1151-1162.

Winters, J. (1984). "Optimum Combining in Digital Mobile Radio with Cochannel Interference", *IEEE Journal in Selected Areas in Communications*", Vol. 2, No. 4, pp. 528-539.

Winters, J. H. (1998). "Smart Antennas for Wireless Systems," *IEEE Personal Communications*, pp. 25-27, Feb.

Wong, P.W. (1990). "Quantization noise, fixed-point multiplicative roundoff noise, and dithering", *IEEE Transactions on Acoustics, Speech, and Signal Processing*, Vol. 38, No. 2, pp. 286-300.

Xiao, P. and Stom, E. (2003). "Pilot-Aided Acquistion Algorithms for Asynchronous DS-CDMA Systems", *European Transactions on Telecommunications*, Vol. 14, No. 1, pp. 89-96.

Xu, G. Liu, H. Tong, L. Kailath, T. "A least-squares approach to blind channel identification", *IEEE Transactions on Signal Processing*, Vol. 43, No. 12, pp. 2982-2993, 1995.

Xu, Z. and Tsatsanis, M. K. (2001). "Blind Adaptive Algorithms for Minimum Variance CDMA Receivers", IEEE Transactions on Communications, Vol. 49, No. 1, pp. 180-193.

Yang, J. and Li, Y. (2002). "A decision-feedback equalizer with tentative chip feedback for the downlink of wideband CDMA", *Proceedings of the IEEE International Conference on Communication*, Vol. 1, pp. 119-123.

Yeap, B. L., Liew, T. H., Hamorsky, J. and Hanzo, L. (2002). "Comparative Study of Turbo Equalization Schemes Using Convolutional Turbo, and Block-Turbo Codes", IEEE Transactions on Wireless Communications", Vol. 1, No. 2, pp. 266-273.

Yoon, Y. C. and Leib, H. (1996). "Matched Filters with Interference Suppression Capabilities for DS-CDMA", *IEEE Journal on Selected Areas in Communications*, Vol. 14, No. 8, pp. 1510-1521.

Yoon, Y. C. and Leib, H. (2001). "Chip-Delay Locked Matched Filter for DS-CDMA Systems Using Long Sequence Spreading", *IEEE Transactions on Communications*, Vol. 49, No. 8, pp. 1468-1478.

Zecevic, N. and Reed, J. H. (1997). "Blind Adaptation Algorithms for Direct-Sequence Spread-Spectrum CDMA Single-User Detection", *IEEE Conference on Vehicular Technology*, Vol. 3, pp. 2133-2137.

Zhenhua, X., Short, R.T. and Rushforth, C.K. (1990). "A family of suboptimum detectors for coherent multiuser communications", *IEEE Journal on Selected Areas in Communications.*, Vol. 8, No. 4, May, pp. 683- 690.

Zobel. (1928). "Distortion Correction in Electrical Circuits with Constant Resistance Recurrent Networks", *Bell Syst. Tech. Journal*, Vol. 7pp. 458.

Zoltowski, M. D., Hillery, W. J. and Krauss, T. P. (2000). "Comparative performance of three MMSE equalizers for the CDMA forward link in frequency selective multipath", *Proceedings of the Asilomar Conference on Signals, Systems and Computers,* Vol. 1, pp. 781-785.

Zoltowski, M. D. and Krauss, T. P. (1999). "Two-channel zero forcing equalization on CDMA forward link: Trade-offs between multi-user access interference and diversity gains", *Proceedings of the Asilomar Conference on Signals, Systems and Computers,* Vol. 2, pp. 1541-1545.

Zvonar, Z. and Brady, D. (1995). "Suboptimal multiuser detector for frequency-selective Rayleigh fading", *IEEE Transactions on Communications,* Vol. 43, No. 2/3/4, pp. 154-157.

Zvonar, Z. and Brady, D. (1994). "Multiuser detection in single-path fading channels", *IEEE Transactions on Communications,* Vol. 42, No. 2/3/4, pp. 154-157.

APPENDIX A
THE RAYLEIGH DISTRIBUTION

Consider $N=X+jY$ complex multivariate Gaussian sources combining at a single point in space modelled with an isotropic antenna where X and Y are statistically independent with first moments $E\{X\}=0$ and $E\{Y\}=0$. The envelope, R, given by the Euclidean distance is a chi-squared random variable with two degrees of freedom [Proakis2001] where $R=\sqrt{X^2+Y^2}$ with $X=R\cos\Phi$ and Y=$R\sin\Phi$. Let

$$p_{X,Y}(x,y)=\frac{1}{2\pi\pi^2}exp\left\{-\frac{1}{2\sigma^2}\left(x^2-y^2\right)\right\} \tag{A.1}$$

denote the joint PDF of the Gaussian random variables and $p_{R,\Phi}(R,\Phi)$ the density function to be obtained. In this case, $p_{R,\Phi}(R,\Phi)=|J|\cdot p_{X,Y}(x,y)$ with the Jacobian

$$J=\left|\frac{\partial(X,Y)}{\partial(R,\Phi)}\right|=\begin{vmatrix}\frac{\partial X}{\partial R} & \frac{\partial Y}{\partial R}\\ \frac{\partial X}{\partial \Phi} & \frac{\partial Y}{\partial \Phi}\end{vmatrix}=\begin{vmatrix}\cos\Phi & \sin\Phi\\ -R\sin\Phi & R\cos\Phi\end{vmatrix} \tag{A.2}$$

equating to $J=R$ where | | represents the determinant function. The joint PDF $p_{R,\Phi}(R,\Phi)$ is thus given as

$$p_{R,\Phi}(R,\Phi)=\frac{R}{2\pi\sigma^2}exp\left\{-\frac{R^2}{2\sigma^2}\right\} \tag{A.3}$$

where the marginal PDF of R, $p_R(R)=\int_0^{2\pi}p_{R,\Phi}(R,\Phi)\ \partial\Phi$ gives the Rayleigh distribution

$$p_R(R)=\frac{R}{\sigma^2}exp\left\{-\frac{R^2}{2\sigma^2}\right\} \tag{A.4}$$

provided $R\geq 0$. Similarly, the marginal PDF for the phase is shown to be uniform where

$$p_\Phi(\Phi)=\int_0^{\infty}p_{R,\Phi}(R,\Phi)\ \partial R=\frac{1}{2\pi} \tag{A.5}$$

The use of the physical scattering model for a set of $N=10$ sources with zero delay spread yields a cumulative distribution function that approximates the Rayleigh function very well

(Fig. A.1). A lack in the number of sources and realizations is the reason why the model does not fit the exact Rayleigh function for *Log(Power) < -3dB*.

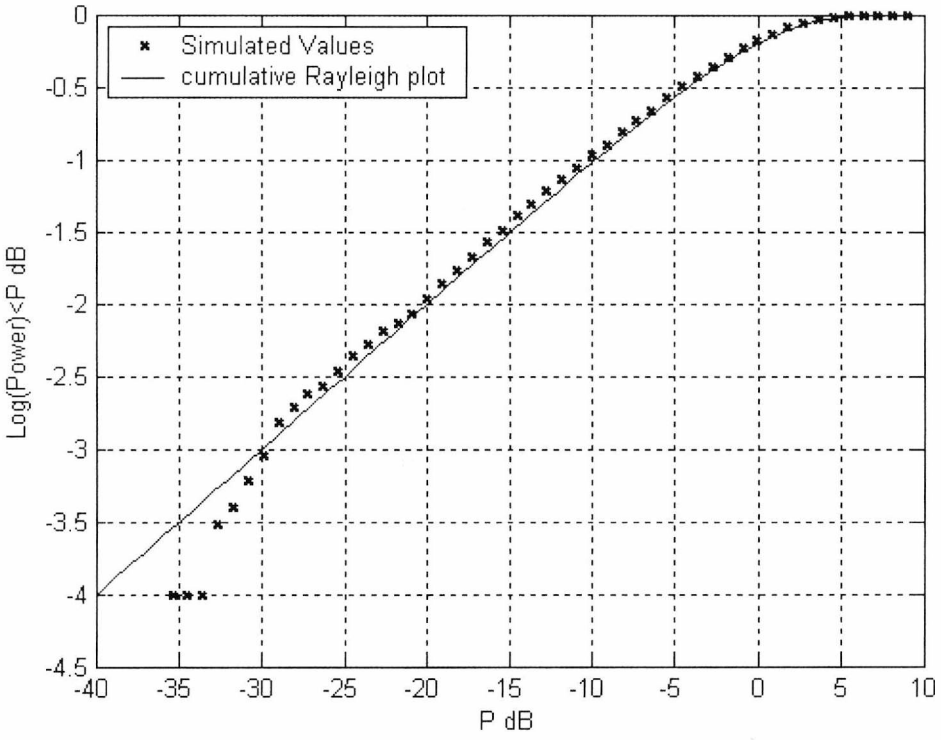

Fig. A.1 A distribution of random sources compared with the exact Rayleigh cumulative distribution function

APPENDIX B
ITU CHANNEL PARAMETERS

This appendix contains the multipath parameters for the downlink in tabular format. The ITU Vehicular A provides a good example of a frequency selective fading channel and the ITU Pedestrian A modelling a nearly flat-fading channel. The Chapter 4 develops multipath estimation filters that are required for channel and delay estimators in rake receivers. This is a very necessary process since the multipath channel filter can be assumed a black box from the receiver perspective.

Table A.1 ITU Vehicular Channel Models

Tap	Channel A		Channel B		Doppler Spectrum
	Relative Delay (ns)	Average Power (dB)	Relative Delay (ns)	Average Power (dB)	
1	0	0	0	-2.5	Classical
2	310	-1.0	300	0	Classical
3	710	-9.0	8900	-12.8	Classical
4	1090	-10.0	12900	-10.0	Classical
5	1730	-15.0	17100	-25.2	Classical
6	2510	-20.0	20000	-16.0	Classical

Table A.2 ITU Pedestrian Channel Models

Tap	Channel A		Channel B		Doppler Spectrum
	Relative Delay (ns)	Average Power (dB)	Relative Delay (ns)	Average Power (dB)	
1	0	0	0	0	Classical
2	110	-9.7	200	-0.9	Classical
3	190	-19.2	800	-4.9	Classical
4	410	-22.8	1200	-8.0	Classical
5	-	-	2300	-7.8	Classical
6	-	-	3700	-23.9	Classical

APPENDIX C
PROBABILITY OF ERROR IN WCDMA WITH DIVERSITY CRITERION

C.1 PROBABILITY OF ERROR ESTIMATION

To analyze the performance of the WCDMA downlink, an important metric of quality measurement is the probability of bit error. This term is usually defined with the input SNR for the channel under investigation. The input SNR is thus the argument against the theoretical BER (depending of course on the mean output SINR of the detector) and is the so called "Symbol energy to noise energy ratio" which in this thesis is taken to be the ideal matched filter output for a single user channel with no interference. This bound is given as the maximum achievable SNR metric in an AWGN channel (given the hypothesis of detection ideology is to generate an optimization/diversity algorithm to approach this bound) with SNR $\gamma_{in} = \frac{2\bar{\varepsilon}_b}{\sigma_n^2}$ yielding a detection probability of error as $P_{minimum} = Q\left(\sqrt{\frac{2\bar{\varepsilon}_b}{\sigma_n^2}}\right)$ that cannot be exceeded at the output of any estimator. The simulations are based on Monte Carlo [Balaban1992] techniques, where the true probability of error is obtained from $P_e = \lim_{N\to\infty}\left\{\frac{N_e}{N}\right\}$ with N_e the number of errors counted over the sample space, N. However, for the estimate of P_e to be within $\beta\times 100\%$ of the true value with probability $1-\alpha$, then $N = \frac{1}{P_e}\frac{Q^{-2}\left(\frac{\alpha}{2}\right)}{\beta^2}$. For large N, $P_e \approx \left\{\frac{N_e}{N}\right\}$ and hence the number of errors to be counted is given by $N_e = \frac{Q^{-2}\left(\frac{\alpha}{2}\right)}{\beta^2}$. The Table C.1 lists some examples of the absolute parametric values and the total number of errors to be counted.

Table C.1 Monte Carlo Simulation Parameters for generating the required error count

A		B	N_e
0.05	95%	0.05	1557
0.02	98%	0.05	1626
0.02	98%	0.02	15550
0.01	99%	0.01	66549

However, due to the error count requiring impermissibly long simulation runs for low additive noise channels, a semi-analytical solution would be more useful for low interference, low additive noise cases. To present a semi-analytical solution, a unified theory is thus presented to enable the probability of error to be calculated for any estimator.

A Unified theory for the Probability of Error as a Function of the Detector Output Signal to Interference + Noise Ratio.

The SINR at the output of any detector can be modelled by the equation (considering the random variable independence assumption)

$$\gamma_k^{(n)} = \frac{\left|d_k^{(n)}\right|^2}{E\left\{\left|\partial_{MAI}^{(n)}\right|^2\right\} + E\left\{\left|\partial_{SI}^{(n)}\right|^2\right\} + \sigma_n^2} \quad \Big| \; n = 1 \ldots N_b \tag{C.1}$$

with $d_k^{(n)}$ the nth demodulated symbol amplitude (assuming cophasing), $\partial_{MAI}^{(n)}$ the MAI at the nth symbol interval, $\partial_{SI}^{(n)}$ the self induced interference, and σ_n^2 the additive noise variance. M is the parameter dependent on the modulation, i.e. for QPSK, $M = 2$. For the Gaussian approximation, (C.1) can be given as

$$\gamma_k^{(n)} = \frac{\left|d_k^{(n)}\right|^2}{\sigma_{MAI}^2 + \sigma_{SI}^2 + \sigma_n^2} \tag{C.2}$$

with mean in Rayleigh Fading channels $\bar{\gamma}_k = \dfrac{\varepsilon_k \cdot E\left\{\left|\alpha_k^{(n)}\right|^2\right\}}{\sigma_{MAI}^2 + \sigma_{SI}^2 + \sigma_n^2}$. Using the known density function $f\left(\bar{\gamma}_k, \gamma_k(n)\right)$ for Rayleigh fading enables calculation of the conditional Probability of Error with

$$P_e = \frac{1}{N_b} \cdot \sum_{n=1}^{N_b} \int_0^{\infty} Q\left(\sqrt{\gamma_k(n)}\right) \cdot f\left(\bar{\gamma}_k, \gamma_k(n)\right) \partial\gamma_k(n) \tag{C.3}$$

where $Q()$ is the Gaussian Error Function and N_b the number of symbols being averaged. The parameters σ^2_{MAI}, σ^2_{SI}, σ^2_n, and $\left|d_k^{(n)}\right|^2$ are all dependent on the type of demodulator used.

C.2 THE SINGLE USER MATCHED FILTER BOUNDS

Consider the implausible frequency-flat fading channel for wideband information, with the received RF signal modeled as

$$r(t) = \sum_{i=1}^{K} \sqrt{\varepsilon_i}\, \alpha \left\{ \chi_I^i(t) cos(\omega_c t + \phi) - \chi_Q^i(t) sin(\omega_c t + \phi) \right\} \tag{C.4}$$

where α is the random fading variables characterized with Rayleigh density function, $\phi \sim U(0, 2\pi^2)$ the uniformly distributed phase[1], with $\chi_I^i(t)$ and $\chi_Q^i(t)$ representing the in-phase and quadrature components of the i^{th} user waveform. After carrier down conversion and filtering of the higher order mixing harmonics, the baseband signal can be represented as (in complex notation)

$$r(t) = \alpha \cdot e^{j\phi} \sum_{i=1}^{K} \sqrt{\varepsilon_i} \left\{ \chi_I^i(t) + j\chi_Q^i(t) \right\} + \eta(t) \tag{C.5}$$

with $\eta(t)$ the additive noise term taking the form of a complex Gaussian RV of two sided PSD in the bandpass region of the signal. Now consider the conventional single user matched filter in a synchronous AWGN channel (formed by equating $\alpha \cdot e^{j\phi} = 1$) with two equiprobable hypotheses[2] under which the observed random variable

$$\boldsymbol{d} = \Re\left\langle \left(\boldsymbol{R}_{SS}\right)_{j,j} \cdot \boldsymbol{E}_{j,j} \cdot \boldsymbol{b}_j + \boldsymbol{\eta}_j \right\rangle \tag{C.6}$$

has density functions

---

[1] The channel phase can also be modified to include the effects of coherent demodulation with differences in the reference and actual carrier phase/frequency.

[2] The data symbols (which we wish to recover with a sign detector) are treated as being a symmetric Bernoulli RV.

$$H_1: \quad \boldsymbol{d} \sim N\left\{\sqrt{\varepsilon_b}, \sigma_n^2\right\}$$
$$H_{-1}: \quad \boldsymbol{d} \sim N\left\{-\sqrt{\varepsilon_b}, \sigma_n^2\right\}.$$

The matched filter (noting that $\chi_1^i(t) = \sum_{g=0}^{G-1}[(\boldsymbol{C} \otimes \boldsymbol{S}^{(n)}) \cdot \partial(n-g)]b_k^{(n)} \cdot \varphi(t - gT_c)$ and assuming orthogonal spreading sequences) is well-known to yield the sufficient decision statistic [Proakis2001, Whalen71] in such a channel, where the optimal decision regions are

$$\Omega_1 = [0, \infty]$$
$$\Omega_{-1} = [-\infty, 0]$$

rendering the most commonly observed single user bound with probability of error

$$P_e = Q\left(\sqrt{\frac{2\varepsilon_b}{\sigma_n^2}}\right) \tag{C.7}$$

with $\bar{\varepsilon}_b$ the average baseband symbol energy and σ_n^2 the matched filter input noise variance based on the measured observations. Note that $j = n + L + (n-1)K$, and $n = 1 \ldots N_b$. In the case of fading channels, the probability of error for any estimator relative to the SNR per symbol (of the nth symbol) at the estimator output $\gamma_b(n)$ (for singular or multiple diversity order) is given by the Gaussian approximation with $\gamma_b(n) = \frac{2 \cdot \alpha(n) \cdot \alpha^*(n) \cdot \varepsilon_b(n)}{\sigma_n^2}$ the SNR relating to the nth data symbol at the output of the matched filter/estimator, $Q\left(\sqrt{\gamma_b(n)}\right) = \int_{\sqrt{\gamma_b(n)}}^{\infty} \frac{1}{\sqrt{2\pi}} exp\left(-\frac{t^2}{2}\right) \partial t$ the well known bit-error probability for signalling over an AWGN channel as a function of the SNR for the nth data symbol, and $f\left(\gamma_b(n)\right)$ the Probability Density Function of the SNR per symbol determined by the fading channel conditions- i.e. in flat Rayleigh fading with diversity order $L=1$, this formula takes the well known form (a chi squared RV with two degrees of freedom) with $f(\gamma_b(n)) = \frac{1}{\bar{\gamma}_b} exp\left\{-\frac{\gamma_b(n)}{\bar{\gamma}_b}\right\}$ where $\bar{\gamma}_b$ is the average channel SNR per realization $\varepsilon_b(n)$ given as $\bar{\gamma}_b = \mathrm{E}\{\gamma_b(n)\} = \frac{2 \cdot E\{\alpha(n) \cdot \alpha^*(n)\} \cdot \varepsilon_b(n)}{\sigma_n^2}$ with $\alpha(n)$ a continuous RV for the nth symbol defined as $\alpha(n) \triangleq \alpha \ \forall \ n$. To indicate this lower bound for a Rayleigh fading channel with $L = 1$, we write (assuming $\varepsilon_b(n)$ is a constant for now)

$$P_{MFbound} = \int_0^{\infty} Q\left(\sqrt{\gamma_b}\right) \cdot f(\gamma_b)\, \partial\gamma_b \tag{C.8}$$

with $\gamma_b = \dfrac{2 \cdot \alpha \cdot \alpha^* \cdot \varepsilon_b}{\sigma_n^2}$ the continuous SNR RV for QPSK with Density function $f(\gamma_b) \triangleq f(\gamma_b(n)) \; \forall n$. In Rayleigh fading, applying the well known formula to the Gaussian error integral [Proakis2001] $Q(\bullet)$, it is relatively trivial to show that

$$P_{MFbound} = \frac{1}{2}\left[1 - \sqrt{\frac{\bar{\gamma}_b}{1+\bar{\gamma}_b}}\right]. \tag{C.9}$$

C.3 THE SEMI ANALYTICAL PERFORMANCE BOUNDS OF THE RAKE RECEIVER

The Rake receiver is a communications device with optimal frequency response for Single User Communications in fading channels. The conventional rake receiver for single user channels can take two forms: A linearly constrained maximum likelihood approach rendering ISI cancellation, or the traditional approach which is to neglect ISI. Both versions of the receiver suffer poor asymptotic efficiency in multi-user channels, particularly if the number of users, K is large and the Near-far ratio large. The derivation of the rake receiver is usually given from a single user perspective, and its performance analyzed in both single and multi-user communication channels. The rake yields the following decision statistic, where

$$y(n) = \sum_{\ell=1}^{L} \left(\hat{\alpha}_\ell^{(n)}\right)^* Z_\ell^{(n)} \tag{C.10}$$

with $Z_\ell^{(n)}$ the output of the l^{th} rake finger (at symbol index, n) and $\hat{\alpha}_\ell^{(n)}$ the corresponding complex channel estimate (weighted with the path loss coefficient and pilot channel symbol energy). The rake finger output $Z_\ell^{(n)}$ prior to combining can be coarsely given by

$$Z_\ell^{(n)} = \frac{1}{sG} \sum_{i=nG_1 s}^{(n+1)G_1 s} r(iT_s) \sum_{j=1}^{G_1} \left(S_j^{(n)}\right)^* C_j^* \varphi\left(iT_s - jT_c - \hat{\tau}_\ell^{(n)}\right) \tag{C.11}$$

with $S_j^{(n)}$ the j^{th} scrambling chip at symbol index, n, C_j the j^{th} channelization/spreading chip, and $\varphi(\bullet)$ the oversampled pulse shape. $\hat{\tau}_\ell^{(n)}$ represents the estimated propagation delay utilizing the timing acquisition techniques presented in the proceeding sections and is a

scalar quantity. To account for probability of error estimation, it is more convenient to represent the rake output in vector format, which can thus be given as

$$\partial_{\text{rake}} = \left\langle \boldsymbol{F}^H \boldsymbol{S}^H r \right\rangle_j \quad \in \mathrm{C}^{N_b} \tag{C.12}$$

where decomposition based on the simulation model yields the decision vector

$$\partial_{\text{rake}}^{(n)} = \left[\underbrace{\underline{\boldsymbol{\Omega} \cdot \boldsymbol{b}}}_{\substack{\text{desired} \\ \text{symbols}}} + \underbrace{\hat{\boldsymbol{F}}^H \left(\boldsymbol{R}_{ss} - diag\left(\boldsymbol{R}_{ss}\right) \right) \boldsymbol{F}\boldsymbol{E}\boldsymbol{b}}_{\text{ISI+MAI}} + \underbrace{\hat{\boldsymbol{F}}^H \boldsymbol{S}^H \boldsymbol{\eta}}_{\text{noise}} \right]_j \tag{C.13}$$

with $j = n + (n\text{-}1)K$, $\boldsymbol{\Omega} = \hat{\boldsymbol{F}}^H diag\left(\boldsymbol{R}_{ss}\right)\boldsymbol{F}\boldsymbol{E}$, $\boldsymbol{R}_{ss} = \boldsymbol{S}^H \boldsymbol{S}$ the signature correlation matrix, $\hat{\boldsymbol{F}}$ the single user channel coefficients/estimates (for the rake MRC solution), and $diag(\bullet)$ representing the diagonal matrix. n is an integer.

The key to this analysis must first consider a method of generating the Gaussian approximation based on the measured SINR. Clearly the SINR will depend chiefly on a number of matters, namely the number of users accessing the channel, the distributions of their powers, the delay spread of the channel, and the processing gain of the desired user being demodulated (with the processing gains of adjacent users also factoring in the level of interference). Treating the MAI and IPI as random noise variables, the rake output SINR per symbol can be given by:

$$\gamma_j^{(k)} = \frac{\left[\left| \boldsymbol{\Omega} \cdot \boldsymbol{b} \right|^2 \right]_{j,j}}{E\left[\left| \hat{\boldsymbol{F}}^H \left(\boldsymbol{R}_{ss} - diag\left(\boldsymbol{R}_{ss}\right) \right) \boldsymbol{F}\boldsymbol{E}\boldsymbol{b} \right|^2 \right]_{j,j} + E\left[\left| \hat{\boldsymbol{F}}^H \boldsymbol{S}^H \boldsymbol{\eta} \right|^2 \right]_{j,j}} \tag{C.14}$$

Denote $\sum_{MAI} = \boldsymbol{R}_{ss} - diag(\boldsymbol{R}_{ss})$, $\boldsymbol{A} = \hat{\boldsymbol{F}}^H \sum_{MAI} \boldsymbol{F}$, $\boldsymbol{d} = \boldsymbol{E}_b$, $\sum_d = E\left(\boldsymbol{d} \cdot \boldsymbol{d}^H\right)$, and $\sum_h = E\left(\hat{\boldsymbol{F}}^H \boldsymbol{F}\right) = diag\left[\nu_{1,1}^{*(0)} \cdot \alpha_{1,1}^{(0)}, \cdots, \nu_{K,L}^{*(Nb)} \cdot \alpha_{K,L}^{(Nb)} \right]^{\mathrm{T}}$. Hence

$$\gamma_j^{(k)} = \frac{\left[\sum_h \sum_d \right]_{j,j}}{\left[\boldsymbol{A} \sum_d \boldsymbol{A}^H \right]_{j,j} + \left[\hat{\boldsymbol{F}}^H \boldsymbol{S}^H \sum_\eta \boldsymbol{S}\hat{\boldsymbol{F}} \right]_{j,j}}. \tag{C.15}$$

For input uncorrelated Gaussian noise, $\sum_\eta = \sigma_n^2 \boldsymbol{I}$ and QPSK signals,

$$\gamma_j^{(k)} = \frac{\left[\sum_h \sum_d \right]_{j,j}}{\left[\boldsymbol{A} \sum_d \boldsymbol{A}^H \right]_{j,j} + \sigma_n^2 \left[\hat{\boldsymbol{F}}^H \boldsymbol{R}_{ss} \hat{\boldsymbol{F}} \right]_{j,j}} \tag{C.16}$$

with $j = n + L + (n\text{-}1)K$, and $n = 1 \ldots N_b$. Equating the density function $f(\gamma_{out})$ for Rayleigh fading allows the conditional probability of error to be calculated with (C.8). The

SINR is conditioned on the channel (where interference and noise is assumed Gaussian), which is also made constant for obtaining the expectations over random bit patterns and signalling powers of MAI. $\boldsymbol{R}_{ss}$ is normalized such that the trace, $tr(\boldsymbol{R}_{ss}) = N_b$. The conditional P_e is obtained from

$$P(y|F) = \frac{1}{N_b}\sum_j \Re\left(Q\left(\sqrt{\gamma_j}\right)\right)$$

For random fading initialisation, we must average over all conditional PDF's (where MAI is also dependent on $\boldsymbol{F}$). Hence

$$P_e = \frac{1}{N_b N_f}\sum_f \sum_j \Re\left(Q\left(\sqrt{\gamma_{j,f}}\right)\right)$$

or rather

$$P_e = \frac{1}{N_b}\sum_j \int_0^\infty \Re\left(Q\left(\sqrt{\gamma_j}\right)\right) \cdot f(\gamma_j)\, \partial\gamma_j$$

C.4 Analytical Derivation for Idealistic L-fold Diversity for a Rake Receiver with Unequal Branch SNR's.

Assume that the noise at the output of the rake receiver is known and Gaussian, where the signal powers scattered over L paths are combined in an optimal manner such that the instantaneous SNR per symbol is maximized [Brenna1959]. The SNR at the ideal rake receiver output is therefore

$$\gamma_{out} = \sum_{i=0}^{L-1} \gamma_i \qquad \text{(C.16)}$$

with $\gamma_i^{(n)} = \dfrac{\alpha_i^{(n)} \cdot \alpha_i^{(n)*} \cdot \varepsilon_b}{\sigma_{N,i}^2}$ the i^{th} diversity branch instantaneous SNR (where $\alpha_i^{(n)}$ is the instantaneous fading coefficient and $\sigma_{N,i}^2$ the variance of the noise floor) of first moment $\bar{\gamma}_i = \dfrac{E\{\alpha_i^{(n)} \cdot \alpha_i^{(n)*}\} \cdot \varepsilon_b}{\sigma_{N,i}^2}$. The i^{th} Moment Generating function for a single Rayleigh distributed channel SNR, $M_i(\nu) = \dfrac{1}{1 - \gamma_i \nu}$ (with ν a transformation variable) can be

extended to a diversity system on the basis of assumption that each multipath component has independent Rayleigh distribution with different second moments. The characteristic

$$M_{out}(\nu) = \prod_{i=0}^{L-1} \frac{1}{1 - \bar{\gamma}_i \nu} \tag{C.17}$$

can be used to calculate the density function, $f(\gamma_{out})$ of the output SNR applying the method of partial fractions. Using the known transform pair $\frac{1}{1-\bar{\gamma}_i \nu} \Leftrightarrow \frac{1}{\bar{\gamma}_i} exp\left\{-\frac{\gamma_i}{\bar{\gamma}_i}\right\}$, $M_{out}(\nu)$ is henceforth represented by

$$M_{out}(\nu) = \sum_{i=0}^{L-1} \frac{A_i}{1 - \bar{\gamma}_i \nu} \tag{C.18}$$

with $A_i = \left[\prod_{\substack{k=0 \\ k \neq i}}^{L-1} \left(1 - \frac{\bar{\gamma}_k}{\bar{\gamma}_i}\right)\right]^{-1}$ formed by equating (C.18) with (C.17). It is relatively easy to show that the density function of the output SNR can be formulated as

$$f(\gamma_{out}) = \sum_{i=0}^{L-1} \left[\bar{\gamma}_i \left\{\prod_{\substack{k=0 \\ k \neq i}}^{L-1} \left(1 - \frac{\bar{\gamma}_k}{\bar{\gamma}_i}\right)\right\}\right]^{-1} \cdot exp\left\{-\frac{\gamma_{out}}{\bar{\gamma}_i}\right\} \tag{C.19}$$

with the probability of error given by the Gaussian approximation

$$\begin{aligned} P_e(\bar{\gamma}) &= \int_0^{\infty} Q\left(\sqrt{\gamma_{out}}\right) \cdot f(\gamma_{out})\, \partial\gamma_{out} \\ &= \sum_{i=0}^{L-1} \frac{1}{\sqrt{2\pi}} \cdot \left[\bar{\gamma}_i \left\{\prod_{\substack{k=0 \\ k \neq i}}^{L-1} \left(1 - \frac{\bar{\gamma}_k}{\bar{\gamma}_i}\right)\right\}\right]^{-1} \int_0^{\infty} \int_{\sqrt{2\gamma_{out}}}^{\infty} exp\left\{-\frac{x^2}{2}\right\} \cdot exp\left\{-\frac{\gamma_{out}}{\bar{\gamma}_i}\right\} \partial x \partial\gamma_{out} \end{aligned} \tag{C.20}$$

There is a closed loop form that can be applied to this double integral. Performing this integral yields the probability of error for the ideal rake receiver where

$$P_e = \frac{1}{2} \sum_{i=0}^{L-1} \left\{\prod_{\substack{k=0 \\ k \neq i}}^{L-1} \left(1 - \frac{\bar{\gamma}_k}{\bar{\gamma}_i}\right)\right\}^{-1} \cdot \left(1 - \sqrt{\frac{\bar{\gamma}_i}{2 + \bar{\gamma}_i}}\right) \tag{C.21}$$

C.5 Analytical Derivation for Idealistic M by L-fold Diversity for a 2D Rake Receiver with Partial Equality in the Branch SNR's.

A very similar analysis can ensue for the 2D Rake receiver employing Maximum Ratio Combining [Simon1998]. Consider the same assumptions as in the single-antenna rake receiver, except this time M diversity antennas are introduced to the system to combat fading. Starting with the SNR

$$\gamma_{out} = \sum_{i=0}^{ML-1} \gamma_i \tag{C.22}$$

and Moment Generating function $M_{out}(\nu) = \prod_{i=0}^{ML-1} \frac{1}{1-\bar{\gamma}_i \nu}$ from a generic sense, it would be highly useful in the model to split the multiplicative chain into corresponding pairs of identically (and assumed independently) distributed adjacent channels of same mean SNR. In this case,

$$M_{out}(\nu) = \prod_{i=0}^{L-1} \frac{1}{(1-\bar{\gamma}_i \nu)^M} \tag{C.23}$$

which has a well-known mapping to a chi-squared distribution with $2M$ degrees of freedom, i.e. $\frac{1}{(1-\bar{\gamma}_i \nu)^M} \Leftrightarrow \frac{\gamma_i^{M-1}}{(M-1)!\,\bar{\gamma}_i^M} exp\left\{-\frac{\gamma_i}{\bar{\gamma}_i}\right\}$. As in the previous example, applying the method of partial fractions yields

$$M_{out}(\nu) = \sum_{d=1}^{M} \sum_{i=0}^{L-1} \frac{A_{d,i}}{(1-\bar{\gamma}_i \nu)^d} \tag{C.24}$$

with $A_i = \left[\prod_{\underbrace{f=1}_{f \neq d}}^{M} \prod_{\underbrace{k=0}_{k \neq i}}^{L-1} \left(1 - \frac{\bar{\gamma}_{k,f}}{\bar{\gamma}_{i,d}}\right) \right]^{-1}$ formed by equating (C.24) with (C.22). The density function of the output SNR can be expressed as:

$$f(\gamma_{out}) = \sum_{d=1}^{M} \sum_{i=0}^{L-1} \left((d-1)!\,\bar{\gamma}_i^d \left\{ \prod_{\underbrace{f=1}_{f \neq d}}^{M} \prod_{\underbrace{k=0}_{k \neq i}}^{L-1} \left(1 - \frac{\bar{\gamma}_{k,f}}{\bar{\gamma}_{i,d}}\right) \right\}^{-1} \cdot \left(\gamma_{out}^{d-1} \cdot \left[exp\left\{-\frac{\gamma_{out}}{\bar{\gamma}_i}\right\} \right] \right) \right) \tag{C.25}$$

and the probability of error given by the Gaussian approximation where

$$P_e(\bar{\gamma}) = \int_0^{\infty} Q\left(\sqrt{\gamma_{out}}\right) \cdot f(\gamma_{out})\, \partial\gamma_{out}$$

$$= \frac{1}{\sqrt{2\pi}} \sum_{d=1}^{M} \sum_{i=0}^{L-1} \left((d-1)!\, \bar{\gamma}_i^{\,d} \prod_{\substack{f=1 \\ f\neq d}}^{M} \prod_{\substack{k=0 \\ k\neq i}}^{L-1} \left(1 - \frac{\bar{\gamma}_{k,f}}{\bar{\gamma}_{i,d}}\right) \right)^{-1} \int_0^{\infty} \int_{\sqrt{2\gamma_{out}}}^{\infty} exp\left\{-\frac{x^2}{2}\right\} \cdot \gamma_{out}^{d-1} \cdot \left[exp\left\{-\frac{\gamma_{out}}{\bar{\gamma}_i}\right\} \right] \partial x \partial \gamma_{out}$$

Assuming a M-antenna diversity assisted MRC system transmitting over Rayleigh flat fading channels, a closed form solution for the component BER can be obtained where

$$P_e = \sum_{d=1}^{M} \sum_{i=0}^{L-1} \left(\prod_{\substack{f=1 \\ f\neq d}}^{M} \prod_{\substack{k=0 \\ k\neq i}}^{L-1} \left(1 - \frac{\bar{\gamma}_{k,f}}{\bar{\gamma}_{i,d}}\right) \right)^{-1} \left\{ \frac{1 - U^{(i)}}{2} \right\}^{d} \sum_{e=0}^{d-1} \binom{d-1+e}{e} \left\{ \frac{1}{2}\left(1 + U^{(i)}\right) \right\}^{e} \qquad \text{(C.26)}$$

where $U^{(i)} = \sqrt{\dfrac{\bar{\gamma}_i}{2 + \bar{\gamma}_i}}$, and $\binom{d-1+e}{e} = \dfrac{(d-1+e)!}{(d-1)!\,e!}$. This model assumes that the L Rake fingers on each diversity antenna branch are uncorrelated and have same mean SNR, i.e. $\bar{\gamma}_i = \bar{\gamma}_{i,d}\ \forall d$.

C.6 Derivation of Rake Mean Finger SINR

We can start with the mean SINR per finger, where

$$\bar{\gamma}_i = \frac{\xi_b^{2(i)}}{\sigma_{MAI,i}^2 + \sigma_{SI,i}^2 + \sigma_{n,i}'^2} \qquad \text{(C.27)}$$

with $\xi_b^{2(i)}$ the desired single user channel symbol energy accounting for path loss, shadowing, the transmitting power control and receiver (plus transmitter) antenna gain. $\sigma_{MAI,i}^2$, $\sigma_{SI,i}^2$ and $\sigma_{n,i}'^2$ represent the multiple access interference, self interference and noise second central moments for the i[th] rake finger respectively.

The simplest model is to assume long RSS codes, allowing the random access code supposition. This can allow a relationship or model to be developed, considering the sliding window dot product between two random codes that exhibit no correlation in the long term. A further useful assumption is that the number of chip boundaries with transitions (where the exact location of the boundaries and their ordering vary from code block to code block).

This is actually a fairly accurate model, when long scrambling PN sequences overlay the Walsh-Hadamard (deterministic) multiuser codes, where provided, the access channel is frequency selective, the digitized signal for a path that constitutes an interference will exhibit little or no correlation with the path-synchronized PN code. Therefore, the demodulated interference prior to matched filtering will 'appear' to be a random code. A further assumption used is that $min[\tau_{delay}] \geq \tau_c$, e.g. the minimum delay acquired by the receiver synchronization equipment is greater than or equal to a chip period. Interference can be treated stochastically at chip and symbol level, where the timing-path difference $\Delta\tau$ defines the correlation metric at the output of the pulse shaping matched filter. The output of the RRC is downsampled to chip rate for simplicity of analysis, for example, each rake receiver consists of a fractional delay offset chip baud rate sampler. The transmitter pulse-shaping filter is assumed to be truncated FIR version of the real impulse response. It may be noted, for any fixed chip time interval (used by the receiver for code acquisition), the chip span of the receiver filter = N_c and that for any chip sample index, the propagation channel incurs past, present and future chip samples that interfere with the desired channel (ignoring the receiver tails at beginning and end of transmission if zero padding is used). We can model the total interference (at chip level) at the output of the RRC, applying a slightly modified version of Model 2 in Chapter 2 where, for any Rake finger, L, the self and multiple access interference can be given by:

$$y_{sI}^{L} = \boldsymbol{Q}_L^T \left\{ \boldsymbol{Q}_I^{(\alpha \neq L} \boldsymbol{\theta}_i \right\} + \left\{ \left\{ \boldsymbol{Q}_L^T \boldsymbol{Q}_L \right\} - \xi_{\max} \cdot \boldsymbol{I} \right\} \boldsymbol{\theta}_L \tag{C.28}$$

where, $\boldsymbol{\theta}_l = \boldsymbol{C}_l \boldsymbol{S}_1 \sqrt{\boldsymbol{E}_b^{2(l)}} \boldsymbol{b}_1$ is the channel modulated desired chip vector (of rank equivalent to the length of the transmitted block minus any tails), $\boldsymbol{\theta}_i = \boldsymbol{C}_{\substack{1:L \\ \alpha \neq L}} \left[\boldsymbol{S}_1 \sqrt{\boldsymbol{E}_b^{(l)}} \boldsymbol{b}_1 \right]$, and $\boldsymbol{Q}_l^{(\alpha \neq L)}$ is the pulse shaping convolution matrix defined for paths $\alpha = 1:L$, $\alpha \neq L$. $\boldsymbol{Q}_l$ is the pulse shaping convolution matrix for path L and $\xi_{\max}$ is the maximum vector inner product of the pulse shapes. The MAI vector can be similarly defined as:

$$\boldsymbol{y}_{MAI}^{(l)} = \boldsymbol{Q}_l^T \left\{ \boldsymbol{Q}_l^{(\alpha \neq l)} \boldsymbol{\theta}_{MAI}^{(\alpha \neq l)} \right\} \tag{C.29}$$

with

$$\boldsymbol{\theta}_{MAI}^{(\alpha \neq l)} = \boldsymbol{C}_{\substack{1:L \\ \alpha \neq l}} \sum_{\substack{\alpha=1 \\ \alpha \neq l}}^{L} \sum_{K=2}^{K} \boldsymbol{S}_k \sqrt{\boldsymbol{E}_k^{(\alpha)}} \cdot \boldsymbol{b}_k \,. \tag{C.30}$$

Now we derive a generic theorem for estimating the chip-level statistics at the output of the receiver front-end matched filter for any sampled output delay offset of τ_l.

We model each individual user and each single path for the interference (self and multiple access) estimate. The total interference per path/finger will be characterized

independently at the output of the chip matched filter, where all path-related, user-path related interference will be summed to form a single discrete RV. For notational convenience, we will assume the channel is static and characterized by a random, complex scalar and a net path-loss term.

Consider the l^{th} propagation path, e.g. the l^{th} Rake finger. The interference due to the M^{th} path $(M \neq l)$ can be defined as:

$$\boldsymbol{y}_{SIM}^{(l)} = \left(\sum_{Q}^{(L)} - \xi_{MAX}\boldsymbol{I}\right)\boldsymbol{\theta}_l \tag{C.31}$$

$$\boldsymbol{y}_{SI}^{(l,m)} = \boldsymbol{Q}_l^T\left\{\boldsymbol{Q}_m\left(\boldsymbol{C}_m\boldsymbol{S}_1\sqrt{\boldsymbol{E}_b^{(m)}}\boldsymbol{b}_1\right)\right\} \tag{C.32}$$

$$\boldsymbol{y}_{MAI}^{(l,m,k)} = \boldsymbol{Q}_l^T\left\{\boldsymbol{Q}_m\left(\boldsymbol{C}_m\boldsymbol{S}_k\sqrt{\boldsymbol{E}_k^{(m)}}\boldsymbol{b}_k\right)\right\} \tag{C.33}$$

Looking at the problem from a 'per sample' basis, define

$$y_{SIM}^{(L)}[u] = \sum_{\substack{i=-Nc \\ i\neq 0}}^{Nc}\left\{\varphi_{(v-\partial_l)}^T \cdot \varphi_{(v-\partial_l - is)}\right\}\cdot x\left[u - \left\lfloor\frac{T_l}{T_c}\right\rfloor - i\right] \tag{C.34}$$

with s = number of samples per chip, v the sampling variable for the continuous pulse mapped to the discrete function spanning $2(F_T - 1)$ samples where F_T is the number of matched filter taps. ∂_l is the l^{th} propagation delay represented by $\partial_l = \left\langle\frac{T_l}{T_c}\right\rangle \cdot s$ with $\langle\cdot\rangle$ the rounding function. u is the chip index, $\lfloor\cdot\rfloor$ the floor function and N_c represents the number of chip samples either side the axis of symmetry of the filter impulse response, which is considered for all past and future chip samples that can interfere with the filter window. This is given by $N_c = \frac{F_T - 1}{2s}$ where the practical FIR filter length, F_T is designed to span 16 chip intervals, e.g., $F_l = 127$ for S=8 samples per chip similarly,

$$y_{SIM}^{(l,m)}[u] = \sum_{i=-Nc}^{Nc}\left\{\varphi_{(v-\partial_l)}^T \cdot \varphi_{(v-\partial_m - is)}\right\}\cdot x\left[u - \left\lfloor\frac{T_m}{T_c}\right\rfloor - i\right] \tag{C.35}$$

With ∂_m, T_m, the m^{th} delay variables with $m \neq l$.

$$y_{MAI}^{(l,m,k)}[u] = \sum_{i=-Nc}^{Nc}\left\{\varphi_{(v-\partial_l)}^T \cdot \varphi_{(v-\partial_m - is)}\right\}\cdot x_k\left[u - \left\lfloor\frac{T_m}{T_c}\right\rfloor - i\right] \tag{C.36}$$

where $x_k[\cdot] = C_m S_k[\cdot]\sqrt{E_k^{(n)}b_k}$. Note that τ_c represents the chip period and $\varphi_{(\bullet)}$ a column from the matrix $\boldsymbol{Q}$ depending on the path delay and relative time interval. Clearly thus far, all interference random variables obtained over the filter window are formed from only a limited number of combinational probabilities if S_c is assumed a Bernoulli RV (provided the channel is completely static). The statistics of y_{SI} and y_{MAI} will span two equiprobable spaces

(where one space contains 'mostly' negative values and the other 'mostly' positive values). The actual density functions are highly difficult to obtain, but it may be assumed that both y_{SI} and y_{MAI} will have certain mean and certain second central moments. The analysis can be simplified if we treat each chip sample of $x^{(n)}$ as a Bernoulli RV and additionally, treat a block of G chips from each contribution as an uncorrelated multivariate problem. Using this assumption (in conjunction with RSS assumption), the statistics at the output of a chip matched filter (with desired Walsh-Hadamard code) will be binomial for any one individual contribution. Provided G is large enough, the central limit theorem comes into play and this random variable can be approximated as zero mean Gaussian. We can then approximate the CMF dot product as producing (for uncorrelated variable assumption):

$$y_{SI}^{(l,m)}[u] \sim N\left(0, \sum_{i=-N_c}^{N_c} \left| \frac{\varphi_{(v-\partial_l)}^T \cdot \varphi_{(v-\partial_m - is)}}{\xi_{\max}^2} \right|^2 \cdot E_b^{(m)} \cdot \frac{\beta^{(m)}}{G}\right) \tag{C.37}$$

$$y_{MAI}^{(l,m,k)}[u] \sim N\left(0, \sum_{i=-N_c}^{N_c} \left| \frac{\varphi_{(v-\partial_l)}^T \cdot \varphi_{(v-\partial_m - is)}}{\xi_{\max}^2} \right|^2 \cdot E_k^{(m)} \cdot \frac{\beta^{(m)}}{G}\right) \tag{C.38}$$

$$y_{SIM}^{(L)}[u] \sim N\left(0, \sum_{\substack{i=-N_c \\ i\neq 0}}^{N_c} \left| \frac{\varphi_{(v-\partial_l)}^T \cdot \varphi_{(v-\partial_l - is)}}{\xi_{\max}^2} \right|^2 \cdot E_b^{(l)} \cdot \frac{\beta^{(l)}}{G}\right) \tag{C.39}$$

This is the analysis for one interference path, so it can be written more generally for the l^{th} Rake finger,

$$\sigma_{SI,l}^2 = \sum_{\substack{m=0 \\ m\neq l}}^{L} \sum_{i=-N_c}^{N_c} \left| \frac{\varphi_{(v-\partial_l)}^T \cdot \varphi_{(v-\partial_m - is)}}{\xi_{\max}^2} \right|^2 \cdot E_b^{(m)} \cdot \frac{\beta^{(m)}}{G} \tag{C.40}$$

$$\sigma_{MAI,l}^2 = \sum_{k=2}^{K} \sum_{\substack{m=0 \\ m\neq l}}^{L} \sum_{i=N_c}^{N_c} \left| \frac{\varphi_{(v-\partial_l)}^T \cdot \varphi_{(v-\partial_m - is)}}{\xi_{\max}^2} \right|^2 \cdot E_k^{(m)} \cdot \frac{\beta^{(m)}}{G} \tag{C.41}$$

$$\sigma_{SIM,l}^2 = \sum_{i=-N_c}^{N_c} \sum_{\substack{i=-N_c \\ i\neq 0}}^{N_c} \left| \frac{\varphi_{(v-\partial_l)}^T \cdot \varphi_{(v-\partial_l - is)}}{\xi_{\max}^2} \right|^2 \cdot E_b^{(l)} \cdot \frac{\beta^{(l)}}{G} \tag{C.42}$$

Denote the general energy variable (relative to the transmitted signal amplitude and signal path loss) as $E \Rightarrow \beta E$. Also treat the self-interference and multiple access interference jointly; where for the i^{th} Rake Finger, the total interference is given by

$$\sigma_{I,l}^2 = \sum_{k=1}^{K} \sum_{\substack{m=0 \\ m \neq l}}^{L} \sum_{i=N_c}^{N_c} \frac{\left| \varphi_{(v-\partial_l)}^T \cdot \varphi_{(v-\partial_m - is)} \right|^2 E_k^{(m)}}{\xi_{\max}^2 G} \tag{C.43}$$

It is thus fairly easy to show that the SINR conditioned for a rake finger $\bar{\gamma}_i$ is given by

$$\bar{\gamma}_i = \frac{\xi_{\max}^2 G \mathrm{E}_1^{(i)}}{\sum_{k=1}^{K} \sum_{\substack{m=0 \\ m \neq i}}^{L} \sigma_{M,i(m)}^2 \mathrm{E}_k^{(m)} + \sigma_{RI,i}^2 + \xi_{\max}^2 G \sigma_\eta^2} \tag{C.44}$$

with σ_η^2 the additive noise floor, $\sigma_{M,i(m)}^2 = \sum_{a=-N_c}^{N_c} \left| \varphi_a^T \varphi_{m-as} \right|^2$ and $\sigma_{RI,i}^2 = \sum_{\substack{a=-N_c \\ a \neq 0}}^{N_c} \left| \varphi_i^T \varphi_{i-as} \right|^2 \mathrm{E}_1^{(i)}$.

FURTHER RAKE ASSUMPTIONS

MAI and SI are Gaussian RV's after CMF. This is a reasonable approximation for static channels given that long filtering windows for each individual path (that is uncorrelated with the Hadamard sequence), produces a binomially distributed RV that tends toward a Gaussian distribution by central limit theorem (particularly if G is quite large). For non-static channels, the fading channel induced envelope produces a PDF more akin to the exponential distribution (for Rayleigh fading) than Gaussian. Further assumptions useful for Chapter 4 are:

(A) The Rake has the MRC decision rule accounting for variances for interference and noise and the envelope, hence, $y_{out} = \sum_{i=l}^{L} y_i$.

(B) The statistics of SINR are characterized by the exponential distribution where this may not necessarily be true.

APPENDIX D
RECURSIVE LEAST SQUARES ALGORITHM

In the RLS algorithm, the cost function (using averaging to calculate the expectation)

$$J(k) = \sum_{i=1}^{n} \lambda^{n-i} \, (|\, \zeta(n)|^2 \,) \tag{D.1}$$

is minimized where $0<<\lambda \leq 1$ is the forgetting factor (i.e. a weighted averaging factor), $i=1,2,...,n$ and $\zeta(n)$ the a priori estimation error defined by $\zeta(n) = d(n) - \mathbf{w}^H(n-1)\,\mathbf{r}(n)$. Note that n and k are sample index/time parameters, where k quantifies the "current" time sample and $n=k-1$. When $\lambda = 1$, the RLS algorithm becomes the method of least squares, i.e. the inverse of $1-\lambda$ is a measure of the memory of the algorithm where the special case $\lambda=1$ corresponds to infinite memory. Some examples of the RLS family of linear adaptive filtering algorithms are classified in [Haykin1996], including the RLS algorithm used in this thesis that assumes adaptive memory to automatically tune the forgetting factor λ. The algorithm can be given by the following derivation where the k^{th} gradient estimate is defined by

$$\psi(k) = \frac{\partial w(k)}{\partial \lambda} \tag{D.2}$$

where differentiating the cost function $J(k)$ with respect to λ yields

$$\nabla_{\lambda}(n) = \frac{\partial J(k)}{\partial \lambda} = -\frac{1}{2} E[\psi^H(k-1)r(k)\xi^*(k) + r^H(k)\psi(k-1)\xi(k)\,] \tag{D.3}$$

The updated weight vector for time k is related to the gain vector $\mathbf{G}(k)$ where

$$\mathbf{w}(k) = \mathbf{w}(k-1) + \mathbf{G}(k)\,\zeta^*(k) \tag{D.4}$$

with $\mathbf{G}(k)$ given by

$$\mathbf{G}(k) = \frac{\lambda^{-1}\hat{\Sigma}_{xx}(k-1)r(k)}{1+\lambda^{-1}r^H(k)\hat{\Sigma}_{xx}(k-1)r(k)} \tag{D.5}$$

and

$$\hat{\Sigma}_{xx}(k) = \lambda^{-1}\,\hat{\Sigma}_{xx}(k-1) - \lambda^{-1}\,\mathbf{G}(k)\,\mathbf{r}^H(k)\,\hat{\Sigma}_{xx}(k-1) \tag{D.6}$$

Let $\mathbf{S}(k)$ denote the derivative of the inverse correlation matrix $\hat{\Sigma}_{xx}(k)$ with respect to λ, where

$$\boldsymbol{S}(k) = \frac{\partial \hat{\Sigma}_{xx}(k)}{\partial \lambda} \tag{D.7}$$

and thus

$$\boldsymbol{S}(k) = \lambda^{-1}[\boldsymbol{I} - \boldsymbol{G}(k)\,\boldsymbol{r}^{H}(k)]\,\boldsymbol{S}(k-1)\,[\boldsymbol{I} - \boldsymbol{r}(k)\boldsymbol{G}^{H}(k)] + \lambda^{-1}\,\boldsymbol{G}(k)\,\boldsymbol{G}^{H}(k) - \lambda^{-1}\,\hat{\Sigma}_{xx}(k) \tag{D.8}$$

Substituting $\zeta(n) = d(n) - \boldsymbol{w}^{H}(n-1)\,\boldsymbol{r}(n)$ and (D.4) and (D.7) into (D.2) yields

$$\psi(k) = [\boldsymbol{I} - \boldsymbol{G}(k)\,\boldsymbol{r}^{H}(k)]\;\psi(k-1) + \boldsymbol{S}(k)\,\boldsymbol{r}(k)\,\zeta^{*}(k) \tag{D.9}$$

The forgetting factor λ(k) adaptively computed and hence

$$\lambda(k) = \lambda(k-1) + \alpha\, Re[\psi^{H}(k-1)\,\boldsymbol{r}(k)\,\zeta^{*}(k)] \tag{D.10}$$

where α is a small, positive learning – rate parameter.

The applicability of the RLS algorithm requires that we initialize the recursion (D.6) by selecting and initial condition $\hat{\Sigma}_{xx}(0)$ that ensures nonsingularity of the correlation matrix [Glisic1997]. The initial value of $\hat{\Sigma}_{xx}(0)$ can be selected as

$$\hat{\Sigma}_{xx}(0) = \delta^{-1}\boldsymbol{I} \tag{D.11}$$

with δ a positive small fractal. The initial value of weight vector is set to the vector of zeros, i.e. $\boldsymbol{w}(0) = \boldsymbol{0}$ with $\boldsymbol{0}$ is the N-by-1 null vector. The positive δ should be small compared to $0.01\sigma^{2}$, with σ^{2} the variance of the data sample $\boldsymbol{r}(k)$. The RLS algorithm with adaptive memory can be summarized as: Initialize $\hat{w}(0)$, $\hat{\Sigma}_{xx}(0)$, $\lambda(0)$, $\boldsymbol{S}(0)$, *and* $\hat{\psi}(0)$, and compute for $n > 0$ the following equations:

$$\boldsymbol{G}(k) = \frac{\lambda^{-1}\hat{\Sigma}_{xx}(k-1)r(k)}{1+\lambda^{-1}r^{H}(k)\hat{\Sigma}_{xx}(k-1)r(k)}$$

$$\zeta(k) = d(k) - \hat{w}^{H}(k-1)\,\boldsymbol{r}(k)$$

$$\boldsymbol{w}(k) = \hat{w}(k-1) + \boldsymbol{G}(k)\,\zeta^{*}(k)$$

$$\boldsymbol{P}(k) = \lambda^{-1}\hat{\Sigma}_{xx}(k-1) - \lambda^{-1}\boldsymbol{G}(k)\,\boldsymbol{r}^{H}(k)\,\hat{\Sigma}_{xx}(k-1)$$

$$\lambda(k) = \lambda(k-1) + \alpha\, Re[\hat{\psi}^{H}(k-1)\,\boldsymbol{r}(k)\,\zeta^{*}(k)]]_{\lambda_{-}}^{\lambda_{+}}$$

$$\boldsymbol{S}(k) = \lambda^{-1}[\boldsymbol{I} - \boldsymbol{G}(k)\,\boldsymbol{r}^{H}(k)]\,\boldsymbol{S}(k-1)\,[\boldsymbol{I} - \boldsymbol{r}(k)\boldsymbol{G}^{H}(k)] + \lambda^{-1}\boldsymbol{G}(k)\,\boldsymbol{G}^{H}(k) - \lambda^{-1}\hat{\Sigma}_{xx}(k)$$

$$\psi(k) = [\boldsymbol{I} - \boldsymbol{G}(k)\,\boldsymbol{r}^{H}(k)]\,\hat{\psi}^{H}(k-1) + \boldsymbol{S}(k)\,\boldsymbol{r}(k)\,\zeta^{*}(k)$$

The parameters λ_{-} and λ_{+} are the conditional limits for the forgetting factor, where if $\lambda > \lambda_{+}$ then $\lambda = \lambda_{+}$ otherwise $\lambda = \lambda_{-}$.

APPENDIX E
ANTENNA ARRAY COMBINING

This Appendix expatiates upon the Maximum Ratio Combiner and the Blind beamforming technique suggested in Chapter 2, section 2.3.2. Brief derivations and appropriate references are yielded for the reader's convenience.

E.1 EQUAL GAIN AND MAXIMUM RATIO COMBINING

Equal Gain and Maximum Ratio Combining (MRC) are now ubiquitous techniques with application in almost every conceivable wireless radio network for over 40 years. Consequently, this thesis will not cover this topic in any detail where the work carried out in [Balaban1992, Vaughan1988, Brennan1959] contains an in-depth account of applying spatial diversity. The Equal Gain combiner simply utilizes unity weights- i.e. combining all channels assuming each is of equal merit in terms of the branch SNR's. Hence in a classical diversity sense, the only requirement is cophasing- which is a technique that utilizes channel phase estimation on each diversity branch to remove the phase content (induced by multipaths and phase errors in the down-conversion) of the channel prior to combining. It is well known that this technique is not optimum in frequency-flat or frequency-selective channels in realistic scenarios [Lee1985] since the instantaneous SNR metrics on adjacent channels are unlikely to be equivalent (and in the frequency-selective channel, the branch SINR is likely to be very different). The MRC technique is marginally more complicated than the EGC technique since the diversity combiner employs a dynamic weight adjustment on each spatial/temporal diversity channel. The maximum ratio combining solution to a generic diversity receiver/beamformer was derived in [Brennan1959], where the weight vector W_{MRC} is given by

$$W_{MRC} = \kappa\sqrt{\gamma} \cdot W_{EGC} \in C^L \tag{E.1}$$

where κ is a constant of proportionality, $W_{EGC} = [\alpha_1^*, \alpha_2^* \ldots, \alpha_L^*]^T \in C^L$ the EGC vector where α_i is the complex phase of the i^{th} channel, and $\gamma = diag\left[\frac{\gamma_1}{\sigma_{n,1}^2}, \frac{\gamma_2}{\sigma_{n,2}^2} \ldots, \frac{\gamma_L}{\sigma_{n,L}^2}\right] \in R^{L\times L}$ the SNR diagonal matrix with

$\gamma_i = \frac{\sigma_{s,i}^2}{\sigma_{n,i}^2} = \frac{\beta_i E_b}{\sigma_{n,i}^2}$ the SNR for channel i (where β_i is the random fading/envelope energy variable for path i) estimated over a finite observation interval. In inner product form, the diversity combiner output $y(t)$ can be modeled (considering L diversity branches) with

$$y(t) = \sum_{i=1}^{L} \frac{\kappa}{\sigma_{n,i}} \cdot \sqrt{\gamma_i(t)} \cdot \alpha_i^*(t) \cdot x_i(t) \tag{E.2}$$

For dual antenna diversity, the two tap combiner can be obtained considering the receiver output signal energy $\left(w_1\sqrt{\beta_1 E_b} + w_2\sqrt{\beta_2 E_b}\right)^2$ and noise energy $\left(w_1 n_1(t) + w_2 n_2(t)\right)^2 = w_1^2\sigma_{n,1}^2 + w_2^2\sigma_{n,2}^2$ (noting that $E\left(n_1(t)\cdot n_2(t)\right) = 0$ for uncorrelated noise) yielding the output SNR

$$\gamma_{out} = \frac{\left(w_1\sqrt{\beta_1 E_b} + w_2\sqrt{\beta_2 E_b}\right)^2}{w_1^2\sigma_{n,1}^2 + w_2^2\sigma_{n,2}^2} \tag{E.3}$$

Finding the minimum of this convex function with respect to w_1 and w_2 yields the simultaneous equations

$$\begin{aligned} \frac{\partial\gamma_{out}}{\partial w_1} &= \sigma_{n,2}^2\sqrt{\beta_1 E_b}\,w_2 + \sigma_{n,1}^2\sqrt{\beta_2 E_b}\,w_1 = 0 \\ \frac{\partial\gamma_{out}}{\partial w_2} &= \sigma_{n,1}^2\sqrt{\beta_2 E_b}\,w_1 + \sigma_{n,2}^2\sqrt{\beta_1 E_b}\,w_2 = 0 \end{aligned} \tag{E.4}$$

which are dependent and therefore

$$\frac{w_1}{w_2} = \frac{\sigma_{n,2}^2}{\sigma_{n,1}^2}\sqrt{\frac{\beta_1}{\beta_2}} = \frac{\sigma_{n,2}}{\sigma_{n,1}}\cdot\sqrt{\frac{\gamma_1}{\gamma_2}} \tag{E.5}$$

The importance of this result rests upon the relative antenna weighting, hence assuming $\frac{\sigma_{n,2}^2}{\sigma_{n,1}^2} = 1$ (i.e. identically but independently distributed noise variables) the MRC solution proportional to the square root of the ratio of input SNR's can be given by the relation

$$w_2 = \frac{\sqrt{\beta_2}}{\sqrt{\beta_1}}\,w_1 \tag{E.6}$$

Table E.1 The diversity array theoretical improvement to the SNR metric over the single channel SNR, Γ for EGC and MRC

Diversity Scheme	SNR for L Diversity Channels
MRC	$L\Gamma$
EGC	$\left[1+(L-1)\frac{\pi}{4}\right]\Gamma$

which requires only an envelope detector per diversity branch. If $w_1 = 1$ then w_2 can be dynamically adjusted according to varying conditions. For more than two diversity branches, the solution is consistent in that if w_1 is known then w_m can be found from (E.6) replacing the *2* subscript with *m*. Generally though, as in rake reception (where the MAI is different on each diversity branch), it would be more useful to consider (E.1) and/or (E.5) for the true solution if noise + interference is not equivalent on each diversity branch. This was done in [Kuo2001], where the authors used a finger variance weight update to make the MRC near optimum for the rake receiver. Note the standard MRC implementation can be readily observed from (E.6) by setting w_1 to the square root of the branch envelope- hence linking (E.1) and (E.6).

The mean SNR for the MRC and EGC schemes are shown in Table E.1, where Γ represents the mean SNR per diversity branch with *L* the number of diversity channels [Lee1985]. It is obvious from this analysis that for a two-element array receiver, the SNR should increase by 3dB for the MRC scheme (since the SNR at the output of the Maximum Ratio Combiner is the sum of the individual branch SNR's), and approximately 2.5dB for the EGC.

E.2 Antenna Array Beamforming with Known Incident Signals

This general approach considers that the DOA's are known a priori. In real life, such knowledge is totally impractical and rather complex to actually estimate unless the number of sensors is greater than the number of incident signals to keep the low rank signal matrix assumptions when utilizing subspace based techniques [Schmidt1986]. However, despite this, a viable solution for the antenna combiner considers *1* desired signal component, and *L-1* interference components. This linear problem can be represented as

$$y = \left(x_d^T(t)\boldsymbol{A}_d\right)^T \boldsymbol{W} + \sum_{i=1}^{L-1}\left(x_d^T(t)\boldsymbol{A}_i\right)^T \boldsymbol{W} \qquad \text{(E.7)}$$

where $\boldsymbol{A}_n = \begin{bmatrix} 1 & 0 \\ 0 & V_2^{\theta_n} \end{bmatrix} \in C^{2\times 2}$ represents the array response to $n=d$ (the desired signal) and $n=i$, $i = 1:L-1$ (the interference signals) with $V_2^{\theta_n} = e^{j\frac{2\pi}{\lambda_0} d\sin\theta_n}$. $\boldsymbol{W} \in C^2$ is the weight vector and $x_n(t) = [x_n, x_n] \in C^2$ the signal vector. Realistically, since L > 2, the solution to this problem is arbitrary for cancellation of all signals with random angular spread, hence consider the case that one interference source is cancelled (i.e. the dominant component) while maximizing the power of the desired component. Therefore the solution for the optimum weight vector can be attained from the system of linear equations $y = \boldsymbol{x}_d^T(\boldsymbol{A}_d\boldsymbol{w}) + \boldsymbol{x}_I^T(\boldsymbol{A}_I\boldsymbol{w})$, with

$$\boldsymbol{x}_d^T(\boldsymbol{A}_d\boldsymbol{w}) = [\boldsymbol{x}_d(t) \quad \boldsymbol{x}_d(t)]^T \begin{bmatrix} 1 & 0 \\ 0 & V_2^{\theta_d} \end{bmatrix} [\boldsymbol{w}_1 \quad \boldsymbol{w}_2] = \boldsymbol{x}_d(t) \text{ and}$$

$$\boldsymbol{x}_I^T(\boldsymbol{A}_I\boldsymbol{w}) = [\boldsymbol{x}_I(t) \quad \boldsymbol{x}_I(t)]^T \begin{bmatrix} 1 & 0 \\ 0 & V_2^{\theta_I} \end{bmatrix} [\boldsymbol{w}_1 \quad \boldsymbol{w}_2] = 0$$

giving rise to the weight vector

$$\boldsymbol{w} = \begin{bmatrix} \dfrac{-V_2^{\theta_I}}{V_2^{\theta_d} - V_2^{\theta_I}} & \dfrac{1}{V_2^{\theta_d} - V_2^{\theta_I}} \end{bmatrix} \tag{E.8}$$

This technique can be referred to as the zero-forcing spatial filter criterion if the number of sensors > the number of interference sources since the interference at the output of the detector is forced to zero while offering unitary gain to the desired signal. An example of this beamformer considering angle of arrivals $\theta_d = -\pi/6$ and $\theta_I = \pi/6$ yields the antenna beam pattern (Fig. E.1) based on the solution from (E.8). In this case, the antenna gain is maximum in the direction of the desired signal, and minimum in the direction of the interference signal.

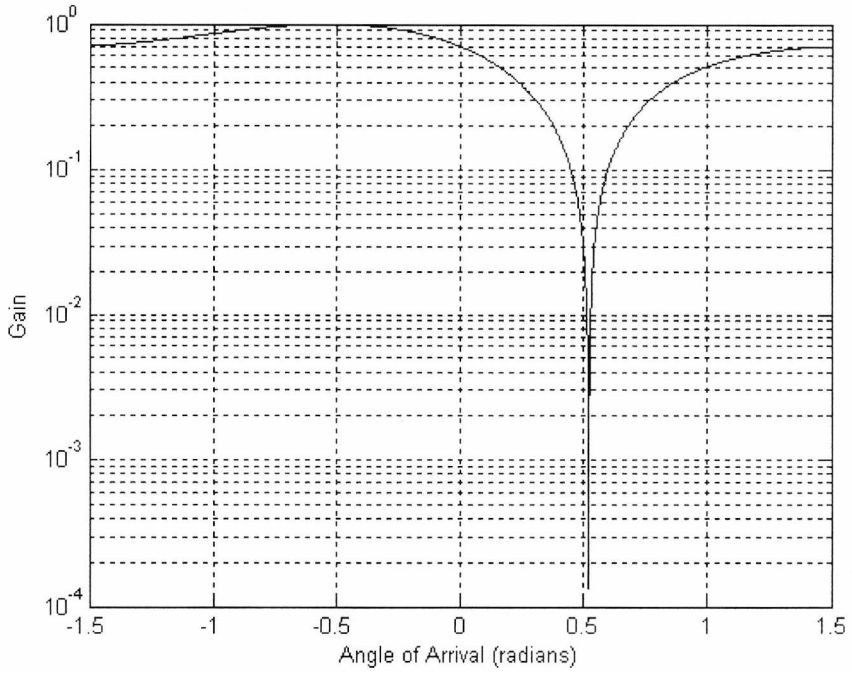

Fig E.2 The antenna gain vs. direction of arrival for diversity coefficients obtained based on known DOA for the desired and interference signal

E.3 A Blind Maximum Ratio Combining Solution

An alternative optimization to the maximum ratio combiner yields a similar criterion based on maximizing the beamformer output SINR [Litva1996] via cancellation of interference. Consider the array output signal $y(t) = \boldsymbol{w}^H \boldsymbol{x}(t)$, with signal power $E\left\{\left|\boldsymbol{w}^H \boldsymbol{x}(t)\right|^2\right\} = \boldsymbol{w}^H \Sigma_s \boldsymbol{w}$, and noise + interference power with decomposition $E\left\{\left|\boldsymbol{w}^H \boldsymbol{u}(t)\right|^2\right\} = \boldsymbol{w}^H \Sigma_u \boldsymbol{w}$. The SINR can be expressed as $SINR = \dfrac{\boldsymbol{w}^H \Sigma_s \boldsymbol{w}}{\boldsymbol{w}^H \Sigma_u \boldsymbol{w}}$ where taking partial derivatives and setting to zero yields

$$\Sigma_s \boldsymbol{w} = \frac{\boldsymbol{w}^H \Sigma_s \boldsymbol{w}}{\boldsymbol{w}^H \Sigma_u \boldsymbol{w}} \Sigma_u \boldsymbol{w} \tag{E.9}$$

which is a joint Eigen-problem. $\dfrac{\boldsymbol{w}^H \Sigma_s \boldsymbol{w}}{\boldsymbol{w}^H \Sigma_u \boldsymbol{w}}$ is bounded by the maximum and minimum eigenvalue of $\gamma = \dfrac{\Sigma_s}{\Sigma_u}$, hence a solution is sought such that $\gamma = \lambda_{max}$ satisfies the equality $\gamma \cdot \boldsymbol{w} = \lambda_{max} \cdot \boldsymbol{w}$, where $\boldsymbol{w}$ is the eigenvector corresponding to the maximum eigenvalue

λ_{max} of $\frac{\sum_s}{\sum_u}$, and is deemed the optimum weights achievable using this criterion. Practically this solution will never be optimum since the multivariate (or bivariate in a dual antenna scheme) array combiner input contains signal + noise quantities where the noise and signal subspaces must be separated to accurately attain the SINR prior to equating the homogeneous problem (the $\boldsymbol{w} \rightarrow \lambda_{max}$ mapping). This approach would require decomposition of the matrix $\sum_{xx}$ into two disjoint subspaces utilizing the well-known orthonormal projection between noise and signal subspaces- i.e. finding the subspace orthogonal (in an eigenvector sense) to the noise subspace [Vaughan2003, Schmidt1986, Kohno1998] thus permitting the weight vector to be calculated according to the spatial signatures of the undesirable signals (it will be seen in the proceeding section that estimation of both $\sum_s$ and $\sum_u$ are reliant on knowledge of the AOA's of all incident signals). However, this is computationally demanding and has severe constraints for applications with a low number of sensors. As discussed previously, solving information-blind[1] antenna optimization problems without knowledge of the AOA of the desired multipath signal (and the interference statistics) presents a formidable challenge, where approaches to overcome this have been explored in [Brunner2000A, Brunner2000B], mainly exploiting the principle of reciprocity in a static multipath environment via using the uplink receiver to provide the necessary degrees of freedom to initiate downlink beamforming[2]. In summary, the $\gamma \cdot \boldsymbol{w} = \lambda_{max} \cdot \boldsymbol{w}$ problem is not so easily solved since $\sum_s$ and $\sum_u$ are assumed unknown initially by the receiver.

1. Alternative Approaches Employing the Second Order Statistics of the Signal

The general eigenproblem can be rewritten as $\sum_s \cdot \boldsymbol{w} = \lambda_{max} \sum_u \cdot \boldsymbol{w}$, where lack of priori's can be partially mitigated by invoking $\sum_{xx} \cdot \boldsymbol{w} = \lambda_{max} \sum_u \cdot \boldsymbol{w}$ with a false assumption $\sum_u = \sigma^2 \boldsymbol{I}$, yielding $\sum_{xx} \cdot \boldsymbol{w} = \sigma^2 \lambda_{max} \cdot \boldsymbol{w}$ which can be solved numerically. The problem with this method is that interference + noise is grouped into a common

[1] By information blind, it is assumed that the training signal offered by the basestation is either too noisy to apply decision directed (or pilot channel-assisted) beamforming or is non-existent.

[2] The downlink receiver for the eigenproblem lacks the full rank assumptions to fully initiate any linear transform to project interference into the noise subspace to obtain the MRC criterion. This is a well-known problem when applying the Multiple Signal Classification (MUSIC) algorithm for parametric estimation in delay acquisition and source estimation.

independently distributed white noise vector hence generating a solution that is somewhat ignorant towards the second order statistics of interference. In this case, the beamformer coefficients are optimized for maximizing the SNR (and not the SINR). An improvement to this technique can be formed when considering that the received signal covariance can be written as

$$\begin{aligned}\Sigma_{xx} &= E\left\{\boldsymbol{x}(n)\boldsymbol{x}^H(n)\right\} = E\left\{\left[\boldsymbol{s}(n)+\boldsymbol{u}(n)\right]\cdot\left[\boldsymbol{s}(n)+\boldsymbol{u}(n)\right]^H\right\} \\ &= \Sigma_s + \Sigma_u\end{aligned}$$

based on the assumption the interference and noise terms are independent. These can be further expressed as $\Sigma_s = E\left\{\left\|d(n)\right\|^2\right\}\boldsymbol{A}(\theta_d)\boldsymbol{A}^H(\theta_d)$ and $\Sigma_u = \boldsymbol{A}_u \Sigma_K \boldsymbol{A}_u^H + \sigma^2 \boldsymbol{I}$ highlighting the importance of knowledge of the channel and the AOA's of all the desired and interfering signals. $\Sigma_K = E\left\{\boldsymbol{z}(n)\cdot\boldsymbol{z}^H(n)\right\}$ where $\boldsymbol{z}(n) = \left[z_0(n), z_1(n), \cdots, z_{N-1}(n)\right]^T$ is the interference signal vector (prior to the array incidence) composed of N independent sources. The $N \times K$ interference array propagation matrix represented by $\boldsymbol{A}_u$ is assumed to have full column rank (with the L^{th} column containing the K dimensional L^{th} propagation vector). K is the number of antenna elements. Another assumption regarding the second order statistics is that the propagation factors and channel attenuation are constant over the symbol interval, thus for optimization at the symbol level, the chip matched filter bank output vector can be used[3]. This is expatiated further by the following Proposition:

PROPOSITION E.1

Using the previous result where $\Sigma_s = E\left\{\left\|d(n)\right\|^2\right\}\boldsymbol{A}(\theta_d)\boldsymbol{A}^H(\theta_d)$, let the chip rate vector $\boldsymbol{d}_{AK}(n) = \left[f_L^{(n)}\boldsymbol{S}^{(n)}\boldsymbol{\xi}^{(n)}\boldsymbol{b}^{(n)}\right]^T$ be the desired multiuser specular signal (i.e. the one synchronized to the receiver via the delay acquisition process), where after chip matched filtering to the time variant signature $\boldsymbol{S}_1^{(n)}$, the desired signal prior to combining is given by $y^{(n)} = f_L^{(n)} b^{(n)}$. Hence $E\left\{\left\|y(n)\right\|^2\right\} = \beta_L$ with $\beta_L = E\left\{f_L^{(n)} \cdot f_L^{*\,(n)}\right\}\varepsilon_b$ the channel gain factor (assuming data is an equiprobable Bernoulli RV). In this case, Σ_s becomes

$$\Sigma_s = \beta_L \boldsymbol{A}(\theta_d)\boldsymbol{A}^H(\theta_d) \qquad \text{(E.10)}$$

A similar treatment for the interference signal at the chip matched filter output can ensue via rendering a composite $K \times G$ matrix with $\boldsymbol{U}(n) = \left[\boldsymbol{u}(n), \boldsymbol{u}(n+1), \cdots, \boldsymbol{u}(n+G)\right]$ where the

[3] The receiver structure contains one chip matched filter per antenna with the coefficients set according to the signatures of the desired user being demodulated.

output vector $y_{int}^{(n)} = \boldsymbol{U}(n) \cdot \boldsymbol{S}_1(n)$. The covariance $E\left\{y_{int}^{(n)} \cdot y_{int}^{*(n)}\right\} = \boldsymbol{U}\boldsymbol{R}_s\boldsymbol{U}^H = \frac{1}{G}\boldsymbol{U}\boldsymbol{U}^H$ invoking the long, non-cyclic random spreading code assumption (which is an approximation and certainly not true for the short term behavior of the model). Due to the linearity and stationary assumption of the operation $\boldsymbol{U}\boldsymbol{U}^H$, Σ_u becomes

$$\Sigma_u = \frac{1}{G}\boldsymbol{A}_u \Sigma_K \boldsymbol{A}_u^H + \sigma^2 \boldsymbol{I} \tag{E.11}$$

In the Proposition E.1, the only low-complexity estimation variable is the channel gain. However, since the problem is that Σ_s and Σ_u are unknown initially, one can consider that the multivariate signal (after matched filtering) has covariance $\Sigma_{yy} = \Sigma_s + \Sigma_u$ where $\Sigma_{xx} = \Sigma_s + G\Sigma_u$, $\Sigma_u = \frac{1}{G-1}\left(\Sigma_{xx} - \Sigma_{yy}\right)$ and $\Sigma_s = \frac{1}{G-1}\left(G\Sigma_{yy} - \Sigma_{xx}\right)$. The joint eigenproblem thus becomes $\frac{1}{G-1}\left(G\Sigma_{yy} - \Sigma_{xx}\right)\cdot \boldsymbol{w} = \frac{\lambda_{max}}{G-1}\left(\Sigma_{xx} - \Sigma_{yy}\right)\cdot \boldsymbol{w}$ which can be algebraically reduced to the solution

$$\Sigma_{yy} \cdot \boldsymbol{w} = \left(\frac{1+\lambda_{max}}{1+G}\right)\Sigma_{xx} \cdot \boldsymbol{w}. \tag{E.12}$$

Denoting $\lambda' = \frac{1+\lambda_{max}}{1+G}$, the generalized optimization becomes one where the eigenvector associated to the maximum eigenvalue is sought from $\Sigma_{xx}^{-1}\Sigma_{yy} \cdot \boldsymbol{w} = \lambda' \cdot \boldsymbol{w}$. The advantage of this approach is that no explicit knowledge of the AOA's or the channel is required (of course a channel estimator would still be required for cophasing the output beamformer signal). The disadvantage is computational complexity since the signal covariance's need to be updated on a sample-by-sample basis where the eigenvector solution must be calculated every new symbol-sample cycle.

2. A Blind Maximum SINR Adaptive Approach

Let the optimum beamformer be one where $\boldsymbol{w}^H \Sigma_s \boldsymbol{w}$ is maximized subject to the constraint $\boldsymbol{w}^H \Sigma_u \boldsymbol{w} = 1$. The Lagrangian is

$$L(\boldsymbol{w}) = \boldsymbol{w}^H \Sigma_s \boldsymbol{w} + \chi(1 - \boldsymbol{w}^H \Sigma_u \boldsymbol{w}) \tag{E.13}$$

with χ the Lagrange multiplier. Applying the steepest "ascent" method,

$$\boldsymbol{w}_n = \boldsymbol{w}_{n-1} + \frac{1}{2}\mu \frac{\partial L(\boldsymbol{w})}{\partial \boldsymbol{w}} \tag{E.14}$$

where the weight vector conditioned on sample index is given as

$$\boldsymbol{w}_n = \boldsymbol{w}_{n-1} + \mu\left[\Sigma_s \boldsymbol{w}_{n-1} - \chi \Sigma_u \boldsymbol{w}_{n-1}\right]. \tag{E.15}$$

The problem now becomes one of calculating the Lagrange multiplier, χ, where for each sample index, $\boldsymbol{w}^H \Sigma_u \boldsymbol{w} = 1$. Hence the solution involving the quadratic (in χ)

$$\left(\boldsymbol{w}_{n-1} + \mu\left[\Sigma_s - \chi \Sigma_u\right]\boldsymbol{w}_{n-1}\right)^H \Sigma_u \left(\boldsymbol{w}_{n-1} + \mu\left[\Sigma_s - \chi \Sigma_u\right]\boldsymbol{w}_{n-1}\right) = 1$$

is sought where expanding the terms (equating $\boldsymbol{w}^H \Sigma_u \boldsymbol{w} = 1$ in the process) and minimizing yields

$$\mu \boldsymbol{w}^H \Sigma_u^3 \boldsymbol{w} \underline{\chi}^2 - \boldsymbol{w}^H \left(2\Sigma_u^2 + \mu \Sigma_s \Sigma_u^2 + \mu \Sigma_u^2 \Sigma_s\right)\boldsymbol{w} \underline{\chi} + \mu \boldsymbol{w}^H \Sigma_s \Sigma_u \Sigma_s \boldsymbol{w}$$
$$+ \boldsymbol{w}^H \Sigma_u \Sigma_s \boldsymbol{w} \boldsymbol{w}^H \Sigma_s \Sigma_u \boldsymbol{w} = 0$$

where $\boldsymbol{w} = \boldsymbol{w}_{n-1}$ indicating that the Lagrange multiplier is updated every symbol interval during training. Solving the above equation requires computation of the roots, where the conventional procedure for obtaining the coefficient(s) when the function = 0 is given by the quadratic formula

$$\chi(n) = \frac{-b - \sqrt{b^2 - 4ac}}{2a} \tag{E.16}$$

with $a = \mu \boldsymbol{w}^H \Sigma_u^3 \boldsymbol{w}$, $b = -\boldsymbol{w}^H \left(2\Sigma_u^2 + \mu \Sigma_s \Sigma_u^2 + \mu \Sigma_u^2 \Sigma_s\right)\boldsymbol{w}$, and $c = \boldsymbol{w}^H \Sigma_s \Sigma_u \Sigma_s \boldsymbol{w} + \boldsymbol{w}^H \Sigma_u \Sigma_s \boldsymbol{w} \boldsymbol{w}^H \Sigma_s \Sigma_u \boldsymbol{w}$. It is apparent that the computational complexity for obtaining the Lagrange multiplier every time the beamformer weights are adapted is a major drawback to this technique. Algebraically, the quadratic solution must be altered by substituting $\Sigma_u = \frac{1}{G-1}\left(\Sigma_{xx} - \Sigma_{yy}\right)$ and $\Sigma_s = \frac{1}{G-1}\left(G\Sigma_{yy} - \Sigma_{xx}\right)$ into the expression. The autocovariance matrices are estimated according to proposition E.2. An application for the maximum SNR solution invoking mathematical simplification of the quadratic term was done in [Kwon1999, Choi2000, Choi2002] for Uplink beamformers. We can similarly follow the analysis from this paper, where for the maximum SINR criterion, the quadratic components are formed from the instantaneous estimated of Σ_u and Σ_s, i.e. $\hat{\Sigma}_s^{(n)} = \boldsymbol{S}_{(n)} \boldsymbol{S}_{(n)}^H$ and $\hat{\Sigma}_u^{(n)} = \boldsymbol{U}_{(n)} \boldsymbol{U}_{(n)}^H$. This gives rise to:

$a = \mu \left|\boldsymbol{w}^H \boldsymbol{U}\right|^2 \left|\boldsymbol{U}^H \boldsymbol{U}\right|^2$, $b = \left|\boldsymbol{w}^H \boldsymbol{U}\right|^2 \left|\boldsymbol{U}^H \boldsymbol{U}\right| + \mu \left|\boldsymbol{U}^H \boldsymbol{U}\right| \Re\left\{\left(\boldsymbol{U}^H \boldsymbol{x}\right) \cdot \left(\boldsymbol{w}^H \boldsymbol{U}\right) \cdot \left(\boldsymbol{w}^H \boldsymbol{x}\right)^*\right\}$, and

$$c = \mu\left|\boldsymbol{U}^H \boldsymbol{x}\right|^2 \left|\boldsymbol{w}^H \boldsymbol{x}\right|^2 + 2 \cdot \Re\left\{\left(\boldsymbol{U}^H \boldsymbol{x}\right) \cdot \left(\boldsymbol{w}^H \boldsymbol{U}\right) \cdot \left(\boldsymbol{w}^H \boldsymbol{x}\right)^*\right\}.$$

The adaptive update (E.15) for the instantaneous approximation becomes

$$\boldsymbol{w}_n = \boldsymbol{w}_{n-1} + \mu\left[\hat{\sum}_s^{(n)} \boldsymbol{w}_{n-1} - \chi^{(n)} \hat{\sum}_u^{(n)} \boldsymbol{w}_{n-1}\right]. \tag{E.17}$$

For adaptive systems, it is important to initialize the weight vector (at the start of the training cycle) where it is usual to use some predetermined value (such as $\boldsymbol{w}(0) = \boldsymbol{0}^T$ or a small fractal constant). In this thesis, $\boldsymbol{w}(0)$ is set to the initial MRC solution (i.e. a complex coefficient vector formed from the desired signal envelope weighted with the complex channel phase). This is to allow faster convergence over setting the initial weights to the null vector.

PROPOSITION E.2

The received signal autocovariance matrices can be estimated on a symbol-by-symbol (or chip-by-chip) basis applying the generic functional

$$\sum_P^{(n)} = g \sum_P^{(n-1)} + P(n) P^H(n) \tag{E.18}$$

with $0 << g < 1$ the forgetting factor.

E.4 THE BLIND MINIMUM VARIANCE BEAMFORMER

The blind Minimum Variance algorithm was originally developed by Capon in the 1960's [Capon1969] and is a very well recognized technique in blind beamforming applications. It is therefore only introduced briefly in this thesis. The usual approach to solving constrained optimization problems involves the use of Lagrange multipliers. Hence consider the unknown parameter vector $\boldsymbol{w}$ acting on the received signal vector $\boldsymbol{r}$ where the output variance $\sigma_r^2 = E\left\{\left|\boldsymbol{w}^H \boldsymbol{r}\right|^2\right\} = \boldsymbol{w}^H \sum_s \boldsymbol{w} + \boldsymbol{w}^H \sum_u \boldsymbol{w}$. The optimization problem is therefore to minimize σ_r^2, i.e. $\min_{\boldsymbol{w}} \left\{\boldsymbol{w}^H \sum_u \boldsymbol{w}\right\}$ subject to the constraint $\boldsymbol{w}^H \boldsymbol{A}(\theta_d) = 1$. The Lagrangian function is

$$L(\boldsymbol{w}, \lambda) = \boldsymbol{w}^H \sum_u \boldsymbol{w} + \lambda\left(\boldsymbol{w}^H \boldsymbol{A}(\theta_d) - 1\right) \tag{E.19}$$

with λ the Lagrange multiplier. To remove the constraint, the gradient of the Lagrangian function is set to zero, i.e. $\frac{\partial L(\boldsymbol{w}, \lambda)}{\partial \boldsymbol{w}} = 0$ giving rise to the weight vector (after some linear algebra and simplifications)

$$\boldsymbol{w} = \frac{\sum_u^{-1} \boldsymbol{A}(\theta_d)}{\boldsymbol{A}^H(\theta_d) \sum_u^{-1} \boldsymbol{A}(\theta_d)} \tag{E.20}$$

APPENDIX F
DIVERSITY COMBINING FOR UNEQUAL BRANCH INTERFERENCE

This Appendix presents the derivation to the optimum combiner presented in Chapter 4, section 4.1.

Due to the noise + interference being different on each rake finger (after spatial combining), the MRC criterion consisting of an envelope detector (with cophasing) is no longer optimum. To overcome this, we must estimate the total interference + noise variance on each diversity finger. Let the despread traffic channel signal be denoted (for the l^{th} rake finger) as

$$Z_l = \sum_{i=1}^{A} \alpha_i^{(l)} \sqrt{E_b^l}\, b + \tilde{\eta}_d^{(l)} \tag{F.1}$$

and the output of the despread Pilot channel as

$$P_l = \sum_{i=1}^{A} \alpha_i^{(l)} \sqrt{\hat{E}_p^l}\, p + \tilde{\eta}_p^{(l)} \tag{F.2}$$

where $\tilde{\eta}_l$ and $\tilde{\eta}_p$ are the uncorrelated interference + noise sources, and $\sqrt{E_b^l}$ and $\sqrt{E_p^l}$ are the real amplitudes of the traffic and pilot channels considering the transmit power, path loss, shadowing, and antenna gain (but not the short-term fading). b is the data symbol. An estimate of the rake coefficient for cophasing is given by

$$\hat{C}_l = \frac{\sum_{i=1}^{A} \alpha_i^{(l)} \sqrt{\hat{E}_p^l}\, p + \tilde{\eta}_p^{(l)}}{\sqrt{\hat{E}_p^l}} \tag{F.3}$$

where $\sqrt{\hat{E}_p^l}$ is an estimate of the pilot amplitude and is a real scalar. Let the dual antenna rake finger soft output be given by $d_l = \hat{C}_l Z_l$. For the l^{th} rake diversity-combining branch, the likelihood function considering the Gaussian approximation is:

$$P\left(d_l \middle| b, E_b^l, E_p^l\right) = \frac{1}{\sqrt{2\pi}\sigma_l} \exp\left[-\frac{\left| d_l - E\{d_l\} \right|^2}{2\sigma_l^2} \right] \tag{F.4}$$

Assuming "L-fold" diversity, the joint density function of the multi-branch Rake outputs is:

$$P\left(d_0, d_1, \cdots, d_{L-1} \middle| b, E_b^0, \cdots, E_b^{L-1}, E_p^0, \cdots, E_p^{L-1}\right) = \prod_{l=0}^{L-1} P\left(d_l \middle| b, E_b^l, E_p^l\right) \tag{F.5}$$

The Log-Likelihood function is given by

$$\sum_{l=1}^{L} log_e P\left\{d_l \middle| b, \sqrt{E_b^l}, \sqrt{E_p^l}\right\} \tag{F.6}$$

which can be equated as

$$-\sum_{l=1}^{L} \frac{\left|d_l - E\{d_l\}\right|^2}{2\sigma_l^2} = -\sum_{l=1}^{L} \frac{\left|\sqrt{\hat{E}_p^l} Z_l - \sqrt{E_b^l} P_l b\right|^2}{2\hat{E}_p^l \sigma_l^2} \tag{F.7}$$

where

$$\begin{aligned} \sigma_l^2 &= E\left\{d_l - E|d_l|^2\right\} \\ &= \left(E\left\{\left|\frac{P_l}{\sqrt{\hat{E}_p^l}}\right|^2\right\} \cdot \left[\sqrt{E_b^l} - \sqrt{\hat{E}_b^l} \cdot \frac{\sqrt{E_p^l}}{\sqrt{\hat{E}_p^l}}\right]^2 + \left\{1 + \frac{\sqrt{E_b^l}}{\sqrt{\hat{E}_p^l}}\right\} \xi_{MAI+SI+\eta} \right). \end{aligned} \tag{F.8}$$

where $\xi_{MAI+SI+\eta}$ is the variance of MAI, self interference, and noise equated as a single random variable. The function $P(\bullet)$ is the conditional probability density function of the variable in the parenthesis. Note the denominator has been left unscaled. This was done for simplicity since for an equiprobable detection hypothesis this scalar is irrelevant.

The likelihood ratio (assuming only the real part of the signal modulation is desired and antipodal) is given by:

$$\lambda\left(d \middle| b \in \{1,-1\}\right) = \prod_{l=0}^{L-1} \frac{P\left(d_l \middle| b_1, E_b^l, E_p^l\right)}{P\left(d_l \middle| b_{-1}, E_b^l, E_p^l\right)} \tag{F.9}$$

and the log-likelihood ratio $\Omega = \log_e\left\{\lambda\left(d \middle| b \in \{1,-1\}\right)\right\}$. After some algebraic manipulation considering (F.4), the decision metric assuming antipodal symbols is

$$\Omega = \log_e\left\{\frac{P\left(d \middle| b=1\right)}{P\left(d \middle| b=-1\right)}\right\} = \sum_{l=1}^{L} \frac{\sqrt{\hat{E}_b^l}}{\sqrt{\hat{E}_p^l}} \times \frac{\Re\left\{P_l^* Z\right\}}{\sigma_l^2} \tag{F.10}$$

i.e. the optimum decisions are centered around a detector that scales the cophased signals on each diversity branch by the inverse "branch" variance. Hence to obtain the diversity improvement, a variance estimator must be implemented (Fig. F.1). Variance estimation applying (F.8) is rather complex. Consider therefore $\sigma_l^2 = E\left\{d_l - E|d_l|^2\right\}$.

If noise + interference is zero mean and uncorrelated, then $E|d_l|$ can be approximated by applying decision directed feedback to remove the symbol modulation. We then can apply a moving average filter to estimate this, where the result can be subtracted from the soft rake finger output to form an approximate interference signal. The square of this signal averaged over a finite interval will give an estimate of the variance. This aspect has also been researched in [Noneaker1998] and [Kong2005] for finding more optimum combining schemes for the rake.

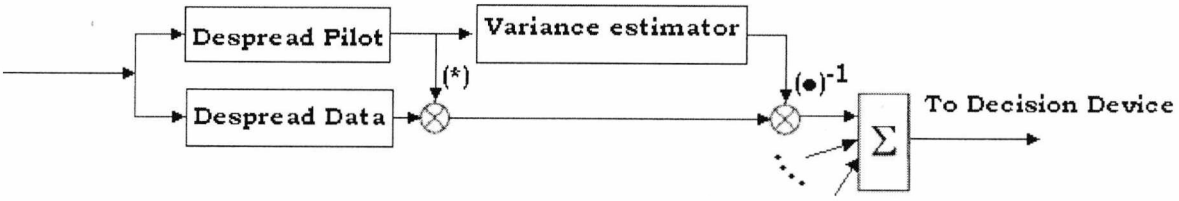

Fig. F.1 Diagram of the new Rake Receiver Finger with inverse variance coefficient

APPENDIX G

NLMS AND SIGNED-REGRESSOR LMS FILTER DERIVATION AND ANALYSIS

In Wiener filter theory, a tapped delay line FIR filter represents the adaptive filter. The matrix form of the Wiener-Hopf equations is the backbone of the method of steepest descent, where the weight vector is altered from its initial or arbitrary state in a direction opposite to that of the gradient of the error criterion. This procedure is continued and updated until the minimum of the error function is reached. The real gradient vector in the Wiener approach depends on the correlation matrix of the input signal vector, and the cross-correlation vector between the desired signal and the input signal vector. In the stochastic gradient descent (SGD) method, an estimate of the gradient vector consisting of instantaneous estimates of the correlation matrix and the cross-correlation vector are used instead of the auto-covariance matrices.

G.1 INTRODUCTION

The following mathematical procedure represents the instantaneous filter output utilizing the vector dot product notation

$$y(n) = \mathbf{w}^H(k)\mathbf{r}(k) \tag{G-1}$$

where $y(n)$ is the filter output at time instant n. The filter coefficients are stacked as a time-variant vector (conditioned with certain impulse response at the n^{th} time interval), with

$$\mathbf{w}(k) = \begin{bmatrix} w_0(k) \\ w_1(k) \\ \vdots \\ w_{N_F-2}(k) \\ w_{N_F-1}(k) \end{bmatrix} \tag{G-2}$$

where N_f are the number of filter taps. Similarly, the filter regressor containing samples of the input signal (shifted along a tap delay line) can be treated as a time variant vector where $r_0(n)$, $r_1(n)$, ..., r_{Nf} are treated as separate time variant signals. However, in equalizer implementation for instance, the sample $r_0(n)$ is the N_f^{th} time shifted sample of $r(n)$, i.e.

r$(n\text{-}N_f)$, hence all multivariate quantities share the same sample space which is unlike that of the adaptive antenna array. A generic vectoral representation of $r(n)$ is given by

$$\boldsymbol{r}(k) = \begin{bmatrix} r_0(k) \\ r_1(k) \\ \vdots \\ r_{N_F-2}(k) \\ r_{N_F-1}(k) \end{bmatrix} \tag{G-3}$$

The output is computed at time nT_c, i.e., at integer multiples of the chip period T_c. The weights of the filter are updated according to

$$\boldsymbol{w}(k+1) = \boldsymbol{w}(k) - \mu\hat{\nabla}(\boldsymbol{J}(k)) \tag{G-4}$$

where μ is a small constant defined as the step-size and $\mu\hat{\nabla}(\boldsymbol{J}(k))$ the instantaneous estimate of the gradient vector. In the method of steepest descent the weight vector follows a deterministic path along the steepest slope on the multi-dimensional error surface. In the SGD method, it follows a random path – see Fig. G1 for a pictoral example considering a two by one dimension filter.

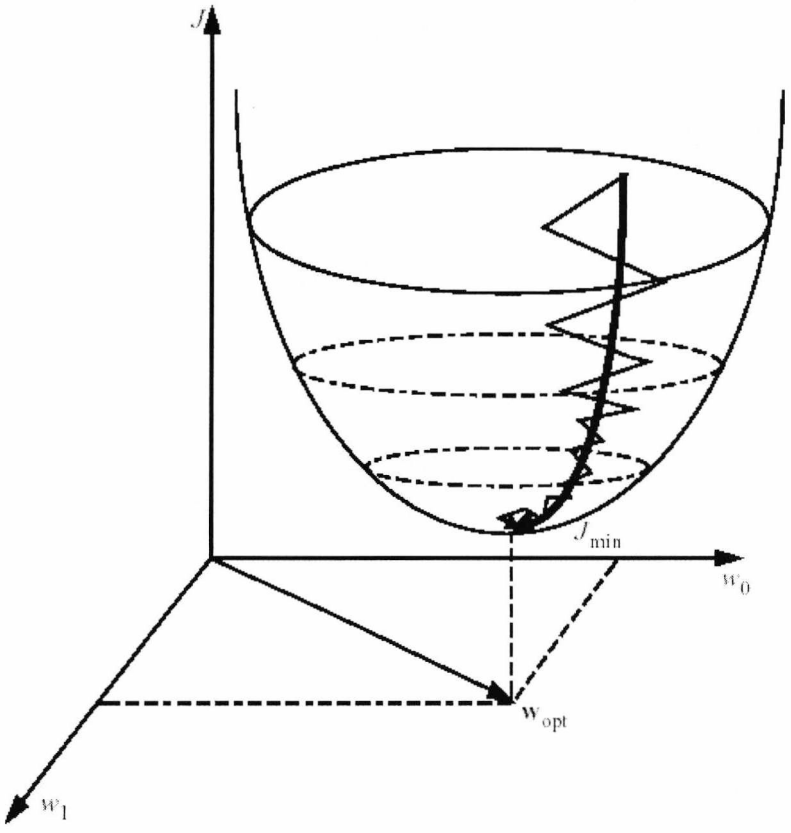

Fig. G1 The Error Surface of the cost function with two filter coefficients. The convergence paths for the SDM and SGD are given with straight and zig-zag lines respectively.

Initiating the instantaneous estimate of the gradient of the steepest slope, the randomized motion occurs due to gradient noise. The step-size parameter, μ, determines the rate of convergence and gradient noise where small step-sizes are preferred since the effect of gradient noise and misadjustment are reduced. However, this comes at the cost of slow convergence. The Bayesian cost function of the MMSE algorithm is given by

$$\begin{aligned} J &= E\left[|e(k)|^2\right] \\ &= E\left[\left|d(k) - \boldsymbol{w}^H \boldsymbol{r}(k)\right|^2\right] \end{aligned} \tag{G-5}$$

where expatiating upon the expected error yields the following function

$$\begin{aligned} J &= E\left[(d(k) - \boldsymbol{w}^H \boldsymbol{r}(k))^* (d(k) - \boldsymbol{w}^H \boldsymbol{r}(k))\right] \\ &= E\left[|d(k)|^2\right] - \boldsymbol{w}^H E[d(k)\boldsymbol{r}(k)] - E\left[d(k)\boldsymbol{r}^H(k)\right]\boldsymbol{w} + \boldsymbol{w}^H E\left[\boldsymbol{r}(k)\boldsymbol{r}^H(k))\right]\boldsymbol{w} \\ &= \sigma_d^2 - \boldsymbol{w}^H \boldsymbol{p} - \boldsymbol{p}^H \boldsymbol{w} + \boldsymbol{w}^H \boldsymbol{R}\boldsymbol{w} \end{aligned} \tag{G-6}$$

where $\boldsymbol{p}$ is the crosscorrelation vector and $\boldsymbol{R}$ the correlation matrix:

$$\begin{aligned} \boldsymbol{p} &\triangleq E[d(k)\boldsymbol{r}(k)] \\ \boldsymbol{R} &\triangleq E[\boldsymbol{r}(k)\boldsymbol{r}^H(k))] \\ \sigma_d^2 &\triangleq E[|d(k)|^2]. \end{aligned} \tag{G-7}$$

The cost function J is minimized when the gradient is minimized, where the gradient is usually a complex multi-dimensional quantity, i.e.

$$\nabla \triangleq \begin{bmatrix} \dfrac{\partial}{\partial w_0^r} + j\dfrac{\partial}{\partial w_0^i} \\ \dfrac{\partial}{\partial w_1^r} + j\dfrac{\partial}{\partial w_l^i} \\ \vdots \\ \dfrac{\partial}{\partial w_{N_F}^r} + j\dfrac{\partial}{\partial w_{N_F}^i} \end{bmatrix} \tag{G-8}$$

The gradient is also related to the conjugate derivative of $\boldsymbol{J}$ with respect to $\boldsymbol{w}$, $\partial \boldsymbol{J} = \partial \boldsymbol{w}$, via the following relation

$$\nabla(\boldsymbol{J}) = 2\frac{\partial \boldsymbol{J}}{\partial \boldsymbol{w}^*} \tag{G-9}$$

The filter is optimum in the MMSE sense if $\nabla(\boldsymbol{J}) = \boldsymbol{0}$ where $\boldsymbol{0}$ is the null vector. Hence

$$\nabla(\boldsymbol{J}) = 2(-\boldsymbol{p} + \boldsymbol{R}\boldsymbol{w}_{opt}) \tag{G-10}$$

and the condition for optimality becomes

$$-\boldsymbol{p} + \boldsymbol{R}\boldsymbol{w}_{opt} = \boldsymbol{0} \tag{G-11}$$

where $\boldsymbol{w}_{opt}$ is the optimum weight vector. Hence

$$\boldsymbol{R}\boldsymbol{w}_{opt} = \boldsymbol{p}. \tag{G-12}$$

which is the matrix formulation of the Wiener-Hopf equations for a transversal filter. Assuming that the correlation matrix $\boldsymbol{R}$ is non-singular, the Wiener solution for the optimum weight vector is given by

$$\boldsymbol{w}_{opt} = \boldsymbol{R}^{-1}\boldsymbol{p}. \tag{G-13}$$

Noting that $\boldsymbol{J} = \boldsymbol{J}_{min}$ when $\boldsymbol{w} = \boldsymbol{w}_{opt}$, (B-6) may be rewritten as

$$\boldsymbol{J}_{\min} = \sigma_d^2 - \boldsymbol{w}_{opt}^H(\boldsymbol{p} - \boldsymbol{R}\boldsymbol{w}_{opt}) - \boldsymbol{p}^H\boldsymbol{w}_{opt} \tag{G-14}$$

with the MMSE given by

$$\boldsymbol{J}_{\min} = \sigma_d^2 - \boldsymbol{p}^H\boldsymbol{R}^{-1}\boldsymbol{p}. \tag{G-15}$$

depending on the variance of the desired signal, the correlation matrix of the received signal at the filter input (the regressor), and the cross-correlation vector between the input signal and the desired signal.

G.2 THE LMS AND NLMS ALGORITHMS

The steepest descent algorithm iteratively changes the weight vector from it's initial state in a direction opposite to the gradient vector, where

$$\boldsymbol{w}(k+1) = \boldsymbol{w}(k) + \frac{\mu}{2}\left[-\nabla(\boldsymbol{J}(k))\right] \tag{G-16}$$

where $\frac{\mu}{2}$ is the real-valued step-size (usually made proportional to a base two signed integer exponent for arithmetic simplicity for a numeric processor). Substituting G-10 into G-16 yields

$$\boldsymbol{w}(k+1) = \boldsymbol{w}(k) + \mu\left[\boldsymbol{p} - \boldsymbol{R}\boldsymbol{w}(k)\right] \tag{G-17}$$

where knowledge of $\boldsymbol{p}$ and $\boldsymbol{R}$ are mandatory for the weight vector adaptation. Accurately attaining both $\boldsymbol{p}$ and $\boldsymbol{R}$ presents a technical challenge particularly for WCDMA environments. If these quantities were estimated applying averaging over a limited time interval, w_{opt} could be computed directly with (B-13). The stochastic gradient descent algorithm rather uses instantaneous estimates $\hat{\boldsymbol{p}} \rightarrow \boldsymbol{p}$ and $\hat{\boldsymbol{R}} \rightarrow \boldsymbol{R}$ from G-7 removing the expectation operators, i.e. $\hat{\boldsymbol{R}} = \boldsymbol{r}(k)\boldsymbol{r}^H(k)$ and $\hat{\boldsymbol{p}} = \boldsymbol{r}(k)d^*(k)$. Hence G-17 in this case becomes the classic LMS algorithm with

$$\boldsymbol{w}(k+1) = \boldsymbol{w}(k) + \mu\left\{d_{(k)} - \boldsymbol{w}^H(k)\boldsymbol{r}(k)\right\}^*\boldsymbol{r}(k) \tag{G-18}$$

We realize the functionality of this filter by the following steps:

I. Computation of filter output,

$$y(k) = \boldsymbol{w}^H(k)\boldsymbol{r}(k);$$

II. Computation of estimation error term,

$$e(k) = d(k) - y(k);$$

III. Update the filter weight vector with,

$$\boldsymbol{w}(k+1) = \boldsymbol{w}(k) + \mu e^*(k)\boldsymbol{r}(k).$$

During the filter training stage, a large input vector can cause gradient noise amplification when the step-size is fixed resulting in a high steady-state MSE or instability of the algorithm. This problem can be mitigated with the normalized LMS (NLMS) algorithm where the weight update factor is normalized with respect to the squared Euclidean norm of the input vector ***r(k)***. Given the input signal vector ***r(k)*** and the desired signal *d(k)*, the problem becomes one where the weight vector ***w(k+1)*** is determined such that the squared Euclidean norm of the change in the weight vector is minimized, i.e. $\delta\boldsymbol{w}(k+1) \triangleq \boldsymbol{w}(k+1) - \boldsymbol{w}(k)$ subject to the constraint $\boldsymbol{w}^H(k+1)\boldsymbol{r}(k) = d(k)$.

Hence the cost function utilizing the complex Lagrange multiplier λ becomes

$$\boldsymbol{J}(k) = \left\|\delta\boldsymbol{w}(+1)\right\|^2 + \lambda\left[d(k) - \boldsymbol{w}^H(k+1)\boldsymbol{r}(k)\right] \tag{G-19}$$

Expanding yields

$$\begin{aligned}\bar{J}(k) &= \left[\boldsymbol{w}(k+1) - \boldsymbol{w}(k)\right]^H\left[\boldsymbol{w}(k+1) - \boldsymbol{w}(k)\right] + \lambda\left[d(k) - \boldsymbol{w}^H(k+1)\boldsymbol{r}(k)\right] \\ &= \boldsymbol{w}^H(k+1)\boldsymbol{w}(k+1) - \boldsymbol{w}^H(k+1)\boldsymbol{w}(k) - \boldsymbol{w}^H(k)\boldsymbol{w}(k+1) \\ &\quad + \boldsymbol{w}^H(k)\boldsymbol{w}(k) + \lambda\left[d(k) - \boldsymbol{w}^H(k+1)\boldsymbol{r}(k)\right]\end{aligned}$$

where the value of *w(k + 1)* that minimizes this cost function, i.e. $\dfrac{\partial\tilde{J}(k)}{\partial\boldsymbol{w}^*(k+1)} = \boldsymbol{0}$ yields

$$\boldsymbol{w}(k+1) - \boldsymbol{w}(k) = \lambda\boldsymbol{r}(k). \tag{G-20}$$

Multiplying both sides of B-20 with $\boldsymbol{r}^H(k)$ renders

$$\boldsymbol{r}^H(k)\left[\boldsymbol{w}(k+1) - \boldsymbol{w}(k)\right] = \lambda\boldsymbol{r}^H(k)\boldsymbol{r}(k) \tag{G-21}$$

where solving for λ yields

$$\lambda = \frac{d^*(k) - \boldsymbol{r}^H(k)\boldsymbol{w}(k)}{\left\|\boldsymbol{r}(k)\right\|^2} = \frac{e^*(k)}{\left\|\boldsymbol{r}(k)\right\|^2} \tag{G-22}$$

With the Lagrange multiplier now known, it is relatively easy to formulate the NLMS update, where

$$\boldsymbol{w}(k+1) = \boldsymbol{w}(k) + \frac{\mu_0}{\left\|\boldsymbol{r}(k)\right\|^2}e^*(k)\boldsymbol{r}(k). \tag{G-23}$$

We usually use (B-23) with the denominator biased with a small fractal quantity α to prevent arithmetic problems when $\frac{\mu_0}{\|\boldsymbol{r}(k)\|^2}$ becomes singular, hence

$$\boldsymbol{w}(k+1) = \boldsymbol{w}(k) + \frac{\mu_0}{\alpha + \|\boldsymbol{r}(k)\|^2} e^*(k)\boldsymbol{r}(k). \tag{G-24}$$

G.3 THE SIGNED-REGRESSOR LMS ALGORITHM

The signed regressor (SR) algorithm has the form

$$\boldsymbol{w}(k+1) = \boldsymbol{w}(k) + \mu e(k)\,\mathrm{sgn}\{\boldsymbol{r}(k)\} \tag{G-25}$$

with $\mathrm{sgn}\{\bullet\} = \begin{Bmatrix} -1 & x < 0 \\ 0 & x = 0 \\ +1 & x > 0 \end{Bmatrix}$.

If μ is of the form 2^{-m}, the only arithmetic operation involved in the weight update is addition. The adaptation problem can be viewed geometrically, where the weight error vector $\boldsymbol{v}(k)$ at the k^{th} iteration is defined by

$$\begin{aligned} &\boldsymbol{v}(\mathrm{k}) = \boldsymbol{w}(\mathrm{k}) - \boldsymbol{w}_{\mathrm{opt}} \\ &\Rightarrow \boldsymbol{v}(\mathrm{k}+1) = \boldsymbol{v}(\mathrm{k}) + \mu \mathrm{e}(\mathrm{k})\boldsymbol{r}(\mathrm{k}) \end{aligned} \tag{G-26}$$

The direction of the update vector is determined by $\boldsymbol{r}(k)$ and the sign of the error $e(k)$ which controls the weight error vector magnitude. The step-size μ scales the instantaneous gradient estimate $-2\mu\mathrm{e}(\mathrm{k})\boldsymbol{r}(\mathrm{k})$ and determines the rate of convergence. For the LMS algorithm, the magnitude of the weight error vector reduces at every iteration until the update converges, i.e. when the magnitude reduces to near zero accounting for any residual due to gradient noise. Consider the geometric interpretation of weight update for the Signed Regressor algorithm in Fig. B.2. The weight error vector update equation is

$$\boldsymbol{v}(\mathrm{k}+1) = \boldsymbol{v}(\mathrm{k}) + \mu \mathrm{e}(\mathrm{k})\,\mathrm{sgn}\{\boldsymbol{r}(\mathrm{k})\}. \tag{G-27}$$

where the vector $\mathrm{sgn}\{\boldsymbol{r}(\mathrm{k})\}$ is not aligned with the input vector $\boldsymbol{r}(k)$. The input vector can have one of $2N$ (in the N-dimensional case) possible directions leading to incorrect adaptation on an instantaneous basis. The degradation of the performance of this algorithm compared with the LMS algorithm arises from the deviation of the equivalent gradient vector $-2\mu\mathrm{e}(\mathrm{k})\,\mathrm{sgn}\{\boldsymbol{r}(\mathrm{k})\}$ from the true instantaneous estimate $-2\mu\mathrm{e}(\mathrm{k})\boldsymbol{r}(\mathrm{k})$ causing incorrect instantaneous adjustments to the weight vector. The algorithm works within this constraint where a monotonic decrease of the weight error vector is not always guaranteed.

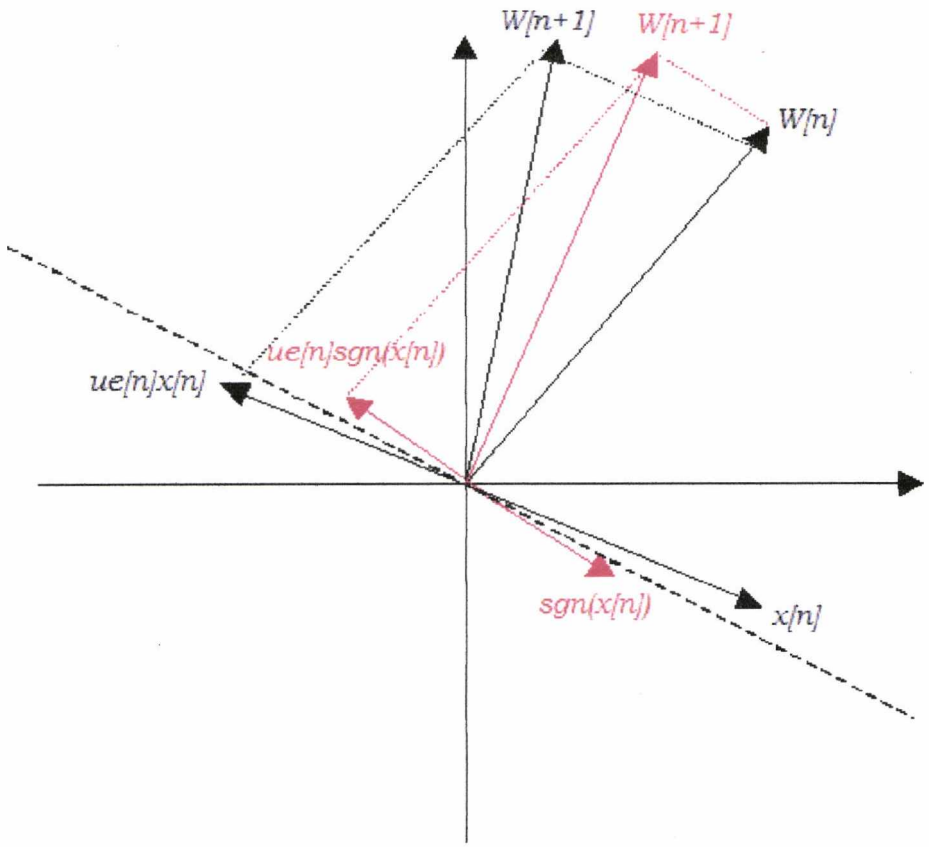

Fig. G.2 Geometric Interpretation of the Weight Vector Update in the SR Algorithm.

The convergence of the Signed Regressor algorithm is now analyzed:

Considering B-27, the expected gradient error can be given as

$$\begin{aligned} \mathrm{E}[\boldsymbol{v}(\mathrm{k}+1)] &= \mathrm{E}[\boldsymbol{v}(\mathrm{k})] + \mu\mathrm{E}[\mathrm{e}(\mathrm{k})\,\mathrm{sgn}\{\boldsymbol{r}(\mathrm{k})\}] \\ &= \mathrm{E}[\boldsymbol{v}(\mathrm{k})] + \mu\mathrm{E}\left[\left\{\mathrm{d}(\mathrm{k}) - (\boldsymbol{w}_{\mathrm{opt}} + \boldsymbol{v}(\mathrm{k}))^{\mathrm{T}}\boldsymbol{r}(\mathrm{k})\right\}\mathrm{sgn}\{\boldsymbol{r}(\mathrm{k})\}\right] \end{aligned} \tag{G-28}$$

where $\boldsymbol{w}_{opt}$ is the optimum vector from the Wiener-Hopf equations. Expanding G-28 yields

$$\begin{aligned} \mathrm{E}[\boldsymbol{v}(\mathrm{k}+1)] &= \mathrm{E}[\boldsymbol{v}(\mathrm{k})] + \mu\mathrm{E}\left[\left\{\mathrm{d}(\mathrm{k}) - \boldsymbol{w}_{\mathrm{opt}}^{\mathrm{T}}\boldsymbol{r}(\mathrm{k})\right\}\mathrm{sgn}\{\boldsymbol{r}(\mathrm{k})\}\right] \\ &\quad - \mu\mathrm{E}\left[\mathrm{sgn}\{\boldsymbol{r}(\mathrm{k})\}\boldsymbol{r}^{\mathrm{T}}(\mathrm{k})\right]\mathrm{E}[\boldsymbol{v}(\mathrm{k})] \\ &= \mathrm{E}[\boldsymbol{v}(\mathrm{k})] + \mu\mathrm{E}\left[\mathrm{e}_{\mathrm{opt}}(\mathrm{k})\,\mathrm{sgn}\{\boldsymbol{r}(\mathrm{k})\}\right] \\ &\quad - \mu\mathrm{E}\left[\mathrm{sgn}\{\boldsymbol{r}(\mathrm{k})\}\boldsymbol{r}^{\mathrm{T}}(\mathrm{k})\right]\mathrm{E}[\boldsymbol{r}(\mathrm{k})] \end{aligned} \tag{G-29}$$

where $e_{opt}(k)$ is the error associated with the optimum weight vector. By the principle of orthogonality where $\boldsymbol{e}_{opt}(k)$ and $\boldsymbol{r}(k)$ are uncorrelated $\mathrm{E}\left[\mathrm{e}_{\mathrm{opt}}(\mathrm{k})\boldsymbol{r}(\mathrm{k})\right] = \boldsymbol{0}$, translating into statistical independence if the Gaussian assumption is invoked. Eweda [Eweda1990] utilized Price's theorem for the individual elements of $\mathrm{E}\left[\mathrm{sgn}\{\boldsymbol{r}(\mathrm{k})\}\boldsymbol{r}^{\mathrm{T}}(\mathrm{k})\right]$ to obtain

$$\mathrm{E}\left[\mathrm{sgn}\{\boldsymbol{r}(\mathrm{k})\}\boldsymbol{r}^{\mathrm{T}}(\mathrm{k})\right] = \frac{1}{\sigma_{\mathrm{r}}}\sqrt{\frac{2}{\pi}}\boldsymbol{R}_{\mathrm{rr}} \tag{G-30}$$

where $\sigma_r = \sqrt{E\{r_i^2(k)\}}$, $i = 1,2,....N$, with $r_i(k)$ being the i^{th} element of the input vector $r(k)$. $\boldsymbol{R}_{rr}$ is the received signal covariance. Substitution into B-29 yields the weight error vector first moment as

$$\begin{aligned} E[\boldsymbol{v}(k+1)] &= E[\boldsymbol{v}(k)] - \frac{\mu}{\sigma_x}\sqrt{\frac{2}{\pi}}\boldsymbol{R}_{rr}E[\boldsymbol{v}(k)] \\ &= \left(\boldsymbol{I} - \frac{\mu}{\sigma_r}\sqrt{\frac{2}{\pi}}\boldsymbol{R}_{rr}\right)E[\boldsymbol{v}(k)]. \end{aligned} \tag{G-31}$$

In a more formal notation, we rewrite (B-31) as

$$\tilde{\boldsymbol{v}}(k+1) = \left(I - \frac{\mu}{\sigma_r}\sqrt{\frac{2}{\pi}}\ \boldsymbol{\Lambda}\right)\tilde{\boldsymbol{v}}(k). \tag{G-32}$$

with $\boldsymbol{\Lambda}$ the signal covariance. The update equation for the i^{th} element of the transformed error vector is given by

$$\tilde{v}_i(k+1) = \left(1 - \frac{\mu}{\sigma_x}\sqrt{\frac{2}{\pi}\lambda}\right)^k \tilde{v}_i(0) \tag{G-33}$$

which renders the following condition for convergence (in the mean) of the Signed Regressor algorithm

$$0 < \mu < \sqrt{2\pi}\frac{\sigma_r}{\lambda_{max}} \tag{G-34}$$

where λ_{max} is again the largest eigenvalue of $\boldsymbol{R}_{rr}$. Since $N\sigma_x^2 = tr\{\boldsymbol{R}_{rr}\} = \sum_{i=1}^{N}\lambda_i$ and $\lambda_{max} < tr(\boldsymbol{R}_{rr})$, a sufficient condition for convergence is $0 < \mu < \sqrt{\frac{2\pi}{N \cdot tr(\boldsymbol{R}_{rr})}}$ where $tr(\bullet)$ represents the trace of the matrix.

The following approximate expression for steady-state MSE with the SR algorithm was derived in [Eweda1990], where

$$\sigma_e^2(\infty) \approx \varepsilon_{min} + \sqrt{\frac{2}{\pi}}\frac{\mu}{2}N\sigma_r\varepsilon_{min}. \tag{G-35}$$

To obtain the same steady-state MSE with the LMS algorithm and the SR algorithm, the step-size μ_R for the SR algorithm is related to μ_{LMS} (for the LMS algorithm) via

$$
\begin{aligned}
\mu_R &= \sqrt{\frac{2}{\pi}} \frac{\sum_{i=1}^{N} \lambda_i}{N \sigma_r} \mu_{LMS} \\
&= \sqrt{\frac{2}{\pi}} \frac{N \sigma_r^2}{N \sigma_r} \mu_{LMS} \\
&= \sqrt{\frac{2}{\pi}} \sigma_r \mu_{LMS}.
\end{aligned}
\tag{G-36}
$$

APPENDIX H

DERIVATION OF MMSE SYMBOL LEVEL DUAL ANTENNA EQUALIZER

For comparative purposes, the MMSE symbol level receiver can be checked against the dual antenna MMSE chip level receiver in section 4.3.3.1. Let the output of the MMSE symbol equalizer be denoted by $\boldsymbol{\theta} = \boldsymbol{w}^H \cdot \boldsymbol{\mathcal{X}}$ with

$$\boldsymbol{\mathcal{X}} = C_1^H \left(\boldsymbol{\mathcal{H}} \left(\boldsymbol{S}_1 \xi_1 \mathbf{b}_1 + \sum_{i=2}^{K} \boldsymbol{S}_i \xi_i \mathbf{b}_i + \boldsymbol{P}_s \xi_s \boldsymbol{p} \right) + \boldsymbol{n} \right) \tag{H.1}$$

the CMF bank output and $C_1 \in \Xi^{(sG+N_f)\times N_f}$ the fractionally delayed single user chip sequence matrix modeling the TDL. The MMSE solution is found by minimizing $\frac{\partial}{\partial \boldsymbol{f}} E\left\{ \left| \boldsymbol{\theta} - \mathbf{b}_1 \right|^2 \right\}$ yielding

$$\boldsymbol{w} = \boldsymbol{\Sigma}_{XX}^{-1} \boldsymbol{\Lambda}_{dX} \tag{H.2}$$

where $\boldsymbol{\Sigma}_{XX} = E\left\{ \boldsymbol{X} \cdot \boldsymbol{X}^H \right\}$ and $\boldsymbol{\Lambda}_{dX} = E\left\{ \mathbf{b}_1^* \cdot \boldsymbol{X} \right\}$. However, considering carrying out the minimization over the symbol period without despreading yields a model alteration where

$$\begin{aligned} \boldsymbol{\mathcal{X}} &= \boldsymbol{\mathcal{H}} \left(\boldsymbol{S}_1 \xi_1 \mathbf{b}_1 + \sum_{i=2}^{K} \boldsymbol{S}_i \xi_i \mathbf{b}_i + \boldsymbol{P}_s \xi_s \boldsymbol{p} \right) + \boldsymbol{n} \\ &= \boldsymbol{\mathcal{H}} \boldsymbol{y} + \boldsymbol{n} \end{aligned} \tag{H.3}$$

with $\boldsymbol{\Sigma}_{XX} = \boldsymbol{\mathcal{H}} \boldsymbol{\Sigma}_{yy} \boldsymbol{\mathcal{H}}^H + \boldsymbol{\Sigma}_n$ and $\boldsymbol{\Lambda}_{dX} = \boldsymbol{\mathcal{H}} E\left\{ \mathbf{b}_1^* \cdot \left(\left(\boldsymbol{S}_1 \xi_1 \mathbf{b}_1 + \sum_{i=2}^{K} \boldsymbol{S}_i \xi_i \mathbf{b}_i + \boldsymbol{P}_s \xi_s \boldsymbol{p} \right) + \boldsymbol{n} \right) \right\}$

Hence

$$\boldsymbol{w} = \left(\boldsymbol{\mathcal{H}} \boldsymbol{\Sigma}_{yy} \boldsymbol{\mathcal{H}}^H + \boldsymbol{\Sigma}_n \right)^{-1} \boldsymbol{\mathcal{H}} E\left\{ \mathbf{b}_1^* \cdot \left(\left(\boldsymbol{S}_1 \xi_1 \mathbf{b}_1 + \sum_{i=2}^{K} \boldsymbol{S}_i \xi_i \mathbf{b}_i + \boldsymbol{P}_s \xi_s \boldsymbol{p} \right) + \boldsymbol{n} \right) \right\} \tag{H.4}$$

For long averaging intervals, random codes and random data, $\boldsymbol{\Sigma}_{yy} \to \mathbf{I}$ with reasonable assumption. Furthermore, provided the minimization is carried out in cyclic intervals (to prevent the expectation in H.4 going to zero), then with reasonable

assumption, $E\left\{ \mathbf{b}_1^* \cdot \left(\left(\boldsymbol{S}_1 \xi_1 \mathbf{b}_1 + \sum_{i=2}^{K} \boldsymbol{S}_i \xi_i \mathbf{b}_i + \boldsymbol{P}_s \xi_s \boldsymbol{p} \right) + \boldsymbol{n} \right) \right\} = \boldsymbol{\mathcal{A}}$ with

$\boldsymbol{A} = \left[\boldsymbol{0}_a^T, \boldsymbol{S}_1^T, \boldsymbol{0}_b^T \right]^T \in \Xi^{N_f+L}$ making the assumption $N_f > G$. Hence

$$\boldsymbol{w} = \left(\boldsymbol{\mathcal{H}} \boldsymbol{\Sigma}_{yy} \boldsymbol{\mathcal{H}}^H + \boldsymbol{\Sigma}_n \right)^{-1} \boldsymbol{\mathcal{H}} \boldsymbol{\mathcal{A}}^{(n)} \tag{H.5}$$

which is a time varying filter (matching the channel codes for user 1). The similarity to the chip level dual antenna equalizer is obvious, particularly when $\boldsymbol{\Sigma}_{yy} \rightarrow \mathbf{I}$.

VITA

Charan Litchfield obtained the degree Electronic Engineering with first class honours from the University of Kent at Canterbury in the year 2000. In the proceeding years 2000 - 2002 he graduated from the same institution obtaining a Masters degree at distinction level in Wireless mobile and Broadband communication systems. The academic dissertation submitted in partial requirement for the degree investigated the performance of the UMTS downlink when non-linear amplifiers were used to transmit multi-channel, multi-carrier broadband information across the wireless interface. Methods of compensating the amplifier-induced intermodulation products via non-linear predistortion and feed-forward circuits were part of the wider objective of the thesis. Charan Litchfield is currently pursuing the degree Doctor of Philosophy where his research interests include statistical signal processing for wireless mobile systems, diversity, multi-user detection, modulation, coding, and number theory for low cost computer arithmetic. Charan Litchfield has worked as a consultant for RFID solutions and undertook a major project developing and simulating wireless readers for RF Identification Tags.